

1981

Kinetic studies of organochromium (III) cations and their hydrido analog

Debra Ann Piering Ryan
Iowa State University

Follow this and additional works at: <https://lib.dr.iastate.edu/rtd>

 Part of the [Inorganic Chemistry Commons](#)

Recommended Citation

Ryan, Debra Ann Piering, "Kinetic studies of organochromium (III) cations and their hydrido analog" (1981). *Retrospective Theses and Dissertations*. 6882.
<https://lib.dr.iastate.edu/rtd/6882>

This Dissertation is brought to you for free and open access by the Iowa State University Capstones, Theses and Dissertations at Iowa State University Digital Repository. It has been accepted for inclusion in Retrospective Theses and Dissertations by an authorized administrator of Iowa State University Digital Repository. For more information, please contact digirep@iastate.edu.

8123127

RYAN, DEBRA ANN PIERING

KINETIC STUDIES OF ORGANOCHROMIUM(III) CATIONS AND THEIR
HYDRIDO ANALOG

Iowa State University

PH.D. 1981

University
Microfilms
International 300 N. Zeeb Road, Ann Arbor, MI 48106

Kinetic studies of organochromium(III) cations and
their hydrido analog

by

Debra Ann Piering Ryan

A Dissertation Submitted to the
Graduate Faculty in Partial Fulfillment of the
Requirements for the Degree of
DOCTOR OF PHILOSOPHY

Department: Chemistry

Major: Inorganic Chemistry

Approved:

Signature was redacted for privacy.

In Charge of Major Work

Signature was redacted for privacy.

For the Major Department

Signature was redacted for privacy.

For the Graduate College

Iowa State University
Ames, Iowa

1981

TABLE OF CONTENTS

	<u>Page</u>
GENERAL INTRODUCTION	1
PART I. AUTOXIDATION OF THE ISOPROPYL (PENTAAQUO)- CHROMIUM(III) COMPLEX	7
INTRODUCTION	8
Statement of Problem	8
Review of Autoxidations	10
EXPERIMENTAL	15
Materials	15
$(\text{CH}_3)_2\text{CHCr}(\text{H}_2\text{O})_5^{2+}$	15
2,3-Dimethyl-2-butyl hydroperoxide	16
Miscellaneous inorganic reagents	16
Reagents for Winkler titration	17
Gases	18
HClO_4 , NaOH , LiClO_4	18
Methods	19
Analyses and characterizations	19
Kinetics obtained with spectrophotometry	25
Kinetics obtained with oxygen-sensing electrode	30
RESULTS	33
Kinetics of Reaction of $(\text{CH}_3)_2\text{CHCr}(\text{H}_2\text{O})_5^{2+}$ with O_2	33
Variation of the concentrations of O_2 and H_3O^+	37
Variation of ionic strength	42
Kinetics at very low $[(\text{CH}_3)_2\text{CHCr}(\text{H}_2\text{O})_5^{2+}]$	48
Radical Scavengers	48
Effect of organic scavengers	48
Effect of miscellaneous metal ions	49
Effect of $\text{Fe}_{\text{aq}}^{2+}$	49
Effect of high $[\text{Cu}^{2+}]$	52

	<u>Page</u>
Products of Reaction of $(\text{CH}_3)_2\text{CHCr}(\text{H}_2\text{O})_5^{2+}$ with O_2	57
Kinetics of Homolysis and Acidolysis	59
Products of Homolysis and Acidolysis	64
DISCUSSION	66
PART II. ACID-CATALYZED CLEAVAGE OF β -HYDROXYETHYL (PENTAAQUO)CHROMIUM(III) ION	83
INTRODUCTION	84
EXPERIMENTAL	96
Materials	96
$\text{Co}(\text{NH}_3)_5\text{H}_2\text{O}(\text{ClO}_4)_3$	96
$[\text{Co}(\text{NH}_3)_5\text{O}_2\text{CCH}_2\text{CH}_2\text{OH}](\text{ClO}_4)_2$	96
$\text{HOCH}_2\text{CH}_2\text{COOH}$	105
$\text{HOCH}_2\text{CH}_2\text{Co}(\text{dmgH})_2\text{py}$	107
$\text{HOCH}_2\text{CH}_2\text{Co}(\text{dmgH})_2\text{H}_2\text{O}$	107
$\text{ClCo}(\text{dmgBF}_2)_2\text{py}$	109
$\text{HOCH}_2\text{CH}_2\text{Co}(\text{dmgBF}_2)_2\text{py}$	109
$\text{Cr}(\text{ClO}_4)_2$	112
HClO_4 , NaOH , LiClO_4	113
Gases	113
Methods	113
Instrumentation	113
Analyses	113
Flash photolysis	115

	<u>Page</u>
RESULTS	117
System 1: $\text{Cr}_{\text{aq}}^{2+} + \text{N}_2\text{O} + \text{CH}_2\text{CH}_2\text{H}_2\text{O} \xrightarrow{h\nu, \text{H}_3\text{O}^+} \text{HOCH}_2\text{CH}_2\text{Cr}(\text{H}_2\text{O})_5^{2+} + \text{N}_2 + \text{H}_2\text{O}$	117
Rate of reaction of $\text{HOCH}_2\text{CH}_2\text{Cr}(\text{H}_2\text{O})_5^{2+}$ with H_3O^+	117
Effect of temperature	123
Effect of ionic strength	126
Spectrum of $\text{HOCH}_2\text{CH}_2\text{Cr}(\text{H}_2\text{O})_5^{2+}$	130
System 2: $\text{HOCH}_2\text{CH}_2\text{Co}(\text{dmgBF}_2)_2\text{py} \xrightarrow{h\nu, \text{Cr}_{\text{aq}}^{2+}, \text{H}_3\text{O}^+}$	
$\text{HOCH}_2\text{CH}_2\text{Cr}(\text{H}_2\text{O})_5^{2+} + \text{Co}(\text{dmgBF}_2)_2 + \text{py}$	134
System 3: $\text{Co}(\text{NH}_3)_5\text{O}_2\text{CCH}_2\text{CH}_2\text{OH}^{2+} \xrightarrow{h\nu, \text{Cr}_{\text{aq}}^{2+}, \text{H}_3\text{O}^+}$	
$\text{HOCH}_2\text{CH}_2\text{Cr}(\text{H}_2\text{O})_5^{2+} + \text{Co}_{\text{aq}}^{2+} + 5\text{NH}_4^+ + \text{CO}_2$	137
Rate of reaction of transients with H_3O^+	138
Product of reaction of $\text{HOCH}_2\text{CH}_2\text{Cr}(\text{H}_2\text{O})_5^{2+}$ with H_3O^+	141
DISCUSSION	142
PART III. PROTONOLYSIS OF HYDRIDO(PENTAAQUO)- CHROMIUM(III) ION	158
INTRODUCTION	159
Statement of Problem	159
Review of Similar Transition Metal Hydrides	164

	<u>Page</u>
EXPERIMENTAL	168
Materials	168
Cr(ClO ₄) ₂	168
CH ₃ Cr(H ₂ O) ₅ ²⁺	169
HClO ₄ , NaOH, LiClO ₄	170
Gases	170
Methods	170
Flash photolysis	170
Conventional kinetics	171
RESULTS	173
Detection of Transient	173
Effect of Scavengers	173
N ₂ O	173
CH ₃ OH	175
Rate of Reaction of HCr(H ₂ O) ₅ ²⁺ with H ₃ O ⁺	176
Dependence on [H ₃ O ⁺]	176
Effect of temperature	179
Effect of ionic strength	182
Effect of deuterium substitution	188
Spectrum of Transient	194
DISCUSSION	196
Assignment of Identity of Transient	196
Spectrum	196
Scavengers	197
Reaction kinetics	200
Ionic strength	201
Mechanism of Protonolysis Reaction	202

	<u>Page</u>
CONCLUSIONS	207
BIBLIOGRAPHY	209
ACKNOWLEDGEMENTS	221
APPENDIX	222
Description of Flash Photolysis Instrument	223
Operation of Spectrophotometer	232
Operation of Flash Photolysis Instrument	238
Initial equipment adjustment	238
Actual experiment	238
Data analysis	240
Simple chemical systems for use as calibration reactions	242

LIST OF TABLES

	<u>Page</u>
Table 1-1. Rate constants for the reaction of $(\text{CH}_3)_2\text{CHCr}(\text{H}_2\text{O})_5^{2+}$ with 1.05 mM O_2 at various $[\text{RCr}^{2+}]_0$	38
Table 1-2. Rate constants for the reaction of $(\text{CH}_3)_2\text{CHCr}(\text{H}_2\text{O})_5^{2+}$ with O_2 at various $[\text{O}_2]$	39
Table 1-3. Rate constants for the reaction of $(\text{CH}_3)_2\text{CHCr}(\text{H}_2\text{O})_5^{2+}$ with O_2 at various $[\text{H}_3\text{O}^+]$	41
Table 1-4. Rate constants for the reaction of $(\text{CH}_3)_2\text{CHCr}(\text{H}_2\text{O})_5^{2+}$ with O_2 at various ionic strengths	45
Table 1-5. Rate constants for the reaction of $(\text{CH}_3)_2\text{CHCr}(\text{H}_2\text{O})_5^{2+}$ with O_2 in the presence of $\text{Cu}^{2+}_{\text{aq}}$	54
Table 1-6. Percent yields of acetone and 2-propanol pro- duced in the reaction of $(\text{CH}_3)_2\text{CHCr}(\text{H}_2\text{O})_5^{2+}$ with O_2	58
Table 1-7. Percent yields of HCrO_4^- , $\text{Cr}(\text{H}_2\text{O})_6^{3+}$, and $[\text{Cr}(\text{OH})(\text{H}_2\text{O})_4]_2^{4+}$	60
Table 1-8. Rate constants obtained for the decomposition of $(\text{CH}_3)_2\text{CHCr}(\text{H}_2\text{O})_5^{2+}$ under N_2	63

Table 2-1. Rate constants for the reaction of $\text{HOCH}_2\text{CH}_2\text{Cr}(\text{H}_2\text{O})_5^{2+}$ with H_3O^+	121
Table 2-2. Rate constants for the reaction of $\text{HOCH}_2\text{CH}_2\text{Cr}(\text{H}_2\text{O})_5^{2+}$ with H_3O^+ at various temperatures	125
Table 2-3. Rate constants for the reaction of $\text{HOCH}_2\text{CH}_2\text{Cr}(\text{H}_2\text{O})_5^{2+}$ with H_3O^+ at various ionic strengths	128
Table 3-1. Rate constants for the reaction of $\text{HCr}(\text{H}_2\text{O})_5^{2+}$ with H_3O^+	180
Table 3-2. Rate constants for the reaction of $\text{HCr}(\text{H}_2\text{O})_5^{2+}$ with H_3O^+ at various temperatures	183
Table 3-3. Rate constants for the reaction of $\text{HCr}(\text{H}_2\text{O})_5^{2+}$ with H_3O^+ at various ionic strengths	186
Table 3-4. Rate constants for the reaction of $\text{DCr}(\text{D}_2\text{O})_5^{2+}$ with D_3O^+	190
Table 3-5. Deuterium isotope effect on reaction rate constants	193
Table A-1. Maximum possible flash energies attainable with various capacitor arrangements	226
Table A-2. Typical PMT voltages for various wavelengths	237

LIST OF FIGURES

- | | <u>Page</u> |
|--|-------------|
| Figure 1-1. The electronic spectrum of the $(\text{CH}_3)_2\text{CHCr}(\text{H}_2\text{O})_5^{2+}$ ion. Concentration = $5.8 \times 10^{-4}\text{M}$; cell length = 1 cm | 20 |
| Figure 1-2. Log-log plot of the instantaneous reaction rate <u>versus</u> the average concentration of the $(\text{CH}_3)_2\text{CHCr}(\text{H}_2\text{O})_5^{2+}$ ion for the reaction of $(\text{CH}_3)_2\text{CHCr}(\text{H}_2\text{O})_5^{2+}$ with O_2 . Rates and concentrations are expressed in absorbance units per 1 cm cell length. The plots include data from four kinetic experiments at two wavelengths. $[\text{O}_2] = 1.05 \text{ mM}$; $[\text{RCr}^{2+}]_0/\text{mM} = 0.098$ (open triangles), 0.20 (solid triangles), 0.50 (open circles), 1.0 (solid circles). Lines are drawn to have a slope of $3/2$ | 34 |
| Figure 1-3. Three-halves-order kinetic plots for the reaction of $(\text{CH}_3)_2\text{CHCr}(\text{H}_2\text{O})_5^{2+}$ with 1.05 mM O_2 . Monitoring $\lambda = 290 \text{ nm}$; cell length = 2 cm | 36 |
| Figure 1-4. Plot of $\log k_{\text{obs}}$ <u>versus</u> $0.509\mu^{1/2}/(1 + \mu^{1/2})$ for the reaction of $(\text{CH}_3)_2\text{CHCr}(\text{H}_2\text{O})_5^{2+}$ with O_2 . The dashed line has a slope of +4 | 47 |
| Figure 1-5. Trace of absorbance at 400 nm <u>versus</u> time for the reaction of $(\text{CH}_3)_2\text{CHCr}(\text{H}_2\text{O})_5^{2+}$ with O_2 in the presence (open circles) of increments of $\text{Fe}_{\text{aq}}^{2+}$ and | |

absence (solid circles). $[\text{RCr}^{2+}]_0 = 0.95 \text{ mM}$;
 $[\text{O}_2] = 1.05 \text{ mM}$. At the numbered arrows the
 following concentrations (mM) of $\text{Fe}_{\text{aq}}^{2+}$ were
 injected (the concentration (mM) of RCr^{2+}
 at this point is in parentheses): (1) 0.58,
 (0.95); (2) 0.28, (0.51); (3) 0.27, (0.29).

The lettered arrows represent the time at which
 all $\text{Fe}_{\text{aq}}^{2+}$ has been consumed

- Figure 1-6. Plot of $k_{\text{obs}}^{\text{Cu}}$ versus $[\text{Cu}^{2+}]^{-1}$ at $[\text{O}_2] = 1.05 \text{ mM}$,
 for the reaction of $(\text{CH}_3)_2\text{CHCr}(\text{H}_2\text{O})_5^{2+}$ with O_2
 in the presence of $\text{Cu}_{\text{aq}}^{2+}$ 50
- Figure 1-7. Plot of $k_{\text{obs}}^{\text{Cu}}$ versus $[\text{O}_2]$ at $[\text{Cu}^{2+}] = 0.10 \text{ M}$,
 for the reaction of $(\text{CH}_3)_2\text{CHCr}(\text{H}_2\text{O})_5^{2+}$ with O_2
 in the presence of $\text{Cu}_{\text{aq}}^{2+}$ 55
- Figure 2-1. ^1H NMR of $\text{Co}(\text{NH}_3)_5\text{O}_2\text{CCH}_2\text{CH}_2\text{OH}(\text{ClO}_4)_2$ in D_2O ,
 referenced to HOD at $\delta = 4.7 \text{ ppm}$ 101
- Figure 2-2. Representative photographs of oscilloscope
 traces showing the reaction of $\text{HOCH}_2\text{CH}_2\text{Cr}(\text{H}_2\text{O})_5^{2+}$
 with H_3O^+ at various acidities. Monitoring
 $\lambda = 390 \text{ nm}$; flash energy = 400 J (a-c), 250 J (d);
 $\mu = 0.05 \text{ M}$ (LiClO_4); $I_0 = 1000 \text{ mV}$; I_{t_∞} (mV) = 915
 (a), 840 (b), 840 (c), 890 (d) 118a
- Figure 2-3. Plots of $\ln(D'_t - D'_\infty)$ versus time for photographs
 of Figure 2-2 120

- Figure 2-4. The dependence of k_{obs} on $[\text{H}_3\text{O}^+]$ for the reaction of $\text{HOCH}_2\text{CH}_2\text{Cr}(\text{H}_2\text{O})_5^{2+}$ with H_3O^+ , using data from Table 2-1. Open circles represent experimental values of k_{obs} ; solid circles are calculated for $T = 24.1^\circ\text{C}$ from activation parameters, using Equation 2-27 122
- Figure 2-5. Plot of $\log k$ versus $0.509\mu^{1/2}/(1 + \mu^{1/2})$ for the reaction of $\text{HOCH}_2\text{CH}_2\text{Cr}(\text{H}_2\text{O})_5^{2+}$ with H_3O^+ . The line is drawn to have a slope of +4 129
- Figure 2-6. The electronic spectrum of the $\text{HOCH}_2\text{CH}_2\text{Cr}(\text{H}_2\text{O})_5^{2+}$ ion. Cell length = 10 cm; flash energy = 250 J 131
- Figure 3-1. Dependence of the absorbance due to $\text{HCr}(\text{H}_2\text{O})_5^{2+}$ at 380 nm on flash energy. Cell length = 10 cm; 1×10^{-3} absorbance unit is approximately 2 mV 174
- Figure 3-2. Representative photographs of oscilloscope traces showing the reaction of $\text{HCr}(\text{H}_2\text{O})_5^{2+}$ with H_3O^+ at various acidities. Monitoring $\lambda = 380$ nm; flash energy = 250 J; $\mu = 0.20$ M (LiClO_4); $I_0 = 1000$ mV; I_{t_∞} (mV) = 950 (a), 960 (b), 994 (c), 975 (d) 177a
- Figure 3-3. Plots of $\ln(D'_t - D'_\infty)$ versus time for photographs of Figure 3-2 178
- Figure 3-4. The dependence of k_{obs} on $[\text{H}_3\text{O}^+]$ for the reaction of $\text{HCr}(\text{H}_2\text{O})_5^{2+}$ with H_3O^+ 181

- Figure 3-5. Plot of $\ln(k/T)$ versus $1/T$ for the reaction of $\text{HCr}(\text{H}_2\text{O})_5^{2+}$ with H_3O^+ 184
- Figure 3-6. Plot of $\log k$ versus $0.509\mu^{1/2}/(1 + \mu^{1/2})$ for the reaction of $\text{HCr}(\text{H}_2\text{O})_5^{2+}$ with H_3O^+ . The line is drawn to have a slope of +4 187
- Figure 3-7. Plot of $\log k$ versus $0.509\mu^{1/2}/(1 + \mu^{1/2})$ for the reaction of $\text{HCr}(\text{H}_2\text{O})_5^{2+}$ with H_3O^+ (open circles) and $\text{DCr}(\text{D}_2\text{O})_5^{2+}$ with D_3O^+ (solid circles). The lines are drawn to have a slope of +4 191
- Figure 3-8. The electronic spectrum of the $\text{HCr}(\text{H}_2\text{O})_5^{2+}$ ion. Cell length = 10 cm; flash energy = 250 J. Values of ϵ are relative to $\epsilon_{380} = 190 \text{ M}^{-1} \text{ cm}^{-1}$ 195
- Figure A-1. Schematic of flash photolysis instrument 224
- Figure A-2. Illustration of trigger wire attachment to flashlamps 229
- Figure A-3. Circuit diagram of PMT dynode chain 231
- Figure A-4. The electronic spectrum of $\text{Co}(\text{NH}_3)_5\text{H}_2\text{O}^{3+}$ obtained with spectrophotometer of flash photolysis instrument (circles) and from Cary 219 spectrophotometer (line) 236
- Figure A-5. Schematic of a kinetic trace for a system where $\epsilon_{\text{transient}} > \epsilon_{\text{product(s)}}$ at the monitoring wavelength. See text for identification of a - d 241

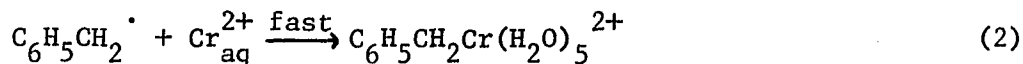
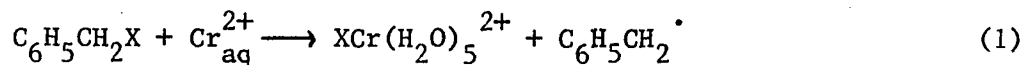
Figure A-6. Decay profile of flashlamps. Monitoring
 $\lambda = 420 \text{ nm}$; flash energy = 250 J; no cell;
680 V on PMT; load resistance = 47 k Ω

GENERAL INTRODUCTION

Organochromium(III) cations with the general formula $\text{RCr}(\text{H}_2\text{O})_5^{2+}$ have been extensively studied due to interest in the chemistry of the carbon-chromium bond. Members of this family are considered to be complexes of chromium(III) in which the metal is octahedrally coordinated to five water molecules and R, the latter through a sigma carbon-chromium bond. In a formal sense, the organo ligand is considered as a carbanion, to conform with the normally accepted convention for organometallic compounds. This assignment is not meant to imply that the C-Cr bond is ionic in nature, indeed many of its reactions can be interpreted only in terms of a covalent interaction. However, the relative solution stability of these complexes is characteristic of chromium(III) complexes, which are generally substitution inert (1). Yet, only recently have solids been isolated (2) of two organochromium(III) perchlorates; the great majority of these species exist only in solution, where their intense UV-visible absorption bands serve as a valuable method of detection.

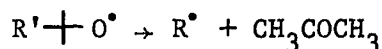
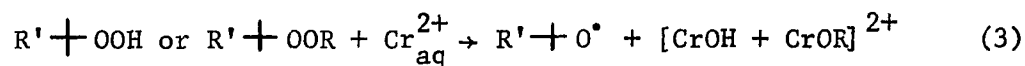
In the late 1950s, Anet and Leblanc (3) reported the first preparation of an organochromium(III) species in this family, the benzyl-pentaaquochromium(III) ion, $\text{C}_6\text{H}_5\text{CH}_2\text{Cr}(\text{H}_2\text{O})_5^{2+}$, obtained and purified as solutions of the cationic complex in aqueous perchloric acid. The preparation consisted of a two-stage reduction of a benzyl halide by the chromium(II) ion. In the first step, chromium(II) abstracts a halogen atom from the halide, generating the benzyl radical. In a rapid subsequent reaction, the radical is scavenged by $\text{Cr}_{\text{aq}}^{2+}$, resulting in formation

of the organochromium(III) complex.



Substituted benzylchromium(III) ions soon followed (4), and more recently (5,6), difunctional complexes of bis(benzylchromium(III)). While the chromium(II) reduction of organic halides is not of general utility for the synthesis of a complete variety of organochromium(III) cations, it has proved successful for "activated" halides. In particular, halomethyl complexes, where R = $-\text{CHCl}_2$ (7,8), $-\text{CH}_2\text{Cl}$; $-\text{CHBr}_2$, $-\text{CH}_2\text{Br}$; $-\text{CHI}_2$, $-\text{CH}_2\text{I}$ (8); $-\text{CCl}_3$ (9); and $-\text{CF}_3$ (10) are all prepared by this route from chloroform, bromoform, iodoform, carbon tetrachloride, and CF_3I , respectively. Likewise, reductions of bromomethylpyridinium bromides lead to the pyridinomethylchromium(III) ions (11,12), or of halogenoacetic acids to $\text{HOOCCH}_2\text{Cr}(\text{H}_2\text{O})_5^{2+}$ (13).

For those complexes which cannot be prepared by reaction with organic halides, because chromium(II) reduction is too slow to be synthetically useful, the reaction of chromium(II) with organic peroxides or hydroperoxides has been exploited (14-16) as a source of organic free-radicals.

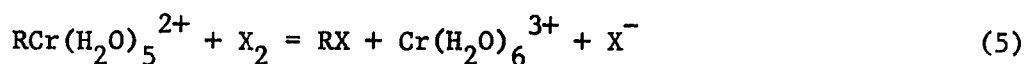


After unimolecular β -scission of the alkoxy radical, the free-radical is scavenged by another $\text{Cr}_{\text{aq}}^{2+}$ ion, forming the organochromium(III) complex,

Reaction 4. This scheme was first used by Kochi and Rust (14) as an alternative route to benzylchromium(III), and has since been useful for the synthesis of $\text{CH}_3\text{Cr}(\text{H}_2\text{O})_5^{2+}$ (16-18), and many other primary and secondary alkylchromium(III) complexes (16,19,20). α -Hydroxy and α -alkoxyalkylchromium(III) species have been synthesized, very recently, using a modified Fenton's reagent as the source of the hydroxyalkyl or alkoxyalkyl radical (18,21-24). Finally, chromium(II) reductions of 3-, 4-pyridineacrylic, maleic, and fumaric acids have resulted in isolation of remarkably stable organochromium(III) complexes (2).

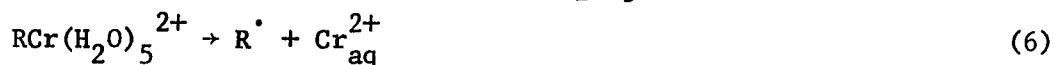
Pulse radiolysis has been useful in detecting the more unstable organochromium(III) species (25), which cannot be investigated by normal methods. Additionally, rates for Reaction 4 have been directly measured by pulse radiolysis for a large series of substituted alkyl radicals, confirming that rates of coupling are competitive with bimolecular reactions of R^\cdot . Second-order rate constants of $(0.34 - 5.1) \times 10^8 \text{ M}^{-1} \text{ s}^{-1}$ have been determined for Reaction 4 (25), having values which do not vary widely for different organic radicals.

Reactions of $\text{RCr}(\text{H}_2\text{O})_5^{2+}$ which have been studied include electrophilic cleavage of the carbon-chromium bond. Kinetic investigations of Br_2 (19,26,27), I_2 (26), and IBr (28) have established dealkylation occurs with formation of the organohalides, RBr , RI , and RI , respectively, and $\text{Cr}(\text{H}_2\text{O})_6^{3+}$, Reaction 5.



The reactions were considered to proceed by an S_E2 mechanism (bimolecular electrophilic substitution). Electrophilic cleavage of some organochromium(III) ions can also be accomplished with mercury(II) or $\text{CH}_3\text{Hg(II)}$ ions (3,8,20) resulting in organomercurials of the general formula RHg^+ or CH_3HgR . Other organochromium(III) complexes react with Hg(II) by an electron-transfer process (8,22). Characterization of organomercurial products has been useful in identifying the starting organochromium(III) ion.

Homolysis of the carbon-chromium bond to form R^\cdot and $\text{Cr}_{\text{aq}}^{2+}$ has been definitely established for several $\text{RCr(H}_2\text{O)}_5^{2+}$ complexes.

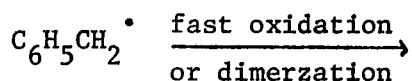
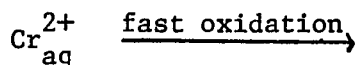
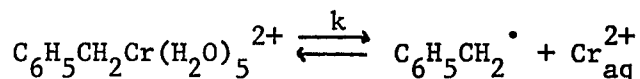


Its importance, relative to other competing reactions, and the rate constant for homolytic cleavage are greatly dependent upon the organo ligand. For example, homolysis is an important pathway leading to decomposition of benzylchromium(III), when in the presence of oxidants. A kinetic investigation (29) of the reaction of $\text{C}_6\text{H}_5\text{CH}_2\text{Cr(H}_2\text{O)}_5^{2+}$ with a variety of oxidants-- $\text{Fe}_{\text{aq}}^{3+}$, $\text{Co(NH}_3)_5\text{Cl}^{2+}$, $\text{Co(NH}_3)_5\text{Br}^{2+}$, $\text{Cu}_{\text{aq}}^{2+}$, H_2O_2 , and O_2 , in aqueous perchloric acid, gave a rate law independent of the nature of the oxidant and its concentration. A first-order dependence on $[\text{C}_6\text{H}_5\text{CH}_2\text{Cr}_{\text{aq}}^{2+}]$ was demonstrated,

$$-\frac{d[\text{RCr}_{\text{aq}}^{2+}]}{dt} = k[\text{RCr}_{\text{aq}}^{2+}] \quad (7)$$

where $\text{R} = \text{C}_6\text{H}_5\text{CH}_2$. The products (29) of reaction were those expected from oxidation of either $\text{Cr}_{\text{aq}}^{2+}$ or benzyl radicals, or both, by the

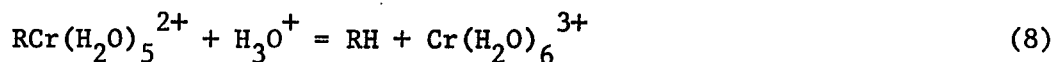
specific oxidant. These results were interpreted (29) as a rate-limiting homolysis of the organochromium(III) ion, followed by rapid oxidation of $\text{Cr}_{\text{aq}}^{2+}$ and/or $\text{C}_6\text{H}_5\text{CH}_2^\bullet$ by the oxidant present:



The experimental rate constant k of Equation 7 was identified with that of homolysis.

Kinetic studies of pyridinomethylchromium(III) ion (30-32); difunctional complexes of bis(benzylchromium(III)) cations (5,6); and α -hydroxy, or α -alkoxyalkylchromium(III) ions (21-24) have similarly demonstrated the importance of homolysis for these species.

Acidolysis (often called protonolysis) of the $\text{RCr}(\text{H}_2\text{O})_5^{2+}$ family of complexes occurs competitively with homolysis, the importance of each pathway depending upon the particular complex. Acidolysis leads to heterolytic cleavage of the carbon-chromium bond to release RH and $\text{Cr}(\text{H}_2\text{O})_6^{3+}$, Reaction 8.



Protonolysis reactions have been studied for a number of simple alkyl (16,18,20); α - and β -hydroxyalkyl (18,24,25); α -alkoxyalkyl (24,25); α -carboxyalkyl (25,27); benzylchromium(III) (33); and organochromium(III)

complexes obtained from pyridineacrylic, maleic, and fumaric acids (34). A general mechanism does not apply for acidolysis of these organochromium(III) complexes. Both acid-independent and acid-dependent pathways may exist, depending on R; in general the rate constant for Equation 8 is of the form $k_0 + k[\text{H}_3\text{O}^+]$. A direct dependence on $[\text{H}_3\text{O}^+]$ is interpreted as electrophilic attack on the carbon-chromium bond (35), while a solvent assisted cleavage is postulated (18) for acid-independent loss of RH.

In an effort to extend the knowledge of the chemistry of carbon-chromium and also the hydrido-chromium bonds, the present study was undertaken. In Part I of this thesis a kinetic analysis of the reaction of $(\text{CH}_3)_2\text{CHCr}(\text{H}_2\text{O})_5^{2+}$ with molecular oxygen is presented. This work represents the first complete study of the oxidation of an organochromium(III) ion of this family by O_2 , which does not involve indirect reaction through simple homolysis. The protonolysis reactions of two highly unstable chromium(III) complexes are presented in Part II and Part III. These reactions were investigated using the flash photolysis technique. A new member of the $\text{RCr}(\text{H}_2\text{O})_5^{2+}$ family, $\text{HOCH}_2\text{CH}_2\text{Cr}(\text{H}_2\text{O})_5^{2+}$, was generated by three different photochemical systems. The hydrido analog, $\text{HCr}(\text{H}_2\text{O})_5^{2+}$, studied previously (36) by pulse radiolysis, was successfully prepared and characterized using flash photolysis. In the Appendix, a description of the flash photolysis instrument, assembled in the course of this study, will be presented along with a guide to its proper usage.

PART I. AUTOXIDATION OF THE ISOPROPYL(PENTAAQUO)CHROMIUM(III) COMPLEX

INTRODUCTION

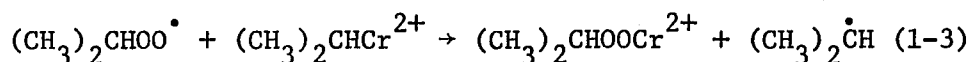
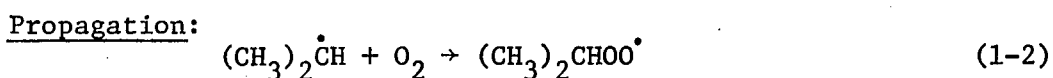
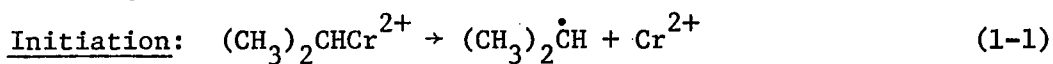
Statement of Problem

Many of the organochromium(III) ions of the family $\text{RCr}(\text{H}_2\text{O})_5^{2+}$ appear to be stable toward molecular oxygen, although this reaction had previously been specifically studied only for the benzylchromium(III) ion. The simple alkylchromium(III) ions such as $-\text{CH}_3$, $-\text{C}_2\text{H}_5$, $-\text{n-C}_3\text{H}_7$, etc., are inert to molecular oxygen, at least within the time they undergo decomposition by acidolysis (20). Likewise, α -carboxymethyl (27), and halomethylchromium(III) (8-10) complexes appear to be air-stable or nearly so. Species which undergo homolysis are, of course, oxygen sensitive, as a result of scavenging of the homolysis fragments by molecular oxygen. Indeed, the above list of oxygen-inert organochromium(III) ions might well be a listing of complexes for which homolysis is unimportant.

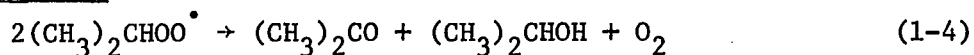
Notable exceptions to these oxygen-stable $\text{RCr}(\text{H}_2\text{O})_5^{2+}$ ions are benzyl- (29), sec-butyl- (20), and isopropylchromium(III) complexes (20), the latter of which is the subject of this part of the thesis. A kinetic study of reactions of $(\text{CH}_3)_2\text{CHCr}(\text{H}_2\text{O})_5^{2+}$ with various oxidants was initiated, with the expectation that this organochromium(III) ion might, like benzylchromium(III), react simply by homolysis. However, the reaction of isopropylchromium(III) with molecular oxygen was unique to this oxidant, occurring faster than with the other oxidants, clearly indicating the chemistry in the presence of O_2 was not only homolysis.

As to be presented in detail later, the rate of reaction of $(\text{CH}_3)_2\text{CHCr}(\text{H}_2\text{O})_5^{2+}$ with O_2 was found to involve a three-halves-order dependence on the concentration of the organochromium(III) ion and a zero-order dependence on the concentration of molecular oxygen. While a number of reasonable reaction mechanisms could be invoked to explain the observed kinetics, only two schemes, both free-radical chain mechanisms, are particularly attractive. Schemes A and B, differing only in the identity of the free-radical which serves as the chain-carrier, are presented below.

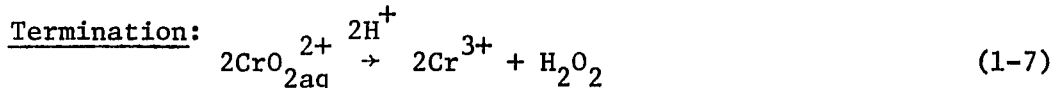
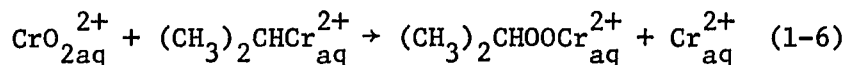
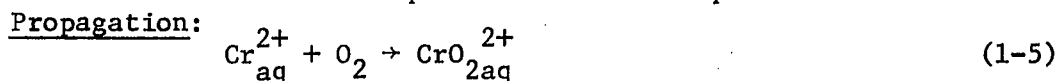
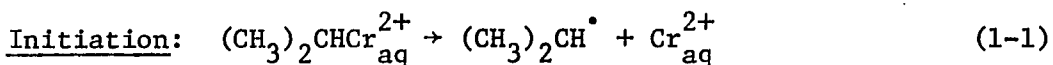
Scheme A:



Termination:



Scheme B:



As either scheme explains the observed reaction kinetics, further experimentation centered on distinguishing between the two schemes by studying the effect of specific radical scavengers.

Scheme A bears a close resemblance to the autoxidation of hydrocarbons. The oxygenation of organometallic compounds (37-40) often involves free-radical intermediates, in mechanisms similar to the degradation of hydrocarbons by molecular oxygen. A concise review of these types of reactions is presented below, with particular attention directed to the role of metal ions or their complexes in autoxidations.

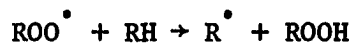
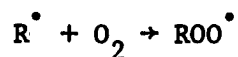
Review of Autoxidations

The oxidation of organic compounds by molecular oxygen is of considerable commercial importance (41). Metal ions often function as homogeneous catalysts for these oxidations, accounting for the intense interest in the ability of soluble metal complexes to activate molecular oxygen (42). Many of the oxidations occur under relatively mild conditions, almost spontaneously, and are known as autoxidations (43). These processes can occur in the absence of metal ions, but their presence increases the overall rate of oxidation (44).

The autoxidations of most organic substrates (including alkanes, alkenes, alcohols, aldehydes, and ethers) proceed by free-radical chain mechanisms in which organic hydroperoxides are generally formed (43).



Uncatalyzed reactions proceed by the following mechanism:

Initiation:Propagation:Termination:

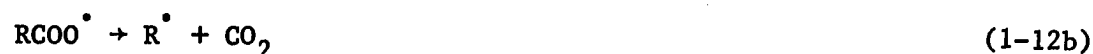
Initiation is often accomplished by addition of thermally unstable azonitriles or peroxides (44). Metal ions also are efficient initiators. Direct interaction of the metal catalyst with the substrate can produce radicals via three possible mechanisms (45). In Reaction 1-9, electron transfer from RH to the metal complex results in a one electron reduction of the catalyst accompanied by radical production.



Electrophilic substitution, Reactions 1-10, or homolytic attack, Reactions 1-11, results in the same products, reduced metal complex and R^\bullet .

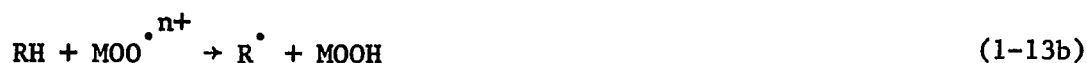


Internal electron transfer (46) from a catalyst ligand to the metal is a particularly important pathway of initiation for carboxylato complexes.



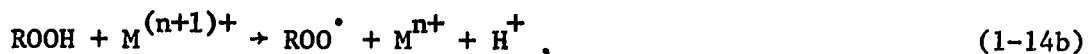
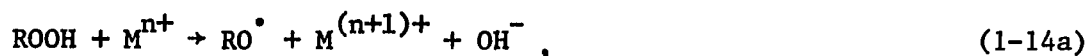
The efficiency of processes involving electron transfer and electrophilic substitution is expected to be dependent upon the oxidizability of the organic substrate, and the oxidation potential of M^{n+} . Likewise, hydrogen transfer from substrate to metal is related to the oxidizing ability of M^{n+} and stability of the radical.

Direct oxygen activation by the metal catalyst may also be responsible for chain initiation. "End-on" coordination of molecular oxygen would form a peroxometal species, which might be expected, like alkylperoxy radicals, to undergo hydrogen transfer from the substrate.

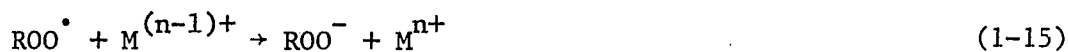


While such initiations have often been proposed (44,46), and may in fact be operative, efforts to obtain direct evidence have been hampered. The difficulty arises from interference by the much more facile reactions of the metal catalyst with hydroperoxide generated in the autoxidation. These reactions tend to mask any direct activation of O_2 which may be occurring simultaneously.

In reality, decomposition of hydroperoxides is by far the most important catalytic pathway for radical generation. The catalyst is recycled between Reactions 1-14,



producing alkoxy and alkylperoxy radicals. In the early stages of an autoxidation, when only trace amounts of ROOH are present, Reactions 1-14 constitute an initiation step, but as the autoxidation proceeds, and the concentration of alkylhydroperoxide increases, the scheme becomes an important source of the chain-carrying RO^\bullet and ROO^\bullet radicals. The Co(II)/Co(III) and Mn(II)/Mn(III) redox systems have been widely exploited for the catalytic decomposition of hydroperoxides (44). Catalysts at high concentrations, however, can act as inhibitors by effectively competing with the substrate RH for alkylperoxy radicals (40,44,47,48).

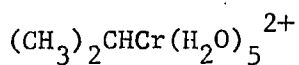


Organometallic complexes are commonly degraded by molecular oxygen, but with a few exceptions the mechanisms of decomposition have been little studied. Alkyls of Groups IA, IIA, IIIA, and IVA metals all give alkylperoxometallic compounds when treated with oxygen (37-40). Kinetic studies, particularly with the organoboranes (49-59), have shown alkylperoxy radicals are intimately involved. The reaction schemes proposed (49-59) bear a close resemblance to those demonstrated for the autoxidation of organic compounds. Alkylperoxo complexes of the transition metals are much less common, although unstable organometallic peroxides of titanium, zirconium, molybdenum, and tungsten have been reported (60). Quite stable solids of alkylperoxocobaloximes (60-67) can be prepared by oxygenation of a solution of the alkylcobaloxime. Peroxo compounds of the early transition metals were believed (60) to be

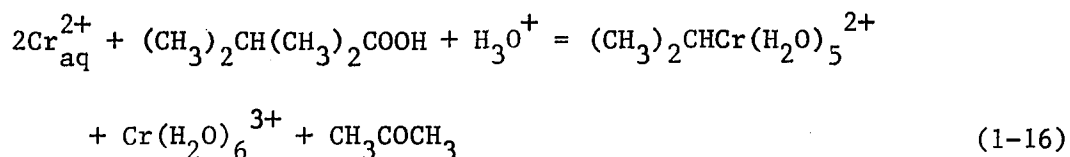
formed by a mechanism similar to the autoxidation of alkylboranes; however, a free-radical mechanism was discounted for the oxygenation of alkylperoxocobaloximes (68), but the evidence for the latter process remains indecisive. Because autoxidations of alkyl metals are relevant to the understanding of metal catalyzed autoxidations of organic compounds, further mechanistic studies are warranted. Therefore, the reaction of isopropylchromium(III) with molecular oxygen can be seen to be of broader relevance than simply the study of carbon-chromium bonds.

EXPERIMENTAL

Materials



The isopropylpentaquo chromium(III) ion was prepared in aqueous perchloric acid by modification of the reported procedure (20). The synthesis involves the two equivalent reduction of 2,3-dimethyl-2-butyl hydroperoxide by chromium(II) perchlorate, Reaction 1-16.



In practice, an excess of alkyl hydroperoxide was used to insure complete reaction of $\text{Cr}_{\text{aq}}^{2+}$, which interfered during ion-exchange chromatography of the products. Excess peroxide was removed before elution by washing with a 20% v/v acetone/water solution (0.001 M HClO_4). In a typical synthesis, 5 mL of 0.2 M $\text{Cr}(\text{ClO}_4)_2$ in 0.1 M HClO_4 , was mixed, under nitrogen, with 0.2 mL of the hydroperoxide (typically ~5 M). Reaction was complete within minutes, and the dark green solution was transferred to a carefully deoxygenated column of Sephadex C-25 cation-exchange resin, in the Na^+ or H^+ form. The column was chilled by circulation of ice water through an external jacket. Elution of the products with cold, deoxygenated 0.2-0.5 M NaClO_4 (in 0.01 M H^+) or HClO_4 caused separation into four bands--the first was the yellow-to-brown isopropylchromium(III) ion, followed by blue-grey $\text{Cr}(\text{H}_2\text{O})_6^{3+}$, and lastly, two dimeric forms of

Cr(III), one blue-green in color, the other dark green. The organochromium(III) ion was collected under nitrogen, at 0°C, and stored in the freezer to slow decomposition. About 15 mL of 0.015 M $(\text{CH}_3)_2\text{CHCr}(\text{H}_2\text{O})_5^{2+}$ was obtained, a 25% yield.

2,3-Dimethyl-2-butyl hydroperoxide

This peroxide was synthesized by the method of Hedaya and Winstein (69), except no vacuum distillation was used. Analysis for hydroperoxide was accomplished by refluxing a sample with excess NaI in 2-propanol, followed by a thiosulfate titration of the liberated iodine (20). Hydroperoxide concentrations of 4.5–5.7 M were obtained; theoretical is about 7.5 M.

Miscellaneous inorganic reagents

$\text{Cr}(\text{ClO}_4)_2$ Aqueous solutions were prepared from chromium(III) perchlorate in dilute acid, by reduction over amalgamated zinc under a nitrogen atmosphere, or from the metal as described in Part III, Experimental.

$\text{Fe}(\text{ClO}_4)_3$ and $\text{Fe}(\text{ClO}_4)_2$ Aqueous solutions of iron(III) perchlorate in HClO_4 were made and analyzed by published procedures (70). Solutions of iron(II) perchlorate were prepared by reduction of iron(III) perchlorate over zinc amalgam, under nitrogen.

$\text{Cu}(\text{ClO}_4)_2$ Aqueous solutions were prepared by dissolving the solid (G. F. Smith) in dilute HClO_4 . Standardization was accomplished iodometrically.

Co(NH₃)₅Br(ClO₄)₂ and Co(NH₃)₅Cl(ClO₄)₂ The perchlorate salts were obtained from the corresponding bromide and chloride by dissolution in room temperature water, with stirring, adding a large excess of concentrated perchloric acid, and cooling in ice.

CrO₂²⁺_{aq} Although perchlorate solutions of CrO₂²⁺_{aq} have been prepared by nonradiolytic techniques before (71), experimental details were not given. The following procedure proved successful.

About 25 mL of a dilute solution of Cr_{aq}²⁺ (2 × 10⁻⁴ M) in 0.1 M H₃O⁺ was transferred into 75 mL of O₂ saturated water, using a 16-gauge double-tipped needle. The solution was mixed well during addition of the Cr_{aq}²⁺ by bubbling a vigorous stream of O₂ through. The exit tip of the transfer needle must be kept below the surface of the water during transfer. Concentrations of (1 - 2) × 10⁻⁵ M were obtained, as calculated from its published (71) UV spectrum.

H₂O₂ Reagent grade, 30% H₂O₂ (Fisher), was used as purchased, its molarity determined by reaction with excess iodide ion followed by thiosulfate titration of the liberated iodine.

Reagents for Winkler titration

Alkaline iodide reagent was prepared by dissolving 20 g NaOH in 25 mL boiled H₂O. Then 45 g NaI were added, dissolved, and the volume made up to 100 mL with boiled H₂O.

MnSO₄ reagent was made by dissolving 18.2 g MnSO₄ in a few mL H₂O, filtering, and diluting to 50 mL.

H₂SO₄ (diluted)--40 mL concentrated H₂SO₄ were mixed with 60 mL H₂O.

Gases

Nitrogen (Air Products) was purified of traces of O_2 by passage through two Cr_{aq}^{2+} scrubbing towers, then aqueous sodium hydroxide, and lastly distilled water. Molecular oxygen (99.6%) was obtained from a lecture bottle (Matheson Gas Products), 52.5% O_2 (balance of N_2) from a Calibration Standard Grade cylinder (Union Carbide Corporation), and 21% O_2 from the compressed air jet in the laboratory, passing the gas stream through glass wool or an air purifier (Koby Inc.) to remove oil.

 $HClO_4$, NaOH, $LiClO_4$

Aqueous solutions of perchloric acid were made by dilution of 70% $HClO_4$ and titrated with standardized NaOH to a phenolphthalein end point. Aqueous NaOH solutions were prepared and standardized by published procedures (72). $LiClO_4$ was prepared by addition of concentrated perchloric acid to an aqueous slurry of the carbonate, until no more CO_2 was evolved. The volume was reduced until crystals of $LiClO_4$ formed, which were collected and recrystallized from water until no longer acidic. An aqueous solution was analyzed for the molarity of Li^+ by addition of an aliquot to a Dowex cation-exchange column in the H^+ form, and titrating the displaced acid with NaOH.

Methods

Analyses and characterizations

$(\text{CH}_3)_2\text{CHCr}(\text{H}_2\text{O})_5^{2+}$ The isopropylpentaquo chromium(III) ion was identified (20) by its UV-visible spectrum, shown in Figure 1-1.

Chromium concentration was determined by conversion of an aliquot to CrO_4^{2-} by hydrogen peroxide oxidation in basic solution, and measuring the absorbance at 372 nm where $\epsilon_{\text{CrO}_4^{2-}} = 4830 \text{ M}^{-1} \text{ cm}^{-1}$. Molar absorptivities for $(\text{CH}_3)_2\text{CHCr}(\text{H}_2\text{O})_5^{2+}$ were then calculated for wavelengths of maximum absorbance to be $(\epsilon/\text{M}^{-1} \text{ cm}^{-1}, (\lambda/\text{nm}))$: 2330, (290); 488, (400); and 10, (560) compared to previous values (20) of 1880, (290); 366, (399); and 10, (556). The disagreement probably arises from the presence of $\text{Cr}(\text{H}_2\text{O})_6^{3+}$ in the latter solutions of $(\text{CH}_3)_2\text{CHCr}(\text{H}_2\text{O})_5^{2+}$.

Organic products Acetone was identified and quantified by gas chromatography. Aliquots of the aqueous product solutions were injected directly onto either a Tenax or 10% FFAP column at 100 or 150°C with N_2 as the carrier gas, using a 5700 A Hewlett-Packard instrument. Positive identification was established on both columns by comparison of the elution time to reagent grade acetone. Aqueous solutions of reagent grade acetone were used to construct a standard curve of peak height versus concentration, from which the unknown acetone concentrations were determined. On the 10% FFAP column, 2-propanol could also be detected. Identification and quantification made use of aqueous standard solutions of reagent grade 2-propanol. These analyses were obtained with the assistance of Mr. J. J. Richard, Ames Laboratory.

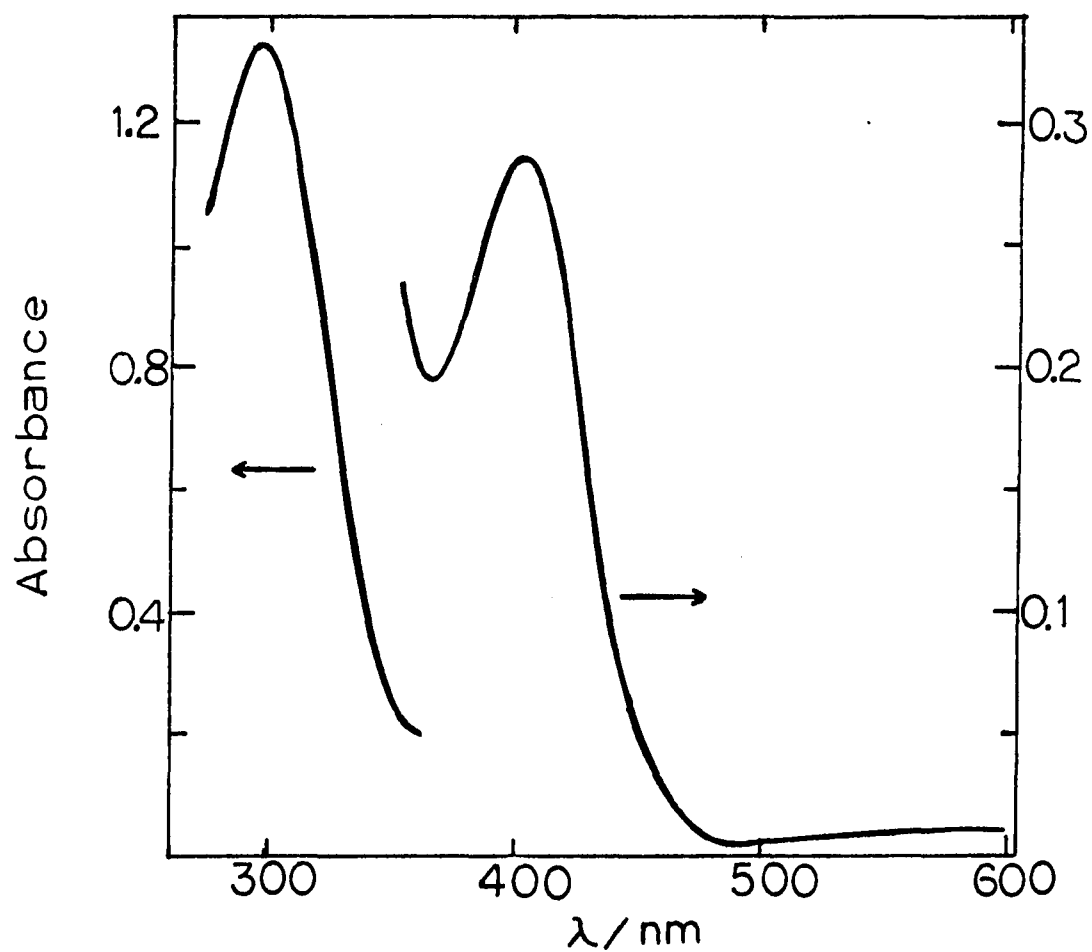


Figure 1-1. The electronic spectrum of the $(\text{CH}_3)_2\text{CHCr}(\text{H}_2\text{O})_5^{2+}$ ion. Concentration = $5.8 \times 10^{-4}\text{M}$; cell length = 1 cm.

Propane was identified by its mass spectrum. A solution of ~ 0.01 M $(\text{CH}_3)_2\text{CHCr}(\text{H}_2\text{O})_5^{2+}$ was decomposed in 0.1 M HClO_4 under a nitrogen atmosphere, by warming in a water bath at 80°C . After the solution had turned from yellow to blue, it was attached to a nitrogen line with the exit stream leading through a glass U-tube immersed in a liquid nitrogen bath. Volatiles from the solution were frozen out in the tube, which was closed off by stopcocks and attached to the mass spectrometer. The nitrogen bath was removed and the trapped products allowed to vaporize into the instrument. The spectrum obtained was compared with authentic propane. Mass spectral analyses were performed with the assistance of Mr. G. D. Flesch, Ames Laboratory.

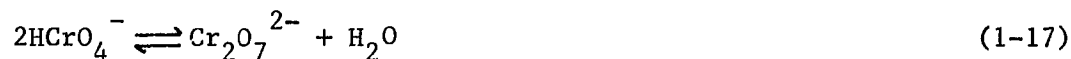
Analysis for alkyl hydroperoxide in the product solution made use of a spectrophotometric method developed by Banerjee and Budke (73). An aliquot of the products, about 0.5 mL, was diluted to the mark in a 10 mL volumetric flask with a 2 to 1 mixture of acetic acid, chloroform in 4% water, and 5.0 mL transferred to a 2.0 cm cylindrical spectrophotometric cell. The dissolved oxygen was removed from the cell by purging with nitrogen for 3 min. 0.2 mL of fresh aqueous 50% KI, also deoxygenated, was added to the cell, and the nitrogen purge continued for an additional 3 min. The cell was capped quickly and placed in the dark for one hour after which the absorbance of the triiodide species was read at 410 nm.

The analysis was calibrated using a standard iodine solution containing 63.7 μg of iodine per mL, which is equivalent to 4.0 μg of active

oxygen¹ per mL. The solution was prepared by dissolving reagent grade iodine in 2 to 1 acetic acid, chloroform, and diluting 0, 2, 4, 7, and 10 mL aliquots to 25.0 mL with a 2 to 1 acetic acid, chloroform solvent containing 4% water. Each standard was analyzed as described above, representing a range in active oxygen concentration of 8-40 µg per 25 mL. A molar absorptivity of 5970 ($\sigma = 400$) $M^{-1}cm^{-1}$ at 410 nm was calculated, in reasonable agreement with the reported (73) value of 5700 $M^{-1}cm^{-1}$.

Prior to the analysis of the products, the chromate ion formed must be removed for it will interfere in the determination. A strongly basic, anion-exchange resin, Dowex 2-X8, was used for this purpose; the product solution was stirred with an excess of the dry resin, centrifuged, and the remaining liquid analyzed. The absorbance at 410 nm was corrected for the remaining cationic chromium(III) products.

Inorganic products The amount of chromate ion formed was determined by its UV-visible spectrum after dilution to a concentration of about 0.1 mM, at acidities of 0.4 to 40 mM $HClO_4$. Under these circumstances, $HCrO_4^-$ ion is the primary species (74), the amount of $Cr_2O_7^{2-}$ ion arising from Reaction 1-17 can be considered negligible, as well as H_2CrO_4 , $HCr_2O_7^-$, and CrO_4^{2-} , which are unimportant at these acidities.

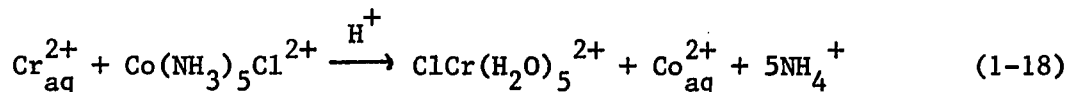


¹Active oxygen is defined as oxygen having a valence of 2 or an equivalent weight of 8. In a hydroperoxide only one of the oxygens is considered "active."

After correction for the absorbance due to the chromium(III) products, the concentration of HCrO_4^- was determined from the absorbance at 350 nm, using $\epsilon = 1528 \text{ M}^{-1} \text{ cm}^{-1}$.

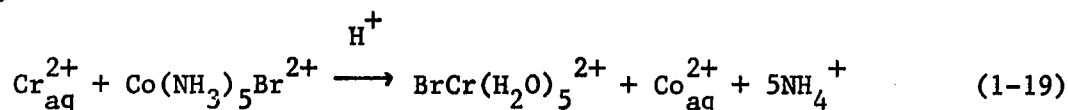
Chromium(III) products were identified by their visible spectra, after separation by ion-exchange chromatography on Sephadex C-25 resin. Each band was analyzed for total chromium after conversion to CrO_4^{2-} , as described above, under " $(\text{CH}_3)_2\text{CHCr}(\text{H}_2\text{O})_5^{2+}$."

Products of homolysis Chromium(II) ion, formed by homolysis, was detected as $\text{ClCr}(\text{H}_2\text{O})_5^{2+}$, after reaction with $\text{Co}(\text{NH}_3)_5\text{Cl}(\text{ClO}_4)_2$, Reaction 1-18.



With the careful exclusion of O_2 , 0.029 mmol Co^{III} and 0.022 mmol $(\text{CH}_3)_2\text{CHCr}(\text{H}_2\text{O})_5^{2+}$ in 0.13 M HClO_4 were placed in the dark at 25°C for 13 hours. The product solution was then eluted in the air on Dowex X8-100 cation-exchange resin in the acid form. Elution with perchloric acid allowed a very dilute, pale green band to be displaced; its visible spectrum was recorded with a very sensitive absorbance range using a Cary 219 spectrophotometer.

Cobalt(II) ion, produced by Reaction 1-19, was also quantitatively analyzed.



Two separate experiments were done. In the first, 0.0595 mmol $\text{Co}(\text{NH}_3)_5\text{Br}^{2+}$ and 0.0272 mmol $(\text{CH}_3)_2\text{CHCr}(\text{H}_2\text{O})_5^{2+}$, in 0.148 M HClO_4 were

allowed to react 22 hours, and in the second experiment, 0.0635 mmol Co^{III} and 0.0232 mmol isopropylchromium(III), in 0.128 M HClO_4 , for 16 hours. An aliquot of the products was analyzed for $\text{Co}_{\text{aq}}^{2+}$ as described in the Experimental section of Part II.

Dissolved oxygen At the completion of a kinetic run an aliquot of the products was removed for analysis of dissolved oxygen. The aliquot was added to a concentration of chromium(II) perchlorate in excess of the amount required for the 4:1 stoichiometric reaction of $\text{Cr}_{\text{aq}}^{2+}$ and O_2 (75). After formation of the green dimeric chromium(III) oxidation product, $[\text{Cr}(\text{OH})(\text{H}_2\text{O})_4]_2^{4+}$, the remaining $\text{Cr}_{\text{aq}}^{2+}$ was analyzed by reaction with a deoxygenated solution of $\text{Co}(\text{NH}_3)_5\text{Cl}^{2+}$. The cobalt(II) ion formed via Reaction 1-18 is equivalent to the amount of excess $\text{Cr}_{\text{aq}}^{2+}$, and was determined by conversion to $\text{Co}(\text{SCN})_4^{2-}$, as described in the Experimental section of Part II.

When 99.6% O_2 was used to saturate the solutions at $[\text{H}_3\text{O}^+] = 0.1 \text{ M}$ and an ionic strength of 1.0 M, maintained by addition of LiClO_4 , the concentration of dissolved oxygen was determined to be $(1.05 \pm 0.11) \times 10^{-3} \text{ M}$ at 25°C , an average of 26 determinations. The concentration of O_2 in runs saturated with 52.5% or 20.95% molecular oxygen was calculated, from the value obtained with 99.6%, by use of Henry's law, Equation 1-20, where k is a proportionality constant.

$$[\text{O}_2] = k \cdot p_{\text{O}_2} \quad (1-20)$$

The partial pressure of O_2 was corrected for water vapor at 25°C , using $p_{\text{H}_2\text{O}} = 0.031$, resulting in values of $[\text{O}_2] = (5.4 \pm 0.6) \times 10^{-4} \text{ M}$ for

52.5% O₂ and $(1.9 \pm 0.2) \times 10^{-4}$ M for 20.95% O₂. These calculations were made for 1 atm barometric pressure.

Kinetics obtained with spectrophotometry

Reaction of $(\text{CH}_3)_2\text{CHCr}(\text{H}_2\text{O})_5^{2+}$ with O₂ The majority of the kinetic data was obtained by following the decrease in the absorbance of the organochromium(III) ion with time, at wavelengths in the region 290-400 nm. The spectroscopic work employed a Cary 14 or Cary 219 spectrophotometer in which constant temperature was maintained by placing the spectrophotometric cell in an externally jacketed water bath inside the cell compartment. Path lengths of 2 or 5 cm were used as required by the molar absorptivity of $(\text{CH}_3)_2\text{CHCr}(\text{H}_2\text{O})_5^{2+}$ at the monitoring wavelength, and by the initial concentration of the complex.

A constant concentration of dissolved oxygen was maintained in the kinetic runs by leading a water-saturated stream of the gas into the spectroscopic cell, through a single-hole rubber stopper, in a narrow Teflon needle. By curling the needle towards the cell wall, away from the light path, the O₂ purge caused no interference with absorbance measurements.

Ionic strength was maintained at a constant concentration, generally 1.0 M, by the addition of LiClO₄. However, the reaction rate was also studied as a function of ionic strength; at very low μ , no LiClO₄ was added and the ionic strength was determined by the concentration of $(\text{CH}_3)_2\text{CHCr}(\text{H}_2\text{O})_5^{2+}$ and the small amount of acid introduced along with the organochromium(III) ion. This acid concentration was determined

at the end of each run, by titration with standardized 5 mM NaHCO_3 to a bromphenol blue end-point. Since some acid is consumed in the auto-oxidation, in runs at very low acid the concentration varied during the run. The initial concentration, $[\text{H}_3\text{O}^+]_0$, was calculated from Equation 1-21 which is based on the stoichiometry of the reaction, determined in 0.10 M H_3O^+ , and shown to be approximately acid-independent.

$$[\text{H}_3\text{O}^+]_0 = [\text{H}_3\text{O}^+]_\infty + \frac{2}{5} [\text{RCr}^{2+}]_0 \quad (1-21)$$

In Equation 1-21, $[\text{H}_3\text{O}^+]_\infty$ is the concentration determined by titration. The initial ionic strength was calculated from Equation 1-22,

$$\mu_0 = \frac{1}{2} \{6[\text{RCr}^{2+}]_0 + 2[\text{H}_3\text{O}^+]_0 + 12[\text{Cr}^{3+}]_0\}, \quad (1-22)$$

where $[\text{Cr}^{3+}]_0$ is the amount of $\text{Cr}(\text{H}_2\text{O})_6^{3+}$ introduced along with $(\text{CH}_3)_2\text{CHCr}(\text{H}_2\text{O})_5^{2+}$, arising from acidolysis. The ionic strength at the conclusion of the kinetic run, μ_∞ , was calculated from the stoichiometry also (determined at 0.10 M H_3O^+); using the inorganic product yields of 70% $\text{Cr}(\text{H}_2\text{O})_6^{3+}$, 10% $[\text{Cr}(\text{OH})(\text{H}_2\text{O})_4]_2^{4+}$, and 10% HCrO_4^- , Equation 1-23 results,

$$\begin{aligned} \mu_\infty = \frac{1}{2} \{ & [\text{RCr}^{2+}]_0 (3^2 \cdot (0.7) + 4^2 \cdot (0.1) + (-1)^2 (3) (0.7) + \\ & + (-1)^2 (4) (0.1)) + 12[\text{Cr}^{3+}]_0 + 2[\text{H}_3\text{O}^+]_\infty \}, \end{aligned} \quad (1-23)$$

where the squared terms in the summation correspond to $\text{Cr}(\text{H}_2\text{O})_6^{3+}$ (formed upon reaction), $[\text{Cr}(\text{OH})(\text{H}_2\text{O})_4]_2^{4+}$, ClO_4^- , and $(\text{ClO}_4^-$ and $\text{HCrO}_4^-)$, respectively. The difference between μ_0 and μ_∞ is significant only at ionic strengths less than 0.1 M. For kinetic runs at ionic strengths

greater than that determined by the chromium species and perchloric acid, LiClO_4 was added.

In a typical experiment, the aqueous medium, containing the required concentrations of HClO_4 and LiClO_4 , was brought to temperature in the spectrophotometer cell, while saturating with the desired partial pressure of O_2 . The reaction was initiated by injection of a small amount of $(\text{CH}_3)_2\text{CHCr}(\text{H}_2\text{O})_5^{2+}$ with a hypodermic syringe, and a recording of absorbance versus time begun and continued until a final, stable value was attained.

The absorbance data were treated according to a three-halves-order dependence on the $(\text{CH}_3)_2\text{CHCr}(\text{H}_2\text{O})_5^{2+}$ ion concentration.

The proper relationship for evaluating the data can be obtained by integration of a three-halves-order rate law, Equation 1-24,

$$\frac{-d[\text{RCr}^{2+}]}{dt} = k_{\text{obs}} [\text{RCr}^{2+}]^{3/2}, \quad (1-24)$$

to give

$$[\text{RCr}^{2+}]_t^{-1/2} - [\text{RCr}^{2+}]_o^{-1/2} = \frac{1}{2} k_{\text{obs}} t. \quad (1-25)$$

After expressing $[\text{RCr}^{2+}]_t$ as a function of absorbance, D ,

$$[\text{RCr}^{2+}]_t = \frac{(D_t - D_\infty)}{(D_o - D_\infty)} [\text{RCr}^{2+}]_o, \quad (1-26)$$

and substituting into Equation 1-25, the required equation is obtained,

$$(D_t - D_\infty)^{1/2} = -\frac{1}{2} k_{\text{obs}} (D_t - D_\infty)^{1/2} [\text{RCr}^{2+}]_o^{1/2} t + (D_o - D_\infty)^{1/2}. \quad (1-27)$$

As suggested by Equation 1-27, a plot of $(D_t - D_\infty)^{1/2}$ versus $(D_t - D_\infty)^{1/2} t$ should be linear with a slope given by,

$$\text{slope} = -\frac{1}{2} k_{\text{obs}} [\text{RCr}^{2+}]_o^{1/2}, \quad (1-28)$$

and an intercept equal to $(D_o - D_\infty)^{1/2}$. Knowledge of $[\text{RCr}^{2+}]_o$ allows k_{obs} to be calculated from Equation 1-28.

At very low initial concentrations of $(\text{CH}_3)_2\text{CHCr}(\text{H}_2\text{O})_5^{2+}$, the data must be treated according to a mixed first- and three-halves-order dependence on $[\text{RCr}^{2+}]$ because of the acidolysis and homolysis reactions (with rate constants k_a and k_h), whose rates are no longer negligible. Integration of the revised rate law, Equation 1-29,

$$\frac{-d[\text{RCr}^{2+}]}{dt} = (k_a + k_h)[\text{RCr}^{2+}] + k_{\text{obs}}[\text{RCr}^{2+}]^{3/2}, \quad (1-29)$$

results in a more complex expression for graphical analysis of the data, Equation 1-30,

$$e^\alpha = (\text{intercept}) + (\text{slope})(D_t - D_\infty)^{1/2}, \quad (1-30)$$

where

$$\alpha = \frac{(k_h + k_a)t}{2} + \ln \left(\frac{D_t - D_\infty}{D_o - D_\infty} \right)^{1/2},$$

$$\text{intercept} = \frac{(k_h + k_a)}{(k_h + k_a) + k_{\text{obs}}[\text{RCr}^{2+}]_o^{1/2}},$$

and

$$\text{slope} = \frac{k_{\text{obs}}[\text{RCr}^{2+}]_o^{1/2}}{[(k_h + k_a) + k_{\text{obs}}[\text{RCr}^{2+}]_o^{1/2}](D_o - D_\infty)^{1/2}}.$$

The three-halves-order rate constant k_{obs} can be obtained from the slope of a plot of e^{α} versus $(D_t - D_{\infty})^{1/2}$ by using Equation 1-31,

$$k_{\text{obs}} = \frac{(\text{slope})(D_o - D_{\infty})^{1/2}(k_h + k_a)}{[\text{RCr}^{2+}]_o^{1/2}[1 - (\text{slope})(D_o - D_{\infty})^{1/2}]} \quad (1-31)$$

However, the function α is dominated by the term $\ln[(D_t - D_{\infty})/(D_o - D_{\infty})]^{1/2}$, so that e^{α} is approximately $[(D_t - D_{\infty})/(D_o - D_{\infty})]^{1/2}$, and the plot of e^{α} versus $(D_t - D_{\infty})^{1/2}$ amounts to essentially plotting $(D_t - D_{\infty})^{1/2}$ against itself. Because of this loss of sensitivity to the data, the graphical treatment is almost meaningless. A better approach is to fit the absorbance at time t , D_t , according to two parallel reactions with first- and three-halves-order dependence on $[\text{RCr}^{2+}]$, and finding the best value for k_{obs} by using a nonlinear-least squares computer program.¹ The data were fit to Equation 1-32,

$$D_t = (D_o - D_{\infty}) \left\{ \frac{(k_{\text{obs}})[\text{RCr}^{2+}]_o^{1/2}}{(k_h + k_a)} \exp \left[\frac{(k_h + k_a)t}{2} - 1 \right] + \exp \frac{(k_h + k_a)t}{2} \right\}^2 + D_{\infty} \quad (1-32)$$

fixing $(k_h + k_a) = 2.85 \times 10^{-4} \text{ s}^{-1}$ (see Results), and D_o , D_{∞} , and $[\text{RCr}^{2+}]_o$ at their known values.

Homolysis and acidolysis The rates of these reactions under nitrogen, were followed spectrophotometrically by programming the Turret

¹The program used was one implemented by Dr. R. B. Pfaff, Ames Laboratory.

assembly of the Cary 219 spectrophotometer. The most reliable data were obtained by using Beckman 1 cm spectrophotometric cells which can be tightly sealed with Aldrich Z10,075-7 rubber septa. The cells, containing all reagents except the organochromium(III) ion, were thoroughly deoxygenated for 20 minutes prior to initiation of the reaction, by injection of $(\text{CH}_3)_2\text{CHCr}(\text{H}_2\text{O})_5^{2+}$. During this time, the cells were also thermostatted.

Kinetics obtained with oxygen-sensing electrode

A few kinetic experiments were conducted using an oxygen-sensing electrode¹ (Hach Portable Dissolved Oxygen Meter Model 16046). The reactants were only saturated with oxygen initially, and the depletion of the dissolved oxygen monitored with time by use of an x-y recorder (Hewlett-Packard Model 7001 A). To prevent equilibration with the air, the reactants had to be sealed from the atmosphere during the reaction. The bottom of a small polyethylene bottle was removed so that when inverted and slipped over the outside of the electrode housing, a reasonably air-tight seal was achieved. With the entire electrode assembly inverted, the oxygen saturated LiClO_4 , HClO_4 reaction medium was transferred to the bottle, filled completely and capped. A magnetic stirring bar was included to eliminate a concentration gradient in the vicinity of the electrode. The assembly was reinverted, magnetic stirring begun, and $(\text{CH}_3)_2\text{CHCr}(\text{H}_2\text{O})_5^{2+}$ injected with a hypodermic syringe

¹ Graciously loaned by Dr. D. C. Johnson, Iowa State University.

through a septum in a small hole in the side of the bottle. Response time of the electrode was 15-30 sec, which severely limited the reaction rates which could be measured, and the temperature could not be controlled during reaction.

The kinetic analysis of the data differed in these experiments, where the concentration of O_2 varied during the run, along with that of organochromium(III). Since $[O_2]_o$ was in slight excess over $[RCr^{2+}]_o$ and assuming that the stoichiometry of the reaction is 1:1 $(CH_3)_2CHCr(H_2O)_5^{2+}$ to O_2 , the oxygen concentration at any time is given by Equation 1-33,

$$[O_2]_t = [O_2]_o - [RCr^{2+}]_o + [RCr^{2+}]_t \quad (1-33)$$

The rate of loss of O_2 equals that of the organochromium(III) ion,

$$\frac{-d[O_2]}{dt} = \frac{-d[RCr^{2+}]}{dt} = k_{obs} ([O_2]_t - \Delta_o)^{3/2}, \quad (1-34)$$

where $\Delta_o = [O_2]_o - [RCr^{2+}]_o$. Upon integration and rearrangement of Equation 1-34, a graphically useful form is obtained,

$$([O_2]_o - \Delta_o)^{-1/2} ([O_2] - \Delta_o)^{1/2} = -\frac{1}{2} k_{obs} ([O_2] - \Delta_o)^{1/2} t + 1, \quad (1-35)$$

which suggests a plot of the quantity on the left-hand side of Equation 1-35 versus $([O_2] - \Delta_o)^{1/2} t$ should be linear with a slope of $-\frac{1}{2} k_{obs}$.

The oxygen-sensing electrode was calibrated by determination of the O_2 concentration using a modified Winkler method (76). A sample (40 mL) of air-saturated or 52.5% oxygen-saturated water was transferred to a 40 mL glass bottle and stoppered. 0.25 mL $MnSO_4$ reagent and 0.50 mL alkaline iodide reagent were added to the bottle quickly, the

stopper replaced, and the solution mixed by inverting. When the precipitate had almost settled, the bottle was reshaken and the precipitate allowed to settle completely. Then 0.60 mL of the diluted sulphuric acid was added, the stopper replaced, and the solution again mixed by inversion. After 10 min an aliquot of the sample was titrated with 0.003 M $\text{Na}_2\text{S}_2\text{O}_3$, which had been standardized using KIO_3 . Readings were made on the oxygen-sensing electrode at the same time; the agreement was quite acceptable. By the Winkler method, air saturation at 24.5°C gave a concentration of dissolved O_2 of 8.61 mg/L, while the electrode gave an average value of 8.63 ($\sigma = 0.21$) mg/L. At 52.5% O_2 saturation and $T = 24.2 \pm 0.2^\circ\text{C}$, the Winkler value was somewhat lower, 16.8 mg/L compared to the electrode response of 17.3 ($\sigma = 0.3$) mg/L.

RESULTS

Kinetics of Reaction of $(\text{CH}_3)_2\text{CHCr}(\text{H}_2\text{O})_5^{2+}$ with O_2

At isopropylchromium(III) concentrations greater than about 0.1 mM, and for a dissolved oxygen concentration of 1.05 mM, the kinetic data were well fit by a three-halves-order dependence on the concentration of the chromium complex, resulting in a rate law of the form,

$$\frac{-d[\text{RCr}^{2+}]}{dt} = k_{\text{obs}} [\text{RCr}^{2+}]^{3/2} . \quad (1-24)$$

This rather unusual fractional dependence is convincingly demonstrated in Figure 1-2, in which the log of the instantaneous loss of $(\text{CH}_3)_2\text{CHCr}(\text{H}_2\text{O})_5^{2+}$ is plotted against the log of the concentration of organochromium(III) at various times of reaction. The relationship plotted is obtained from the rate law by taking the logarithm of both sides of Equation 1-24, and allowing the differentials to be approximated by the finite difference Δ ,

$$\log \frac{\Delta[\text{RCr}^{2+}]}{\Delta t} = \frac{3}{2} \log k_{\text{obs}} + \frac{3}{2} \log [\text{RCr}^{2+}] . \quad (1-36)$$

Substitution of the expression,

$$[\text{RCr}^{2+}] = \left(\frac{D_t^* - D_\infty^*}{D_o^* - D_\infty^*} \right) [\text{RCr}^{2+}]_o , \quad (1-37)$$

where $D^* = D/l$, into Equation 1-36 results in,

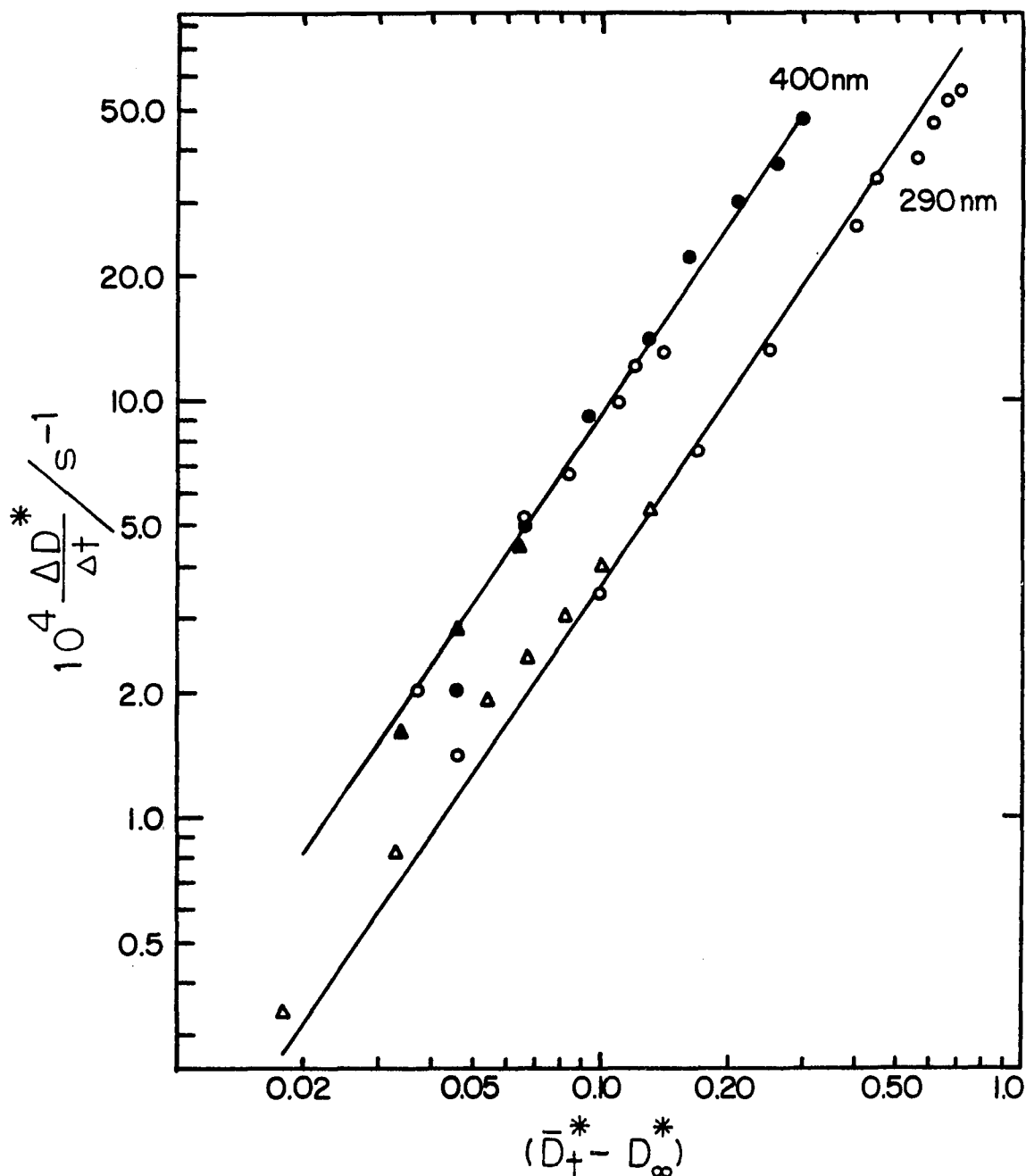


Figure 1-2. Log-log plot of the instantaneous reaction rate versus the average concentration of the $(\text{CH}_3)_2\text{CHCr}(\text{H}_2\text{O})_5^{2+}$ ion for the reaction of $(\text{CH}_3)_2\text{CHCr}(\text{H}_2\text{O})_5^{2+}$ with O_2 . Rates and concentrations are expressed in absorbance units per 1 cm cell length. The plots include data from four kinetic experiments at two wavelengths. $[\text{O}_2] = 1.05 \text{ mM}$; $[\text{RCr}^{2+}]_0/\text{mM} = 0.098$ (open triangles), 2.20 (solid triangles), 0.50 (open circles), 1.0 (solid circles). Lines are drawn to have a slope of $3/2$

$$\log \frac{\Delta D_t^*}{\Delta t} = \frac{3}{2} \log (\bar{D}_t^* - D_\infty^*) + \frac{3}{2} \log k_{\text{obs}} + \frac{1}{2} \log \frac{[\text{RCr}^{2+}]_0}{(D_0^* - D_\infty^*)} \quad (1-38)$$

\bar{D}_t^* was evaluated as the average absorbance during the time interval Δt . The lines in Figure 1-2 have been drawn to a slope of exactly 3/2, as predicted by Equation 1-38 if the concentration dependence of $(\text{CH}_3)_2\text{CHCr}(\text{H}_2\text{O})_5^{2+}$ is three-halves-order. Data from two wavelengths, 290 and 400 nm, are presented in the figure, as well as runs differing in the initial concentration of $(\text{CH}_3)_2\text{CHCr}(\text{H}_2\text{O})_5^{2+}$ -- 0.10, 0.20, 0.50, and 1.0 mM, all with $[\text{O}_2] = 1.05$ mM. The fit of the data to the 3/2 slope is quite reasonable for all the runs indicated in the plot, suggesting the three-halves-order kinetics apply to both wavelengths and are independent of $[\text{RCr}^{2+}]_0$ in the range 0.1-1.0 mM.

The three-halves-order rate constant, k_{obs} , was obtained from the slope of plots of $(D_t - D_\infty)^{1/2}$ versus $(D_t - D_\infty)^{1/2} t$ from Equation 1-39,

$$k_{\text{obs}} = \frac{-(2)(\text{slope})}{[\text{RCr}^{2+}]_0^{1/2}} \quad (1-39)$$

The initial organochromium(III) concentration was calculated by dilution of a known stock solution, but its value is somewhat uncertain due to the slow decomposition of the chromium complex under nitrogen, introducing an uncertainty in k_{obs} . The three-halves-order kinetic plots were generally linear for 2 to 3 half-lives, at least for $[\text{RCr}^{2+}]_0$ in the range ~ 0.1 -1.2 mM. Some typical kinetic plots for experiments at 1.05 mM O_2 and four initial concentrations of the isopropylchromium(III) ion are shown in Figure 1-3.

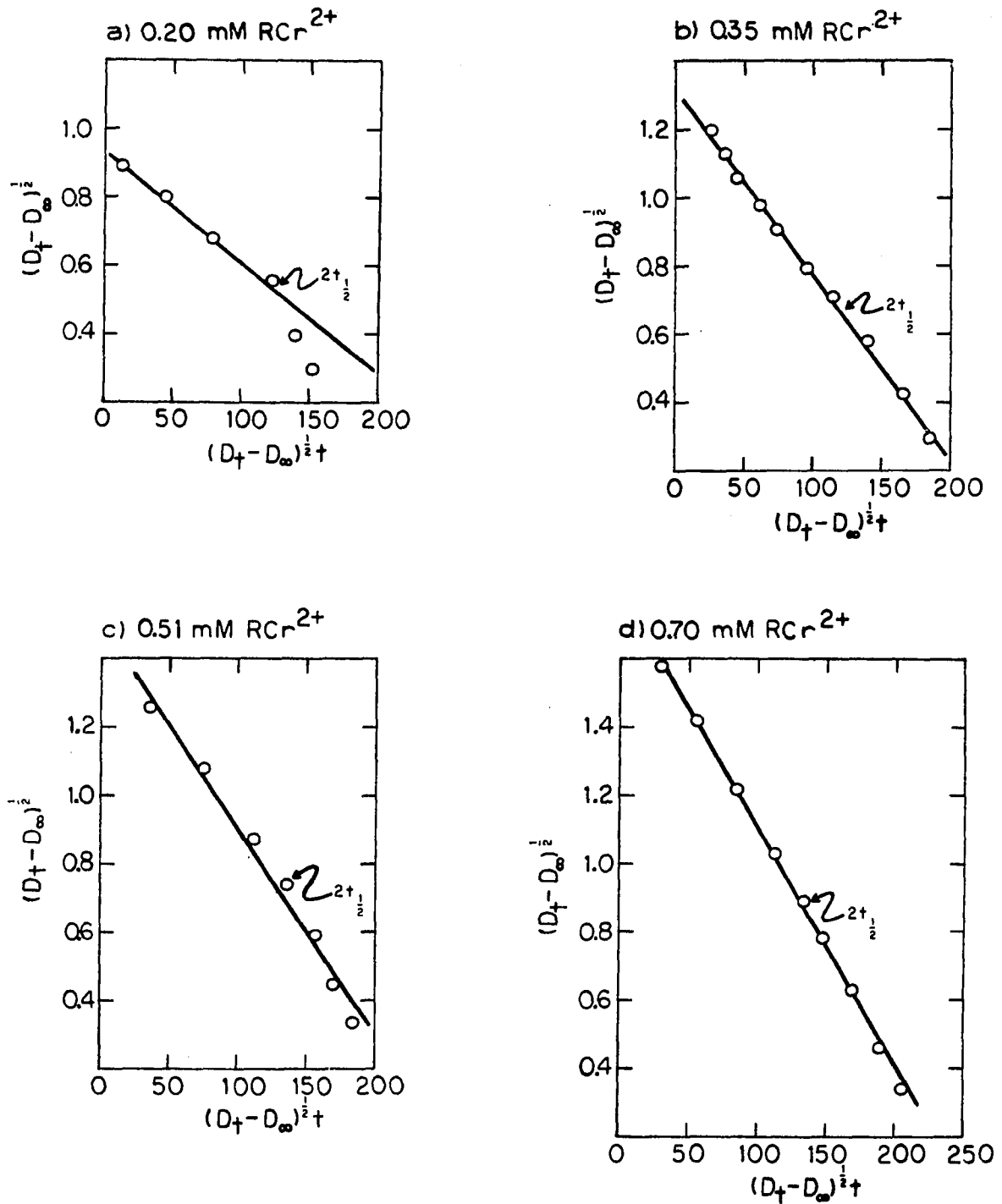


Figure 1-3. Three-halves-order kinetic plots for the reaction of $(\text{CH}_3)_2\text{CHCr}(\text{H}_2\text{O})_5^{2+}$ with 1.05 mM O_2 . Monitoring $\lambda = 290 \text{ nm}$; cell length = 2 cm

While kinetic plots at the three monitoring wavelengths--290, 330, and 400 nm--were equally linear, values for k_{obs} obtained at the different wavelengths were not in agreement--larger at longer wavelength; a suggestion for this anomaly is deferred to the Discussion. Values from monitoring at 290 nm, where the HCrO_4^- by-product absorbs relatively least, are deemed the best measure of the reaction rate, and are collected in Table 1-1, along with values from 330 nm, at $[\text{O}_2] = 1.05 \text{ mM}$, $T = 25 \pm 1^\circ\text{C}$. The individual values of k_{obs} have a rather large error associated with them, a phenomenon probably associated with the free-radical nature of the reaction. However, within the estimated uncertainty, the value of k_{obs} shows no dependence on the initial concentration of $(\text{CH}_3)_2\text{CHCr}(\text{H}_2\text{O})_5^{2+}$, further substantiating that the rate law is properly defined by Equation 1-24.

Variation of the concentrations of O_2 and H_3O^+

The dependence of k_{obs} on the concentration of molecular oxygen was assessed by lowering its concentration to 0.54 and 0.19 mM. Again, the three-halves-order kinetic plots were linear for 2 to 3 half-lives, and the value of k_{obs} was independent of the initial concentration of isopropylchromium(III). The rate constants obtained at the lower partial pressures of O_2 are listed in Table 1-2. While the reproducibility from run to run is again rather poor, it is clearly evident that k_{obs} is not a function of the oxygen concentration. The interpretation of the data is complicated somewhat by monitoring the absorbance at a variety of

Table 1-1. Rate constants for the reaction of $(\text{CH}_3)_2\text{CHCr}(\text{H}_2\text{O})_5^{2+}$ with 1.05 mM O_2 at various $[\text{RCr}^{2+}]_0^a$

λ/nM	$[\text{RCr}^{2+}]_0/\text{mM}$	$k_{\text{obs}}/\text{M}^{-1/2}\text{s}^{-1}$
290	0.20-0.23	0.46 ± 0.04 (3)
	0.30-0.40	0.55 ± 0.03 (5)
	0.50-0.58	0.46 ± 0.06 (5)
	0.70	0.52 (1)
	0.97	0.40 (1)
		$\bar{k}_{\text{obs}} = 0.49 \pm 0.06$ (15)
330	0.43	0.57 (1)
	0.51-0.53	0.72 ± 0.09 (4)
	0.70-0.71	0.84 ± 0.01 (2)
	0.78-0.84	0.72 ± 0.09 (5)
	1.0	0.70 (1)
		$\bar{k}_{\text{obs}} = 0.73 \pm 0.09$ (13)

^aUncertainties represent 1σ ; number in parentheses is number of kinetic runs; $[\text{H}_3\text{O}^+] = 0.10 \text{ M}$; $\mu = 1.0 \text{ M (LiClO}_4)$; $T = 25 \pm 1^\circ\text{C}$.

Table 1-2. Rate constants for the reaction of $(\text{CH}_3)_2\text{CHCr}(\text{H}_2\text{O})_5^{2+}$ with O_2 at various $[\text{O}_2]^a$

$[\text{O}_2]/\text{mM}$	$[\text{RCr}^{2+}]_0/\text{mM}$	λ/nm	$k_{\text{obs}}/\text{M}^{-1/2}\text{s}^{-1}$
1.0	0.54	400	0.60 ± 0.05 (2)
	0.21	400	0.55 (1)
0.5	0.54	320	0.65 (1)
	0.21	320	0.54 (1)
0.3	0.54	320	0.64 ± 0.04 (2)
	0.54	290	0.50 ± 0.09 (2)
	0.19	290	0.43 ± 0.07 (2)
0.1	0.54	290	0.55 (1)
	0.19	290	0.83 (1)
			$\bar{k}_{\text{obs}} = 0.59 \pm 0.11$ (13)

^aUncertainties represent 1σ ; number in parentheses is number of kinetic runs; $[\text{H}_3\text{O}^+] = 0.1 \text{ M}$; $\mu = 1.0 \text{ M}$ (LiClO_4); $T = 25 \pm 1^\circ\text{C}$

wavelengths. However, the average value of k_{obs} ($0.59 \pm 0.11 \text{ M}^{-1/2} \text{ s}^{-1}$) obtained at 0.54 or 0.19 mM O_2 and a variety of wavelengths, is in reasonable agreement with the values of \bar{k}_{obs} at 1.05 mM O_2 , at either 290 nm ($0.49 \pm 0.06 \text{ M}^{-1/2} \text{ s}^{-1}$) or 330 nm ($0.73 \pm 0.09 \text{ M}^{-1/2} \text{ s}^{-1}$), within the uncertainties indicated.

The effect of acid concentration on the reaction rate was evaluated at two different ionic strengths; the data are presented in Table 1-3. The rate is unaffected by a change in $[\text{H}_3\text{O}^+]$ in the region 0.003 to 0.10 M.

Therefore, the complete rate law for the reaction is given by,

$$\frac{-d[\text{RCr}^{2+}]}{dt} = k_{\text{obs}} [\text{RCr}^{2+}]^{3/2} [\text{O}_2]^0 [\text{H}_3\text{O}^+]^0 \quad (1-40)$$

Only a few reaction rates were measured using the oxygen-sensing electrode because of experimental limitations. Due to the electrode response time (15-30 s), only low concentrations of $(\text{CH}_3)_2\text{CHCr}(\text{H}_2\text{O})_5^{2+}$ could be studied so as to maintain the reaction rate within the capabilities of the electrode. Air-saturated solutions, with $[\text{RCr}^{2+}]_0 = 0.1 \text{ mM}$, were found to be satisfactory. The electrode was extremely sensitive to mechanical shock when a large electrolyte concentration was used; therefore, the ionic strength was not adjusted to 1.0 M as in the spectrophotometric work. An acid concentration of 0.01 M was also used, instead of 0.10 M, to further lower the ionic strength, independent work (see above) demonstrating k_{obs} is unaffected by $[\text{H}_3\text{O}^+]$. With $[\text{RCr}^{2+}]_0 = 0.086 - 0.12 \text{ mM}$, and $[\text{O}_2]_0 = 0.26 - 0.27 \text{ mM}$, values for k_{obs}

Table 1-3. Rate constants for the reaction of $(\text{CH}_3)_2\text{CHCr}(\text{H}_2\text{O})_5^{2+}$ with O_2 at various $[\text{H}_3\text{O}^+]$ ^a

$[\text{H}_3\text{O}^+]/\text{mM}$	$[\text{RCr}^{2+}]_0/\text{mM}$	μ/mM	$k_{\text{obs}}/\text{M}^{-1/2}\text{s}^{-1}$
3.0, 3.2	0.58, 0.56	41.9, 43.1	0.276, 0.313
6.7, 6.8, 7.0	0.68, 0.75, 0.72	43.4, 43.4, 43.8	0.310, 0.314, 0.306
37.0	0.58	40.7	0.297
11.7	0.74	1070	0.530
84.6	0.70	978	0.521
97.2	0.35	1070	0.577

^a $[\text{O}_2] = 1.05 \text{ mM}; T = 25.1 \pm 0.1^\circ\text{C}; \text{ monitoring } \lambda = 290 \text{ nm.}$

of $0.5-0.7 \text{ M}^{-1/2} \text{ s}^{-1}$ were obtained at $T = 21-22^\circ\text{C}$, in reasonable agreement with the spectrophotometric results at $0.10 \text{ M H}_3\text{O}^+$, $\mu = 1.0 \text{ M}$.

Variation of ionic strength

The variation of the rate constant for the reaction of $(\text{CH}_3)_2\text{CHCr}(\text{H}_2\text{O})_5^{2+}$ with O_2 was also investigated as a function of ionic strength, for the purpose of determining the ionic charge of the chain-propagating radical. Knowledge of the charge would help in distinguishing between the two alternative mechanisms, Schemes A and B, as presented earlier. The three-halves-order rate constant, k_{obs} , is given by a composite term of individual rate constants, Equation 1-41 (Scheme A) or 1-42 (Scheme B), where k_{h} is the rate constant for homolysis, Reaction 1-1.

$$k_{\text{obs}} \text{ (Scheme A)} = k_3 \left(\frac{k_{\text{h}}}{2k_4} \right)^{1/2} \quad (1-41)$$

$$k_{\text{obs}} \text{ (Scheme B)} = k_6 \left(\frac{k_{\text{h}}}{2k_7} \right)^{1/2} \quad (1-42)$$

Equation 1-41 (and by analogy, 1-42) will be derived in the Discussion. Each elementary rate constant of Equations 1-41 and 1-42 was analyzed as suggested by Brønsted-Debye-Hückel theory (77-81). Equation 1-43 relates the magnitude of the rate constant k for any elementary reaction to the ionic strength of the reaction medium.

$$\log k = \log k^{\circ} + \frac{(\Delta Z_i^{\ddagger})^2 \alpha \mu^{1/2}}{1 + \mu^{1/2}} \quad (1-43)$$

Equation 1-43 originates from the theories of Brønsted and Bjerrum, and relies on the Debye-Hückel relation, 1-44,

$$-\log \gamma_i = \frac{Z_i^2 \alpha \mu^{1/2}}{1 + \beta a \mu^{1/2}}, \quad (1-44)$$

to express activity coefficients (γ) as a function of μ . In these equations k^0 is the rate constant at infinite dilution ($\mu = 0$), $(\Delta Z_i^2)^\ddagger$ is the difference in the square of the ionic charges between the activated complex, (Z_\ddagger^2) , and the reactant(s), $\sum_i Z_i^2$, and α and β are physical constants which are functions of temperature and dielectric constant of the medium. At 25.0°C, in aqueous medium, $\alpha = 0.509$ and $\beta = 3.29 \times 10^7$. The quantity a is an average distance of closest approach of the ions; for ions of size 3 Å, βa is about unity. When Equation 1-43 is applied to the individual rate constants of Equations 1-41 or 1-42, the following relationships are obtained:

(Scheme A)

$$\begin{aligned} \log k_{\text{obs}} &= \log k_3 - \frac{1}{2} \log(2k_4) + \frac{1}{2} \log k_h \\ &= \log k_3^0 - \frac{1}{2} \log(2k_4^0) + \frac{1}{2} \log k_h^0 \end{aligned} \quad (1-45)$$

(Scheme B)

$$\begin{aligned} \log k_{\text{obs}} &= \log k_6 - \frac{1}{2} \log(2k_7) + \frac{1}{2} \log k_h \\ &= \log k_6^0 - \frac{1}{2} \log(2k_7^0) + \frac{1}{2} \log k_h^0 + \{[(4)^2 - (2)^2 - (2)^2] \\ &\quad - \frac{1}{2} [(4)^2 - (2)^2 - (2)^2] + \frac{1}{2} [(2)^2 - (2)^2]\} \frac{\alpha \mu^{1/2}}{1 + \mu^{1/2}} \\ &= \log k_6^0 - \frac{1}{2} \log(2k_7^0) + \frac{1}{2} \log k_h^0 + \frac{4\alpha \mu^{1/2}}{1 + \mu^{1/2}} \end{aligned} \quad (1-46)$$

Equation 1-46 predicts that a plot of $\log k_{\text{obs}}$ versus $\alpha\mu^{1/2}/(1 + \beta\alpha\mu^{1/2})$ will be linear with a slope of +4 if Scheme B is operative,¹ whereas a slope of zero is expected¹ if Equation 1-45 (Scheme A) correctly describes k_{obs} .

A study of k_{obs} as a function of ionic strength in the range 0.004 to 1.0 M was carried out with $[O_2] = 1.05 \text{ mM}$, $[RCr^{2+}]_0 = 0.35\text{-}0.88 \text{ mM}$, at a temperature of $25.1 \pm 0.1^\circ\text{C}$, while monitoring at 290 nm. Values of k_{obs} are collected in Table 1-4 and a plot of $\log k_{\text{obs}}$ versus $\alpha\mu^{1/2}/(1 + \beta\alpha\mu^{1/2})$, with $\alpha = 0.509$, and $\beta\alpha = 1$, is shown in Figure 1-4. It can be seen from the figure that k_{obs} is roughly independent of ionic strength at very low μ , over a rather narrow region of 0.004 to 0.034 M. However, around $\mu = 0.04 \text{ M}$, an abrupt increase in k_{obs} occurs, increasing linearly to $\mu = 1.0 \text{ M}$, with a slope of $\sim +1.5$. At these high ionic strengths, clearly outside the region where Equation 1-43 is valid, this result is more likely attributable to medium effects. Especially for a scheme such as B, where the bimolecular reactions involve two dipositive cations, the validity of equations such as 1-43 have been particularly criticized at higher ionic strengths (81). Consequently, judgement on the effect of μ on k_{obs} should be restricted to data at very low ionic strengths, where it can be concluded from Figure 1-4 that k_{obs} has approximately no dependence on μ , supporting Scheme A.

¹Equation 1-44 is rigorously correct only at $\mu < 0.01 \text{ M}$; to extend its validity to higher ionic strengths a term linear in μ (77-81) is often included, in which case $\log k$ becomes a linear function of $[\mu^{1/2}/(1+\mu^{1/2}) - C\mu]$ and with a slope no longer equal to simply $(\Delta Z_i^2)^\ddagger$.

Table 1-4. Rate constants for the reaction of $(\text{CH}_3)_2\text{CHCr}(\text{H}_2\text{O})_5^{2+}$ with O_2 at various ionic strengths^a

μ_0/mM	μ_∞/mM	$[\text{H}_3\text{O}^+]_\infty/\text{mM}$	$[\text{RCr}^{2+}]_0/\text{mM}$	$\frac{0.509\mu^{1/2}}{1 + \mu^{1/2}}$	$k_{\text{obs}}/\text{m}^{-1/2}\text{s}^{-1}$
3.3- 3.6	4.0- 4.4	1.4- 1.6	0.40	0.0277- 0.0317	0.258 \pm 0.004 (2)
5.8- 8.1	6.7- 9.4	3.4- 6.0	0.48- 0.79	0.0360- 0.0450	0.259 \pm 0.013 (7)
11.1- 11.5	12.3- 12.8	8.6- 8.9	0.59- 0.74	0.0485- 0.0517	0.257 \pm 0.005 (3)
15.8- 15.9	17.4	11.5- 11.6	0.80- 0.88	0.0568- 0.0593	0.249 \pm 0.008 (3)
23.9- 25.4	24.7- 26.2	22.3- 23.6	0.44- 0.47	0.0682- 0.0709	0.264 \pm 0.012 (2)
32.0- 32.9	33.0- 33.6	29.7- 30.0	0.41- 0.56	0.0772- 0.0788	0.262 \pm 0.007 (2)
40.2- 43.1	41.2- 44.4	3.0- 37.0	0.56- 0.75	0.0850- 0.0886	0.303 \pm 0.014 (6)
74.3- 75.3	75.3- 76.7	2.9- 7.0	0.56- 0.78	0.109- 0.110	0.335 \pm 0.01 (4)
107.	108.	7.5	0.56- 0.62	0.125- 0.126	0.322 \pm 0.008 (2)
173.- 174.	174.- 175.	9.5- 11.5	0.69- 0.74	0.150	0.340 \pm 0.002 (2)
210.	211.	7.4	0.53- 0.54	0.160 0.160	0.375 \pm 0.006 (2)

^aData has been grouped according to ionic strength; kinetic runs with very similar μ are listed together--each column represents the range in concentration, or k_{obs} within the group. Uncertainties represent 1 σ ; number in parentheses is number of kinetic runs; $T = 25.1 \pm 0.1^\circ\text{C}$; monitoring $\lambda = 290$ nm. Ionic strengths (μ_0 and μ_∞) and $[\text{H}_3\text{O}^+]_\infty$ were calculated from Equations (1-21)-(1-23).

Table 1-4. Continued

μ_o /mM	μ_∞ /mM	$[H_3O^+]_\infty$ /mM	$[RCr^{2+}]_o$ /mM	$\frac{0.509\mu^{1/2}}{1 + \mu^{1/2}}$	$k_{obs}/m^{-1/2}s^{-1}$
254.	255.	32.2	0.75	0.171	0.353 (1)
317.	318.	11.6	0.70	0.183	0.396 (1)
565.	566.	9.5	0.69- 0.71	0.218	0.440 \pm 0.015 (2)
764.	766.	9.5- 9.6	0.7	0.237	0.505 \pm 0.025 (2)
977.	978.	84.6	0.70	0.253	0.521 (1)
1070.	1070.	11.7	0.74	0.259	0.530 (1)
1070.	1070.	97.2	0.35	0.259	0.577 (1)

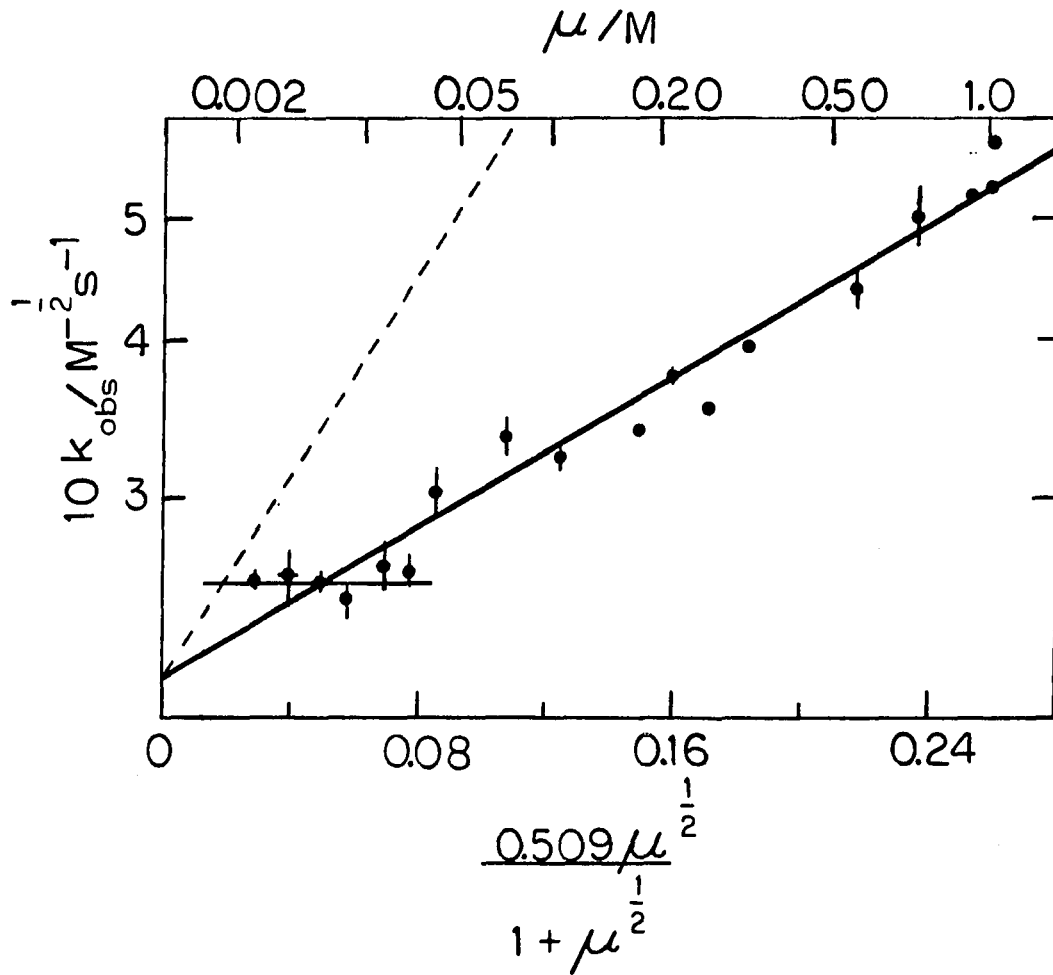


Figure 1-4. Plot of $\log k_{\text{obs}}$ versus $0.509\mu^{1/2}/(1 + \mu^{1/2})$ for the reaction of $(\text{CH}_3)_2\text{CHCr}(\text{H}_2\text{O})_5^{2+}$ with O_2 . The dashed line has a slope of +4

Kinetics at very low $[(\text{CH}_3)_2\text{CHCr}(\text{H}_2\text{O})_5]^{2+}$

For initial organochromium(III) concentrations less than 0.2 mM, Equation 1-32 was used, as described in the Experimental section, to obtain values for the three-halves-order rate constant, k_{obs} . For runs monitored at 290 nm, with $[\text{RCr}^{2+}]_0 = 0.04\text{--}0.20$ mM, 1.05 mM O_2 , 0.10 M H_3O^+ , $\mu = 1.0$ M (LiClO_4), and $T = 25 \pm 1^\circ\text{C}$, an average value for k_{obs} of $0.43 \pm 0.05 \text{ M}^{-1/2} \text{ s}^{-1}$ was obtained, in reasonable agreement with those values in Table 1-1, at higher organochromium(III) concentration.

Radical Scavengers

Effect of organic scavengers

The effect of various radical scavengers was investigated to gain further mechanistic information on the reaction of $(\text{CH}_3)_2\text{CHCr}(\text{H}_2\text{O})_5^{2+}$ with O_2 . Galvinoxyl is an efficient scavenger for both alkyl and alkylperoxy radicals (82,83). It is too insoluble in water to be used as a scavenger in aqueous medium, so a 65:35 V/V% acetone to water solvent was used. In the absence of galvinoxyl, this solvent change was shown not to affect the reaction kinetics. Experiments in the presence of a very low concentration of galvinoxyl, 1×10^{-5} M, were unsuccessful, however, as there appeared to be a direct reaction between galvinoxyl and $(\text{CH}_3)_2\text{CHCr}(\text{H}_2\text{O})_5^{2+}$ itself. Another scavenger, diphenylamine (43), present at the same concentration of isopropylchromium(III), caused an interference in the absorption measurements and was not further studied.

Effect of miscellaneous metal ions

Radical scavengers in the form of metal ions were also investigated. Hexaaquacobalt(II), manganese(II), and copper(II) perchlorates at concentrations equimolar to that of the organochromium(III) ion had no effect on the kinetics of the reaction at 1.05 mM O₂. Three-halves-order rate constants obtained in the presence of these metal ions agreed well with the values listed in Table 1-1.

Effect of Fe_{aq}²⁺

However, iron(II) perchlorate, added to the reaction medium saturated with 1.05 mM O₂ before injection of the organochromium(III) ion, resulted in a remarkable inhibition of the reaction. An actual absorbance versus time trace, monitored at 400 nm, is reproduced in Figure 1-5. Complete quenching did not occur, as long as the amount of iron(II) added was less than the amount of (CH₃)₂CHCr(H₂O)₅²⁺. After a very slow, first-order loss in organochromium(III) concentration, $k = (4.27 \pm 0.03) \times 10^{-4} \text{ s}^{-1}$, the reaction rate abruptly increased. A three-halves-order kinetic plot of the ensuing data was linear, with a value for k_{obs} of the correct magnitude. The length of time of inhibition was related to the amount of iron(II) injected, but due to difficulties in reproducibility, this was not quantified. The stoichiometry of the reaction was about 3-4 Fe(II) consumed per (CH₃)₂CHCr(H₂O)₅²⁺. Quenching could be repeated by addition of more iron(II), apparently indefinitely, until all the organochromium(III) ion was depleted.

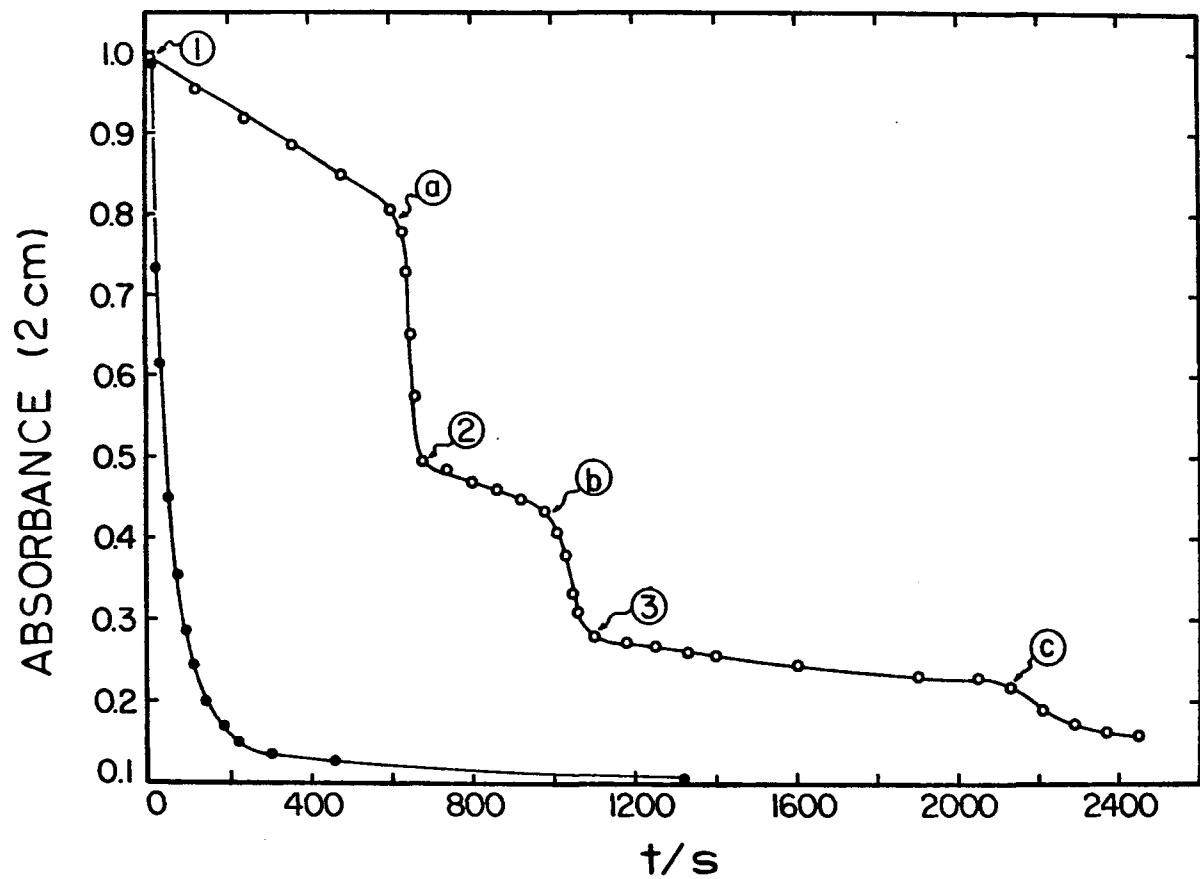
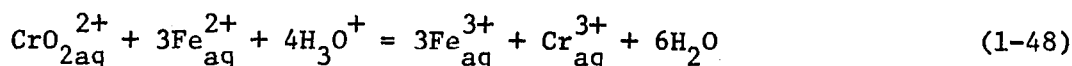
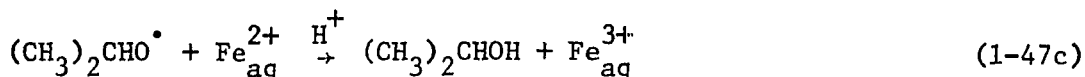
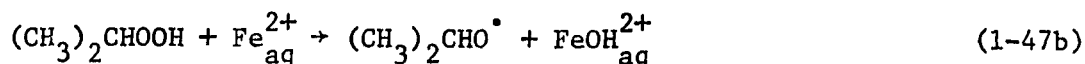
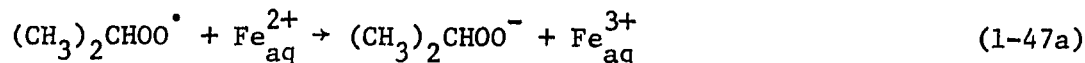


Figure 1-5. Trace of absorbance at 400 nm versus time for the reaction of $(\text{CH}_3)_2\text{CHCr}(\text{H}_2\text{O})_5^{2+}$ with O_2 in the presence (open circles) of increments of $\text{Fe}_{\text{aq}}^{2+}$ and absence (solid circles). $[\text{RCr}^{2+}]_0 = 0.95 \text{ mM}$; $[\text{O}_2] = 1.05 \text{ mM}$. At the numbered arrows the following concentrations (mM) of $\text{Fe}_{\text{aq}}^{2+}$ were injected (the concentration (mM) of RCr^{2+} at this point is in parentheses): (1) 0.58, (0.95); (2) 0.28, (0.51); (3) 0.27, (0.29). The lettered arrows represent the time at which all $\text{Fe}_{\text{aq}}^{2+}$ has been consumed

The dramatic inhibition of the reaction by $\text{Fe}_{\text{aq}}^{2+}$ suggests the involvement of free-radical intermediates, because it is certainly reasonable to expect either isopropylperoxy radicals or $\text{CrO}_{2\text{aq}}^{2+}$ to be capable of oxidizing iron(II) ions, Reactions 1-47 and 1-48.



Alkylperoxy radicals oxidize $\text{Co}_{\text{aq}}^{2+}$ or $\text{Mn}_{\text{aq}}^{2+}$ (44,47) which have more negative oxidation emf's (-1.808 and -1.51 V, respectively) than $\text{Fe}_{\text{aq}}^{2+}$ (-0.771 V) in acidic solution, so Reaction 1-47a appears likely. Subsequent reaction with $\text{Fe}_{\text{aq}}^{2+}$ will presumably occur via Reactions 1-47b and 1-47c, in analogy to reactions suggested (84) for the reduction of t-butyl hydroperoxide by $\text{Fe}_{\text{aq}}^{2+}$. Three equivalents of $\text{Fe}_{\text{aq}}^{3+}$ should be consumed for every isopropylperoxy radical. Confirmation of Reaction 1-48 was obtained by injecting iron(II) perchlorate into a solution of $\text{CrO}_{2\text{aq}}^{2+}$ in 0.1 M HClO_4 ; the UV spectrum revealed the formation of $\text{Fe}_{\text{aq}}^{3+}$, and loss of the maximum at 290 nm, characteristic of $\text{CrO}_{2\text{aq}}^{2+}$ (71,85,86). A stoichiometry of about 3.2 $\text{Fe}_{\text{aq}}^{2+}$ consumed per $\text{CrO}_{2\text{aq}}^{2+}$ was estimated. If the rate of reaction of the chain-propagating radical with $\text{Fe}_{\text{aq}}^{2+}$ is rapid enough, (Reaction 1-47a or 1-48), to compete with attack on $(\text{CH}_3)_2\text{CHCr}(\text{H}_2\text{O})_5^{2+}$, inhibition by $\text{Fe}_{\text{aq}}^{2+}$ is readily

explained. The observed consumption of $\text{Fe}_{\text{aq}}^{2+}$ per $(\text{CH}_3)_2\text{CHCr}(\text{H}_2\text{O})_5^{2+}$ of 3-4, rather than a total of 6, implies the rates of Reactions 1-47 and 1-48 are not competitive.

The lack of inhibition by low concentrations of $\text{Co}_{\text{aq}}^{2+}$, $\text{Mn}_{\text{aq}}^{2+}$, and $\text{Cu}_{\text{aq}}^{2+}$ may be due to slowness of reaction with the chain-propagating radical(s) or unfavorable emf's.

Effect of high $[\text{Cu}^{2+}]$

Although millimolar concentrations of copper(II) perchlorate did not interfere with the reaction of $(\text{CH}_3)_2\text{CHCr}(\text{H}_2\text{O})_5^{2+}$ with O_2 , concentrations of 10 to 100 fold greater were found to have a dramatic effect. Not only is the rate of reaction slowed considerably, but the form of the rate law changes. The kinetics were studied in detail by monitoring the decrease in absorbance of the organochromium(III) ion with time at 400 nm where Cu(II) does not absorb. A concentration range of copper(II) ion from 0.02 to 0.40 M was investigated at molecular oxygen concentrations of 0.19, 0.54, 1.05 mM, again maintained constant throughout the reaction. All runs contained 0.6-1.0 mM isopropylchromium(III), in 0.1 M H_3O^+ , with the ionic strength maintained at 1.0 M, except for $[\text{Cu}^{2+}] = 0.40$ M, where by necessity, $\mu = 1.3$ M. The temperature was controlled at $25.0 \pm 0.1^\circ\text{C}$.

A pseudo-first-order dependence on isopropylchromium(III) concentration is seen in the presence of high concentrations of Cu(II), rather than the three-halves-order dependence in its absence. Pseudo-first-order rate constants, $k_{\text{obs}}^{\text{Cu}}$, were calculated from the slopes of

$\ln(D_t - D_\infty)$ versus time plots. Values obtained at various $[O_2]$, $[Cu^{2+}]_0$, and $[RCr^{2+}]_0$ are collected in Table 1-5.

The dependence of k_{obs}^{Cu} on the concentrations of Cu_{aq}^{2+} and O_2 was analyzed graphically. Plotting k_{obs}^{Cu} , obtained at 1.05 mM O_2 , versus $[Cu^{2+}]^{-1}$ resulted in the linear relationship,

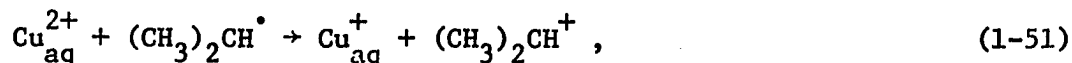
$$k_{obs}^{Cu}/s^{-1} = (6.46 \pm 0.69) \times 10^{-4} + (4.84 \pm 0.26) \times 10^{-5} [Cu^{2+}]^{-1}, \quad (1-49)$$

demonstrated in Figure 1-6. A direct dependence on $[O_2]$ was indicated, although some scatter in the data points is apparent. From Figure 1-7, the relationship,

$$k_{obs}^{Cu}/s^{-1} = (3.8 \pm 0.9) \times 10^{-4} + (0.84 \pm 0.15 [O_2]), \quad (1-50)$$

was obtained, with the copper(II) concentration maintained constant at 0.10 M.

The kinetic effect of high concentrations of copper(II) ion presented an opportunity to distinguish between Schemes A and B. If Scheme A were operative either the isopropyl or isopropylperoxy radicals must be scavenged by Cu_{aq}^{2+} to explain the kinetic results. Much literature precedent exists for the reduction of Cu_{aq}^{2+} to Cu_{aq}^+ by alkyl radicals. Specifically, for the isopropyl radical,



the rate constant for Reaction 1-51 has been estimated as $5.0 \times 10^7 M^{-1} s^{-1}$ at 57°C in 66% V/V acetic acid/water (87), and $5.0 \times 10^6 M^{-1} s^{-1}$ at 25.5°C in 44% V/V acetonitrile/acetic acid (88). At high concentrations of copper(II), ca. 0.20 M, the apparent rate constant of

Table 1-5. Rate constants for the reaction of $(\text{CH}_3)_2\text{CHCr}(\text{H}_2\text{O})_5^{2+}$ with O_2 in the presence of $\text{Cu}_{\text{aq}}^{2+}$ ^a

$[\text{O}_2]/\text{mM}$	$[\text{Cu}^{2+}]/\text{M}$	$10^3 k_{\text{obs}}/\text{s}^{-1}$
1.05	0.020	2.89 ± 0.23
	0.025	2.78 ± 0.20
	0.033	2.15
	0.038	1.97
	0.050	1.50 ± 0.04
	0.10	1.26 ± 0.07
	0.20	0.890 ± 0.03
	0.30	0.728 ± 0.02
0.54	0.40 ^b	0.727 ± 0.01
	0.05	1.03
	0.10	0.796 ± 0.02
0.19	0.05	0.780
	0.10	0.676 ± 0.04
	0.20	0.589 ± 0.01
	0.30	0.65 ± 0.08
0 ^c	0.10	0.291 ± 0.021

^aUncertainties represent 1 σ from 2 duplicate runs; $[\text{H}_3\text{O}^+] = 0.1 \text{ M}$; $\mu = 1.0 \text{ M}$ (LiClO_4), except as noted; $T = 25.0 \pm 0.1^\circ\text{C}$; monitoring $\lambda = 400 \text{ nm}$.

^b $\mu = 1.3 \text{ M}$.

^cUnder a N_2 atmosphere.

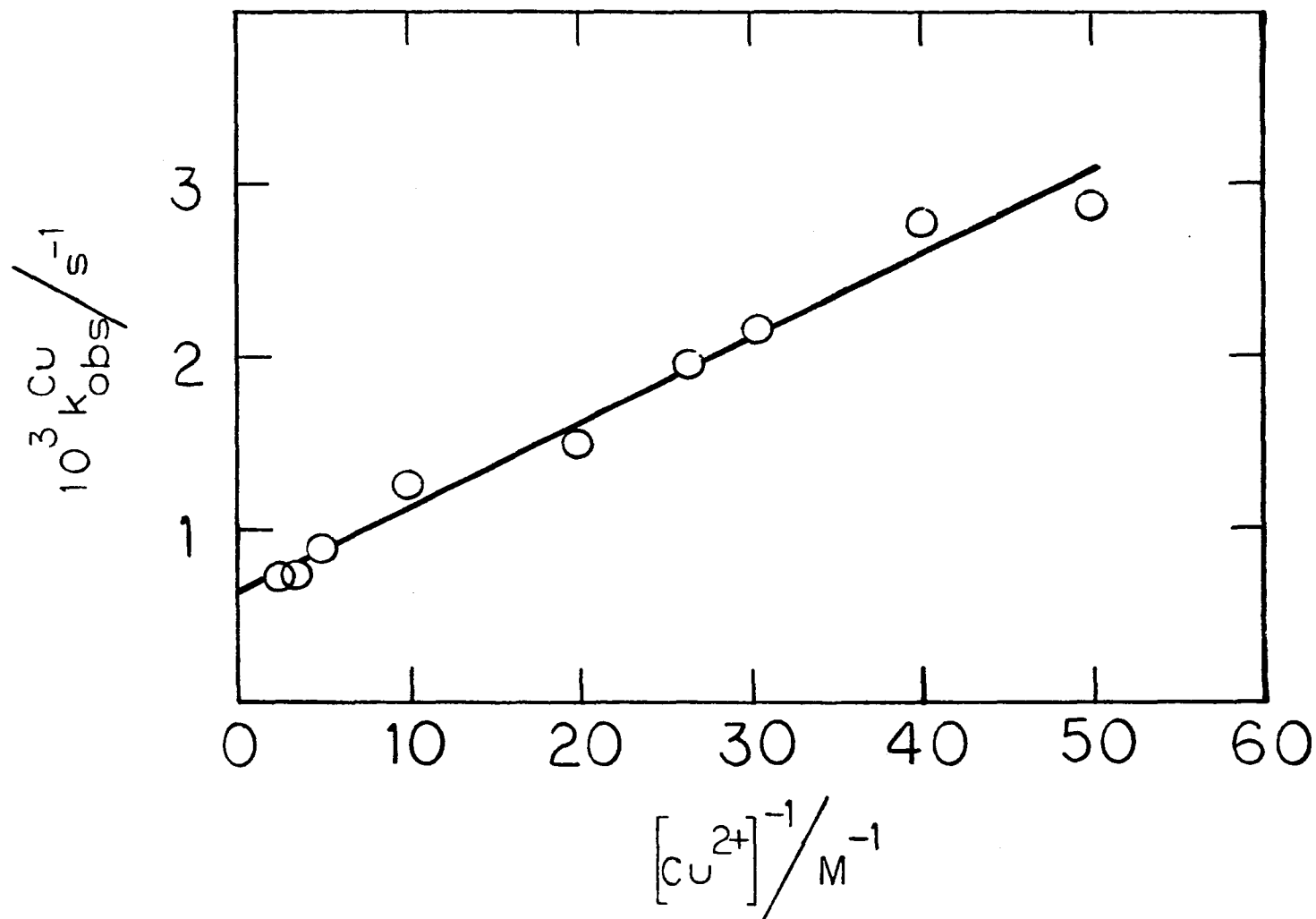


Figure 1-6. Plot of k_{obs}^{Cu} versus $[Cu^{2+}]^{-1}$ at $[O_2] = 1.05$ mM, for the reaction of $(CH_3)_2CHCr(H_2O)_5^{2+}$ with O_2 in the presence of Cu_{aq}^{2+}

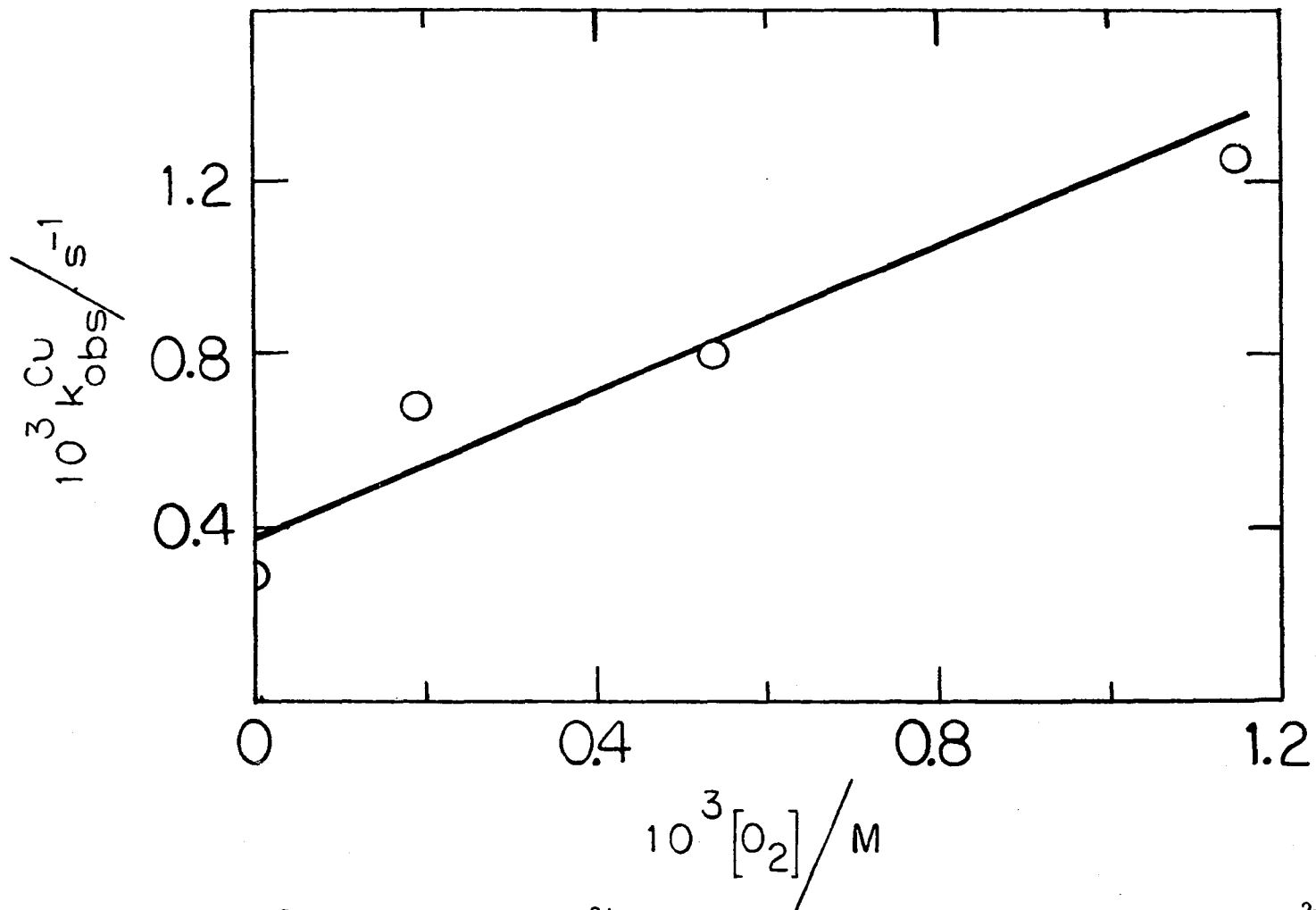


Figure 1-7. Plot of k_{obs}^{Cu} versus $[O_2]$ at $[Cu^{2+}] = 0.10 M$, for the reaction of $(CH_3)_2CHCr(H_2O)_5^{2+}$ with O_2 in the presence of Cu_{aq}^{2+}

Reaction 1-51 will be $(1 - 10) \times 10^6 \text{ s}^{-1}$, or rapid enough to compete with millimolar O_2 for the isopropyl radical, Reaction 1-2 ($k_2 \sim 1 \times 10^9 \text{ M}^{-1} \text{ s}^{-1}$ (47)) and inhibit the chain reaction. Oxidation of $\text{Cu}_{\text{aq}}^{2+}$ by $(\text{CH}_3)_2\text{CHOO}^\bullet$ to $\text{Cu}_{\text{aq}}^{3+}$ can be disregarded on the basis of thermodynamics.

However, if Scheme B is the correct mechanism, either $\text{Cr}_{\text{aq}}^{2+}$ or $\text{CrO}_{2\text{aq}}^{2+}$ must be capable of being scavenged by copper(II) ion. The reduction of copper(II) by chromium(II) ions is too slow in $0.1 \text{ M H}_3\text{O}^+$ to compete with the formation of $\text{CrO}_{2\text{aq}}^{2+}$. For example, with $[\text{Cu}^{2+}] = 0.20 \text{ M}$ and $[\text{H}_3\text{O}^+] = 0.10 \text{ M}$, the apparent rate constant for reduction of copper(II) ions is 1.21 s^{-1} at 24.6°C , $\mu = 1.00 \text{ M}$ (89), compared to $1.6 \times 10^5 \text{ s}^{-1}$ for Reaction 1-5 ($k_5 = 1.6 \times 10^8 \text{ M}^{-1} \text{ s}^{-1}$ (71,85,86)). The reactivity of $\text{Cu}_{\text{aq}}^{2+}$ toward $\text{CrO}_{2\text{aq}}^{2+}$ was investigated by comparing the UV spectrum before and after addition of copper(II) perchlorate to a solution of $\text{CrO}_{2\text{aq}}^{2+}$ at pH 2. Clearly, no reaction occurred--the final spectrum consisted of the sum of the individual spectra of $\text{Cu}_{\text{aq}}^{2+}$ and $\text{CrO}_{2\text{aq}}^{2+}$. Therefore, Scheme B can be eliminated from further consideration.

Products of Reaction of $(\text{CH}_3)_2\text{CHCr}(\text{H}_2\text{O})_5^{2+}$ with O_2

Acetone and 2-propanol were the only organic products detected. Their yields, reported as a percentage based on the starting concentration of $(\text{CH}_3)_2\text{CHCr}(\text{H}_2\text{O})_5^{2+}$, were studied as a function of $[\text{H}_3\text{O}^+]$, and are reported in Table 1-6. There is a slight dependence of the yields of both products on the acidity. Acetone production parallels the increase in $[\text{H}_3\text{O}^+]$, while 2-propanol decreases, so that their sum remains constant.

Table 1-6. Percent yields of acetone and 2-propanol produced in the reaction of $(\text{CH}_3)_2\text{CHCr}(\text{H}_2\text{O})_5^{2+}$ with O_2^a

$[\text{H}_3\text{O}^+]/\text{M}$	% CH_3COCH_3	% $\text{CH}_3\text{CHOHCH}_3$
$\sim 0.002^b$	57.7 ± 1.4	28.3 ± 1.6
0.01	66.8 ± 0.4	24.1 ± 0.1
0.10	69.0	18.9
0.10^c	75.4	-
0.10^c	70.8	-

^aUncertainties represent 1σ of duplicate injections; $[\text{RCr}^{2+}]_0 = 0.45\text{--}0.65$ mM; 1.05 mM O_2 ; $\mu \approx 0.5$ M + $[\text{H}_3\text{O}^+]$; T = ambient; FFAP column used, except as noted.

^bApproximate $[\text{H}_3\text{O}^+]$ used to elute $(\text{CH}_3)_2\text{CHCr}(\text{H}_2\text{O})_5^{2+}$ from ion-exchange column.

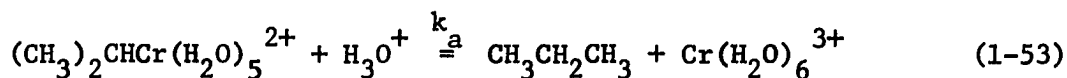
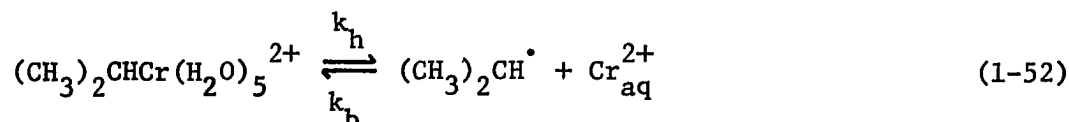
^cTenax column.

Essentially no hydroperoxide could be detected in the product solutions, after correcting for residual active oxygen (presumably traces of $(\text{CH}_3)_2\text{CH}(\text{CH}_3)_2\text{COOH}$ from the synthesis) in the $(\text{CH}_3)_2\text{CHCr}(\text{H}_2\text{O})_5^{2+}$ ion's stock solution. The analyses were further hampered by the large uncertainty introduced when the absorbance of I_3^- at 410 nm was corrected for the amount of Cr(III) present, because the numbers were of similar magnitude.

The percent yields of HCrO_4^- , $\text{Cr}(\text{H}_2\text{O})_6^{3+}$, and $[\text{Cr}(\text{OH})(\text{H}_2\text{O})_4]_2^{4+}$ ions are summarized in Table 1-7. Only the yield of hydrogen chromate was studied as a function of $[\text{H}_3\text{O}^+]$. From 0.011 to 0.90 M H_3O^+ it decreases by 28%.

Kinetics of Homolysis and Acidolysis

Under a nitrogen atmosphere, with the strict exclusion of molecular oxygen, the decomposition of $(\text{CH}_3)_2\text{CHCr}(\text{H}_2\text{O})_5^{2+}$ in aqueous perchloric acid is a consequence of both homolysis and acidolysis, Reactions 1-52 and 1-53, respectively.



Reaction 1-52 is written as an equilibrium where the forward reaction, homolysis, occurs with a rate constant k_h , and the back reaction, by which $(\text{CH}_3)_2\text{CHCr}(\text{H}_2\text{O})_5^{2+}$ is made, has a rate constant designated k_b .

Table 1-7. Percent yields of HCrO_4^- , $\text{Cr}(\text{H}_2\text{O})_6^{3+}$, and $[\text{Cr}(\text{OH})(\text{H}_2\text{O})_4]_2^{4+}$ produced in the reaction of $(\text{CH}_3)_2\text{CHCr}(\text{H}_2\text{O})_5^{2+}$ with O_2^a

$[\text{H}_3\text{O}^+]/\text{M}$	% HCrO_4^-	% $\text{Cr}(\text{H}_2\text{O})_6^{3+}$	% $[\text{Cr}(\text{OH})(\text{H}_2\text{O})_4]_2^{4+}$
0.011	12.9 (1)	-	-
0.10	12.6 ± 2.6 (8)	70.1 ± 8.3 (5)	10.1 ± 1.2 (5)
0.50	10.0 ± 0.5 (2)	-	-
0.70	9.8 ± 1.6 (4)	-	-
0.90	9.3 ± 1.8 (2)	-	-

^aUncertainties represent 1σ ; numbers in parentheses indicate number of analyses; $[\text{RCr}^{2+}]_0 = 0.01\text{-}0.02 \text{ M}$; 1.05 mM O_2 ; $\mu \approx 0.5 \text{ M} + [\text{H}_3\text{O}^+]$; $T = \text{ambient}$.

The kinetics of acidolysis were not studied in detail, so the mechanism is not known. However, the rate of acidolysis has no dependence on the acid concentration in the region $[\text{H}_3\text{O}^+] = 0.05\text{--}0.17\text{ M}$, and consequently Reaction 1-53 is not an elementary reaction.

By addition of a variety of reagents in separate experiments, the individual values for k_h and k_a may be obtained. In the presence of an oxidant, reactive towards $\text{Cr}_{\text{aq}}^{2+}$ ion and/or the isopropyl radical, the sum of the rate constants of homolysis and acidolysis will be measured. The oxidant serves to scavenge (29) one or both products of homolysis, effectively eliminating the back reaction of 1-52. Oxidants such as iron(III) or copper(II) ions, and acidopentaamminecobalt(III) complexes, are useful for this purpose. In the presence of one of these species, the experimentally measured rate constant will be,

$$k_{\text{obs}} = k_h + k_a . \quad (1-54)$$

However, if the kinetics of decomposition are measured in the presence of a millimolar concentration of $\text{Cr}_{\text{aq}}^{2+}$ ion, homolysis will be suppressed because the rate of the back reaction of 1-52 will be quite fast (25), $k_p[\text{Cr}^{2+}] \approx 10^4 - 10^5\text{ s}^{-1}$. The observed rate constant is then identified with k_a ,

$$k_{\text{obs}} = k_a , \quad (1-55)$$

the rate constant of acidolysis.

The rates in the presence of oxidants or chromium(II) ion were obtained by following the decrease in absorbance of the organochromium(III) ion with time at 400 nm where the other complexes have minimal

absorbance. Values of k_{obs} were obtained from plots of $\ln(D_t - D_\infty)$ versus time, which were linear for at least three half-lives. The rate constants are collected in Table 1-8.

The rates in the presence of iron(III) perchlorate are faster than with copper(II) ion or the cobalt(III) complex, and also depend on the concentration of $\text{Fe}_{\text{aq}}^{3+}$. The rate should be independent of the oxidant's concentration, hence there appears to be a direct reaction between $\text{Fe}_{\text{aq}}^{3+}$ and $(\text{CH}_3)_2\text{CHCr}_{\text{aq}}^{2+}$.¹ The rates in the presence of the cobalt(III) complex are reasonably independent of its concentration, except at the lowest, for which an explanation is not available. The rate of homolysis, plus acidolysis is probably best given by the average of the values at higher $[\text{Co}(\text{NH}_3)_5\text{Br}^{2+}]$, 3.7-9.6 mM, and for $\text{Cu}_{\text{aq}}^{2+}$ scavenging, with $k_{\text{obs}} = (2.85 \pm 0.10) \times 10^{-4} \text{ s}^{-1}$.

The rate constant for acidolysis, $k_a = (1.067 \pm 0.008) \times 10^{-4} \text{ s}^{-1}$ obtained in the presence of $\text{Cr}_{\text{aq}}^{2+}$, was not obtained at 0.1 M H_3O^+ , as in the above work, but at 0.05 M. Additional experiments (90) at 0.17 M H_3O^+ have established that the rate has no dependence on $[\text{H}_3\text{O}^+]$ in the region 0.05-0.17 M, not unexpected as the rate of acidolysis of $\text{Cr}(\text{H}_2\text{O})_5^{2+}$ is largely acid-independent (16). Using $k_a = 1.067 \times 10^{-4} \text{ s}^{-1}$, the value of k_h obtained from Equation 1-54 is $(1.78 \pm 0.11) \times 10^{-4} \text{ s}^{-1}$.

¹An $\text{Fe}_{\text{aq}}^{3+}$ -dependent pathway has been detected for difunctional complexes of bis(benzylchromium) cations (5).

Table 1-8. Rate constants obtained for the decomposition of
 $(\text{CH}_3)_2\text{CHCr}(\text{H}_2\text{O})_5^{2+}$ under N_2^{a}

Species present	[species]/M	$[\text{RCr}^{2+}]_0/\text{mM}$	$10^4 k/\text{s}^{-1}$
$\text{Fe}^{3+ \text{b}}$	0.10	0.98	4.56 ± 0.26 (2)
	0.050	0.98	3.98 ± 0.02 (3)
$\text{Cu}_{\text{aq}}^{2+}$	0.10	0.93	2.91 ± 0.21 (2)
$\text{Co}(\text{NH}_3)_5\text{Br}^{2+}$	0.0096	0.93	2.862 ± 0.007 (4)
	0.0048	0.88	2.80 ± 0.13 (3)
	0.0037	0.88	2.87 (1)
	[0.0024	1.1	3.17 ± 0.02 (4)] ^c
$\text{Cr}_{\text{aq}}^{2+ \text{b,d}}$	0.0038	1.0	1.067 ± 0.008 (4)

^aUncertainties represent 1 σ ; number in parentheses is number of kinetic runs; $[\text{H}_3\text{O}^+] = 0.10$ M, except as noted; $\mu = 1.0 \pm 0.05$ M (LiClO_4); $T = 25.0 \pm 0.1^\circ\text{C}$, except as noted; monitoring $\lambda = 400$ nm.

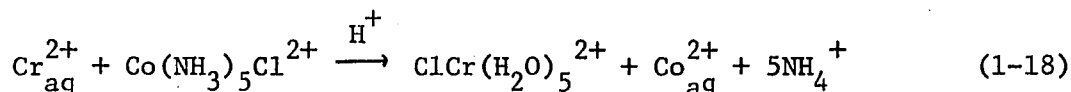
^b $T = 24.7^\circ\text{C}$.

^cSee text.

^d $[\text{H}_3\text{O}^+] = 0.05$ M.

Products of Homolysis and Acidolysis

In addition to the kinetic evidence for homolysis, product studies, designed to detect $\text{Cr}_{\text{aq}}^{2+}$, were carried out. Decomposition in the presence of $\text{Co}(\text{NH}_3)_5\text{Cl}^{2+}$ (under N_2) should produce $\text{ClCr}(\text{H}_2\text{O})_5^{2+}$ and cobalt(II) ion if homolysis is important.



In the experiment constructed to observe $\text{ClCr}_{\text{aq}}^{2+}$, (see Experimental) maxima at 428 and 609 nm in the visible spectrum, with an intensity ratio of 1.20:1, confirmed its presence.

In other experiments the amount of $\text{Co}_{\text{aq}}^{2+}$ ion formed via Reaction 1-19 was quantified, using $\text{Co}(\text{NH}_3)_5\text{Br}^{2+}$ as the oxidant. Two separate determinations were examined, the results of which are reported below.

<u>mmol $\text{RCr}_{\text{o}}^{2+}$</u>	<u>mmol $\text{Co}_{\text{aq}}^{2+}$ (analyzed)</u>	<u>mmol $\text{Co}_{\text{aq}}^{2+}$ ("expected")</u>
0.0272	0.0349	0.0169
0.0232	0.0315	0.0144

The mmol $\text{Co}_{\text{aq}}^{2+}$ ("expected") were calculated from the kinetic data. Since only homolysis leads to $\text{Co}_{\text{aq}}^{2+}$ ion, the fraction of isopropylchromium(III) which reacts by this pathway is given as,

$$\frac{k_{\text{h}}}{k_{\text{h}} + k_{\text{a}}} = \frac{1.78 \times 10^{-4} \text{ s}^{-1}}{2.85 \times 10^{-4} \text{ s}^{-1}} = 0.624,$$

so mmol $\text{Co}_{\text{aq}}^{2+}$ "expected" = $0.624[\text{RCr}^{2+}]_{\text{o}}$. However, it is apparent twice as much $\text{Co}_{\text{aq}}^{2+}$ was produced than calculated, 2.06 or 2.19. This implies

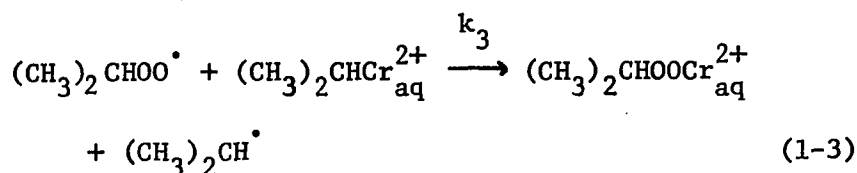
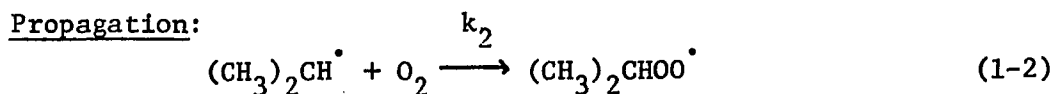
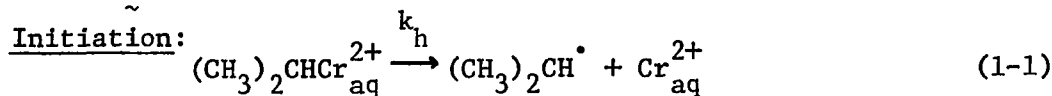
the isopropyl radical is also being oxidized by $\text{Co}(\text{NH}_3)_5\text{Br}^{2+}$, accounting for the additional equivalent of $\text{Co}_{\text{aq}}^{2+}$. Therefore, the kinetic results appear to be in good agreement with the product analysis.

The only products detected from acidolysis of ~ 0.01 M $(\text{CH}_3)_2\text{CHCr}(\text{H}_2\text{O})_5^{2+}$ in 0.10 M H_3O^+ were propane and $\text{Cr}(\text{H}_2\text{O})_6^{3+}$. Acetone or other low molecular weight organic compounds were not present.

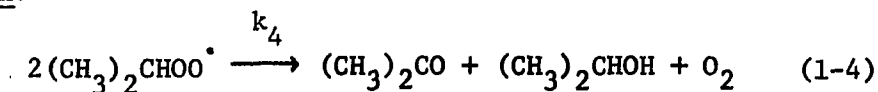
DISCUSSION

Scheme A is the preferred reaction mechanism for the autoxidation of $(\text{CH}_3)_2\text{CHCr}(\text{H}_2\text{O})_5^{2+}$. Scheme B was eliminated because of the inability to explain the effect of high concentrations of $\text{Cu}_{\text{aq}}^{2+}$ on the kinetics, and the absence of a large ionic strength dependence on k_{obs} . Another mechanistic scheme might be considered, and will be presented after a thorough discussion of the individual reactions in Scheme A, reproduced below.

Scheme A:



Termination:



Initiation occurs by homolysis of isopropylchromium(III), Reaction 1-1, to form the isopropyl radical and chromium(II) ion. Homolysis, while a rather inefficient process for $(\text{CH}_3)_2\text{CHCr}(\text{H}_2\text{O})_5^{2+}$, nonetheless proceeds with a rate constant of $1.78 \times 10^{-4} \text{ s}^{-1}$. Both homolysis products are known to react very rapidly with molecular oxygen.

The isopropylperoxy radical is formed with a rate constant of $k_2/M^{-1}s^{-1} \approx 1 \times 10^9$ (47); likewise the formation of CrO_{2aq}^{2+} occurs with a rate constant of $(1.6 \pm 0.2) \times 10^8 M^{-1}s^{-1}$ (71,85,86), measured by pulse radiolysis. The second propagating reaction is the subsequent attack of the peroxy radical on the isopropylchromium(III) ion, releasing an isopropyl radical, Reaction 1-3, and forming an (unstable) isopropylperoxochromium(III) ion. The isopropyl radical continues the chain reaction by Reaction 1-2.

Termination of alkylperoxy radicals via the bimolecular Reaction 1-4 is well established, although the mechanism is still somewhat doubtful. In the Russell Mechanism (91) the self-reaction of secondary (and primary) alkylperoxy radicals is theorized as involving the decomposition of a tetroxide, formed in a cyclic transition state. Transfer of an α -hydrogen atom from one radical to the α -oxygen of the other results in the formation of ketone (or aldehyde), alcohol, and an oxygen molecule. For isopropylperoxy radicals, the rate of termination has been measured only in hydrocarbon solvents, where a value of $2k_4/M^{-1}s^{-1} = 3 \times 10^6$ was reported (92).

The rate law derived from Scheme A can be shown to be in agreement with that obtained experimentally, Equation 1-24. The isopropylchromium(III) complex disappears by two pathways, Reactions 1-1 and 1-3, which defines the rate law as ($k_1 \equiv k_h$),

$$\frac{-d[RCr]}{dt} = k_h [RCr^{2+}] + k_3 [RCr^{2+}][ROO^\bullet] \quad (1-56)$$

If the steady-state approximation is made for the free-radicals, R^\bullet and ROO^\bullet , as a consequence, the rate of initiation must be equal to the rate of termination,

$$k_h [RCr^{2+}] = 2k_4 [ROO^\bullet]_{s.s.}^2 \quad (1-57)$$

From Equation 1-57, the steady-state concentration of the peroxy radical can be obtained in terms of the concentration of the organochromium(III) ion,

$$[ROO^\bullet]_{s.s.} = \left[\frac{k_h [RCr^{2+}]}{2k_4} \right]^{1/2}, \quad (1-58)$$

which is substituted into the rate law, Equation 1-55. The assumption of long chains reduces Equation 1-56 to the experimentally observed form.

This approximation states that the major pathway by which

$(CH_3)_2CHCr(H_2O)_5^{2+}$ reacts is via the propagation step, and not initiation (homolysis), $k_3 [RCr^{2+}] [ROO^\bullet] \gg k_h [RCr^{2+}]$, giving the following rate law,

$$\frac{-d[RCr^{2+}]}{dt} = k_3 \left(\frac{k_h}{2k_4} \right)^{1/2} [RCr^{2+}]^{3/2} \quad (1-59)$$

The experimental rate constant, k_{obs} , is identified with the individual rate constants,

$$k_{obs} = k_3 \left(\frac{k_h}{2k_4} \right)^{1/2} \quad (1-41)$$

The chain length or efficiency of the propagating steps is defined as the rate of reaction divided by the rate of initiation,

$$\text{chain length} = \frac{k_{\text{obs}} [\text{RCr}^{2+}]^{3/2}}{k_h [\text{RCr}^{2+}]} = \frac{k_{\text{obs}} [\text{RCr}^{2+}]^{1/2}}{k_h} \quad (1-60)$$

It is dependent on the concentration of organochromium(III) so decreases continually throughout the reaction. Typical values are 90 at $1 \times 10^{-3} \text{M}$ $(\text{CH}_3)_2\text{CHCr}(\text{H}_2\text{O})_5^{2+}$ and 64 at $5 \times 10^{-4} \text{M}$; justifying the long chain approximation for about 90% reaction. However, at very low $[\text{RCr}^{2+}]$, the chain length will drop substantially and a mixed first- and three-halves-order dependence on organochromium(III) is predicted. Also the rate of acidolysis will no longer be negligible at very low $[\text{RCr}^{2+}]$, so the rate law will change form somewhat,

$$\frac{-d[\text{RCr}^{2+}]}{dt} = (k_h + k_a)[\text{RCr}^{2+}] + k_{\text{obs}}[\text{RCr}^{2+}]^{3/2} \quad (1-29)$$

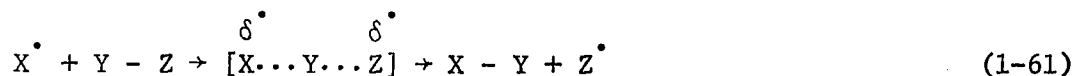
For $[\text{RCr}^{2+}]_0 = 5 \times 10^{-5} \text{M}$, a chain length of only 20 is calculated, and the contribution of the term first-order in $[\text{RCr}^{2+}]$ to the loss of organochromium(III) is

$$\frac{(2.85 \times 10^{-4})(5 \times 10^{-5})}{(2.85 \times 10^{-4})(5 \times 10^{-5}) + (0.51)(5 \times 10^{-5})^{3/2}} \times 100 = 7.3\%$$

at the start of the reaction, increasing to 13.6% after two half-lives. Therefore, it is apparent a simple three-halves-order treatment of the data is not sufficient at these low isopropylchromium(III) concentrations, as was seen experimentally.

The second propagating step, Equation 1-3, deserves further discussion. This reaction involves the homolytic attack of the isopropylperoxy radical on the chromium center in a reaction classified as a

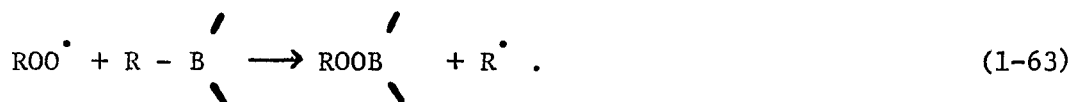
bimolecular homolytic substitution, or S_H2 reaction (40). In more general terms, an S_H2 reaction involves attack of a radical X^\cdot on a molecule YZ , displacing Z^\cdot , while forming a new bond between X and Y .



Hydrogen-abstraction is the simplest and most common type of radical displacement reaction; the autoxidation of organic compounds involves hydrogen-abstraction by peroxy radicals in a chain-propagating step (see Introduction).



Radical displacement by peroxy radicals at a multivalent center is more rare, although there are a few authentic examples. In particular, in the autoxidation of organoboranes to organoperoxyboranes, it is now widely held (49-59) that a free-radical mechanism is operative, in which the rate-controlling, chain-propagating step is an S_H2 displacement by ROO^\cdot on the boron center,



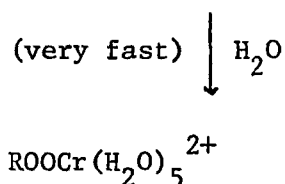
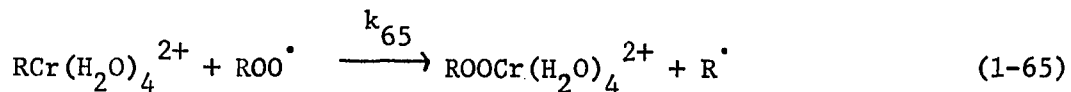
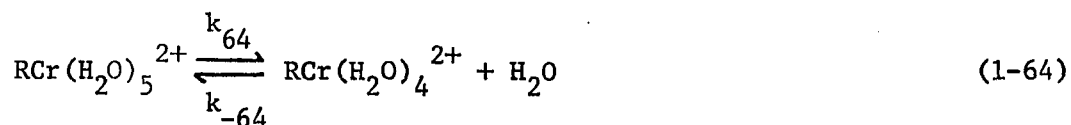
Evidence (49-59) for this reaction type is supported by stereochemical arguments, the ability to scavenge radical intermediates with powerful inhibitors, and ESR studies. Rates for Reaction 1-63 have been determined for several R groups, with values for k_{63} ranging from 1×10^3 to $\sim 1 \times 10^7 M^{-1} s^{-1}$ (56,57,59). Likewise, the autoxidations of Grignard reagents (93) and organometallic compounds of zinc, cadmium, aluminum, and tin (94) can be explained in terms of a S_H2 attack at the metal.

Studies involving similar reactions with organometallic compounds of the transition metals are quite scarce (40). A reaction analogous to 1-63 was presented for the formation of unstable organometallic peroxides of alkyltitanium, -zirconium, and -dimolybdenum, and -tungsten compounds (58).

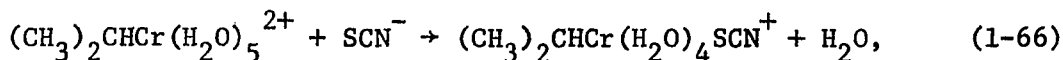
The rate of S_H2 displacement at $(CH_3)_2CHCr(H_2O)_5^{2+}$ can be estimated from the kinetic data. From Equation 1-41,

$$\begin{aligned}
 k_3 &= k_{\text{obs}} \left(\frac{2k_4}{k_h} \right)^{1/2} \\
 &\approx 0.51 \left(\frac{3 \times 10^6}{1.78 \times 10^{-4}} \right)^{1/2} \\
 &\approx 6.6 \times 10^4 \text{ M}^{-1} \text{ s}^{-1} .
 \end{aligned}$$

This rapid a substitution reaction at chromium(III) is highly unusual. For example, the aquation of acidopentaaquochromium(III) complexes, $XCr(H_2O)_5^{2+}$, proceeds (95) by the following first-order rate constants at 25.0°C (k/s^{-1} , X): 5.14×10^{-6} , Br; 1.10×10^{-4} , I; and 7.35×10^{-5} , NO_3 . The mechanism for aquation of these complexes is believed (96) to be an associative interchange (I_a) substitution. The alkyl group of the organochromium(III) complexes is known to labilize the trans-water to a large extent (97,98) which suggested the possibility that the isopropylperoxy radical may attack at this vacant position, eliminating the need to invoke a seven-coordinate transition state.



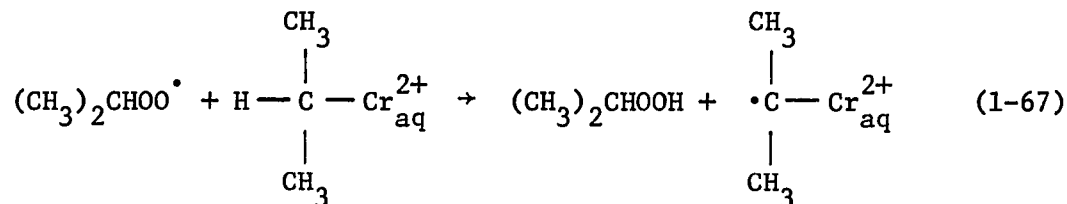
The rate of incorporation of SCN^- into the coordination sphere of $(\text{CH}_3)_2\text{CHCr}(\text{H}_2\text{O})_5^{2+}$ was measured (98) to determine the feasibility of a reaction scheme such as Reactions 1-64 and 1-65. For Reaction 1-66,



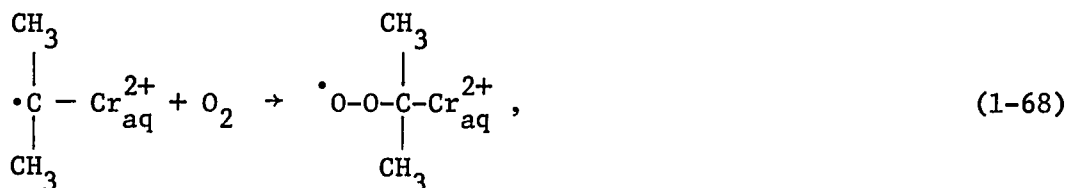
a second-order rate constant of only $1.25 \pm 0.02 \text{ M}^{-1} \text{ s}^{-1}$ at 25.0°C was calculated, far less than the rate required for $\text{S}_{\text{H}}2$ attack by $(\text{CH}_3)_2\text{CHOO}^\bullet$, thereby eliminating a dissociative-type mechanism. One must conclude, therefore, from the available data that substitution occurs via a seven-coordinate intermediate, or by an associative mechanism, as postulated (see earlier) for other chromium(III) complexes. Supportive of this assignment is the reduction of cobalt(III) and ruthenium(III) complexes by hydroxyalkyl radicals. The mechanism is believed (99-102) to proceed by an inner-sphere electron transfer process, although there is disagreement (102) on the intimate mechanistic details. These reactions are very rapid; second-order rate constants of 10^6 - $10^8 \text{ M}^{-1} \text{ s}^{-1}$ are common (101), although it is possible direct attack

at the metal center is occurring only for $\text{Ru}(\text{NH}_3)_6^{3+}$ (101), and hydroxyalkyl radicals reduce $\text{Co}(\text{III})$ complexes via a ligand-bridged intermediate (101,102). Further study of the $\text{S}_{\text{H}}2$ reactions of other alkylperoxy radicals with organochromium(III) is necessary to formulate a more complete mechanism.

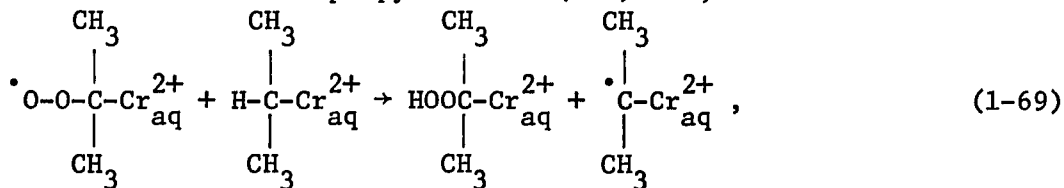
For the sake of completeness, another scheme for the autoxidation of $(\text{CH}_3)_2\text{CHCr}(\text{H}_2\text{O})_5^{2+}$ ought to be considered. Abstraction of the hydrogen atom from the α -carbon of $(\text{CH}_3)_2\text{CHCr}(\text{H}_2\text{O})_5^{2+}$ by $(\text{CH}_3)_2\text{CHOO}^\bullet$ would lead to $(\text{CH}_3)_2\text{CHOOH}$ and an alkyl radical-chromium(III) complex.



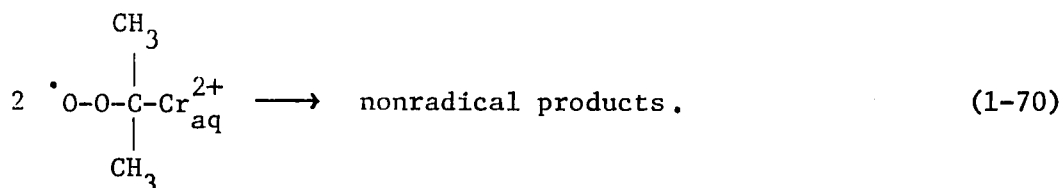
It is possible this species may mimic the reactivity of alkyl free-radicals towards O_2 ,



forming a peroxychromium(III) ion which subsequently abstracts a hydrogen atom from another isopropylchromium(III) ion,



releasing $\cdot\text{C}(\text{CH}_3)_2\text{Cr}_{\text{aq}}^{2+}$ to continue the chain-reaction via Reaction 1-68. In order for this scheme to give the experimentally observed rate law, only Reactions 1-68 and 1-69 can be the chain-propagating steps, and a new termination reaction must be operative,



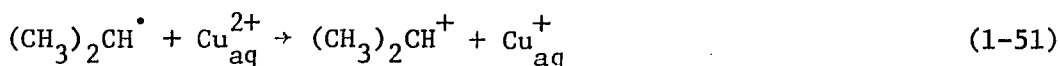
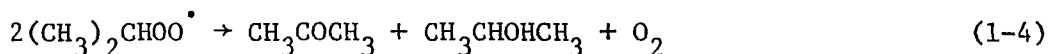
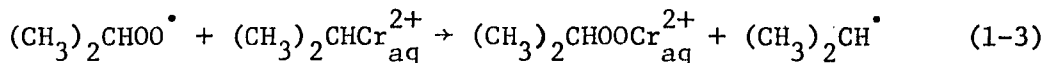
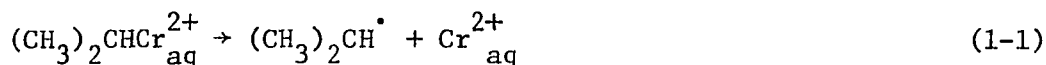
The products expected from such a scheme must derive from $\text{HOOC}(\text{CH}_3)_2\text{Cr}(\text{H}_2\text{O})_5^{2+}$. Reaction with H_3O^+ could conceivably produce the ultimate products of acetone and $\text{Cr}(\text{H}_2\text{O})_6^{3+}$.

However, there is a serious problem with such a scheme. Peroxy radicals are comparatively unreactive, and hence rather selective hydrogen abstractors (47). Abstraction of even allylic or benzylic hydrogen is quite slow--for example, abstraction from cumene by the cumylperoxy radical has $k/M^{-1}\text{s}^{-1} = 0.18$ at 30°C (103). Rates are also affected by polar and steric factors, increasing with substitution of electron-donating groups and with less steric bulk on the substrate and peroxy radical. Because the α -H of the isopropyl ligand is a secondary hydrogen, in addition to its close proximity to the bulky, electro-positive chromium(III) center, the rate of abstraction should be quite slow, several orders of magnitude less than the measured rate constant of $\text{ca. } 10^4 \text{ M}^{-1} \text{ s}^{-1}$. Surely it is unlikely that hydrogen abstraction by the $\cdot\text{OOC}(\text{CH}_3)_2\text{Cr}(\text{H}_2\text{O})_5^{2+}$ ion would be any more favorable, so this scheme is eliminated.

An estimation of the rate of oxidation of $\text{Fe}_{\text{aq}}^{2+}$ by $(\text{CH}_3)_2\text{CHOO}^\bullet$ can be made from the kinetic results obtained in its presence. The slow first-order loss in isopropylchromium(III) measured in the presence of $\text{Fe}_{\text{aq}}^{2+}$, is faster, $k = (4.27 \pm 0.03) \times 10^{-4} \text{ s}^{-1}$, than just homolysis and acidolysis, $(k_h + k_a) = 2.85 \times 10^{-4} \text{ s}^{-1}$. If the propagating step, Reaction 1-3, was eliminated by $\text{Fe}_{\text{aq}}^{2+}$, then the rates should be equal; the fact that they aren't implies $\text{Fe}_{\text{aq}}^{2+}$ is not completely effective in scavenging the chain-propagating radical. Since the concentrations of $\text{Fe}_{\text{aq}}^{2+}$ and $(\text{CH}_3)_2\text{CHCr}(\text{H}_2\text{O})_5^{2+}$ were of similar magnitude in the kinetic runs, each must react with a similar rate towards the peroxy radical. Hence, the rate of oxidation of $\text{Fe}_{\text{aq}}^{2+}$ by $(\text{CH}_3)_2\text{CHOO}^\bullet$, Reaction 1-47, must be about $10^4 - 10^5 \text{ M}^{-1} \text{ s}^{-1}$.

The kinetic effect of high concentrations of $\text{Cu}_{\text{aq}}^{2+}$ follows directly from Scheme A, when an additional termination step, Reaction 1-51, is included.

Scheme A in the presence of $\text{Cu}_{\text{aq}}^{2+}$:



Because Reaction 1-51 is a much more effective termination step (at high $[\text{Cu}_{\text{aq}}^{2+}]$) than the bimolecular reaction of isopropylperoxy radicals, Reaction 1-4 may be considered unimportant. The rate law can be derived by making the steady-state approximation for the free-radicals, from which it follows that the rate of initiation is equal to that of termination ($k_1 \equiv k_h$),

$$k_h [\text{RCr}^{2+}] = k_{51} [\text{R}^\bullet]_{\text{s.s.}} [\text{Cu}^{2+}] \quad (1-71)$$

The steady-state concentration of isopropylperoxy radicals is given by,

$$[\text{ROO}^\bullet]_{\text{s.s.}} = \frac{k_2 [\text{R}^\bullet]_{\text{s.s.}} [\text{O}_2]}{k_3 [\text{RCr}^{2+}]}, \quad (1-72)$$

which, after substitution of $[\text{R}^\bullet]_{\text{s.s.}}$ derived from Equation 1-71, simplifies to,

$$[\text{ROO}^\bullet]_{\text{s.s.}} = \frac{k_1 k_2 [\text{O}_2]}{k_3 k_{51} [\text{Cu}^{2+}]} \quad (1-73)$$

The rate law in the presence of $\text{Cu}_{\text{aq}}^{2+}$ becomes,

$$\frac{-d[\text{RCr}^{2+}]}{dt} = \left[(k_h + k_a) + \frac{k_h k_2 [\text{O}_2]}{k_{51} [\text{Cu}^{2+}]} \right] [\text{RCr}^{2+}] \quad (1-74)$$

where the rate constant for acidolysis has been included for these slow reactions. The experimentally obtained rate constant is then identified as,

$$k_{\text{obs}}^{\text{Cu}} = (k_h + k_a) + \frac{k_h k_2 [\text{O}_2]}{k_{51} [\text{Cu}^{2+}]} \quad (1-75)$$

Equation 1-75 predicts that a plot of $k_{\text{obs}}^{\text{Cu}}$ versus $[\text{Cu}^{2+}]^{-1}$ at constant $[\text{O}_2]$ should be linear, as was confirmed experimentally, Figure 1-6. The slope of this line is equal to $k_h k_2 [\text{O}_2] / k_{51}$ with an intercept equal to $(k_h + k_a)$. An estimation of k_{51} can be obtained from the slope since k_h is known, and an approximate value for k_2 exists:

$$k_{51} = \frac{k_h k_2 [\text{O}_2]}{(\text{slope})} = \frac{(1.78 \times 10^{-4})(\sim 1 \times 10^9)(1.05 \times 10^{-3})}{4.84 \times 10^{-5}}$$

$$\approx 3.9 \times 10^6 \text{ M}^{-1} \text{ s}^{-1}.$$

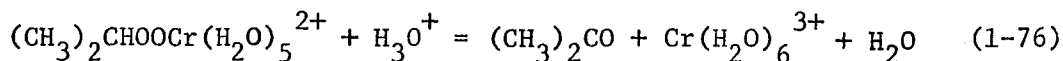
The intercept from Figure 1-6 is $(6.46 \pm 0.69) \times 10^{-4} \text{ s}^{-1}$, or about two times larger than the value measured independently for $(k_h + k_a)$, $2.85 \times 10^{-4} \text{ s}^{-1}$, not unreasonable agreement.

Similarly, from Equation 1-75 a plot of $k_{\text{obs}}^{\text{Cu}}$ versus $[\text{O}_2]$ at a constant $\text{Cu}_{\text{aq}}^{2+}$ concentration should be linear, with a slope, $(k_h k_2) / (k_{51} [\text{Cu}^{2+}])$, and intercept $(k_h + k_a)$. From Figure 1-7, k_{51} is estimated as,

$$k_{51} = \frac{k_h k_2}{(\text{slope}) [\text{Cu}^{2+}]} = \frac{(1.78 \times 10^{-4})(\sim 1 \times 10^9)}{(0.84)(0.10)} \approx 2.1 \times 10^6 \text{ M}^{-1} \text{ s}^{-1},$$

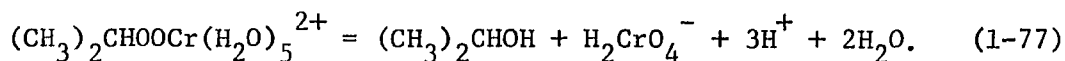
similar to the value obtained from Figure 1-6. Both estimates are in good agreement with the rate constants estimated by other workers-- $5.0 \times 10^7 \text{ M}^{-1} \text{ s}^{-1}$ at 25.5°C in 66% V/V acetic acid/water (87) and $5.0 \times 10^6 \text{ M}^{-1} \text{ s}^{-1}$ at 25.5°C in 44% V/V acetonitrile/acetic acid (88). The sum of k_h and k_a , from the intercept of Figure 1-7, is $(3.8 \pm 0.9) \times 10^{-4} \text{ s}^{-1}$, in good agreement with the independently obtained value.

The major products of the autoxidation reaction--acetone and $\text{Cr}(\text{H}_2\text{O})_6^{3+}$ --can be readily explained as the products of a rapid reaction of the isopropylperoxochromium(III) ion.



In addition, some acetone will be produced by the termination of two isopropylperoxy radicals. The analogous isopropylperoxocobaloxime reacts via two parallel reactions in aqueous perchloric acid to form acetone and isopropyl hydroperoxide in a 42:58 ratio (104). Acetone was accounted for (104) by O-O bond-cleavage accompanied by breakage of the α -C-H bond of the isopropyl ligand. Isopropyl hydroperoxide arises from O-Co bond-cleavage, assisted by proton transfer from an oxime oxygen to the α -O-atom of the peroxo linkage (104). Since an internal proton transfer mechanism is precluded for the decomposition of the peroxochromium complex, the absence of isopropyl hydroperoxide may result from the inability of a free proton to assist in O-Cr bond-breaking, at a rate competitive with acetone formation via O-O bond-cleavage.

The small amount of 2-propanol produced can conceivably be formed from two sources--the termination reaction, 1-4, and an internal redox reaction of the isopropylperoxochromium(III) ion, acting in competition to protonolysis.



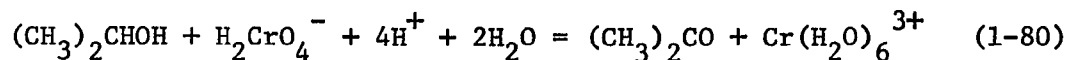
Formation of chromium(V) is suggested as the oxidation product because reduction of the isopropylperoxo ligand to 2-propanol requires a

two-electron transfer from chromium(III). Reaction 1-77 is analogous to processes suggested for $\text{CrO}_2\text{H}^{2+}$ (105) and $\text{FeO}_2\text{H}^{2+}$ (106),



in which Cr(V) and Fe(V), respectively, are the oxidation products.

The ultimate fate of Cr(V) is too complex in such a system to predict, although it is possible oxidation of 2-propanol may produce acetone and $\text{Cr}(\text{H}_2\text{O})_6^{3+}$ (107).



If this is the case, the termination reaction is the only source of 2-propanol. The slight dependence of the yields of acetone and 2-propanol on $[\text{H}_3\text{O}^+]$ probably means the rate of Reaction 1-76 (or 1-80, possibly) is acid-catalyzed in order to explain the decreased yield of acetone at lower acid concentrations, accompanied by an increase in 2-propanol. The inability to isolate the isopropylperoxochromium(III) intermediate is unfortunate in that it limits a complete analysis of its decomposition reactions.

The small amount of HCrO_4^- ion probably arises from $\text{CrO}_{2\text{aq}}^{2+}$ produced by Reaction 1-5. Solutions of $\text{CrO}_{2\text{aq}}^{2+}$ are known to be unstable at $\text{pH} < 3$, resulting in the formation of HCrO_4^- (71,86,105,108).

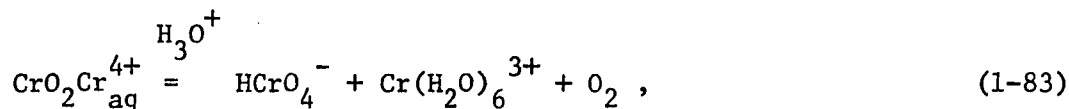


From pulse radiolysis studies (71) at pH \sim 2, $\text{CrO}_{2\text{aq}}^{2+}$ was reported to react by a second-order process, with a rate constant $\sim 2.4 \times 10^6 \text{ M}^{-1} \text{ s}^{-1}$, whereas preparation of $\text{CrO}_{2\text{aq}}^{2+}$ by mixing $\text{Cr}_{\text{aq}}^{2+}$ with excess O_2 resulted (71) in a first-order decomposition, with $t_{1/2} \sim 20$ min at pH 2. The large disparity between these rates is unexplained (71); however, it appears the latter value is more reliable.

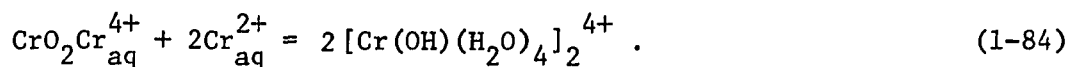
When $\text{CrO}_{2\text{aq}}^{2+}$ is produced in a solution containing a high concentration of chromium(II) ion, relative to that of oxygen, rapid scavenging by $\text{Cr}_{\text{aq}}^{2+}$ to form the peroxo-bridged intermediate, $\text{CrO}_2\text{Cr}_{\text{aq}}^{4+}$ (75), has been postulated (85,86).



$\text{CrO}_2\text{Cr}_{\text{aq}}^{4+}$ itself may slowly decompose ($t_{1/2} \sim 25$ min at 25.5°C) to HCrO_4^- and $\text{Cr}(\text{H}_2\text{O})_6^{3+}$ (105),



or be reduced by two equivalents of $\text{Cr}_{\text{aq}}^{2+}$ to $[\text{Cr}(\text{OH})(\text{H}_2\text{O})_4]_2^{4+}$ (85,86),



In the present system, however, a low concentration of $\text{Cr}_{\text{aq}}^{2+}$ is produced in a solution saturated with molecular oxygen, so it is highly unlikely that Reaction 1-82 can compete with the oxidation of $\text{Cr}_{\text{aq}}^{2+}$ to $\text{CrO}_{2\text{aq}}^{2+}$. This would require Reaction 1-82 to have a pseudo-first-order rate constant of $1 \times 10^5 \text{ s}^{-1}$, or greater, to divert $\text{Cr}_{\text{aq}}^{2+}$ from scavenging by O_2 ;

the concentration of CrO_2^{2+} actually present during a kinetic run will be low enough to require the second-order rate constant of Reaction 1-82 to approach the diffusion-controlled limit, in order that $k_{81}[\text{CrO}_2^{2+}]$ be $\sim 1 \times 10^5 \text{ s}^{-1}$, a rather unreasonable expectation. Consequently, Reactions 1-82 through 1-84 probably are unimportant in the autoxidation of $(\text{CH}_3)_2\text{CHCr}(\text{H}_2\text{O})_5^{2+}$, and the source of $[\text{Cr}(\text{OH})(\text{H}_2\text{O})_4]_2^{4+}$ in the present system is not readily apparent.

HCrO_4^- ion, once formed, appears to be stable toward further reaction with other autoxidation products. Reduction of 2-propanol is quite slow in $0.10 \text{ M H}_3\text{O}^+$, occurring with a second-order rate constant of $3.3 \times 10^{-4} \text{ M}^{-1} \text{ s}^{-1}$ at 40°C (109). Reaction of HCrO_4^- with $\text{Cr}_{\text{aq}}^{2+}$ ion may be precluded by the latter's rapid oxidation to CrO_2^{2+} . CrO_2^{2+} is not reactive towards HCrO_4^- , either, as indicated by the quantitative conversion of the former ion to the latter (71).

From the work cited (71) above for the rate of formation of HCrO_4^- ion, it appears this is not a rapid process, that is the rate of formation of HCrO_4^- is not expected to equal the rate of disappearance of $(\text{CH}_3)_2\text{CHCr}(\text{H}_2\text{O})_5^{2+}$. This may explain the dependence of the rate of autoxidation on the wavelength of monitoring. At wavelengths where the molar absorptivity of HCrO_4^- is comparable to that of $(\text{CH}_3)_2\text{CHCr}(\text{H}_2\text{O})_5^{2+}$, faster rates of reaction were measured; i.e., at 330 and 400 nm. A comparison of the molar absorptivities at the three monitoring wavelengths follows.

λ/nm	$\epsilon_{\text{HCrO}_4^-}/\text{M}^{-1}\text{cm}^{-1}$	$\epsilon_{(\text{CH}_3)_2\text{CHCr}_{\text{aq}}^{2+}}/\text{M}^{-1}\text{cm}^{-1}$
400	340	488
330	1100	1108
290	1250	2330

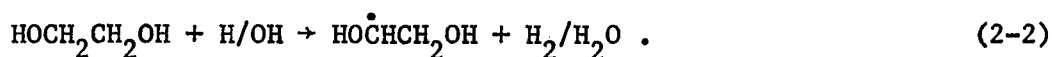
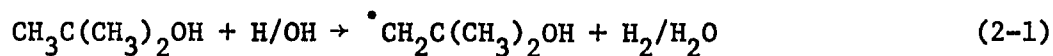
At any of the wavelengths studied, the decrease in absorbance monitored upon reaction is due to replacement of the intensely absorbing organochromium(III) by primarily $\text{Cr}(\text{H}_2\text{O})_6^{3+}$ and $[\text{Cr}(\text{OH})(\text{H}_2\text{O})_4]_2^{4+}$, which by comparison absorb very weakly, and also small quantities of HCrO_4^- of comparable molar absorptivity. If some delay occurs in the production of HCrO_4^- , the decreasing organochromium(III) absorbance will be superimposed on the slowly increasing absorbance due to appearance of HCrO_4^- . This will cause the reaction to appear to be reaching infinity more rapidly, falsely reflecting a more rapid reaction rate. The data collected at 290 nm are deemed the best measure of the rate of autoxidation.

PART II. ACID-CATALYZED CLEAVAGE OF
 β -HYDROXYETHYL(PENTAAQUO)CHROMIUM(III) ION

INTRODUCTION

Over the past several years, the chemistry of organopentaaquo-chromium(III) ions containing functional groups such as alcohols or ethers has been actively studied with the goal of understanding their effect on the reactivity of the carbon-chromium bond. Kinetic studies of the acid-catalyzed reactions of a few α -hydroxy-substituted complexes, $\text{HO}(\text{R},\text{R}')\text{CCr}(\text{H}_2\text{O})_5^{2+}$, and an α -alkoxyalkyl species, $\text{R}(\text{R}'\text{O})\text{CCr}(\text{H}_2\text{O})_5^{2+}$, were investigated by Schmidt, Swinehart, and Taube (18) in 1971. Using the pulse radiolysis technique, Cohen and Meyerstein (25) in 1974 extended these protonolysis studies to include several highly unstable α -hydroxy- and α -alkoxyalkyl complexes. Recently, a number of more highly substituted analogs of these organochromium(III) ions have been investigated using either a multimix stopped-flow instrument or conventional methods to study the kinetics (21-24). Reactions explored have included acidolysis and homolysis of the C-Cr bond (24) as well as oxidations by copper(II) and iron(III) ions (21,22) and reaction with mercury(II) ion (23).

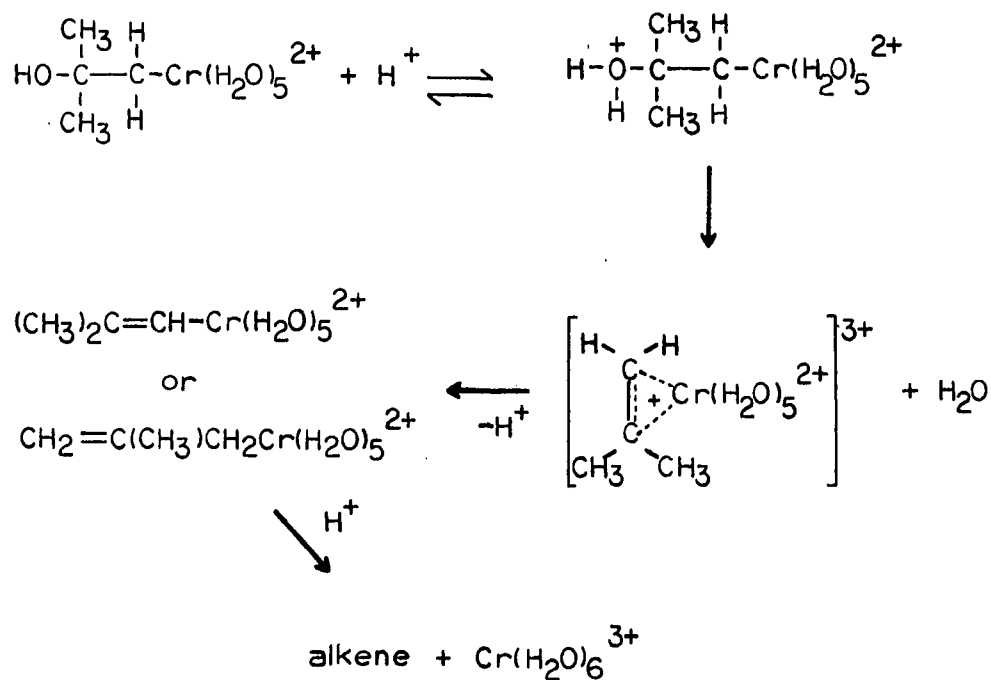
A related series of organochromium(III) ions, characterized by hydroxy- or alkoxy-substitution at the carbon atom β to the C-Cr bond, have been little explored. Cohen and Meyerstein (25) prepared the $\text{HO}(\text{CH}_3)_2\text{CCH}_2\text{Cr}(\text{H}_2\text{O})_5^{2+}$ ion, which contains a β -OH group, and $\text{HOCH}_2(\text{OH})\text{CHCr}(\text{H}_2\text{O})_5^{2+}$ with both α - and β -hydroxyl substitution, by pulse radiolysis. The organic radicals were generated in the presence of $\text{Cr}_{\text{aq}}^{2+}$ from the corresponding alcohols by H^\bullet or OH^\bullet abstraction,



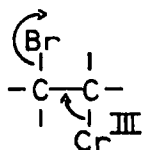
The organochromium(III) ions were formed in a subsequent reaction by the rapid coupling of $\text{Cr}_{\text{aq}}^{2+}$ and the radical (25),



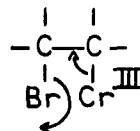
The kinetics of acidic decomposition and the absorption spectra of these highly unstable complexes were reported (25). In particular, the reaction of $\text{HO}(\text{CH}_3)_2\text{CCH}_2\text{Cr}(\text{H}_2\text{O})_5^{2+}$ with H_3O^+ was seen to follow a more complex rate law than the organochromium(III) ions with α -OH or α -OR substitution. Two separate processes, both first-order in $[\text{RCr}_{\text{aq}}^{2+}]$, were detected after formation of the complex; each process occurred by two pathways--one acid-independent and the other with a first-order dependence on $[\text{H}_3\text{O}^+]$. The acid-dependent pathway was interpreted by a mechanism proceeding through a pi-bonded intermediate, formed in a proton-assisted elimination of the β -hydroxyl group. It was suggested this intermediate rearranges to a more stable sigma-bonded alkenylchromium(III) ion, which slowly undergoes acidolysis by cleavage of the C-Cr bond to $\text{Cr}(\text{H}_2\text{O})_6^{3+}$ and the corresponding alkene.



It was of interest in this work to extend these studies by making the β -hydroxyethylpentaquo chromium(III) ion, $\text{HOCH}_2\text{CH}_2\text{Cr}(\text{H}_2\text{O})_5^{2+}$, and investigate its decomposition reaction in acidic solution. Electrophilic attack by H_3O^+ at the β -OH group could lead to elimination of water and the formation of a highly unstable π -bonded ethylenechromium(III) intermediate, easily releasing ethylene in a final step. However, if attack by H_3O^+ at the C-Cr bond were the preferred mode of reaction, rather than productive protonation of the β -OH group, acidolysis would lead to formation of ethanol as the organic product.



(2-7a)
trans-elimination

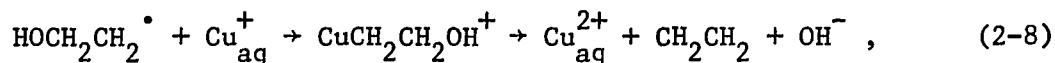


(2-7b)
cis-elimination

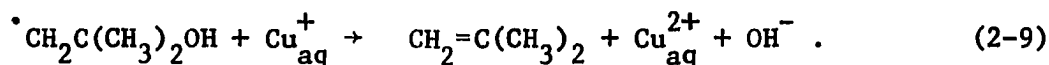
In Reaction 2-5 bromine atom abstraction by Cr^{II} generates a haloalkyl radical, which is scavenged by another Cr^{II} in Reaction 2-6 to form a β -bromoalkylchromium(III) intermediate. Elimination of the second bromine, as a bromide ion, can occur by two different pathways--one in which halide and Cr^{III} are released trans to one another (2-7a), and the other involving cis-elimination, in which the halogen is captured by chromium to form $\text{Cr}^{\text{III}}\text{Br}^{2+}$ (2-7b).

The reaction scheme was generalized (110) to include similar reductions of β -substituted alkyl halides by Cr^{II} ; in particular, β -hydroxyalkyl bromides preferred cis-elimination (2-7b) to form CrOH^{2+} .

The oxidation of metal ions, other than $\text{Cr}_{\text{aq}}^{2+}$, by β -hydroxyalkyl radicals has also been interpreted in terms of a π -bonded intermediate. The β -hydroxyethyl radical reacts with Cu_{aq}^+ to form an unstable organocopper(II) intermediate (111-113). Ethylene was the suggested product (111-113) of Reaction 2-8,

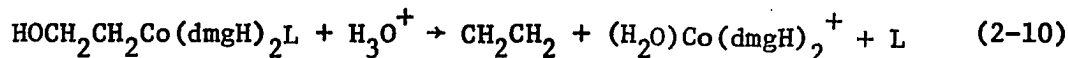


by analogy to a reaction where products were more completely characterized (112),



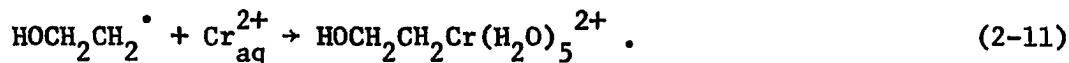
Reactions similar to 2-9 have been proposed for the oxidation of Ni^+ (114) and Cd^+ (115) by $\cdot\text{CH}_2\text{C}(\text{CH}_3)_2\text{OH}$.

The acid-catalyzed evolution of ethylene (2-10) from $\text{HOCH}_2\text{CH}_2\text{Co}(\text{dmgH})_2\text{L}$ (L = py or H_2O), which can be obtained in solid form, has been well studied (116-119).



The mechanism has been shown (118,119) to proceed through a pi-bonded intermediate in which ethylene is coordinated to cobalt.

Because of the expected instability of the $\text{HOCH}_2\text{CH}_2\text{Cr}(\text{H}_2\text{O})_5^{2+}$ ion, a rapid technique was necessary to detect and study its reactions. Flash photolysis was deemed suitable, in which the synthetic route to this organochromium(III) complex would be photochemical. In particular, a photochemical source of β -hydroxyethyl radicals, produced in the presence of $\text{Cr}_{\text{aq}}^{2+}$ ion, was needed,



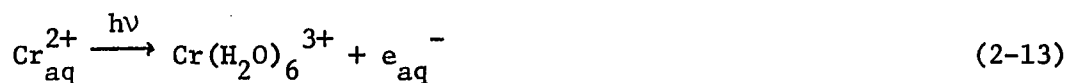
Three photochemical systems for generation of $\text{HOCH}_2\text{CH}_2\cdot$ were selected for study, on the basis of efficiency of radical production, water solubility, and thermal stability towards $\text{Cr}_{\text{aq}}^{2+}$.

System 1 is based upon the very efficient addition of a hydroxyl radical to ethylene, to form $\text{HOCH}_2\text{CH}_2\cdot$.



$$k_{12}/\text{M}^{-1}\text{s}^{-1} = 2.1 \times 10^9 \quad (120)^1$$

Hydroxyl radicals were indirectly obtained by taking advantage of the UV photochemistry of chromium(II) ion. As detailed in Part III, UV excitation of aqueous solutions of $\text{Cr}_{\text{aq}}^{2+}$ results in the production of hydrated electrons (Reaction 2-13).



In dilute acid (10^{-3}M or less) hydrated electrons can be competitively scavenged by nitrous oxide to form hydroxyl radicals (Reactions 2-14 and 2-15), rather than conversion to hydrogen atoms by reaction with H_3O^+ (Reaction 2-16).



$$k_{14}/\text{M}^{-1}\text{s}^{-1} = 8.7 \times 10^9 \quad (121)$$



$$\text{p}K_{15} = 11.9 \pm 0.2 \quad (122)$$



$$k_{16}/\text{M}^{-1}\text{s}^{-1} = 2.3 \times 10^{10} \quad (123)$$

¹ k_{12} was obtained as explained on page 133.

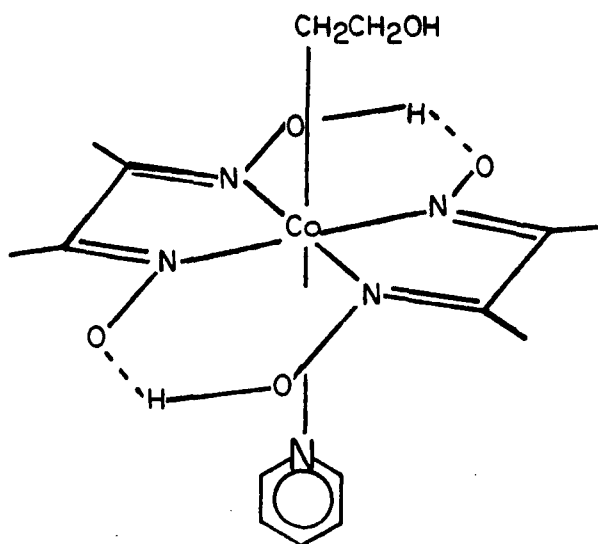
Therefore, flash photolysis of a weakly acidic solution of $\text{Cr}_{\text{aq}}^{2+}$, saturated with N_2O and ethylene, will generate $\text{HOCH}_2\text{CH}_2^\bullet$ radicals by the rapid sequence of Reactions 2-13, 2-14 and 2-15, and 2-12. The organochromium(III) ion will be formed in a subsequent reaction, 2-11. The nitrous oxide, ethylene system is chemically very simple, with the advantage that complicating side reactions of the substrate are eliminated. However, OH^\bullet and not H^\bullet radicals, can be produced from e_{aq}^- only in dilute acid, so the usefulness of System 1 is somewhat limited.

The quantum yield¹ for formation of $\text{HOCH}_2\text{CH}_2^\bullet$ radicals can be no larger than $\phi(e_{\text{aq}}^-)$ and will actually be considerably less due to loss of hydrated electrons to H_3O^+ , reduction of $\text{Cr}_{\text{aq}}^{2+}$ to Cr^+ , scavenging of OH^\bullet by $\text{Cr}_{\text{aq}}^{2+}$ rather than ethylene, and self-reactions of e_{aq}^- and OH^\bullet radicals. Although $\phi(e_{\text{aq}}^-)$ has not been measured directly, the quantum yield for hydrogen gas formation in acid solution has been reported (124) to be 0.13; hence $\phi(e_{\text{aq}}^-) = 0.26$.

Flash photolysis of an alkylcobaloxime² complex was investigated as another source of the β -hydroxyethyl radical, System 2. Maillard and Giannotti (125) studied the visible continuous photolysis ($\lambda > 420 \text{ nm}$) of the (β -hydroxyethyl)pyridinacobaloxime,

¹Quantum yield is a measure of the efficiency of a photochemical process. For product formation, it is defined as the number of species formed divided by the number of photons absorbed.

²Cobaloxime is a trivial name given to complexes of bis(dimethylglyoximate)cobalt, $\text{Co}(\text{dmgH})_2$.

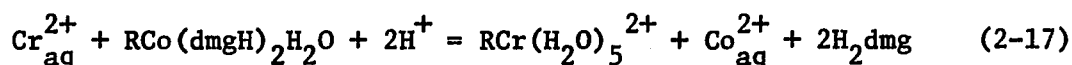


by ESR spectroscopy, including the use of spin-trapping techniques. At room temperature, in methanol or aqueous solution (pH 7), two free-radical species are produced--a hydrogen atom and the β -hydroxyethyl radical. In aqueous medium, release of $\text{HOCH}_2\text{CH}_2^\bullet$ is strongly favored over formation of H^\bullet . Light-induced Co-C bond homolysis produces the alkyl free radical and $\text{Co}(\text{dmgH})_2$; the hydrogen atom originates from the dimethylglyoximate chelate after photo-excitation, presumably (125) from the chelated proton of the dimethylglyoximate chelate. In very recent work the photo-induced homolysis of similar alkylcobaloximes, to form the alkyl free-radical, has been studied (126) by flash photolysis.

The quantum yield of free-radical formation was measured (127) in aqueous deoxygenated solution for a number of alkylcobaloximes, $\text{RCo}(\text{dmgH})_2\text{H}_2\text{O}$. Using irradiation at 380 nm, the quantum yields of photodecomposition (equivalent to yield of R^\bullet) were seen to be acid-

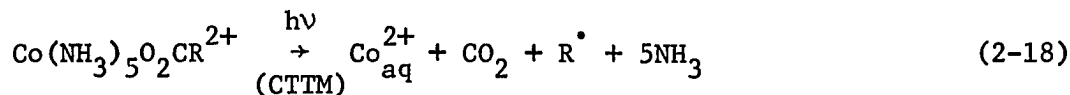
dependent in the region $1 \leq \text{pH} < 7$, maximizing around pH 2. The quantum yields were not particularly sensitive to the axial ligand R, ranging from 0.12 to 0.27 at pH 2, for the particular series of alkylcobaloximes studied. The results indicate that alkyl free-radicals are efficiently produced by the visible photolysis of alkylcobaloximes.

Alkylcobaloximes are known (128) to be cleaved by chromium(II) ion in a reaction where the alkyl ligand is transferred from the cobalt(III) center to the chromium(II) ion, forming an organochromium(III) ion and the cobalt(II) macrocycle (Reaction 2-17). The latter rapidly decomposes in acidic medium to $\text{Co}_{\text{aq}}^{2+}$.



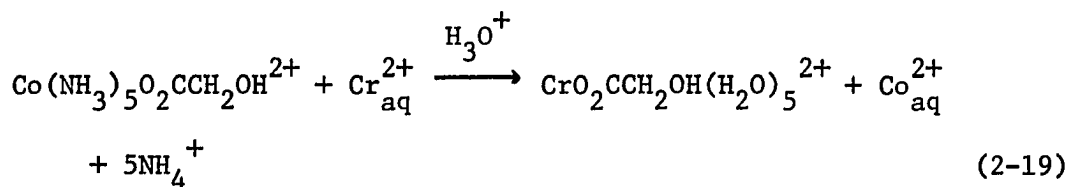
Although the rate of Reaction 2-17 had not been determined for $\text{R} = \text{CH}_2\text{CH}_2\text{OH}$, it was expected to be similar to that for $\text{R} = \text{CH}_2\text{CH}_3$ or $-\text{CH}_2\text{CH}_2\text{CH}_3$, which have apparent second-order rate constants of $8.8 \times 10^{-3} \text{ M}^{-1} \text{ s}^{-1}$ and $8.7 \times 10^{-4} \text{ M}^{-1} \text{ s}^{-1}$ at $0.4 \text{ M H}_3\text{O}^+$ (128).

System 3 is based on the UV photochemistry of a carboxylatopentaamminecobalt(III) complex, $[\text{Co}(\text{NH}_3)_5\text{O}_2\text{CCH}_2\text{CH}_2\text{OH}](\text{ClO}_4)_2$. Campano et al. (99) reported an extensive study in 1974 on the generation of organic free-radicals from the UV excitation of a series of $\text{Co}(\text{NH}_3)_5\text{O}_2\text{CR}^{2+}$ ions, where R was an alkyl or aryl group. Irradiation with 254 nm light in their intense ($\epsilon > 10^3 \text{ M}^{-1} \text{ cm}^{-1}$) ligand-to-metal charge transfer (CTTM) band was seen to induce photoreduction of the cobalt(III) center by electron-transfer from the carboxylato ligand, producing $\text{Co}_{\text{aq}}^{2+}$, CO_2 , and R^\bullet in a 1:1:1 stoichiometry (99,129), Reaction 2-18.



Direct observation of R^\bullet was accomplished using ESR (99,130-132); $\text{R} = \text{}^\bullet\text{CH}_2\text{C}_6\text{H}_5$ and $\text{}^\bullet\text{CH}_2\text{CO}_2\text{H}$ were also detected by their characteristic UV spectrum using flash photolysis (99). The quantum yield for $\text{Co}_{\text{aq}}^{2+}$, $\phi(\text{Co}^{2+})$, was determined at 254 nm and fell within the rather narrow range of 0.15-0.25 for most of the carboxylato complexes studied (99). By virtue of the stoichiometry of Equation 2-18, $\phi(\text{Co}^{2+})$ is equal to $\phi(\text{R})$, demonstrating CTTM excitation of $\text{Co}(\text{NH}_3)_5\text{O}_2\text{CR}^{2+}$ complexes is an efficient source of organic free-radicals for aqueous solution.

While the UV photochemistry of the $\text{Co}(\text{NH}_3)_5\text{O}_2\text{CCH}_2\text{CH}_2\text{OH}^{2+}$ complex has not been previously studied, nor has even a report of its synthesis appeared, there is every indication that this type of photoredox chemistry can be generalized to any $\text{Co}(\text{NH}_3)_5\text{O}_2\text{CR}^{2+}$ complex. However, for the $\text{Co}(\text{NH}_3)_5\text{O}_2\text{CCH}_2\text{CH}_2\text{OH}^{2+}$ species to be a useful source of $\text{}^\bullet\text{CH}_2\text{CH}_2\text{OH}$ for this work, it must be relatively stable towards reduction by $\text{Cr}_{\text{aq}}^{2+}$. While most cobalt(III) complexes of this family are reduced by $\text{Cr}_{\text{aq}}^{2+}$ in an inner-sphere-electron-transfer process (133,134), reaction with the structurally similar $\text{Co}(\text{NH}_3)_5\text{O}_2\text{CCH}_2\text{OH}^{2+}$ ion is slow enough to allow mixing of the cobalt(III)

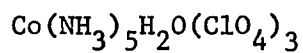


$$k_{19}(25^\circ\text{C}, 0.1-1.00 \text{ M H}^+)/\text{M}^{-1}\text{s}^{-1} = 3.06 \quad (135)$$

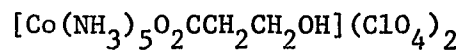
complex and chromium(II) ion immediately prior to a flash photolysis experiment. An additional methylene group in the carboxylato ligand is not expected to alter the rate of electron-transfer for the β -hydroxypropionato complex appreciably.

EXPERIMENTAL

Materials



The aquo derivative was made from $\text{Co}(\text{NH}_3)_5\text{CO}_3(\text{NO}_3) \cdot 1/2 \text{H}_2\text{O}$ (136) by treating (137) a slurry with an equivalent amount of concentrated HClO_4 . The precipitate was collected, washed with ethanol, then ether.



No report has appeared of the successful synthesis of this compound. In fact, in 1965 Butler and Taube (136) remarked, "complexes [of pentaamminecobalt(III)] with β -hydroxy acids as ligands could not be prepared because of their marked tendency to form lactones and polymeric species." In spite of this observation, several routes to synthesize this compound were attempted. Two methods were unsuccessful--the procedure of Fan and Gould (138) which involves refluxing $\text{Co}(\text{NH}_3)_5\text{CO}_3^+$ in methanol in the presence of a 10-fold excess of β -hydroxypropionic acid, and the preparation used by Dockal, Everhart, and Gould (139), which also utilizes the carbonato complex as starting material, but employs diethylene glycol as the solvent.

The synthetic method of Jackman et al. (140) was more promising. In this method, the carboxylato complex is made by reaction of hydroxopentaamminecobalt(III) ion with the anhydride of the carboxylic acid. The success of the synthesis depends on the ability to make the

corresponding anhydride. It need not be isolated, but can be made in situ, by reaction of the carboxylic acid with dicyclohexylcarbodiimide. It was not known if the β -hydroxy group would be stable to the dehydration, which could lead to the vinylic anhydride instead. However, it was thought it would be possible to distinguish the resulting acrylate complex from the β -hydroxypropionate complex, by NMR methods. Hydroxopentaamminecobalt(III) ion is obtained by deprotonation of the aquo complex with N,N-dimethylbenzylamine, in solution.

The procedure was followed as published, except for modifications necessary to isolate the product. 3.95 mmol (0.82 g) dicyclohexylcarbodiimide in 8 mL DMF were stirred with 9.21 mmol (0.91 g) β -hydroxypropionic acid (see below) in 3 mL DMF, for 1 hr. The corresponding urea precipitates almost immediately. 1.35 mmol (0.062g) $\text{Co}(\text{NH}_3)_5\text{H}_2\text{O}(\text{ClO}_4)_3$ in 10.2 mmol (1.52 mL) N,N-dimethylbenzylamine and 5 mL DMF were added, and the mixture allowed to stir for 15 min. After cooling 15 min in ice-water, the urea was removed by filtration, and the filtrate evaporated under reduced pressure, at 50° , to remove the DMF. This solution was treated with water (3 x 5 mL), followed by further evaporation after each addition at $30-40^\circ$. Any remaining urea was filtered off. At this point the reference calls for addition of ethanol to cause the precipitation of the product. However, only a very viscous syrup was obtained, which had to be taken back up in water, and then precipitated by addition of perchlorate ion. Both concentrated HClO_4 and 5 M NaClO_4 were used, the latter giving more satisfactory results. The light-pink product was then washed with ethanol, ethanol-ether (1:1), and then ether.

Recrystallization was attempted in dilute HClO_4 at $\sim 60^\circ\text{C}$, but only a noncrystalline type material could be recovered.

The cobalt content of the solid was determined by a photochemical procedure described below. Values of 10.12 to 11.50% Co were measured, for different preparations, much lower than the expected 13.64%. The visible spectrum gave maxima at 352 and 502 nm, with molar absorptivities of 60.3-61.6 and $72.3 \text{ M}^{-1} \text{ cm}^{-1}$, respectively, based on percent Co. The position of the maxima and the magnitude of the absorptions are characteristic of carboxylatopentaamminecobalt(III) complexes (135). The ^1H NMR in D_2O or deuterated DMSO consisted of two broad resonances centered at $\sim \delta = 2.5$ ppm and $\sim \delta = 3.75$ ppm; integration gave a ratio of the downfield to upfield resonances of 2.8 to 1. The downfield resonance is presumably due to the protons of the 5 - cis - NH_3 , the β -methylene group of the carboxylato ligand, and, depending on the solvent, the hydroxyl group; the upfield resonance can be assigned to the trans- NH_3 and α -methylene protons. A ratio of from 2.8-3 to 1 is calculated, dependent upon the inclusion of the O-H proton. Distinct methylene resonances were expected, however, but were not clearly visible. A ^{13}C NMR was obtained in acidified D_2O with a sample concentration of about 0.3 M. Although it was much more complex than it should have been for such a simple carboxylato ligand, the presence of bound acid was indicated. There were a number of unassigned resonances, presumably impurities. The IR of the material was obtained as Nujol and Fluorolube mulls. It was compared to that of the glycolatopentaamminecobalt(III)

perchlorate. No clear evidence existed for the O-H absorption, expected at $\sim 3500 \text{ cm}^{-1}$, as present in the glycolato complex, although this may have been masked by N-H stretches at 3250 and 3320 cm^{-1} . Some C-H stretches were apparent; however, the IR spectra does not provide conclusive evidence for the identity of the material.

Since the method of synthesis of $\text{Co}(\text{NH}_3)_5\text{O}_2\text{CCH}_2\text{CH}_2\text{OH}(\text{ClO}_4)_2$ using the procedure of Jackman, et al. (140) was not completely successful, the final route employed was based on the traditional preparation for carboxylato complexes of pentaamminecobalt(III)--heating an excess of the carboxylic acid in the presence of $\text{Co}(\text{NH}_3)_5\text{H}_2\text{O}^{3+}$. 10 mmol (0.9 g) $\text{HOCH}_2\text{CH}_2\text{COOH}$ were mixed with a cold solution of 5 mmol (0.2 g) NaOH in about 5 mL H_2O to half-neutralize the acid. This solution was added to 2 mmol (0.9 g) $\text{Co}(\text{NH}_3)_5\text{H}_2\text{O}(\text{ClO}_4)_3$ dissolved in about 20 mL H_2O . The solution was stirred for about 20 hours at 45°C . The visible spectrum was indicative of a carboxylato complex. In some of the preparations, extractions with ether were done at this point, although in later preparations it was eliminated. Ion exchange separation of the solution was carried out successfully on the cooled solution, using Sephadex SP C-25 cation-exchange resin. A very long column was required, 25 cm, to separate the components from this size preparation. Elution with 0.01 M HClO_4 displaced a small volume of a pink-red solution which gave a visible spectrum indicative of a carboxylato complex. An attempt to isolate a solid product from this fraction resulted, after evaporation, to a very thick, syrupy material, which would not dry even under high vacuum. With 0.25 or 0.50 M HClO_4 , a large cherry-red fraction

was eluted, well-separated from the orange-red band of unreacted $\text{Co}(\text{NH}_3)_5\text{H}_2\text{O}^{3+}$ remaining on the column. The eluant required to displace the cherry-red band was indicative of a +2 charged species. Evaporation of this solution at 40-45^o, under reduced pressure, resulted in a wet precipitate, which after further drying over desiccant and then with ether, yielded a pink powder.

The percent Co in the sample was again very low, ranging from 9-12%. However, the visible spectrum was indicative of a carboxylato complex-- molar absorptivities of 70.4 $\text{M}^{-1}\text{cm}^{-1}$ at 502 nm and 57.7 $\text{M}^{-1}\text{cm}^{-1}$ at 351 nm were calculated, based on the percent Co actually determined. Minima were present at 316 and 404 nm. The ¹H NMR spectrum was obtained in D₂O using the HOD resonance at $\delta = 4.7$ ppm as the reference; it is shown in Figure 2-1. The α -methylene protons of the carboxylato ligand are seen as a multiplet, closely resembling a triplet, at $\delta = 2.6$ ppm, superimposed on a small broad trans-NH₃ resonance. Farther downfield, a larger broad resonance at $\sim \delta = 3.8$ ppm was assigned to the cis-NH₃ groups; splitting of this signal was taken as indicative of the triplet expected for the β -methylene protons. The O-H resonance is not expected in D₂O. Integration was attempted but resonances are broad and overlap with one another. A ¹³C NMR spectrum was cleaner than that found for the material prepared by the Jackman et al. (140) procedure, but like the ¹³C of the free acid (see below) consisted of a pair of resonances for each unique carbon atom of the carboxylato group, rather than simply three single absorbances. The spectrum was obtained in acidified D₂O

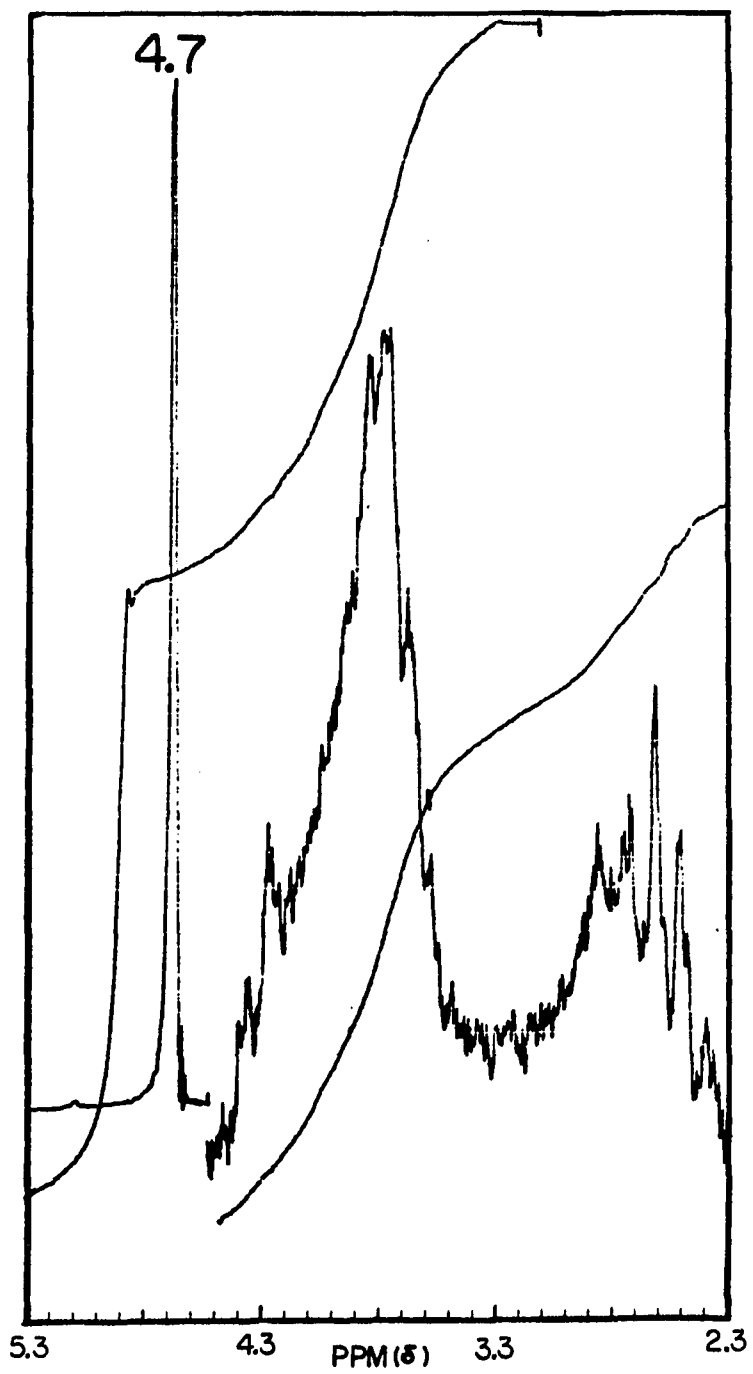


Figure 2-1. ^1H NMR of $\text{Co}(\text{NH}_3)_5\text{O}_2\text{CCH}_2\text{CH}_2\text{OH}(\text{ClO}_4)_2$ in D_2O , referenced to HOD at $\delta = 4.7$ ppm

with a sample concentration of 0.2 M and p-dioxane as internal reference. The pairs of resonances detected and their likely assignments are given below:

<u>ppm</u> ¹	<u>assignment</u> ²
185.4, 185.0 ³	bound $\text{-}\overset{\text{O}}{\parallel}\text{C}\text{-}\text{CH}_2\text{CH}_2\text{OH} + ?$
67.6, 58.8	bound $\text{-}\overset{\text{O}}{\parallel}\text{C}\text{-}\text{CH}_2\text{CH}_2\text{OH} + ?$
66.2, 57.8	free $\text{HO}-\overset{\text{O}}{\parallel}\text{C}-\text{CH}_2\text{CH}_2\text{OH} + ?$
62.3	not assigned
61.1	not assigned
40.9, 38.3	bound $\text{-}\overset{\text{O}}{\parallel}\text{C}\text{CH}_2\text{CH}_2\text{OH} + ?$
34.7, 33.6	free $\text{HOC}\overset{\text{O}}{\parallel}\text{CH}_2\text{CH}_2\text{OH} + ?$

¹Relative to p-dioxane = 67.0 ppm.

²Underlined carbon indicates assignment.

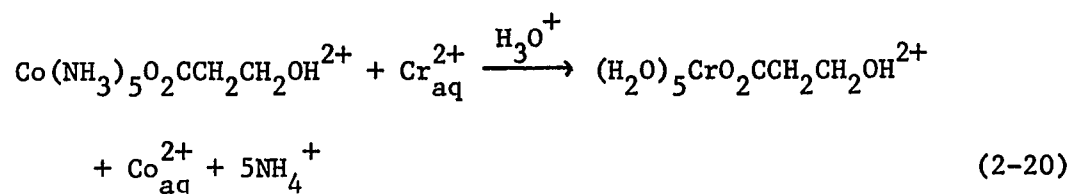
³No resonance (or pair of) assignable to the carboxylato C of the free acid was discernible over the baseline noise. This may not be totally unexpected as these resonances are the least intense in the spectrum of the free acid.

The assignments for the free carboxylic acid resonances were made after comparison to its spectrum, reported below. Complexation of the carboxylic acid to cobalt is expected to cause a downfield shift of the resonances, most apparent for the carbonato carbon; the assignments for bound acid were made on this premise. Two resonances are unaccounted for and must be impurities. The presence of pairs of resonances for the bound ligand(s) suggests there are two carboxylato cobalt complexes, with very similar chemical structures. It appears the impurity present in the spectrum of the free acid has been complexed to cobalt(III) also, along with the desired β -hydroxypropionato complex.

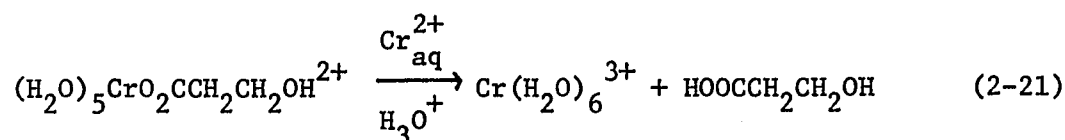
In summary, the ^1H NMR provides good evidence for coordination of the β -hydroxypropionato ligand to the pentaamminecobalt(III) ion. The visible spectrum and molar absorptivities also support a carboxylato complex. The ^{13}C NMR parallels that seen for free $\text{HOCH}_2\text{CH}_2\text{COOH}$; both appear to be contaminated with a very similar organic compound.

The percent Co of the cobalt complex is too low, again indicating the sample is impure. Unfortunately, the inability to recrystallize the material, without evaporation to dryness, does not allow it to be purified.

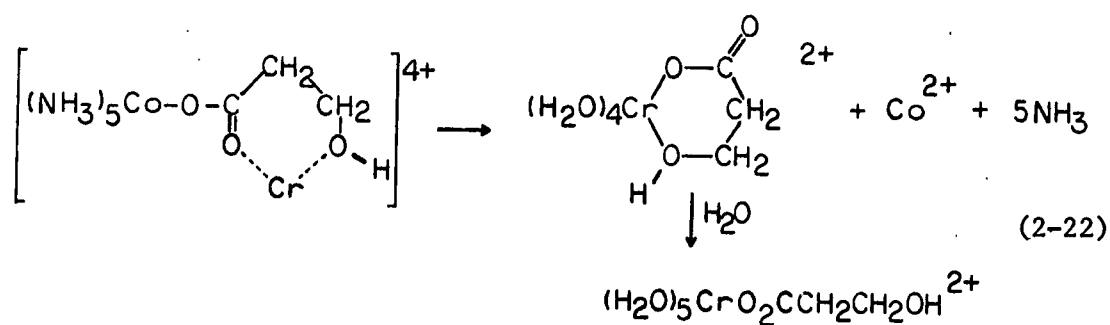
The rate of reaction of the cobalt complex with $\text{Cr}_{\text{aq}}^{2+}$ was measured to determine if the reactants were compatible long enough to be used in flash photolysis experiments. The reaction (Reaction 2-20) was followed spectroscopically, with either a large excess of the cobalt(III) complex or chromium(II) ion.



Rather than an expected simple pseudo-first-order reaction, a much slower, secondary reaction, whose rate was accelerated somewhat by a large excess of $[\text{Cr}^{2+}]$, was observed. This slower loss of absorbance might be a chromium(II) ion-catalyzed decomposition (Reaction 2-21) of the β -hydroxypropionatochromium(III) ion formed in Reaction 2-20.



Similar chromium(III) complexes have been reported (141) to undergo such catalysis. Another possible explanation is that the chromium(III) complex formed upon electron-transfer is metastable, reverting to $(\text{H}_2\text{O})_5\text{CrO}_2\text{CCH}_2\text{CH}_2\text{OH}^{2+}$ with time,



The rate of the first reaction was analyzed independently of the secondary step by the usual methods (142). In 0.10 M H_3O^+ , $\mu = 0.50$ M, $t \sim 25^\circ\text{C}$, a second-order rate constant of $0.8\text{--}1.1 \text{ M}^{-1}\text{s}^{-1}$ was obtained, similar to that for $\text{Cr}_{\text{aq}}^{2+}$ reduction of $\text{Co}(\text{NH}_3)_5\text{O}_2\text{CCH}_2\text{OH}^{2+}$ (135), as expected.

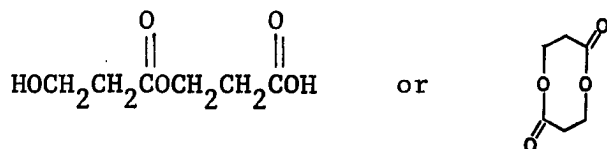
$\text{HOCH}_2\text{CH}_2\text{COOH}$

The literature preparation (143) was followed exactly. The percent purity was determined by titration with standardized NaOH. A weighed sample was dissolved in water and diluted to a known volume. Aliquots were titrated to a phenolphthalein end point. A percent acid of $95.4 \pm 2.3\%$ was measured, somewhat higher than the reported (143) value of 75–80%; the remainder was claimed (143) to be water. A ^1H NMR in D_2O , with Tiers' salt as the internal reference, consisted of a triplet at $\delta = 2.65$ ppm, assigned to the α -methylene protons, and a multiplet at $\delta \approx 3.8$ ppm, due to the β -methylene protons. Another multiplet at $\delta = 4.3$ ppm is probably due to the presence of a bimolecular esterification product, claimed as the contaminant in Aldrich supplied material. Splitting of the 2.65 ppm triplet (< 0.5 ppm), and the presence of a multiplet at 3.8 ppm, rather than a triplet, probably are indicative of this contaminant also. The integration of the 3.8 and 4.3 ppm multiplets is equal to that of the 2.65 ppm triplet. ^{13}C NMR spectra obtained in D_2O substantiated the presence of an impurity in the acid. Rather than the single resonance, expected for each of the three carbon atoms in the

β -hydroxypropionic acid molecule, a pair of resonances, separated by about 2 ppm, were detected where only a single absorption was predicted. The spectra were unaffected by pH (at pH 8 the entire spectrum was shifted downfield as expected) or dilution of the acid by a factor of 10. The resonances obtained at pH 0.2 are as follows:

<u>ppm</u> ¹	<u>Assignment</u> ²
176.8, 176.3	$\begin{array}{c} \text{O} \\ \\ \text{HOC}\underline{\text{C}}\text{H}_2\text{CH}_2\text{OH} + ? \end{array}$
66.3, 57.9	$\begin{array}{c} \text{O} \\ \\ \text{HOC}\text{CH}_2\underline{\text{C}}\text{H}_2\text{OH} + ? \end{array}$
36.9, 34.7	$\begin{array}{c} \text{O} \\ \\ \text{HOC}\text{CH}_2\text{C}\underline{\text{H}}_2\text{OH} + ? \end{array}$

These values are reasonable for this compound based on calculations (144). It is not possible to assign a structure to the impurity based on these numbers, but it is consistent with a bimolecular esterification product, acyclic or cyclic,



¹Relative to p-dioxane = 67.0 ppm.

²Underlined carbon indicates assignment.

HOCH₂CH₂Co(dmgh)₂py

This cobaloxime was made following the procedure reported by Wang (145). Details were sketchy as to the exact amount of 2-bromoethanol to add--a total of 12 mL were used in this procedure, added over a period of 6 hours, 2 mL per hour. A 1 min H₂ purge was done prior to each addition. After 21 hours of total reaction time, the TLC (Eastman 13181 silica gel) with 20% V/V 2-propanol/CHCl₃ showed most of the cobalt was present as the alkylated form. The reaction mixture itself looked bright yellow-brown. Ether was used to dry the product after recrystallization from CH₂Cl₂. A 48% yield was obtained. The ¹H NMR in CDCl₃ gave a singlet at δ = 2.19, one triplet at δ = 1.72, and another at δ = 3.07, all in ppm relative to TMS. These are assigned as the methyl resonances of dmg, and the α-methylene, and β-methylene protons, respectively. The characteristic spectrum for pyridine was seen as a series of resonances in the region 7 to 9 ppm. The integration was indicative of the desired material. The cobalt analysis gave 13.90%, compared to the theoretical of 14.26%, and the visible spectrum had maxima at 440 and 375 nm.

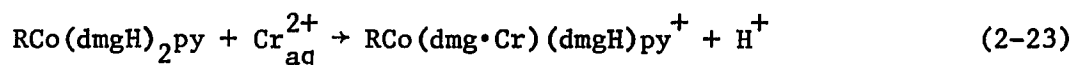
HOCH₂CH₂Co(dmgh)₂H₂O

The py adduct was converted (117) to the aquo by stirring 2 g (4.84 mmol) with a 3.75 fold excess (3.5 g) of AG50W-X8 cation-exchange resin, in ~ 350 mL H₂O for 1 min. The resin was removed by filtration, immediately, and the filtrate evaporated to dryness under reduced pressure at

35°. The orange-yellow material which remained was added to CHCl_3 , as suggested (Ref.145, p. 14), but some would not dissolve. The CHCl_3 soluble fraction, after silica gel chromatography (with 10% CH_3OH in CHCl_3), was evaporated under reduced pressure to dryness. The dark orange crystals were identified as the py adduct, by NMR. The CHCl_3 -insoluble material was shown to be the aquo complex, by ^1H NMR in d_4 -MeOH, from the absence of the pyridine resonance. An impurity with a resonance at $\delta = 2.1$ ppm was present. Since the percent Co was very low, 11.51% compared to the theoretical of 16.73%, the material was subjected to a purification procedure. It was taken up in MeOH, and eluted on silica gel with 20% MeOH/ CHCl_3 . The eluant was evaporated to dryness under reduced pressure, and washed with ether. The percent Co was 14.37%, still low, and the NMR was not cleaner. No further purification was attempted.

The rate of reaction of $\text{Cr}_{\text{aq}}^{2+}$ and $\text{HOCH}_2\text{CH}_2\text{Co}(\text{dmgH})_2\text{H}_2\text{O}$ was measured to determine if these reagents would be compatible long enough for a flash photolysis experiment, before substantial thermal reaction occurred. The reaction was followed, by monitoring the spectrum of the cobaloxime with time, of a solution of 7.6×10^{-5} M $\text{HOCH}_2\text{CH}_2\text{Co}(\text{dmgH})_2\text{H}_2\text{O}$ and 1.3×10^{-3} M $\text{Cr}_{\text{aq}}^{2+}$ in 0.050 M HClO_4 ($\mu = 0.054$ M (LiClO_4)). The rate of acidolysis in the absence of $\text{Cr}_{\text{aq}}^{2+}$ was measured at the same acidity and ionic strength. The difference in observed rates gives k_{obs} for reaction with $\text{Cr}_{\text{aq}}^{2+}$, $k_{\text{obs}} = (2.81 - 1.20) \times 10^{-3} \text{ s}^{-1}$; assuming a first-order dependence on $[\text{Cr}_{\text{aq}}^{2+}]$, the second-order rate constant of $1.23 \text{ M}^{-1} \text{ s}^{-1}$ is calculated. However, at low $[\text{H}_3\text{O}^+]$, $\sim 5 \times 10^{-3}$ M, reaction with $\text{Cr}_{\text{aq}}^{2+}$

was no longer simple, each reaction producing a species with λ_{\max} at 446 nm. Cleavage of halomethylcobaloximes by $\text{Cr}_{\text{aq}}^{2+}$ was previously seen (146) to generate unidentified complexes, characterized by maxima at 460 nm. It was suggested (146) these species were organocobaloxime-chromium binuclear complexes in which a chromium atom was coordinated to the dimethylglyoximate ligand through the oxygen atoms of two oxime groups.



To prevent Reaction 2-23 from occurring the di- BF_2 adduct of $\text{HOCH}_2\text{CH}_2\text{Co}(\text{dmgH})_2\text{py}$ was made; this would effectively block the oxime oxygens from coordination by $\text{Cr}_{\text{aq}}^{2+}$.

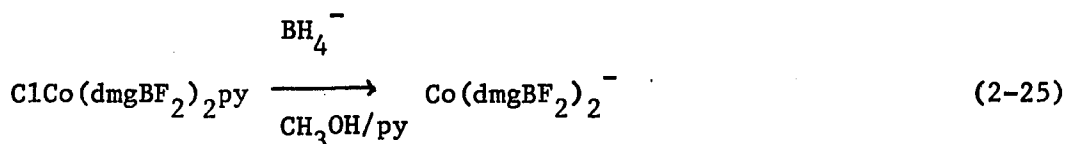
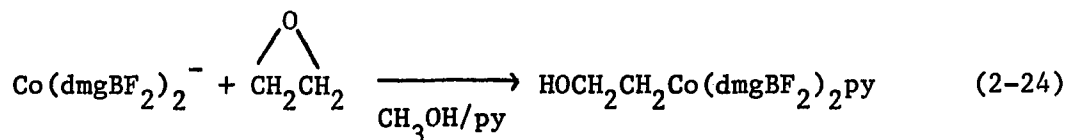
$\text{ClCo}(\text{dmgBF}_2)_2\text{py}$

The starting material $\text{ClCo}(\text{dmgH})_2\text{py}$ was prepared by the procedure reported by Schrauzer (147). However, a purer material can be obtained by an adaptation of the method reported by Costa, Tazher, and Puxeddu (148). $\text{ClCo}(\text{dmgH})_2\text{py}$ was converted to the BF_2 adduct by reaction with $\text{BF}_3 \cdot (\text{CH}_3\text{CH}_2)_2\text{O}$ as reported (149).

$\text{HOCH}_2\text{CH}_2\text{Co}(\text{dmgBF}_2)_2\text{py}$

The procedure was based on that reported by Wang (145), for the analogous β -hydroxy-n-propylcobaloxime. Although the preparation was successful, the procedure may be far from optimized.

The reaction makes use of the nucleophilic addition of the reduced cobaloxime to ethylene oxide, Reaction 2-24; $(\text{Co}^{\text{I}})^{-}$ is produced in situ by BH_4^- reduction of chlorocobaloxime, Reaction 2-25.



Since ethylene oxide is extremely volatile, boiling at 10°C , the reaction must, at least in the early states, be maintained at low enough temperature to ensure a sufficiently high concentration of the oxide in the solvent. Aliquots of liquid ethylene oxide were transferred by using a pre-cooled syringe, and working as rapidly as possible. Transfers were only semiquantitative, though, due to the difficulty of keeping the oxide liquified in the syringe.

A slurry of 3.85 g $\text{ClCo}(\text{dmgBF}_2)_2\text{py}$ (7.71 mmol) in 100 mL 1 M py in CH_3OH was deoxygenated by bubbling with nitrogen for 20 min, while cooling to -10°C in a $\text{CH}_3\text{OH}/\text{ice}$ bath. 1.2 g NaBH_4 (30.8 mmol) and a small amount of PdCl_2 were added; the solution turned dark-blue almost immediately. About 50 mL ethylene oxide (50x excess) were added over a period of about one hour, at which time the solution was greenish colored. Stirring was continued for another 1 1/2 hours at -10°C , while nitrogen flowed over the solution. Then the nitrogen purge was discontinued, the flask sealed, and the solution stirred at room

temperature for 24 hours. The solution was yellow-brown at this point, and a yellow-green precipitate was removed by filtration, dried with ether, and stored in the desiccator. The visible spectrum resembled that of β -hydroxy- η -propylcobaloxime (145), with a maximum at 440 nm and a broad shoulder around 380 nm. The solid was recrystallized from CH_2Cl_2 by precipitation with hexane. 1.6 g of a bright yellow powder was recovered, or a 41% yield.

The proton NMR in d_6 -acetone gave a singlet at $\delta = 2.48$ ppm, presumably due to the methyl protons of the dmg ligand. The triplets expected for the methylene protons of the organo ligand were not clearly resolved from the baseline; however, the α -protons appeared to give a triplet in the region of $\delta \sim 1.8$ ppm while the β -protons resonated at about $\delta = 3.1$ ppm. In the corresponding $\text{HOCH}_2\text{CH}_2\text{Co}(\text{dmgH})_2\text{py}$ compound, the α - and β -protons of the organo group give triplets centered at $\delta = 1.72$ and 3.07 ppm, respectively, similar to that seen above. A broadish singlet at $\delta = 2.85$ ppm could not be assigned, but was perhaps water. The presence of py was definitely indicated. The IR, in a Nujol mull, with KBr plates, showed the expected B-F vibrations at 1168, 1015, and 825 cm^{-1} . A C,H,N analysis of the material indicated the presence of an impurity.

	<u>% Observed</u>	<u>% Calculated</u>
C	34.64	35.40
N	4.28	4.36
H	13.18	13.76

Likewise, the percent Co was slightly low; 11.23% was measured as compared to the theoretical value of 11.58%. TLC on Eastman 13181 silica gel plates showed a 20% ethyl acetate, 20% isopropanol mixture in CHCl_3 caused separation into two components, but the very low solubility of the material in CHCl_3 limited the feasibility of purification by column chromatography.

The rate of reaction between $\text{Cr}_{\text{aq}}^{2+}$ and $\text{HOCH}_2\text{CH}_2\text{Co}(\text{dmgBF}_2)_2\text{py}$ was measured only approximately to determine if these reagents were compatible long enough for flash photolysis experiments. The reaction was followed by monitoring the appearance of the product, $\text{Co}(\text{dmgBF}_2)_2$, at 452 nm with time, under conditions where $[\text{Cr}_{\text{aq}}^{2+}] \gg [\text{RCo}(\text{dmgBF}_2)_2\text{py}]$, and $[\text{H}_3\text{O}^+] = 0.01 \text{ M}$. Assuming a first-order dependence on $[\text{Cr}_{\text{aq}}^{2+}]$, a second-order rate constant of $0.8 \pm 0.1 \text{ M}^{-1}\text{s}^{-1}$, at ambient temperature, was estimated. However, this increase in absorbance appeared to be preceded by a much faster absorbance increase (at 452 nm), which occurred upon mixing. Also it was seen that the final absorbance of the products depended upon the initial $[\text{Cr}_{\text{aq}}^{2+}]$. These complexities in the thermal reaction are probably due to impurities in the cobaloxime, perhaps $\text{HOCH}_2\text{CH}_2\text{Co}(\text{dmgH})_2\text{py}$. Since the flash photolysis studies were free of complications the impurities were deemed innocent.

$\text{Cr}(\text{ClO}_4)_2$

Aqueous solutions were prepared and analyzed by the procedure described in Part III, Experimental.

HClO₄, NaOH, LiClO₄

Aqueous solutions were prepared and standardized as described in Part I, Experimental.

Gases

Nitrous oxide, Matheson, 98.0% minimum purity, and nitrogen, Air Products, were used to saturate solutions. Trace amounts of O₂ present in either gas were removed by passing through Cr_{aq}²⁺ scrubbing towers. Ethylene, 99.98% research purity, was used as such. The low level of O₂ present in the tank was ascertained by bubbling directly into a solution of Cr_{aq}²⁺ and noting any spectral change due to reaction with O₂.

MethodsInstrumentation

All ¹H NMR spectra were recorded with a Hitachi-Perkin Elmer R-20B spectrometer. ¹³C NMR were obtained on a Jeol FX-90Q instrument, with the assistance of Bill McGranahan or Tom Lyttle. Analysis by mass spectrometry was accomplished with the assistance of Jerry Flesch. For recording absorption spectra a Cary 219 spectrophotometer was employed.

Analyses

% Co-photochemical decomposition (150) This procedure is better for carboxylatopentaamminecobalt(III) perchlorates than the following method. A weighed sample (~ 5 mg) is dissolved in 6.00 mL 0.1 M HClO₄

in a 2 cm quartz spectrophotometric cell. After capping, the cell is suspended inside a Raytheon "Photochemical Generator" which supplies intense UV light. The solution is photolyzed about 1 hr, then the cell is removed from the generator and allowed to cool. 5.00 mL is removed by pipet and transferred to a 50 mL volumetric flask. The amount of $\text{Co}_{\text{aq}}^{2+}$ is determined spectrophotometrically, as described below.

% Co-HClO₄ decomposition This method is more satisfactory for the cobaloxime complexes. A weighed sample (~ 10 mg) is transferred to a 50 mL volumetric flask and a few mL of concentrated HClO₄ added. It is fumed until almost colorless, then cooled. To determine the concentration of $\text{Co}_{\text{aq}}^{2+}$, 5 mL 12 M NH₄SCN (extracted until colorless with methylisobutyl ketone) is added, 25 mL acetone, and the flask is cooled to room temperature. After diluting to the mark with water, the absorbance is read at 623 nm; the concentration of $\text{Co}(\text{SCN})_4^{2-}$ is calculated using $\epsilon = 1842 \text{ M}^{-1} \text{ cm}^{-1}$.

Ethylene A solution containing $3.8 \times 10^{-3} \text{ M}$ $\text{Co}(\text{NH}_3)_5\text{O}_2\text{CCH}_2\text{CH}_2\text{OH}(\text{ClO}_4)_2$ in 0.10 M HClO₄ was deoxygenated with nitrogen in a 5 cm quartz spectrophotometric cell. An aliquot of $\text{Cr}_{\text{aq}}^{2+}$ was injected so $[\text{Cr}_{\text{aq}}^{2+}] = 5.0 \times 10^{-3} \text{ M}$, and the cell was suspended in a Raytheon "Photochemical Generator" which served as a source of UV light. After 2 hours of photolysis, a stream of N₂ was passed into the cell, while leading the effluent to a glass U-tube immersed in liquid N₂. The exit stream was bubbled into water, before venting to the air. The U-tube was sealed, still immersed in liquid N₂, and attached to the mass

spectrometer. The N_2 was removed, and trapped gases allowed to vaporize into the instrument.

Flash photolysis

Preparation of solutions In System 1, 23.2 mL of water, containing the necessary amounts of perchloric acid and $LiClO_4$, were placed in a quartz 10 cm spectrophotometric cell, which was sealed with a septum, and saturated with N_2O . The cell was removed from the N_2O line and 5.8 mL of water saturated with ethylene were injected. This amounted to 1 to 4 V/V dilution such that $[N_2O] = 0.020$ M and $[CH_2CH_2] = 8.8 \times 10^{-4}$ M (151) at $25^\circ C$. A small aliquot of $Cr(ClO_4)_2$ solution was injected into the cell which was then photolyzed.

In Systems 2 and 3, the cobalt compound was dissolved in water and transferred to a 10 cm quartz spectrophotometric cell. Aqueous perchloric acid and $LiClO_4$ were used to adjust acidity and ionic strength to their desired concentrations. After sealing the cell with a septum, the solution was saturated with nitrogen gas, or, in some experiments, N_2O . Immediately prior to a flash photolysis experiment, a small aliquot of $Cr(ClO_4)_2$ solution was injected.

Temperature control When room temperature kinetic data were desired, the photolysis solutions generally were not thermostatted. The temperature fluctuated somewhat as the day to day ambient temperature of the laboratory varied, but was measured precisely at the conclusion of the kinetic run. A Cole-Parmer Model 8502-20 thermometer was used for this purpose, immersing the temperature probe directly into the spectro-

photometric cell, after removal of the septum. In many experiments solutions were flashed more than once, but the temperature could be measured only after the last flash.

To obtain temperatures different from the ambient, the filled spectrophotometric cells were brought to temperature in a dish of hot or cold water as needed. Since the solutions could not be thermostatted during the actual photolysis, it was necessary to work rapidly to avoid a large drift in the temperature before it could be recorded at the end of the experiment.

Equipment Details of the instrument and data analysis are given in the Appendix. In Systems 1 and 3, 250 J flashes of nonfiltered flash light were used. In System 2 light was restricted to $\lambda > 380$ nm using jacketed spectroscopic cells¹ filled with 0.1 M NaNO_2 , or $\lambda > 280$ nm, obtained by slipping each flashlamp inside a tube of Pyrex glass. Energy was increased to 400 J.

Spectrum of transient To obtain the spectrum of the transient, its absorbance was measured, point by point at several wavelengths, using an identical, fresh solution for each wavelength. The same energy flash and flashlamps were used to insure delivery of the same amount of energy to each solution. Different spectrophotometric cells were employed, however, for efficiency, but no differences between them were noted, at least for this photoreaction. The absorbance due to the transient was determined at its maximum value, before reaction occurred,

¹Kindly loaned by Professor D. S. Martin.

²See the Appendix for details.

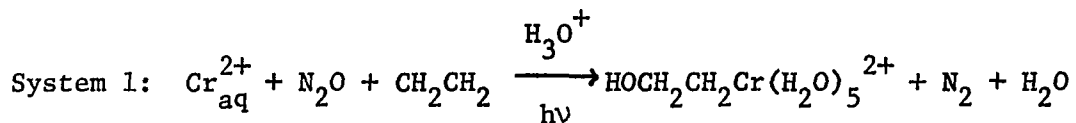
to maximize the measurement. By judicious choice of the oscilloscope time base, an accurate reading of the transmittance, before decay of the transient, I_{\max} , could be measured. The final transmittance, $I_{t_{\infty}}$, of the solution after reaction was also noted, and the absorbance of the transient calculated by use of Equation A-4,²

$$D_{\text{trans.}} = -\log \frac{I_{\max}}{I_0} + \log \frac{I_{t_{\infty}}}{I_0}, \quad (\text{A-4})$$

where I_0 is the transmittance of the solvent.

RESULTS

Results from flash photolysis studies of the three systems introduced earlier will be discussed separately.



Rate of reaction of $\text{HOCH}_2\text{CH}_2\text{Cr}(\text{H}_2\text{O})_5^{2+}$ with H_3O^+

Flash photolysis of 5×10^{-4} M chromium(II) perchlorate, saturated with 0.020 M N_2O and 8.8×10^{-4} M ethylene, using 250 or 400 J flashes, produced a transient which was detected at 390 nm. After the decay of the flashlamps, about 0.6 ms, a species absorbing more than the reactants had formed, which then decayed with a rate dependent upon the perchloric acid concentration. The final absorbance was slightly larger than before photolysis.

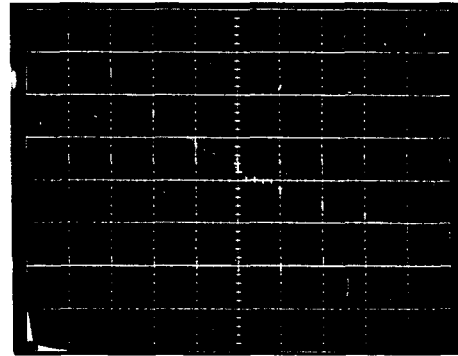
The reaction rate of the transient with H_3O^+ was investigated in the region $0.1 \leq [\text{H}_3\text{O}^+] \leq 3.0$ mM, by monitoring the loss of absorbance at 390 nm as a function of time. Ionic strength was maintained at 0.05 M, and the temperature was $24.1 \pm 0.5^\circ\text{C}$.

Oscilloscope sensitivities of 5 mV/div ($I_0 = 1000$ mV) and time bases of from 5 to 50 ms/div (depending on $[\text{H}_3\text{O}^+]$) were used to obtain kinetic data. Representative photographs of the transient decay, at four different $[\text{H}_3\text{O}^+]$, are reproduced in Figure 2-2. The kinetic traces were analyzed according to a pseudo-first-order treatment in transient

Figure 2-2. Representative photographs of oscilloscope traces showing the reaction of $\text{HOCH}_2\text{CH}_2\text{Cr}(\text{H}_2\text{O})_5^{2+}$ with H_3O^+ at various acidities. Monitoring $\lambda = 390 \text{ nm}$; flash energy = 400 J (a-c), 250 J (d); $\mu = 0.05 \text{ M}$ (LiClO_4); $I_0 = 1000 \text{ mV}$; $I_{t_\infty} (\text{mV}) = 915$ (a), 840 (b), 840 (c), 890 (d)

a) 0.1mM H_3O^+

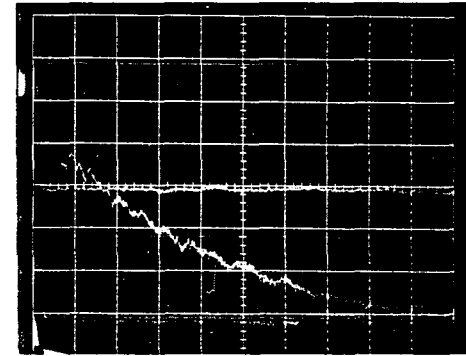
$\frac{5mV}{d}$



50ms/d

b) 0.75mM H_3O^+

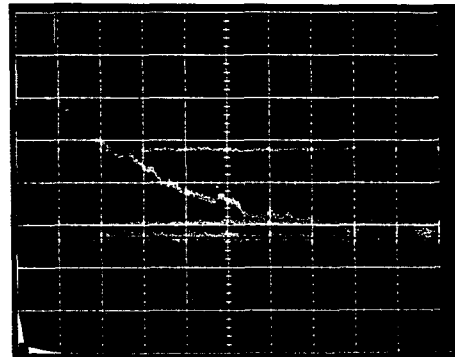
$\frac{5mV}{d}$



20 ms/d

c) 1.25mM H_3O^+

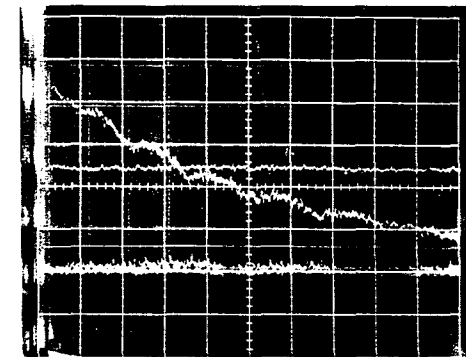
$\frac{5mV}{d}$



20ms/d

d) 2.5 mM H_3O^+

$\frac{5mV}{d}$



5ms/d

concentration by plotting $\ln(D'_t - D'_\infty)^{-1}$ versus time. While linear plots over about the last 90% of reaction were obtained at all acidities, often the initial points of a $\ln(D'_t - D'_\infty)$ versus time plot fell below the line defined by data at longer times. This could not be interference from the formation reaction of the transient, which would be complete well within the decay of the flash profile. Instead, it appeared to be the result of formation of an additional species, also absorbing at 390 nm; the half-life of formation was about 20 ms. It is not known if this species is stable within the time bases used, or if it too decays along with the transient of interest. Since the absorbance due to this secondary reaction is small (< 20% of the absorbance changes monitored at 390 nm), it was disregarded. However, neither the origin, nor the identity of this additional species was apparent.

In Figure 2-3, the kinetic plots corresponding to the photographs in Figure 2-2, are given. The pseudo-first-order rate constants, k_{obs} , obtained from these and similar plots, are listed in Table 2-1 at the acidities studied.

The observed rate constants were seen to have a linear dependence on $[\text{H}_3\text{O}^+]$, as given by,

$$k_{\text{obs}} = k_0 + k [\text{H}_3\text{O}^+] , \quad (2-26)$$

shown graphically in Figure 2-4. A least-squares fit of the data from Table 2-1 to Equation 2-26 yields $k_0/\text{s}^{-1} = 2.9 \pm 0.4$ and $k/\text{M}^{-1}\text{s}^{-1} = (1.43 \pm 0.02) \times 10^4$. These values were calculated for $T = 24.1^\circ\text{C}$;

¹D' is linearly related to D, see Appendix.

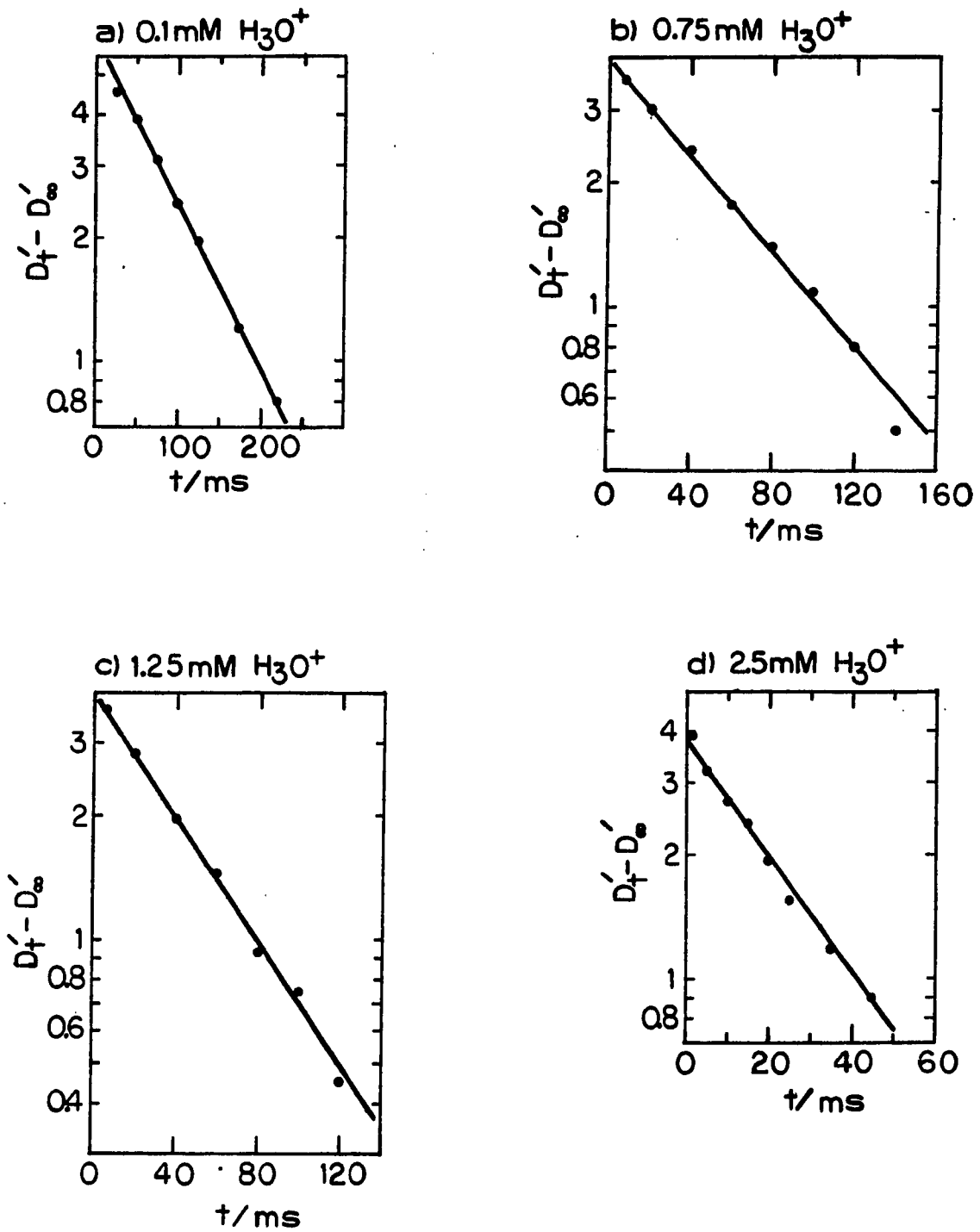


Figure 2-3. Plots of $\ln(D'_t - D'_\infty)$ versus time for photographs of Figure 2-2

Table 2-1. Rate constants for the reaction of $\text{HOCH}_2\text{CH}_2\text{Cr}(\text{H}_2\text{O})_5^{2+}$ with H_3O^+ ^a

$[\text{H}_3\text{O}^+]/\text{mM}$	$k_{\text{obs}}/\text{s}^{-1}$
0.1	4.38 ± 0.14 (3)
0.25	7.38 ± 1.3 (3)
0.5	9.9 ± 1.0 (2)
0.75	13.7 ± 1.5 (3)
1.25	20.1 ± 2.1 (3)
1.5	23.7 ± 6.6 (3)
2.0	$27.4 \pm 1.5^{\text{b}}$ (3) [30.7] ^c
2.5	$35.2 \pm 1.7^{\text{d}}$ (3) [38.6] ^c
3.0	$42.2 \pm 3.4^{\text{e}}$ (3) [46.7] ^c

^aUncertainties represent 1σ ; number in parentheses is number of kinetic runs; monitoring $\lambda = 390$ nm; flash energy = 250 or 400 J; $\mu = 0.05$ M (LiClO_4); $[\text{Cr}_{\text{aq}}^{2+}] = 5 \times 10^{-4}$ M; $[\text{N}_2\text{O}] = 0.020$ M; $[\text{CH}_2\text{CH}_2] = 8.8 \times 10^{-4}$ M; $T = 24.1 \pm 0.5^\circ\text{C}$ except as noted.

^b $T = 22.4^\circ\text{C}$.

^cNumber in brackets is k_{obs} calculated for $T = 24.1^\circ\text{C}$ from experimental data at lower temperature using Equation 2-27.

^d $T = 22.8^\circ\text{C}$.

^e $T = 22.6^\circ\text{C}$.

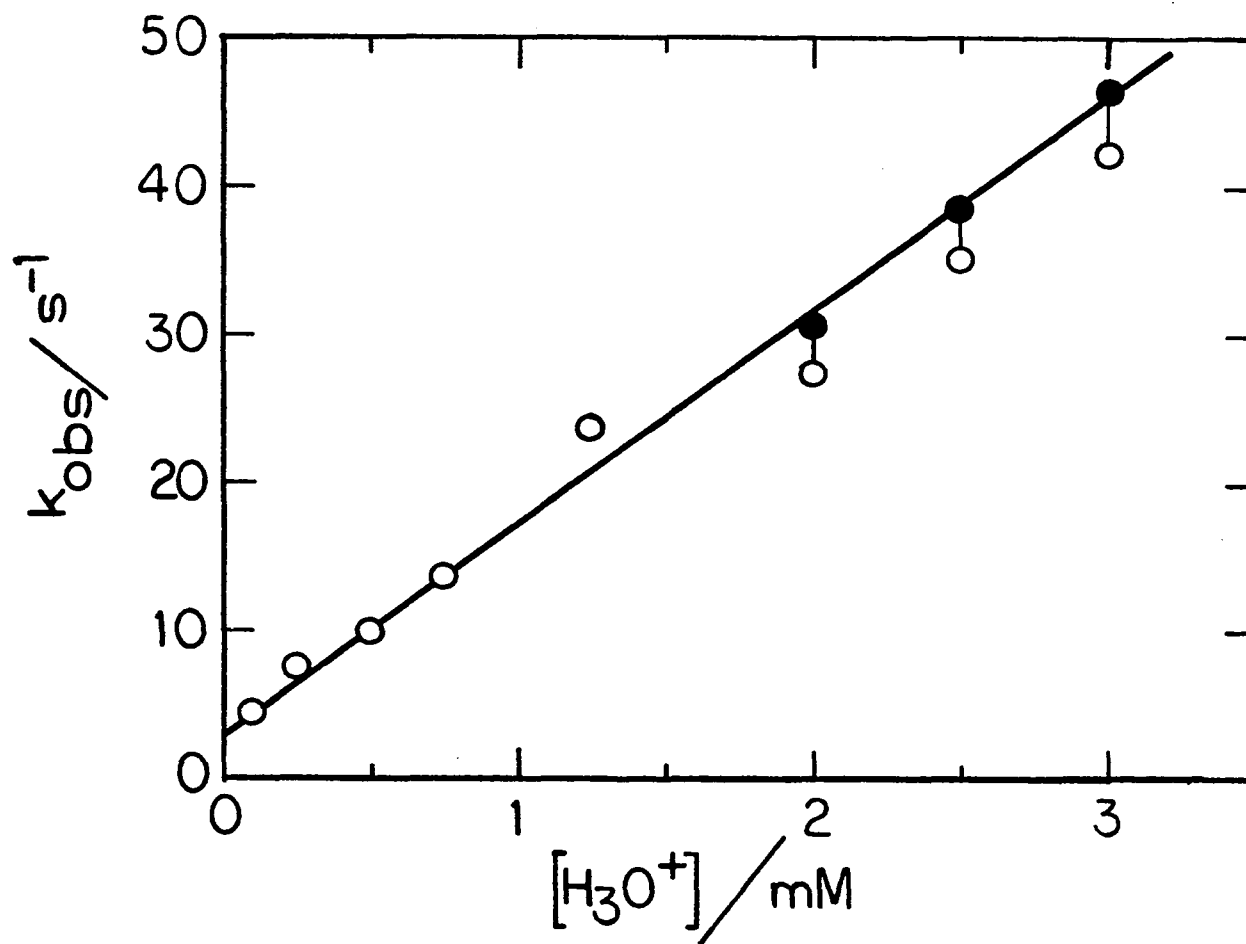


Figure 2-4. The dependence of k_{obs} on $[\text{H}_3\text{O}^+]$ for the reaction of $\text{HOCH}_2\text{CH}_2\text{Cr}(\text{H}_2\text{O})_5^{2+}$ with H_3O^+ , using data from Table 2-1. Open circles represent experimental values of k_{obs} ; solid circles are calculated for $T = 24.1^\circ\text{C}$ from activation parameters, using Equation 2-27

although not all the data was obtained at this temperature, values of k_{obs} were so adjusted by using the activation energies determined separately (see below). Because of the necessity of working only at very low $[\text{H}_3\text{O}^+]$, the concentration of acid in these experiments is probably not of the accuracy needed to assign an absolute value to the k_0 term with complete confidence. The concentrations of H_3O^+ listed in Table 2-1 were obtained by calculation only, based upon dilution of a stock solution of more concentrated HClO_4 . Contributions from acid present in the $\text{Cr}(\text{ClO}_4)_2$ or LiClO_4 stock solutions were neglected, as they were too small to be determined with any accuracy. Taking these points into consideration, it is quite likely the error limit stated for k_0 is much larger than that estimated from the least-squares fit of the data. Consequently, it is possible k_0 is zero; the amount of acid introduced by the $\text{Cr}_{\text{aq}}^{2+}$ and Li^+ stock solutions would only have to be as large as 0.2 mM, in order for the line in Figure 2-4 to pass through the origin.

Effect of temperature

The temperature dependence of the reaction of H_3O^+ with the transient was investigated by determining its rate over a 29° range in temperature, while maintaining $[\text{H}_3\text{O}^+] = 0.10$ mM, and $\mu = 0.05$ M. At 16°C, the acid concentration was varied to include kinetic runs at 0.10, 0.20, 1.0, and 2.0 mM H_3O^+ , all at $\mu = 0.05$ M. The absorbance of the transient was monitored at 390 nm, and 250 J flashes were used.

The solubilities (151) of the gases, N_2O and ethylene, will, of course, vary with the temperature of the experiment. At the lowest temperature studied, $13.2^\circ C$, the concentrations of N_2O and CH_2CH_2 will increase to approximately 0.026 M and $1.2 \times 10^{-3} M$, respectively, and at $42.6^\circ C$, decrease to approximately 0.011 M and $4.2 \times 10^{-4} M$. At higher temperatures the scavenging of e_{aq}^- by N_2O , and of OH^\cdot by ethylene, will not be able to compete as effectively with H_3O^+ , and Cr_{aq}^{2+} , respectively, if the rate constants are assumed to vary only slightly with temperature. The yield of $HOCH_2CH_2^\cdot$ radicals will be lowered; as expected the amount of transient formed was reduced by about 25% over the 29° range in temperature.

Pseudo-first-order rate constants (k_{obs}) obtained at various temperatures, are collected in Table 2-2. The rate constants were analyzed as a function of temperature and acid concentration to sort out the individual activation parameters for the acid-independent, and acid-dependent paths, Equation 2-26. By applying the Eyring equation to k_o and k individually, Equation 2-26 becomes,

$$k_{obs} = \frac{RT}{Nh} \left(e^{\frac{\Delta S_o^\ddagger}{R} - \frac{\Delta H_o^\ddagger}{RT}} + [H^+] e^{\frac{\Delta S_1^\ddagger}{R} - \frac{\Delta H_1^\ddagger}{RT}} \right), \quad (2-27)$$

where

R = Gas constant

T = Absolute temperature

N = Avogadro's number

h = Planck's constant

Table 2-2. Rate constants for the reaction of $\text{HOCH}_2\text{CH}_2\text{Cr}(\text{H}_2\text{O})_5^{2+}$ with H_3O^+ at various temperatures^a

$T/^\circ\text{C}$	$k_{\text{obs}}/\text{s}^{-1}$
13.2	1.38 ± 0.12
16.0 ^b	2.92 ± 0.58
16.1 ^c	18.4 ± 1.4
16.4	1.83 ± 0.17
16.5 ^d	10.2 ± 1.4
24.1	4.38 ± 0.14
29.8	7.43 ± 0.52
38.6	15.4 ± 0.81
42.6	24.9 ± 4.2

^aUncertainties represent 1σ of three replicate runs; monitoring $\lambda = 390 \text{ nm}$; flash energy = 250 J; $[\text{H}_3\text{O}^+] = 0.10 \text{ mM}$, except as noted; $\mu = 0.05 \text{ M}$ (LiClO_4); $[\text{Cr}_{\text{aq}}^{2+}] = 5 \times 10^{-4} \text{ M}$; $[\text{N}_2\text{O}]$ and $[\text{CH}_2\text{CH}_2]$, see text.

^b0.20 mM H_3O^+ .

^c2.0 mM H_3O^+ .

^d1.0 mM H_3O^+ .

$\Delta S_o^\ddagger / \Delta H_o^\ddagger$ = entropy/enthalpy of activation for acid-independent pathway

$\Delta S_1^\ddagger / \Delta H_1^\ddagger$ = entropy/enthalpy of activation for acid-dependent pathway.

The values of k_{obs} were fit to Equation 2-27 as a function of temperature and acidity, by a nonlinear-least-squares computer program. The following activation parameters were obtained.

	<u>k_o path</u>	<u>k_1 path</u>
$\Delta S^\ddagger / \text{e.u.}$	9.4 ± 2.6	-5.0 ± 3.9
$\Delta H^\ddagger / \text{kcal mol}^{-1}$	19.6 ± 0.8	10.3 ± 1.1

In view of the questions raised earlier about the reality of a k_o pathway, if k_o is set to zero by adding 0.20 mM H_3O^+ to each calculated acid concentration, the data in Table 2-2 can be reevaluated to give $\Delta S^\ddagger / \text{e.u.} = 13.8 \pm 2.5$ and $\Delta H^\ddagger / \text{kcal mol}^{-1} = 15.8 \pm 0.8$.

Effect of ionic strength

The variation of the rate constant for the reaction of the transient with H_3O^+ was also investigated as a function of ionic strength, for the purpose of establishing its charge. At a perchloric acid concentration of 0.1 mM, the ionic strength was varied from 0.0081 to 0.10 M by the addition of LiClO_4 . Ionic strength was calculated from Equation 2-28.

$$\mu = \frac{1}{2} \{ [\text{H}_3\text{O}^+] + [\text{Li}^+] + 4[\text{Cr}_{\text{aq}}^{2+}] + [\text{ClO}_4^-] \} \quad (2-28)$$

The data were treated according to Equation 2-29, once again setting $k_o = 0$ ($[\text{H}_3\text{O}^+] = [\text{H}_3\text{O}^+]_{\text{calc.}} + 0.20 \text{ mM}$), as justified by the uncertainty in $[\text{H}_3\text{O}^+]$.

$$\log k = \log k^{\circ} + \frac{2Z_A Z_B \alpha \mu^{1/2}}{1 + \beta_a \mu^{1/2}} \quad (2-29)$$

A discussion of the Brønsted-Debye-Hückel equation (Equation 2-29) was presented earlier in Part I, Results, and will not be restated here.

The rate constants obtained as a function of μ are collected in Table 2-3, and a plot of $\log k_{\text{obs}}$ versus $\alpha \mu^{1/2}/(1 + \beta_a \mu^{1/2})$, with $\alpha = 0.509$, $\beta_a = 1$, is presented in Figure 2-5. If the transient is properly formulated as $\text{HOCH}_2\text{CH}_2\text{Cr}(\text{H}_2\text{O})_5^{2+}$, the charge product of Equation 2-29, $2Z_A Z_B$ should be $2(+2)(+1) = +4$. The slope of the line in Figure 2-5 is drawn to exactly +4, and can be seen to approximate the data within its stated uncertainty, in the region $0.02 \text{ M} \leq \mu \leq \text{M}$, after which the experimental values fall below the theoretical line.

This type of behavior is not unexpected at ionic strengths greater than about 0.01 M where the Debye-Hückel equation is no longer valid. To extend its useful region, a term linear in ionic strength (77-81) is often included, so Equation 2-29 becomes,

$$\log k = \log k^{\circ} + \frac{2Z_A Z_B \alpha \mu^{1/2}}{1 + \beta_a \mu^{1/2}} - C\mu. \quad (2-30)$$

The kinetic data from Table 2-3 were fit to Equation 2-30 using a least-squares computer program¹ which allowed k° , $2Z_A Z_B$, and C to be treated as adjustable parameters. With $\alpha = 0.509$, $\beta_a = 1$, the following values were computed,

¹The least-squares program used was one implemented by Dr. R. B. Pfaff, Ames Laboratory.

Table 2-3. Rate constants for the reaction of $\text{HOCH}_2\text{CH}_2\text{Cr}(\text{H}_2\text{O})_5^{2+}$ with H_3O^+ at various ionic strengths

μ/M^a	$k_{\text{obs}}/\text{s}^{-1}{}^b$	$\frac{0.509 \mu^{1/2}}{1 + \mu^{1/2}}$
0.0081	3.49 ± 0.09	0.0416
0.010	3.26 ± 0.19	0.0458
0.020	3.40 ± 0.16	0.0629
0.030	3.75 ± 0.33	0.0751
0.040	4.34 ± 0.30	0.0848
0.050	4.38 ± 0.14	0.0930
0.080	4.67 ± 0.21	0.112
0.090	4.23 ± 0.14	0.117
0.10	4.41 ± 0.51	0.122

^a $\mu = \mu(\text{calc.}) + 2.0 \times 10^{-4} \text{M } \text{H}_3\text{O}^+$.

^bUncertainties represent 1 σ of three replicate runs; monitoring $\lambda = 390 \text{ nm}$; flash energy = 400 J; $[\text{H}_3\text{O}^+] = 3 \times 10^{-4} \text{M}$ (assumed, see text); $[\text{Cr}_{\text{aq}}^{2+}] = 5 \times 10^{-4} \text{M}$; $[\text{N}_2\text{O}] = 0.020 \text{ M}$; $[\text{CH}_2\text{CH}_2] = 8.8 \times 10^{-4} \text{M}$; $T = 23.8 \pm 0.3^\circ\text{C}$.

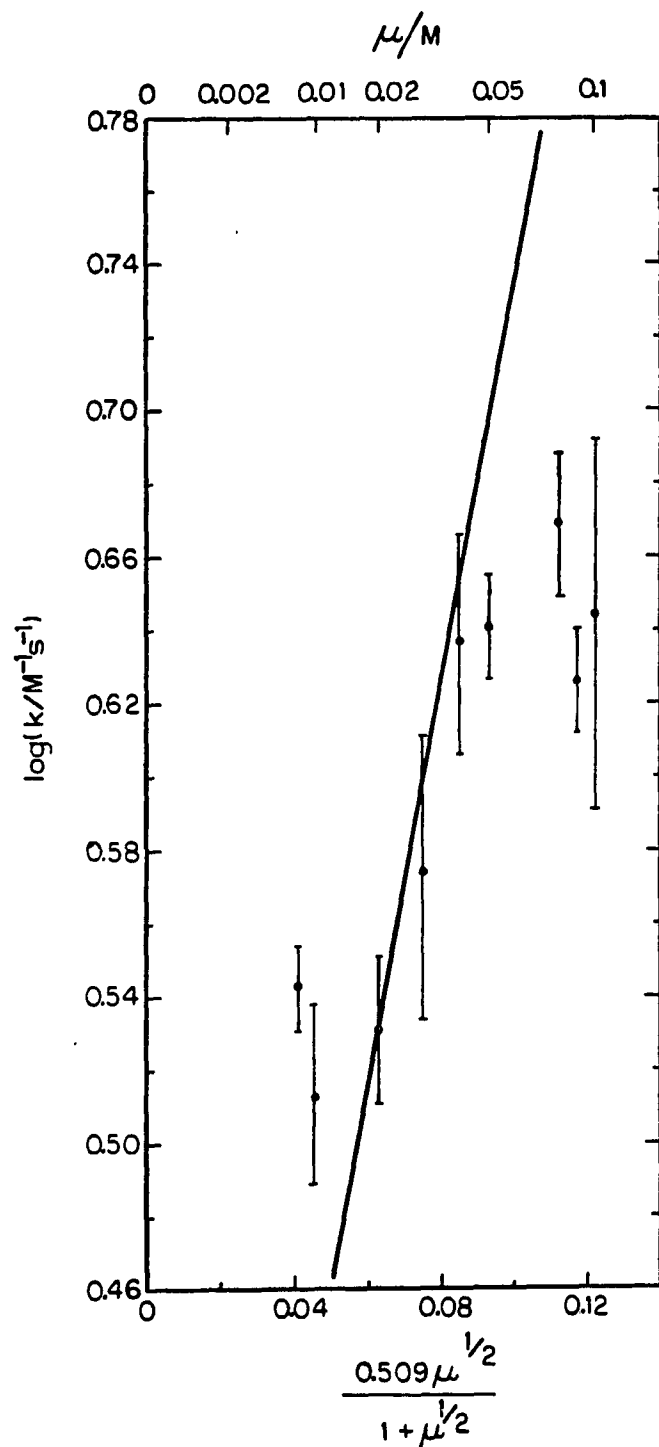


Figure 2-5. Plot of $\log k$ versus $\frac{0.509\mu^{1/2}}{1+\mu^{1/2}}$ for the reaction of $\text{HOCH}_2\text{CH}_2\text{Cr}(\text{H}_2\text{O})_5^{2+}$ with H_3O^+ . The line is drawn to have a slope of +4

$$k^0 = 2.4 \pm 0.4$$

$$2Z_A Z_B = 3.4 \pm 1.7$$

$$C = 1.5 \pm 1.4.$$

These values reflect the uncertainty in the kinetic data; the assignment of a charge of +2 to the transient on the basis of the calculated value of $2Z_A Z_B$, 3.4 ± 1.7 , is somewhat speculative, although without a doubt the transient can definitely be identified as cationic.

Spectrum of $\text{HOCH}_2\text{CH}_2\text{Cr}(\text{H}_2\text{O})_5^{2+}$

The spectrum of the transient was obtained in the region 310-440 nm, and is reproduced in Figure 2-6. A maximum is present at 390 ± 5 nm, a minimum at 365 ± 10 nm, and a rising absorbance into the UV region. A shoulder at 330 nm may be an artifact due to optical restrictions at these shorter wavelengths.

Absolute values of molar absorptivities cannot be calculated unless the concentration of the transient is known. It can be estimated, from the yield of $\text{HCr}(\text{H}_2\text{O})_5^{2+}$ produced when no N_2O or ethylene are present (see Part III). In 0.01 M H_3O^+ , an absorbance change of 0.0223 ± 0.0011 ($\ell = 10$ cm) was measured at 380 nm due to the formation of $\text{HCr}(\text{H}_2\text{O})_5^{2+}$. Using the published (36) value for ϵ_{380} of $190 \pm 20 \text{ M}^{-1}\text{cm}^{-1}$, $[\text{HCr}(\text{H}_2\text{O})_5^{2+}]$ is calculated to be $(1.17 \pm 0.21) \times 10^{-5} \text{ M}$. The yield of hydrated electrons from the UV photolysis of $\text{Cr}_{\text{aq}}^{2+}$ (Equation 2-13) can then be determined after calculation of the fraction of e_{aq}^- which react to form hydrogen atoms (and eventually $\text{HCr}(\text{H}_2\text{O})_5^{2+}$). From Reactions 2-16 and 2-31,

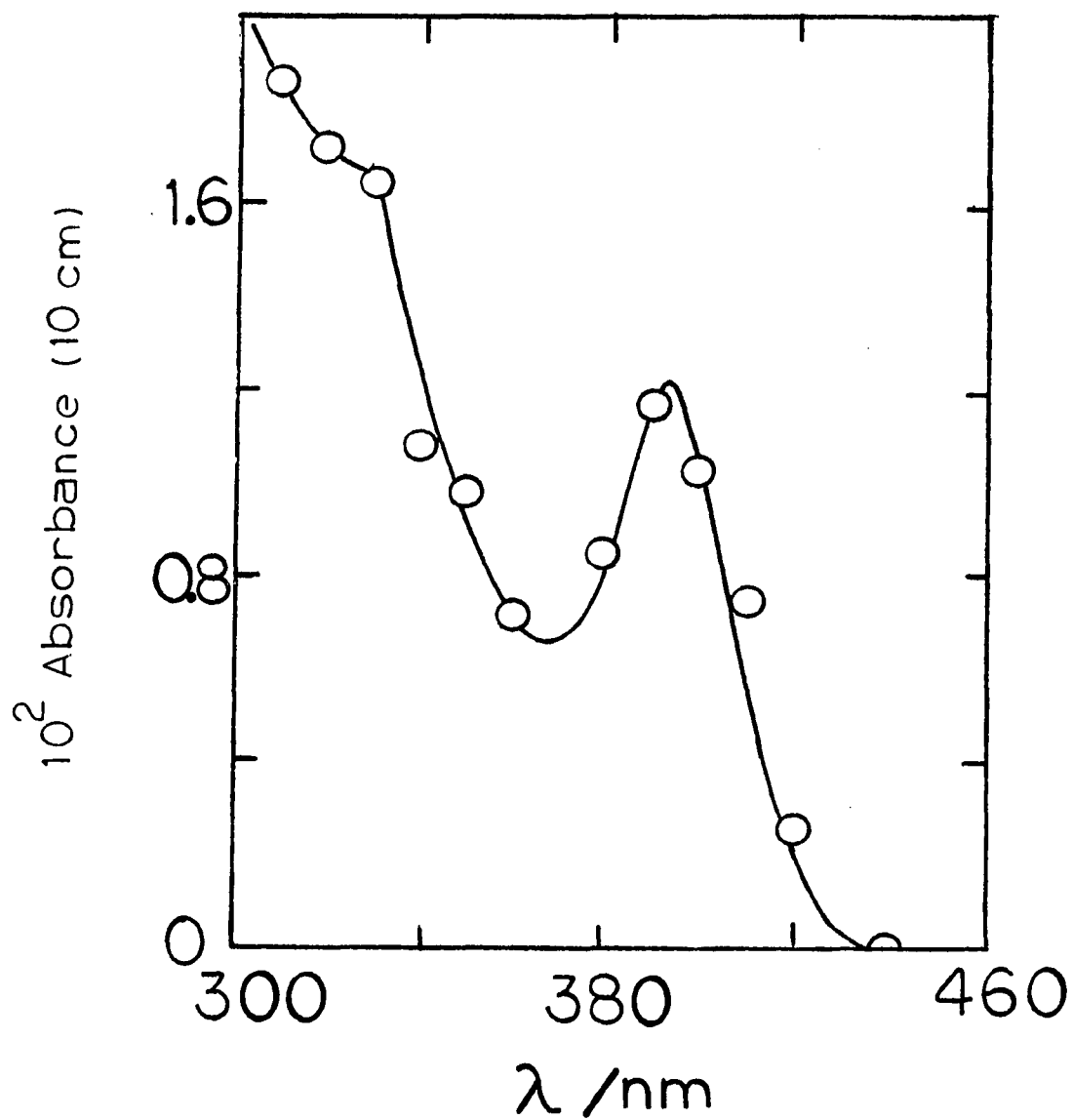


Figure 2-6. The electronic spectrum of the $\text{HOCH}_2\text{CH}_2\text{Cr}(\text{H}_2\text{O})_5^{2+}$ ion. Cell length = 10 cm; flash energy = 250 J



$$k_{16}/\text{M}^{-1}\text{s}^{-1} = 2.3 \times 10^{10} \quad (123)$$



$$k_{31}/\text{M}^{-1}\text{s}^{-1} = 1.4 \times 10^{10} \quad (36)$$

it can be seen this fraction is equal to 0.94 under the experimental conditions of $[\text{Cr}_{\text{aq}}^{2+}] = 1 \times 10^{-3}\text{M}$, and $[\text{H}_3\text{O}^+] = 0.01\text{M}$. The concentration of e_{aq}^- is therefore $(1.17 \pm 0.21) \times 10^{-5}/0.943 = (1.24 \pm 0.22) \times 10^{-5}\text{M}$. In the presence of N_2O , most e_{aq}^- will be scavenged to form OH^\bullet radicals, in competition with Reactions 2-16 and 2-31.

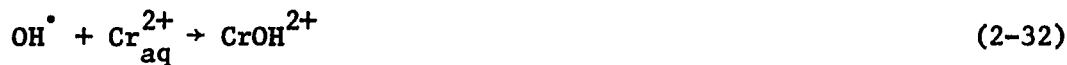


$$k_{14}/\text{M}^{-1}\text{s}^{-1} = 8.7 \times 10^9 \quad (121)$$

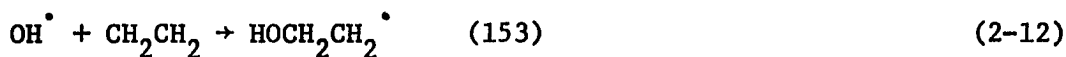


$$\text{pK}_{15} = 11.9 \pm 0.2 \quad (122)$$

The fraction of e_{aq}^- which will be converted to OH^\bullet is 0.949 for $[\text{N}_2\text{O}] = 0.020\text{M}$, $[\text{H}_3\text{O}^+] = 1 \times 10^{-4}\text{M}$, and $[\text{Cr}_{\text{aq}}^{2+}] = 5 \times 10^{-4}\text{M}$. Hydroxyl radicals can react with $\text{Cr}_{\text{aq}}^{2+}$, or add to ethylene, Reactions 2-32 and 2-12.



$$k_{32}/\text{M}^{-1}\text{s}^{-1} = 4.8 \times 10^9 \quad (152)$$



$$k_{12}/\text{M}^{-1}\text{s}^{-1} = 2.1 \times 10^9 \quad (120)^1$$

The fraction which react by addition is calculated to be 0.44 at $[\text{Cr}_{\text{aq}}^{2+}] = 5 \times 10^{-4}\text{M}$, $[\text{CH}_2\text{CH}_2] = 8.8 \times 10^{-4}\text{M}$. If it is assumed that $\phi(e_{\text{aq}}^-)$ is independent of acid concentration, then $\phi(e_{\text{aq}}^-)$ will depend only on the amount of light absorbed by $\text{Cr}_{\text{aq}}^{2+}$, $[e_{\text{aq}}^-] = \phi I_a$. While I_a itself is unknown, I_a/I_o can be calculated for any particular wavelength using Equation 2-33 (Ref. 154, p. 11),

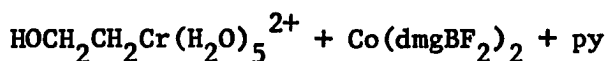
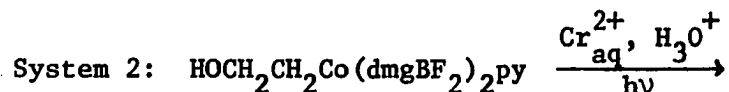
$$\frac{I_{a,i}}{I_o} = 1 - 10^{-\ell \sum_i \epsilon_i C_i} \frac{\epsilon_i C_i}{\sum_i \epsilon_i C_i}, \quad (2-33)$$

where I_a is the amount of light absorbed by species i ; I_o is the amount of incident light, ℓ is the path length, ϵ_i is the molar absorptivity of the i^{th} species, and C_i is its concentration. For example, at 265 nm $\epsilon_{\text{Cr}_{\text{aq}}^{2+}} \approx 15 \text{ M}^{-1}\text{cm}^{-1}$ (155), so I_a/I_o is 0.0171 for $5 \times 10^{-4}\text{M Cr}_{\text{aq}}^{2+}$, and 0.0339 for $1 \times 10^{-3}\text{M}$. Hence, $[e_{\text{aq}}^-]$ at $5 \times 10^{-4}\text{M Cr}_{\text{aq}}^{2+}$ will be equal to $0.504[e_{\text{aq}}^-]$ for $1 \times 10^{-3}\text{M Cr}_{\text{aq}}^{2+}$. Finally, the yield of $\text{HOCH}_2\text{CH}_2^\bullet$ radicals is given by Equation 2-34,

¹ k_{12} represents the average of the reported (120) rate constants for the reaction of HO^\bullet with ethylene; i.e., 4.8×10^9 , 1.0×10^9 , and 4.9×10^8 , all in $\text{M}^{-1}\text{s}^{-1}$. The former value is reported (120) as the sum of k_{12} and the rate constant for hydrogen abstraction by HO^\bullet to form the vinyl radical. In more recent work (153) H-abstraction has been determined to be unimportant, and hence this reaction was neglected in the above scheme.

$$\begin{aligned}
& \{[e_{\text{aq}}^-] \text{ produced in } 5 \times 10^{-4} \text{ M Cr}_{\text{aq}}^{2+}\} \\
& \cdot \{\text{fraction of } e_{\text{aq}}^- \text{ converted to OH}^\bullet\} \\
& \cdot \{\text{fraction of OH}^\bullet \text{ converted to HOCH}_2\text{CH}_2^\bullet\}, \quad (2-34) \\
& = \{0.504((1.24 \pm 0.22) \times 10^{-5} \text{ M})\} \cdot \{0.94\} \cdot \{0.44\} \\
& = (2.6 \pm 0.4) \times 10^{-6} \text{ M}.
\end{aligned}$$

The absorbance measured at the 390 nm maximum of $\text{HOCH}_2\text{CH}_2\text{Cr}(\text{H}_2\text{O})_5^{2+}$ was 0.0117 ± 0.0006 ($l = 10$ cm); assuming that all $\text{HOCH}_2\text{CH}_2^\bullet$ radicals are scavenged by $\text{Cr}_{\text{aq}}^{2+}$, a molar absorptivity of $450 \pm 100 \text{ M}^{-1} \text{ cm}^{-1}$ is approximated. The large uncertainty in this value reflects that it clearly is useful only as an estimation of the order of magnitude of ϵ_{390} for $\text{HOCH}_2\text{CH}_2\text{Cr}(\text{H}_2\text{O})_5^{2+}$.



Flash photolysis of aqueous solutions of $(2.0 \pm 0.2) \times 10^{-5} \text{ M}$ $\text{HOCH}_2\text{CH}_2\text{Co}(\text{dmgBF}_2)_2\text{py}^1$ and $1.0 \times 10^{-3} \text{ M Cr}_{\text{aq}}^{2+}$ produced a transient which was detected at 390 nm. 400 J flashes of light of $\lambda > 280$ or 380 nm were used. During the decay of the scattered flashlight (~ 1 ms), an absorbance grew in which then decreased, at a rate dependent on $[\text{H}_3\text{O}^+]$, to an absorbance lower than before photolysis.

¹The thermal reaction of $\text{HOCH}_2\text{CH}_2\text{Co}(\text{dmgH})_2\text{py}$ and $\text{Cr}_{\text{aq}}^{2+}$ (see Experimental) prevented any flash photolysis experiments with this cobaloxime.

Permanent spectral changes were more completely analysed using a Cary 219 spectrophotometer. A $3.7 \times 10^{-5} \text{ M HOCH}_2\text{CH}_2\text{Co(dmgBF}_2)_2\text{py}$ solution containing $\sim 1 \times 10^{-3} \text{ M Cr}_{\text{aq}}^{2+}$, in $1 \times 10^{-3} \text{ M H}_3\text{O}^+$, was photolyzed with a 400 J flash, and the spectrum recorded on the Cary 219 before and after the flash. Initially, the spectrum was due only to the organocobaloxime with a 442 nm maximum and 380 nm shoulder ($\text{Cr}_{\text{aq}}^{2+}$ absorbs very weakly). After the flash a more intense maximum at 456 nm and a minimum at 326 nm appeared, in excellent agreement with the spectrum of authentic $\text{Co(dmgBF}_2)_2$ (90). The amount of $\text{Co(dmgBF}_2)_2$ formed can be calculated from the spectral changes. At 400 nm, an increase in absorbance of 0.635 was measured; using $(\epsilon_{\text{Co}^{\text{II}}} - \epsilon_{\text{R}(\text{Co}^{\text{III}})})$ as $(4.05 - 1.17) \times 10^3 \text{ M}^{-1} \text{ cm}^{-1}$, the concentration of $\text{Co(dmgBF}_2)_2$, produced by one flash, is calculated to be $2.2 \times 10^{-5} \text{ M}$.

Flash experiments conducted in the presence of 2 or 5 M CH_3OH , at $[\text{H}_3\text{O}^+] = 0.01 \text{ M}$, showed no reduction in the size of the transient detected, nor its rate of reaction. Because methanol is an effective scavenger for H^\bullet atoms,



$$k_{35}(0.1 \text{ M H}^+)/\text{M}^{-1} \text{ s}^{-1} = (2.0 \pm 0.8) \times 10^6 \quad (156)$$

it may be concluded that H^\bullet atoms are not a precursor to the transient detected. This eliminates the possibility that the unstable species detected might be $\text{HCr(H}_2\text{O)}_5^{2+}$, formed by the scavenging of H^\bullet atoms by $\text{Cr}_{\text{aq}}^{2+}$, a concern since the visible photolysis of organocobaloximes has

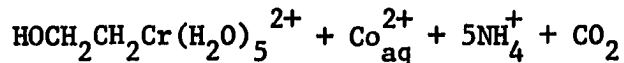
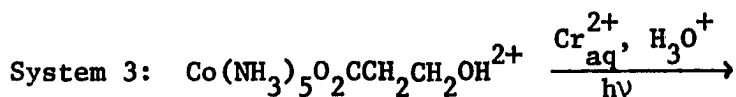
been reported (125) to produce small yields (as compared to R^\bullet) of hydrogen atoms in protic solvents. H abstraction from CH_3OH by $HOCH_2CH_2^\bullet$ radicals is very slow, so no β -hydroxyethyl radicals would be scavenged.

The reaction rate of the transient with H_3O^+ was investigated by monitoring the decrease of its absorbance at 390 nm with time. Rates were determined as a function of perchloric acid concentration, $[H_3O^+] = 0.001 - 0.01$ M, at a constant ionic strength of 0.01 M; the temperature was ambient, $25 \pm 1^\circ C$.

Oscilloscope sensitivities of 5 mV/div ($I_0 = 1000$ mV) and time bases of 2 to 10 ms/div (depending on $[H_3O^+]$) were used to follow the transients. The kinetic data fit a pseudo-first-order treatment in transient concentration at all acid concentrations investigated, as evidenced by linear $\ln(D_t' - D_\infty')$ versus time plots. The rate constants obtained from the slopes of these plots were seen to vary linearly with $[H_3O^+]$,

$$k_{obs} = k_0 + k[H_3O^+] \quad (2-36)$$

A least-squares fit of the data to Equation 2-36 gives $k_0/s^{-1} = 33 \pm 12$ and $k/M^{-1}s^{-1} = (1.5 \pm 0.2) \times 10^4$. Because of the large uncertainty in k_0 , it can be assumed to be zero so that k_{obs} has no acid-independent component.

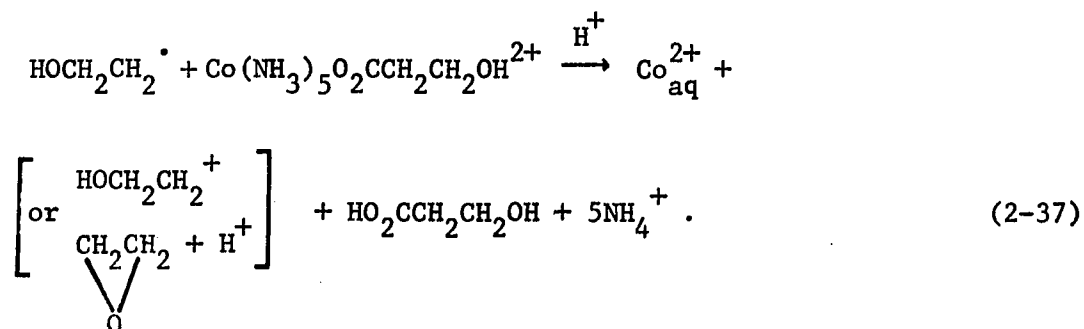


When aqueous solutions of $(0.5 - 1.0) \times 10^{-3} \text{ M Co}(\text{NH}_3)_5\text{O}_2\text{CCH}_2\text{CH}_2\text{OH}^{2+}$ and $(0.5 - 1.0) \times 10^{-3} \text{ M Cr}_{\text{aq}}^{2+}$ were photolyzed with 250 J flashes of light, a transient was detected at 380 or 390 nm. During the decay of the scattered flashlight, about 0.6 ms, an absorbance grew in which then decreased, at a rate dependent on the perchloric acid concentration. The final absorbance was slightly higher than before photolysis.

Saturating the photolysis solution with nitrous oxide, instead of with nitrogen gas, had no effect on the size of the transient detected, nor on its rate of reaction with H_3O^+ . This confirmed the transient was not $\text{HCr}(\text{H}_2\text{O})_5^{2+}$, formed from the UV photolysis of $\text{Cr}_{\text{aq}}^{2+}$, because the precursor to H^\bullet atoms, hydrated electrons, are efficiently scavenged by N_2O .

Indeed, considerably more of the UV flashlight will be absorbed by the cobalt(III) complex than $\text{Cr}_{\text{aq}}^{2+}$, because of the former's intense UV absorbance. At any particular wavelength, the fraction of light absorbed by either component can be calculated by application of Equation 2-33. For example, at 270 nm, using $\epsilon_{\text{Cr}_{\text{aq}}^{2+}} \approx 15 \text{ M}^{-1} \text{ cm}^{-1}$ (155), $\epsilon_{\text{Co}^{\text{III}}} = 646 \text{ M}^{-1} \text{ cm}^{-1}$, $[\text{Co}^{\text{III}}] = 5 \times 10^{-4} \text{ M}$, and $\ell = 1 \text{ cm}$, $I_{\text{a Co}^{\text{III}}}/I_{\text{o}} = 0.44$ and $I_{\text{a Cr}^{2+}}/I_{\text{o}} = 0.020$, or Co^{III} absorbs 95% more of the flashlight at 270 nm than $\text{Cr}_{\text{aq}}^{2+}$.

When a deoxygenated solution of the cobalt(III) complex at a concentration of 1×10^{-4} M in 0.01 M HClO_4 is photolyzed with a 250 J flash of light, in the absence of $\text{Cr}_{\text{aq}}^{2+}$, no transient is detected at 390 nm. Only a simple loss in absorbance occurs, due to photolysis of the cobalt(III) substrate to $\text{Co}_{\text{aq}}^{2+}$. This result indicates that the transient detected in the presence of $\text{Cr}_{\text{aq}}^{2+}$ is a direct consequence of a reaction involving chromium(II) ion, and the transient behavior cannot be attributed to a reaction of the type,



Rate of reaction of transients with H_3O^+

The reaction rate of the transient with H_3O^+ was investigated by monitoring the decrease of its absorbance at 380 or 390 nm with time, as a function of the perchloric acid concentration in the range 0.0025–0.25 M. Ionic strength was maintained at 0.50 M, and the temperature of the runs was $24.8 \pm 0.7^\circ\text{C}$. Oscilloscope sensitivities of 5 or 10 mV/div ($I_0 = 1000$ mV) and time bases of from 0.2 to 20 ms/div (depending on $[\text{H}_3\text{O}^+]$) were used to follow the transients.

Attempts to analyze the kinetic data according to a pseudo-first-order treatment in transient concentration gave curved plots of

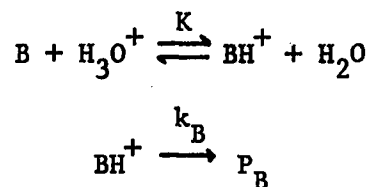
$\ln(D'_t - D'_\infty)$ versus time, when $[H_3O^+]$ was less than about 0.1 M.

However, the data in this acidic region was successfully analyzed by treating the loss in absorbance with time as due to parallel reactions of two transients, with substantially different lifetimes. At any given acidity the kinetic data was fit to Equation 2-38 by using a nonlinear least-squares computer program.¹

$$D'_t = [A]_0(\epsilon_A - \epsilon_{P_A})e^{-k'_A t} + [B]_0(\epsilon_B - \epsilon_{P_B})e^{-k'_B t} + D'_\infty \quad (2-38)$$

In Equation 2-38 A and B designate the faster and slower reacting transient, respectively; P_A and P_B denote their products.

The pseudo-first-order rate constants k'_A and k'_B were then analyzed as a function of $[H_3O^+]$. A first-order dependence on $[H_3O^+]$ was found for k'_A , such that $k'_A = k_A[H_3O^+]$, and in a least-squares fit of the data, $k'_A/M^{-1}s^{-1} = (3.6 \pm 0.4) \times 10^4$. The acid-dependence of k'_B was more complex but fit a reaction scheme in which B is protonated to a reactive form BH^+ , which then goes on to product with a rate constant k_B . This scheme identifies the measured



rate constant k'_B as,

$$k'_B = \frac{k_B K [H_3O^+]}{1 + K [H_3O^+]} \quad (2-39)$$

¹The least-squares program used was one implemented by Dr. R. B. Pfaff, Ames Laboratory.

A more useful form is obtained by inversion,

$$\frac{1}{k'_B} = \frac{1}{k_B} + \frac{1}{k_B K [\text{H}_3\text{O}^+]} \quad , \quad (2-40)$$

which demonstrates that a plot of $1/k'_B$ versus $1/[\text{H}_3\text{O}^+]$ must be linear if the above scheme is operative. The intercept of such a plot will give k_B^{-1} ; with this value, the equilibrium constant K can be calculated from the slope.

For acidities in the range $0.075 \leq [\text{H}_3\text{O}^+] \leq 0.25$ M the kinetic data fit the simpler treatment of $\ln(D'_t - D'_\infty)$ versus time, suggesting that only the reaction of transient B was being followed. At these higher acid concentrations the decay of transient A would have been too fast to detect with the available instrumentation. For example, at 0.2 M H_3O^+ , A would have a half-life given by only,

$$t_{1/2} = \frac{0.693}{(3.6 \times 10^4 \text{ M}^{-1} \text{ s}^{-1})(0.2 \text{ M})} = 0.096 \text{ ms} \quad ,$$

while the "dead" time of the flash photolysis apparatus is ~ 0.6 ms under these conditions. This calculation assumes $k_A = 3.6 \times 10^4 \text{ M}^{-1} \text{ s}^{-1}$ is valid in this acidic region. The slopes of plots of $\ln(D'_t - D'_\infty)$ versus time gave $-k'_B$ directly.

When values for k'_B in the region $0.01 \leq [\text{H}_3\text{O}^+] \leq 0.25$ M were treated according to Equation 2-40, a reasonably linear plot was obtained. Values at the lowest $[\text{H}_3\text{O}^+]$, 0.0025 and 0.005 M, deviated from this line, however, indicating this treatment was not valid at low acid. A least-squares fit of the data in the region $0.01 \text{ M} \leq [\text{H}_3\text{O}^+] \leq 0.25 \text{ M}$

gave $k_B/s^{-1} = (1.9 \pm 0.7) \times 10^3$, and $k_B K/M^{-1}s^{-1} = (5.60 \pm 0.53) \times 10^3$;
hence, $K = 2.9 \pm 2 M^{-1}$.

Product of reaction of $HOCH_2CH_2Cr(H_2O)_5^{2+}$ with H_3O^+

The organic product of the photolysis of $Co(NH_3)_5O_2CCH_2CH_2OH^{2+}$ in the presence of Cr_{aq}^{2+} was identified as containing ethylene and carbon dioxide by comparison of the m/e peaks and their intensities with published spectra.

DISCUSSION

Of the three photochemical systems studied for generation of $\text{HOCH}_2\text{CH}_2^\bullet$ radicals in the presence of $\text{Cr}_{\text{aq}}^{2+}$, System 1, based on the addition of the hydroxyl radical to ethylene, proved to be the most free of complicating side reactions. Consequently, the transient produced in this system was characterized most thoroughly. In all three systems, the rate of the disappearance of the transient as a function of acid concentration was determined, but only in System 1 were activation energies of the reaction, a semi-quantitative study of the effect of ionic strength on the reaction rate, and the spectrum of the transient obtained.

The reactions which must be considered in System 1 are summarized:



$$k_{14}/\text{M}^{-1}\text{s}^{-1} = 8.7 \times 10^9 \quad (121)$$



$$\text{pK}_{15} = 11.9 \pm 0.2 \quad (122)$$



$$k_{16}/\text{M}^{-1}\text{s}^{-1} = 2.3 \times 10^{10} \quad (123)$$



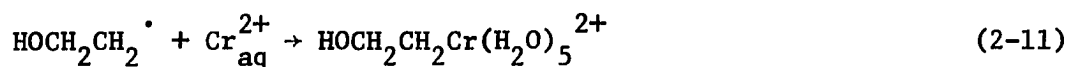
$$k_{31}/\text{M}^{-1}\text{s}^{-1} = 1.4 \times 10^{10} \quad (36)$$



$$k_{12}/\text{M}^{-1}\text{s}^{-1} = 2.1 \times 10^9 \quad (120)^1$$



$$k_{32}/\text{M}^{-1}\text{s}^{-1} = 4.8 \times 10^9 \quad (152)$$



$$k_{11} \text{ estimated as } 1 \times 10^8 \text{ M}^{-1}\text{s}^{-1} \quad (125)$$



$$k_{41}/\text{M}^{-1}\text{s}^{-1} \approx 2 \times 10^6 \quad (112)^2$$



$$2k_{42}/\text{M}^{-1}\text{s}^{-1} = 5.6 \times 10^8 \quad (153,157)^3$$

In order to form $\text{HOCH}_2\text{CH}_2\text{Cr}(\text{H}_2\text{O})_5^{2+}$, the rates of Reactions 2-14, 2-12, and 2-11 must be optimized to compete effectively with Reactions 2-16, 2-31, 2-32, 2-41, and 2-42 for the reactive intermediates.

¹ k_{12} was obtained as explained on p. 133.

²Three different values for k_{41} have been reported-- $\sim 1 \times 10^7$ (157), $\sim 2 \times 10^6$ (112), and 3×10^4 (153), all $\text{M}^{-1}\text{s}^{-1}$. The middle value was deemed the most reliable.

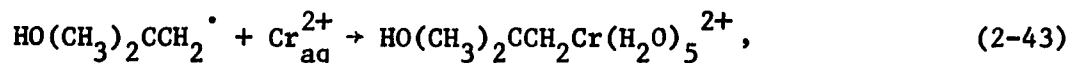
³ k_{42} is an average of the values in the literature (153,157).

High concentrations of N_2O and ethylene favor formation of OH^\bullet and $HOCH_2CH_2^\bullet$ radicals, but the actual concentrations which can be obtained are limited by the solubilities of the gases in water. To eliminate reactions of Cr_{aq}^{2+} with e_{aq}^- and OH^\bullet , Reactions 2-31 and 2-32, a low chromium(II) concentration is suggested, but Reaction 2-11 must be able to compete with Reaction 2-41 and self-reaction, Reaction 2-42.

Fortunately, nitrous oxide is quite soluble in water, 0.025 M at 1 atm, 25°C. Reaction 2-14 would have an apparent rate constant of $2.2 \times 10^8 s^{-1}$ in a solution saturated with N_2O , competing effectively with H_3O^+ up to concentrations of about $5 \times 10^{-3} M H_3O^+$ ($k_{16} (5 \times 10^{-3} M) = 1.2 \times 10^8 s^{-1}$) for e_{aq}^- . Likewise, Reaction 2-31 does not constitute a serious loss of e_{aq}^- , when $[Cr_{aq}^{2+}]$ is less than $1 \times 10^{-2} M$ ($k_{31} (1 \times 10^{-2} M) = 1.4 \times 10^8 s^{-1}$). However, the reaction of OH^\bullet radicals with ethylene occurs at approximately the same rate as oxidation of chromium(II), Reactions 2-12 and 2-32. Because ethylene is not especially soluble in water, $4.41 \times 10^{-3} M$ at 1 atm, 25°C, the concentration of Cr_{aq}^{2+} ion must be less than [ethylene], so Reaction 2-12 will predominate. Since both N_2O and ethylene must be present in solution, the solubilities of both gases will decrease from that at 1 atm in accordance with Henry's law. So as not to limit the range of $[H_3O^+]$ which could be investigated to lower than about $3 \times 10^{-3} M$, a 1 to 4 V/V dilution of ethylene saturated water was made with a saturated solution of nitrous oxide, resulting in $8.8 \times 10^{-4} M CH_2CH_2$ in 0.020 M N_2O . Hydrated electrons are still effectively converted to OH^\bullet radicals at this N_2O concentration,

$k_{14}(\text{N}_2\text{O}) = 1.74 \times 10^8 \text{ s}^{-1}$. The concentration of $\text{Cr}_{\text{aq}}^{2+}$ ion is limited by the low concentration of ethylene; $5 \times 10^{-4} \text{ M}$ $\text{Cr}_{\text{aq}}^{2+}$ ion was chosen for these experiments, much lower concentrations would make scavenging of $\text{HOCH}_2\text{CH}_2^\bullet$ by $\text{Cr}_{\text{aq}}^{2+}$, Reaction 2-11, too slow, allowing Reactions 2-41 and 2-42 to interfere. Also, the yield of e_{aq}^- from photochemical excitation, Equation 2-13, decreases as $[\text{Cr}_{\text{aq}}^{2+}]$ does. Yet, at $5 \times 10^{-4} \text{ M}$ $\text{Cr}_{\text{aq}}^{2+}$ ion about 60% of the OH^\bullet radicals are lost to Reaction 2-32.

The rate of formation of $\text{HOCH}_2\text{CH}_2\text{Cr}(\text{H}_2\text{O})_5^{2+}$ could not be determined in this work because it is faster than the time limitations of the flash photolysis instrument. The rate of formation can be estimated from similar reactions of $\text{Cr}_{\text{aq}}^{2+}$ and hydroxyalkyl radicals. Cohen and Meyerstein (25) have shown that the rate of reaction of several α - and β -hydroxyalkyl radicals with $\text{Cr}_{\text{aq}}^{2+}$ are actually quite similar, with second-order rate constants of $(0.34-3.5) \times 10^8 \text{ M}^{-1} \text{ s}^{-1}$. The rates were seen to depend slightly on the identity of the radical in a predictable manner, but steric effects were not particularly important. Substitution at the α -carbon with an electron-donating group decreased the rate of reaction with chromium(II), while an electron-withdrawing substituent had the opposite effect. For the β -hydroxy-2,2-dimethylethyl radical,



a rate constant of $1.0 \times 10^8 \text{ M}^{-1} \text{ s}^{-1}$ was measured (25). Since the substituents at the α -carbon are similar to those of the β -hydroxyethyl radical, the rate of Reaction 2-11 should be about the same. Therefore,

the half-life for Reaction 2-11 will be about $(1 \times 10^8 \text{ M}^{-1} \text{ s}^{-1}) [\text{Cr}_{\text{aq}}^{2+}]$ or 0.014 ms, because $[\text{Cr}_{\text{aq}}^{2+}]$ is in large excess compared to $[\text{HOCH}_2\text{CH}_2\cdot]$. The flash decay profile eliminates absorbance measurements to times greater than 0.6 ms, so the inability to detect the formation reaction is as expected.

The evidence used to establish the identity of the transients generated by flash photolysis of the three systems is 1) the spectrum, 2) the results of scavenging experiments, and 3) the independence of the transient's reaction rate with H_3O^+ on the photochemical source.

The spectrum, Figure 2-6, consists of a maximum at 390 ± 5 nm which is characteristic of an organochromium(III) carbon-chromium sigma bond. This absorption has been assigned to a d-d transition (25), ${}^4\text{A}_{2g} \rightarrow {}^4\text{T}_{1g}$ (2). The intensity of these transitions is always much larger than most d-d absorptions (2,20,25); molar absorptivities generally fall within the range 200 to $700 \text{ M}^{-1} \text{ cm}^{-1}$. For the transient detected from System 1, a value for ϵ_{390} of $450 \pm 100 \text{ M}^{-1} \text{ cm}^{-1}$ was estimated, which is clearly reasonable for a complex of this type. The UV absorption spectrum of $\text{HOCH}_2\text{CH}_2\text{Cr}(\text{H}_2\text{O})_5^{2+}$ is expected to consist of a very intense maximum, probably in the region 260-310 nm (2,20,25), due to a charge-transfer transition from the ligand to chromium. The "shoulder" at 330 nm is probably of too low an energy and intensity to be this transition and is more likely an artifact arising from poor monochromation of near UV light.

From scavenging experiments in Systems 2 and 3, the transient definitely cannot be identified as $\text{HCr}(\text{H}_2\text{O})_5^{2+}$ (36), which has a similar absorption spectrum and rate of reaction with H_3O^+ (see Part III). Methanol was used as a scavenger for hydrogen atoms in System 2, since it is possible visible photolysis of $\text{HOCH}_2\text{CH}_2\text{Co}(\text{dmgBF}_2)_2\text{py}$ can produce H^\cdot along with $\text{HOCH}_2\text{CH}_2^\cdot$, as reported for $\text{CH}_3\text{Co}(\text{dmgBF}_2)_2\text{py}$ in CHCl_3 (158). Since the size and decay rate of the transient were unaffected by a concentration of methanol sufficient to divert virtually all H^\cdot atoms from $\text{Cr}_{\text{aq}}^{2+}$, it can be safely concluded the transient in System 2 is not $\text{HCr}(\text{H}_2\text{O})_5^{2+}$. Likewise, in System 3, when the photolysis solutions were saturated with N_2O , no change in the transient concentration, nor reactivity, was detected. Since the possibility existed that a small amount of photolysis of $\text{Cr}_{\text{aq}}^{2+}$ was occurring, with production of e_{aq}^- , and ultimately H^\cdot atoms, it was necessary to determine if a scavenger specific for the e_{aq}^- had any effect. While no scavenging experiments were carried out in System 1, the magnitude of the activation parameters measured for the reaction of this transient with H_3O^+ are quite different, $\Delta S^\ddagger = 13.8$ e.u., $\Delta H^\ddagger = 15.8$ kcal/mol, from those for the corresponding reaction of $\text{HCr}(\text{H}_2\text{O})_5^{2+}$, $\Delta S^\ddagger = -19.1$ e.u., $\Delta H^\ddagger = 6.3$ kcal/mol, providing good evidence that $\text{HCr}(\text{H}_2\text{O})_5^{2+}$ is not formed in this system either.

Irrespective of the system in which it was detected, the kinetics of decomposition of the transient with H_3O^+ were shown to occur predominately, if not entirely, by a rate law involving a first-order dependence on both the concentration of the transient and H_3O^+ .

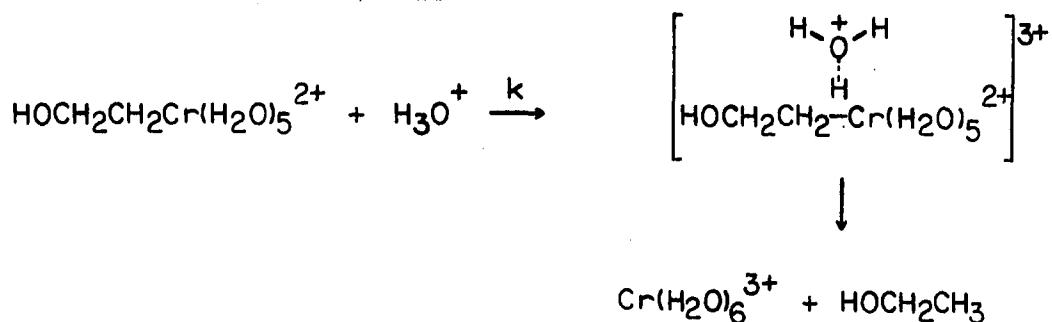
$$\frac{-d[\text{transient}]}{dt} = k[\text{H}_3\text{O}^+][\text{transient}] \quad (2-44)$$

The second-order rate constants (k), measured in each system, are all of the same order of magnitude, in spite of minor differences in the ionic strength and temperature. For Systems 1, 2, and 3 the rate constants are $(1.43 \pm 0.02) \times 10^4 \text{M}^{-1} \text{s}^{-1}$ ($\mu = 0.05 \text{M}$, $T = 24.1^\circ\text{C}$); $(1.5 \pm 0.2) \times 10^4 \text{M}^{-1} \text{s}^{-1}$ (0.01M , $25 \pm 1^\circ\text{C}$); $(3.6 \pm 0.4) \times 10^4 \text{M}^{-1} \text{s}^{-1}$ (0.50M , 24.8°C), respectively. In System 3, the loss of absorbance with time was seen to involve two separate reactions, most reasonably interpreted as due to two different transients, previously designated A and B. The faster reacting species (A) gave a rate law of the form seen for Systems 2 and 3, and a value for k at least of the correct magnitude. Considering the method used for its extraction from the experimental data, and the differences in ionic strength, transient A is identified as the same species detected in the less complex Systems 1 and 2. Transient B cannot be identified on the basis of the available data. Agreement of the rate constants between Systems 1 and 2 is excellent. It is highly encouraging that the transient detected in the three systems reacts with H_3O^+ by similar kinetics, yet each source of $\text{HOCH}_2\text{CH}_2^\cdot$ is chemically independent, only the presence of $\text{Cr}_{\text{aq}}^{2+}$ is common to all three. On the basis of the spectrum, scavenging experiments, and the kinetic data, along with the well-documented photochemistry of carboxylatopentaamminecobalt(III) complexes (99,129-132), alkylcobaloximes (125-127), and $\text{Cr}_{\text{aq}}^{2+}$ ion (Part III), it is reasonable to propose that $\text{HOCH}_2\text{CH}_2\text{Cr}(\text{H}_2\text{O})_5^{2+}$ has been formed in each system.

Three mechanisms by which $\text{HOCH}_2\text{CH}_2\text{Cr}(\text{H}_2\text{O})_5^{2+}$ reacts with H_3O^+ can be imagined, both consistent with the observed rate law, Equation 2-44.

In Scheme 1 rate-determining electrophilic attack by the proton on the carbon-chromium bond (18,24,25,34) would result in formation of ethanol and $\text{Cr}(\text{H}_2\text{O})_6^{3+}$.

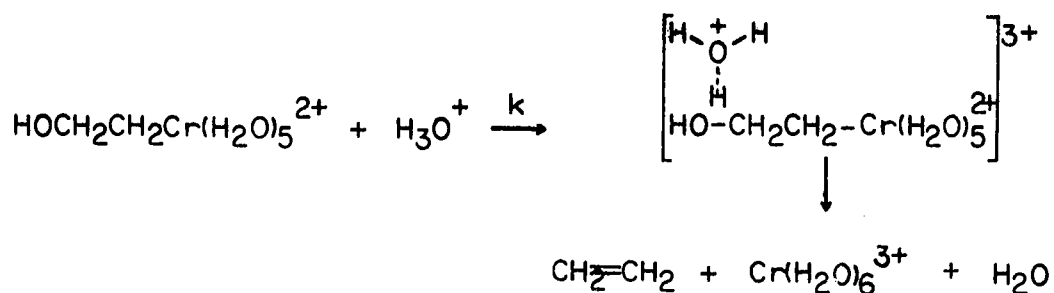
Scheme 1:



However, this scheme is inconsistent with the observed organic product; in System 3, ethylene, not ethanol was detected, so Scheme 1 can be eliminated from consideration.

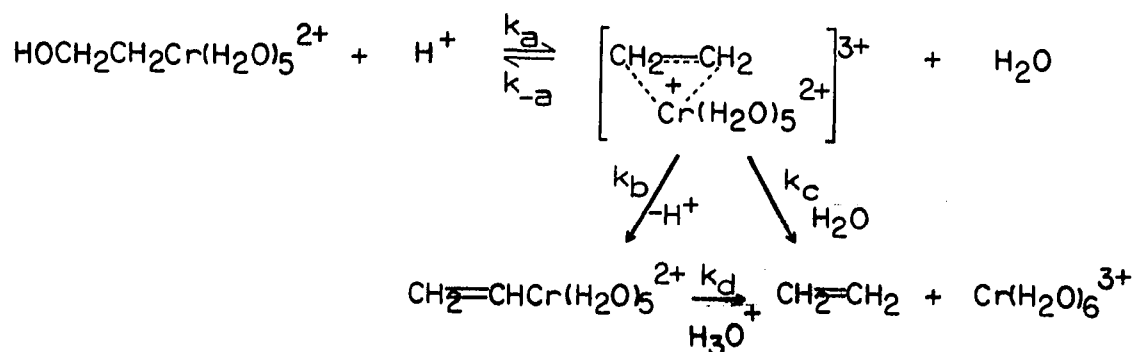
An alternative mechanism is suggested by Scheme 2, in which the rate-limiting step is attack of the proton at the β -hydroxyl group of the organo ligand. Loss of a water molecule with simultaneous cleavage of the carbon-chromium bond would produce the required products.

Scheme 2:



An interesting alternative to Scheme 2 is given by Scheme 3, in which the hydroxyl group and organo ligand are not lost simultaneously, but in subsequent steps. Reaction might proceed through a π -bonded intermediate which rearranges to a more stable σ -bonded alkenylchromium(III) ion (k_b) or loses ethylene directly (k_c).

Scheme 3:



If the σ -alkenylchromium(III) intermediate is formed, further protonolysis, at the carbon-chromium bond, is necessary to arrive at the final products.

Scheme 3 predicts the observed rate law, Equation 2-44, if the steady-state approximation is made for the concentration of the π -intermediate. The observed rate constant, k , is then identified as a composite of individual terms,

$$k = \frac{k_a(k_b + k_c)}{k_{-a} + k_b + k_c} \quad (2-45)$$

If k_b and k_c are both very large compared to k_{-a} , then Equation 2-45 simplifies to $k \approx k_a$, and the rate of formation of the π -intermediate can be considered as rate-determining. On the other hand, if k_b and/or k_c are much smaller than k_{-a} , rearrangement to the σ -alkenyl and/or loss of ethylene will be rate-limiting. It is not possible from the kinetic data to distinguish between these alternatives; however, it is possible to suggest which is more likely. It is reasonable to expect k_d to be quite slow, similar to the slow ($t_{1/2} \sim 10$ -100 min) acidolysis of alkylchromium(III) complexes; and hence, if the σ -alkenylchromium(III) species were formed, it would be stable on the flash photolysis time-scale. However, it is difficult to explain the magnitude of the molar absorptivity of the transient calculated at 390 nm, if the metastable σ -alkenylchromium(III) ion is formed, and not the weakly absorbing $\text{Cr}(\text{H}_2\text{O})_6^{3+}$ ion. Consequently, it appears loss of ethylene rather than $\pi \rightarrow \sigma$ rearrangement is more favorable; i.e., $k_c \gg k_b$. The expected

relative magnitudes of k_c and k_{-a} may best be assessed after further consideration of the bonding in the π -intermediate.

Bonding of an olefin to a chromium(III) center is likely to be quite weak. The Dewar-Chart-Duncanson theory describes the bonding in metal-alkene complexes in terms of two components. A sigma bond is formed from overlap of the filled pi orbitals on the olefin with a vacant metal orbital, and a pi bond results from back-donation of electrons from a filled metal orbital to pi antibonding orbitals on the carbon atoms. While the first mode of bonding is conceivable for octahedral chromium(III), back-bonding could be of little or no importance (159) because the orbitals of the correct symmetry for overlapping with the π^* orbitals of ethylene, the t_{2g} levels, are only half-filled. The high +3 charge on the metal center will further inhibit electron flow into the ethylene molecule.

The acid decomposition of $\text{HOCH}_2\text{CH}_2\text{Co}(\text{dmgh})_2\text{H}_2\text{O}$ was shown to proceed through a π -bonded ethylenecobaloxime intermediate (118,119). Direct observation of this species was obtained from Fourier transfer ^1H NMR spectroscopy (119). It is not unreasonable that the ethylene-cobalt complex should be more stable than that of chromium; with its filled t_{2g} orbitals back-bonding from cobalt will be more effective. Also, electron donation from the dimethylglyoximate macrocycle reduces the formal oxidation state of the cobalt atom somewhat.

For β -hydroxyethylcobaloxime, the rate of loss of H_2O , resulting from protonation of the β -OH group, is several orders of magnitude

slower (118) than for the β -hydroxyethylchromium(III) ion. The cobaloxime reaction was interpreted (118) by a mechanism similar to Scheme 3, except $\pi \rightarrow \sigma$ rearrangement was not considered likely ($k_b = 0$). It was suggested that $k_c \gg k_{-a}$, or that formation of the π -intermediate was rate-limiting, on the basis of acid-cleavage reactions of similar β -hydroxycobaloximes, where k_c/k_{-a} could be directly measured (118). Hence, with this assumption k_a was identified with the experimentally determined rate constant, k , of $3.09 \times 10^{-2} \text{ M}^{-1} \text{ s}^{-1}$ at 25.1°C . In light of the above comments about the expected stability of a π -bonded organochromium(III) ion, it is reasonable to expect loss of ethylene from $[\text{CH}_2\text{CH}_2\text{Cr}(\text{H}_2\text{O})_5]^{2+}$ to be more facile than from the cobaloxime, and that formation of the π -bonded organochromium(III) ion is rate-limiting, $k_c \gg k_{-a}$. Therefore, the value of k_a for the reaction of $\text{HOCH}_2\text{CH}_2\text{Cr}(\text{H}_2\text{O})_5^{2+}$ with H_3O^+ is given by the experimentally measured rate constant, k , of $1.43 \times 10^4 \text{ M}^{-1} \text{ s}^{-1}$ (System 1), at 24.1°C . A comparison of these rate constants for the organocobaloxime and the organochromium(III) ion reveals an enormous difference in reactivity towards loss of H_2O from the β -hydroxyethyl ligand.

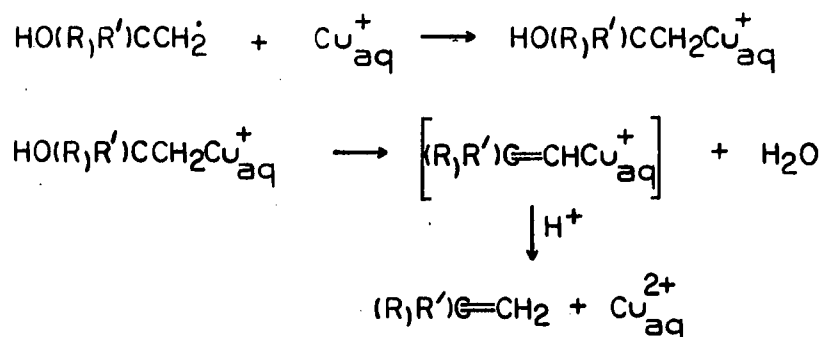
It is interesting that the entropy of activation, ΔS^\ddagger , for both the organochromium and cobaloxime reactions are similar--large positive numbers, 13.8 and 29.9 e.u. (118), respectively, lending further support to Scheme 3, for the acid-cleavage reaction of the organochromium(III) ion.

Cohen and Meyerstein suggested (25) the reaction of the analogous $\text{HO}(\text{CH}_3)_2\text{CCH}_2\text{Cr}(\text{H}_2\text{O})_5^{2+}$ ion with H_3O^+ proceeded by a scheme similar to Scheme 3, except direct loss of isobutylene (pathway k_c) was not considered. Instead, the σ -isobutylenechromium(III) ion appeared to be formed, which then slowly underwent acidolysis to the final products--isobutylene and $\text{Cr}(\text{H}_2\text{O})_6^{3+}$. Again, no direct observation of the π -bonded isobutylenechromium(III) intermediate was made. The kinetics of both reaction steps involved a first-order dependence on the concentration of the organochromium(III) ion, with observed rate constants given by $k_{\text{obs}} = k_0 + k[\text{H}_3\text{O}^+]$. For the production of $\sigma - (\text{CH}_3)_2\text{C}=\text{CHCr}(\text{H}_2\text{O})_5^{2+}$ from $\text{HO}(\text{CH}_3)_2\text{CCH}_2\text{Cr}(\text{H}_2\text{O})_5^{2+}$, individual values for k_0 and k of $1.0 \times 10^2 \text{ s}^{-1}$, and $1.1 \times 10^3 \text{ M}^{-1} \text{ s}^{-1}$, respectively, were measured, while acidolysis of $\sigma - (\text{CH}_3)_2\text{C}=\text{CHCr}(\text{H}_2\text{O})_5^{2+}$ to the products occurred with $k_0 = 1.4 \times 10^{-4} \text{ s}^{-1}$, and $k = 3.9 \times 10^{-4} \text{ M}^{-1} \text{ s}^{-1}$.

The stability of the π -bonded isobutylene-chromium intermediate might be expected to be less than that of ethylene, if the "normal" stability order for metal-olefin bonding is followed. Generally speaking, increasing alkyl substitution about the double bond lowers the stability of the complex (160). This can be explained in terms of increasing the electron density on the double bond which strengthens the σ -bond to the metal, but at the expense of the π -back-bond. For Cr(III) where back-bonding is probably negligible, strengthening the σ -bond may be a more important factor, and a "reversed" stability order may be operative. If it's true then than isobutylene forms a more

stable π -bond to chromium(III) than ethylene, this may account for why $\pi \rightarrow \sigma$ rearrangement is observed rather than loss of isobutylene directly. This argument is highly speculative and the stability order may be affected by steric hindrance also (160).

The oxidation of Cu_{aq}^+ by $\text{HOCH}_2\text{CH}_2^\cdot$, $\text{HO}(\text{CH}_3)\text{CHCH}_2^\cdot$, or $\text{HO}(\text{CH}_3)_2\text{CCH}_2^\cdot$ radicals, has been suggested (112,113) as proceeding through a π -intermediate also, resulting in formation of an unstable (not detectable) σ -bonded alkenylcopper(II) ion. For reaction with $\text{HOCH}_2\text{CH}_2^\cdot$, ethylene is the expected product, but this could not be ascertained (112)



since the experiments were conducted in solutions saturated with ethylene. However, it was clear that ethanol was not the product. Isobutylene was detected as the product of oxidation of Cu_{aq}^+ by $\text{HO}(\text{CH}_3)_2\text{CCH}_2^\cdot$ (112).

The acid-catalyzed decomposition of $\text{HOCH}_2\text{CH}_2\text{Cu}_{\text{aq}}^+$ followed kinetics (113) showing a first-order dependence on the organocopper(II) ion, with an observed rate constant given by $k_{\text{obs}} = k_0 + k[\text{H}_3\text{O}^+]$, where

$k_o = 3.2 \times 10^3 \text{ s}^{-1}$ and $k = 3.8 \times 10^7 \text{ M}^{-1} \text{ s}^{-1}$. The β -hydroxyethylcopper(II) complex is strikingly less stable to dehydration than the corresponding organochromium(III) ion; the value for k differs by a factor of 10^3 between the two complexes. Similarly, the CH_3Cu^+ ion (116) undergoes carbon-chromium bond cleavage by H_3O^+ (acidolysis) about 10^{10} times faster than liberation of CH_4 from $\text{CH}_3\text{Cr}(\text{H}_2\text{O})_5^{2+}$ (16,18).

In summary, all three photochemical systems were successful as a source of the $\text{HOCH}_2\text{CH}_2\text{Cr}(\text{H}_2\text{O})_5^{2+}$ ion, whose identity was established on the basis of its UV-visible absorption spectrum, scavenging experiments, and kinetics of reaction with H_3O^+ . System 1 is believed to be the most reliable source of the kinetic data, for which the second-order rate constant, as defined by Equation 2-44, is $(1.43 \pm 0.02) \times 10^4 \text{ M}^{-1} \text{ s}^{-1}$, at 24.1°C , $\mu = 0.05 \text{ M}$. The form of the rate law can be explained by either Scheme 2 or 3, although the latter is favored by analogy to similar systems in the literature (112,113,118). In Scheme 3, the question of $\pi \rightarrow \sigma$ rearrangement versus direct loss of ethylene, while impossible to answer definitively on the basis of the available data, is best addressed by the magnitude of the absorbance changes monitored, which imply $\text{Cr}(\text{H}_2\text{O})_6^{3+}$ and ethylene are formed directly via decomposition of the π -intermediate, and not through a σ -alkenylchromium(III) ion. Likewise, assignment of the rate-limiting step to formation of the π -intermediate or to release of olefin is not possible; however, it is tempting to suggest that loss of ethylene (pathway k_c) is favored over return to the β -OH complex (pathway k_{-a}), by attack of H_2O on the

olefin, on the basis of the expected instability of a π -bonded chromium(III) complex.

PART III. PROTONOLYSIS OF HYDRIDO(PENTAAQUO)CHROMIUM(III) ION

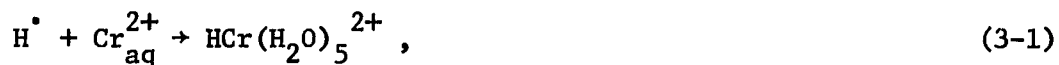
INTRODUCTION

Statement of Problem

As detailed in the General Introduction, organochromium(III) cations of the general formula $\text{RCr}(\text{H}_2\text{O})_5^{2+}$ have been extensively studied over the past several years. As a result, some general theories of reactivity have emerged. In contrast, the hydrido analog to this family of organochromium(III) complexes, $\text{HCr}(\text{H}_2\text{O})_5^{2+}$, has been only briefly investigated. It was of interest to study the nature of the hydrido-chromium bond in order to compare its reactivity with organo-complexes.

The absence of extensive chemical studies of the hydridochromium(III) species probably stems from lack of a simple method of preparation of this highly reactive complex. Using the pulse radiolysis technique, Cohen and Meyerstein (36) first generated the $\text{HCr}(\text{H}_2\text{O})_5^{2+}$ ion in aqueous perchloric acid. Because pulse radiolysis requires an electron accelerator for production of intense pulses of radiation, its use is limited to only a few laboratories worldwide. Therefore, it appears worthwhile to develop an alternative route.

Preparation of the hydrido complex can be accomplished by the coupling of a hydrogen atom and a chromium(II) ion (36),

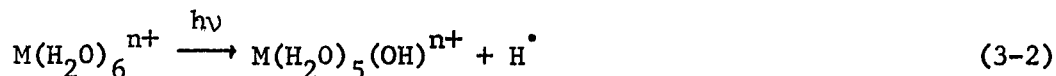


in analogy to the synthesis of organochromium(III) cations by the reaction of organic free-radicals and chromium(II) ions. Generation of hydrogen atoms in the presence of chromium(II) ions will lead to the

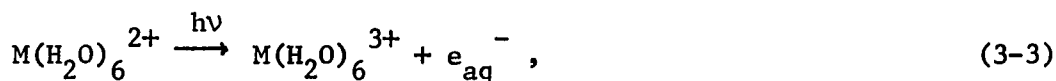
formation of the hydrido complex. To actually observe the species, however, a rapid method of detection is necessary, as Cohen and Meyerstein (36) reported it to be highly unstable in acidic solution.

The technique of flash photolysis is ideally suited to kinetic studies of reactions of $\text{HCr}(\text{H}_2\text{O})_5^{2+}$. Hydrogen atoms can be generated photochemically, in the presence of chromium(II) ions, by taking advantage of the UV photochemistry of chromium(II) ion itself. The hydrido complex is easily detected by its UV absorption spectrum (36), allowing kinetic data to be obtained by monitoring absorbance as a function of time. Finally, flash photolysis is a technique which responds rapidly enough to allow study of some reactions of the $\text{HCr}(\text{H}_2\text{O})_5^{2+}$ ion.

It has been known for at least 40 years that irradiation of aqueous solutions of chromium(II) ion with UV light causes evolution of hydrogen gas (Ref. 154, pp. 116-117). The photoreaction proceeds with oxidation of the metal ion to chromium(III) ion, and concurrent reduction of the proton to atomic hydrogen. Production of molecular hydrogen by photo-oxidation of ions in acidic solution has been demonstrated for a number of metal cations, $\text{Fe}_{\text{aq}}^{2+}$ (Ref. 154, pp. 159-161 and Ref. 162), $\text{Ce}_{\text{aq}}^{3+}$ (Ref. 154, pp. 317-318 and Ref. 162), $\text{Co}_{\text{aq}}^{2+}$ (Ref. 154, p. 193), $\text{Eu}_{\text{aq}}^{2+}$ (162,163), and $\text{V}_{\text{aq}}^{2+}$ (162,164). For all these ions, including $\text{Cr}_{\text{aq}}^{2+}$, it was generally believed that the primary photochemical process involved formation of a hydrogen atom.



In more recent years, however, absorption of UV radiation by $\text{Fe}_{\text{aq}}^{2+}$ (165,166) or $\text{Cr}_{\text{aq}}^{2+}$ (165,167,168) ions, is now believed to lead to a process in which an electron is ejected from the cation to the solvent, forming the hydrated electron and oxidized metal ion. Hydrogen atoms are produced from e_{aq}^- in a secondary reaction by the reduction of protons,



for which $k_4 = 2.3 \times 10^{10} \text{M}^{-1} \text{s}^{-1}$ (123). The rate of Reaction 3-4 is so rapid that even in dilute acid, $1 \times 10^{-3} \text{M} \text{H}_3\text{O}^+$, the hydrated electron has a half-life of only 0.03 μs . Irrespective of the nature of the primary photoreaction, molecular hydrogen is formed by dimerization of H^\bullet ,



accounting for the observed product.

For $\text{Cr}_{\text{aq}}^{2+}$ ion, Hartmann et al. (167) obtained indirect evidence for process 3-3 by trapping experiments. In some product studies, aqueous chromium(II) perchlorate at pH 2.6 was photolyzed with UV light in the presence of nitrous oxide, known to be an efficient scavenger for hydrated electrons.



$$k_6 / \text{M}^{-1} \text{s}^{-1} = 8.7 \times 10^9 \quad (121)$$



$$\text{pK}_7 = 11.9 \pm 0.2 \quad (122)$$

Nitrogen gas was detected as one of the products, presumably formed by Reaction 3-6. This result, coupled with a study of the ratio of H_2 to N_2 produced as a function of nitrous oxide concentration, gave further evidence for the hydrated electron. As $[\text{N}_2\text{O}]$ was increased, the ratio $\text{H}_2:\text{N}_2$ decreased as expected for a competition between Reactions 3-4 and 3-6 for e_{aq}^- . Although there appears to be no report in the literature for the direct observation of the hydrated electron from the UV photolysis of $\text{Cr}_{\text{aq}}^{2+}$, the product studies of Hartmann et al. (167) provide unequivocal evidence for its existence.

The photolytic process responsible for production of a hydrated electron results from absorption of light by an ion's charge-transfer-to-solvent, CTTS, transition. Well-documented examples of photoelectron production from CTTS excitation exist for several anions--the simple halides, Cl^- , Br^- , I^- , and pseudohalide NCS^- ; oxo anions, SO_4^{2-} , SO_3^{2-} , $\text{S}_2\text{O}_3^{2-}$, H_2PO_4^- , HPO_4^{2-} , $\text{P}_2\text{O}_7^{2-}$, CO_3^{2-} (169); and anionic metal complexes $\text{Fe}(\text{CN})_6^{4-}$ (Ref. 154, pp. 148-151 and Refs. 162,170), $\text{Ru}(\text{CN})_6^{4-}$ (Ref. 154, p. 308 and Ref. 170), $\text{W}(\text{CN})_8^{4-}$ and $\text{Mo}(\text{CN})_8^{4-}$ (Ref. 154, pp. 124-127 and Refs. 162,170), IrCl_6^{3-} (Ref. 154, p. 311 and Ref. 170), CuCl_2^- and CuCl_3^{2-} (171,172). Basco et al. (173) also reported e_{aq}^- production from photolysis of some monovalent metal cations, Co^+ , Ni^+ , Zn^+ , and Cd^+ . Although the assignment of the CTTS transition in metal complexes is

often difficult due to overlap with other charge-transfer transitions in the same spectral region, the CTTS transition of $\text{Cr}_{\text{aq}}^{2+}$ ion in aqueous HClO_4 has been assigned (165) to a well-defined shoulder at 270 nm, superimposed on a large absorption extending further into the UV. The molar absorptivity at 270 nm is a rather small number, $\sim 15 \text{ M}^{-1} \text{ cm}^{-1}$ (155).

The efficiency of formation of e_{aq}^- from UV photolysis of $\text{Cr}_{\text{aq}}^{2+}$ can be inferred from the data of Collinson et al. (124). These workers measured the quantum yield¹ of hydrogen formation, $\phi(\text{H}_2)$, for irradiations at 254 and 265 nm of aqueous solutions of chromium(II) ion in hydrochloric acid. At low HCl concentrations, where Cr(II) ion is present as the uncomplexed $\text{Cr}_{\text{aq}}^{2+}$, $\phi(\text{H}_2) = 0.13$ was reported (124). Since $\phi(\text{H}_2)$ is stated to be one-half of $\phi(\text{Cr}_{\text{aq}}^{3+})$, and $\phi(\text{Cr}_{\text{aq}}^{3+})$ must equal $\phi(e_{\text{aq}}^-)$, the quantum yield for hydrated electron production is 0.26. This result means that 26% of the excitations of the CTTS band are productive in generating e_{aq}^- , a reasonably efficient process. Aqueous $\text{Cr}_{\text{aq}}^{2+}$ ion satisfies at least one of the important criteria for use as a photochemical source of hydrated electrons--the quantum yield for e_{aq}^- is appreciable; however, the CTTS transition has a rather low molar absorptivity, resulting in poor light absorption of wavelengths necessary to initiate the desired photochemistry. An additional advantage offered by this source of e_{aq}^-

¹Quantum yield is a measure of the efficiency of a photochemical process. For product formation, it is defined as the number of species formed divided by the number of photons absorbed.

is the formation of $\text{Cr}(\text{H}_2\text{O})_6^{3+}$ as a by-product. By virtue of its relative inertness, no complicating side-reactions are possible.

Review of Similar Transition Metal Hydrides

The widespread interest in transition metal hydrides results from their involvement as reactive intermediates in the activation of molecular hydrogen (174-180). One of the earliest observations of a homogeneous catalyzed hydrogenation reaction was made by Calvin in 1938 (181). He reported that copper(I) acetate, in quinoline solution, catalyzed the reduction of benzoquinone and copper(II) ions by molecular hydrogen. Peters and Halpern (182,183) and Halpern et al. (184) investigated the catalysis of the reduction of dichromate ion, in aqueous perchloric acid, by copper(II) ion. On the basis of the kinetic results, a hydridocopper(II) intermediate was postulated, arising from the heterolytic cleavage of the hydrogen molecule.



In a subsequent reaction, copper(I) ion was formed which was believed to be the species responsible for the reduction of $\text{Cr}_2\text{O}_7^{2-}$.



In other work, copper(I) itself was shown to be capable of reacting directly with molecular hydrogen, forming CuH from a heterolytic splitting of H_2 (174).

A similar catalysis by silver(I) ion was seen by Webster and Halpern (185) to occur by two pathways in which the hydrogen molecule is activated. At higher temperatures, a heterolytic cleavage of H_2 forms the intermediate AgH .



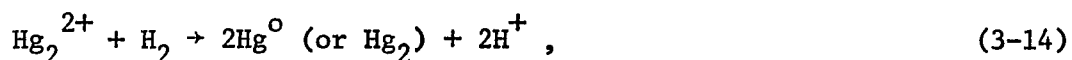
A homolytic cleavage is favored at lower temperatures.



Although both mercury(II) and mercury(I) ions are capable of catalyzing the homogeneous reductions of molecular hydrogen, there is no evidence for the participation of hydride intermediates (186). Instead, Korinek and Halpern (186) proposed a two-electron process, for $Hg(II)$,



and for $Hg(I)$,



in which the mercury cation is reduced to elemental mercury by H_2 in an electron-transfer process. Similar processes for $Cu(II)$ or $Ag(I)$ were shown (187) to be thermodynamically unreasonable.

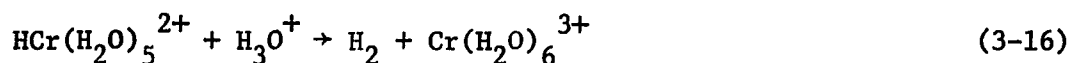
Many metal complexes also have the ability to catalyze homogeneous hydrogenations, with formation of intermediate hydrido species. Some earlier examples are $HRuCl_5^{3-}$, $HRhCl_5^{3-}$, $HCo(CN)_5^{3-}$, $IrH_2Cl(CO)(PPh_3)_2$ and $HPdCl_3^{2-}$ (174,175). Several additional complexes have been found

to be catalytically active towards hydrogen, serving as useful homogeneous catalysts for the reduction of organic compounds. Many reviews and books dealing with this active area of research have appeared (176-180).

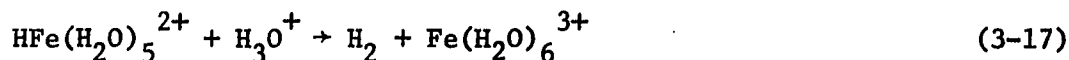
The advent of pulse radiolysis made possible the study of unstable transition metal hydrides. Hydrogen atoms are easily generated in the presence of the metal ion to produce the hydrido complex.



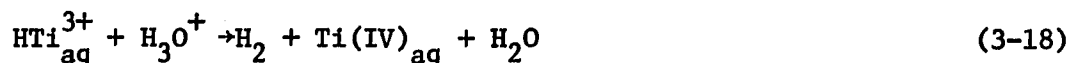
In general, the pulse radiolytic technique has been applied more to the study of aquated metal ions than metal complexes (188,189). As discussed earlier, the $HCr(H_2O)_5^{2+}$ ion is one such intermediate which has been prepared by pulse radiolysis, and its reaction with H_3O^+ to produce H_2 and $Cr(H_2O)_6^{3+}$ ions studied (36).



The species formed by reaction of a hydrogen atom with the iron(II) ion was first proposed (190,191) to be $HFe(H_2O)_5^{2+}$, which was later confirmed (192,193) by pulse radiolysis. This hydrido species also reacts with H_3O^+ to liberate molecular hydrogen and iron(III) ion, the kinetics of which have been determined (192,193).



HTi_{aq}^{3+} was detected recently (194-196), and its decomposition in acidic solution to H_2 and Ti(IV) ions briefly studied (196).



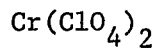
In its reaction with $\text{Cr}_{\text{aq}}^{2+}$, $\text{Fe}_{\text{aq}}^{2+}$, and Ti(III) the hydrogen atom has been shown, in the above studies, to act as an oxidizing agent towards these reducing metal ions. Using radiolysis to generate atomic hydrogen, several other metal ions have been found which are also oxidized by hydrogen atoms, namely V^{2+} (197); Pu(III) (198); Cd^+ and Ni^+ (199); Ni(CN)_4^{2-} (200); and Al^{2+} (201). This is somewhat unusual as hydrogen atoms are generally considered as strongly reducing ($E^0 = -2.1 \text{ V}$ (202)); for instance hydrogen atoms can reduce Ce(IV) , Tl^+ , and Cu^{2+} , but not Co^{2+} , Ni^{2+} , Mn^{2+} , Cd^{2+} , Pb^{2+} , or Co(III) amines (203).

A study using flash photolysis to form a hydrido complex was recently reported. Ferraudi (172) showed UV photolysis of acidic solutions of CuCl_3^- produces the transient HCuCl_3^{2-} species by reaction of the substrate with photochemically generated hydrogen atoms. Excitation of the CTTS transition of CuCl_3^- was reported to lead to photoelectron production, which are scavenged by H_3O^+ ions to form hydrogen atoms.

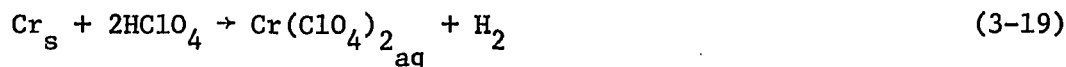
Certainly photochemical production of hydrated electrons is a convenient source of hydrogen atoms. Presumably, flash photolysis has a promising future as a technique complementary to pulse radiolysis for the study of reactive hydrido intermediates.

EXPERIMENTAL

Materials

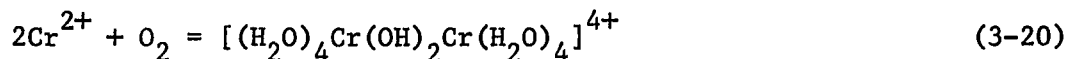


Aqueous solutions of chromium(II) perchlorate were prepared from the metal by oxidation with perchloric acid. Chromium pellets of 99.999% purity (Apache Chemicals, Inc.) were pretreated with 1 M HCl by warming with a heat gun until gas evolution began. The pellets were quickly rinsed with water and rapidly introduced into 5 M HClO₄, while flushing with nitrogen (204). In order to obtain solutions with a pH of 2 or greater, a slight stoichiometric excess of metal was used (36). After several hours, when evolution of hydrogen had ceased, the solution



was withdrawn from the unreacted chromium, and diluted to about 0.2 M Cr²⁺_{aq}. The concentration of Cr²⁺_{aq} ion was determined spectrophotometrically by measuring the absorbance of the broad maximum around 715 nm, using $\epsilon = 4.85 \text{ M}^{-1} \text{ cm}^{-1}$.

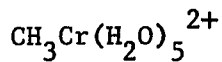
The perchloric acid concentration was determined by titration. An aliquot of the solution was first air-oxidized, converting the chromium(II) ion to the hydroxo-bridged dimer of chromium(III) (75), and then applied to a column of Dowex 50W-X8 cation-exchange resin in



the acid form. Elution was accomplished with water and continued until the eluent was no longer acidic by pH paper. The eluent was titrated with standardized NaOH solution to a phenolphthalein end-point. The amount of acid present in the chromium(II) perchlorate solution was calculated from the total amount titrated by the following equation,

$$[\text{H}^+]_{\text{Cr}(\text{ClO}_4)_2} = [\text{H}^+]_{\text{titrated}} - 4[\text{Cr}(\text{III})], \quad (3-21)$$

where $4[\text{Cr}(\text{III})]$ is equivalent to the amount of acid displaced from the ion-exchange resin by the +4 charged chromium(III) species. The concentration of the dimeric chromium(III) complex, after air-oxidation, was calculated from the concentration of chromium(II) ion, before oxidation, plus any chromium(III) present originally, determined by its visible spectrum. Typically, solutions millimolar in H_3O^+ were obtained.



Aqueous solutions of this organochromium(III) ion were prepared by the chromium(II) reduction of *t*-butyl hydroperoxide in dilute perchloric acid (20). 14 μl 70% $(\text{CH}_3)_3\text{COOH}$ (7.3 M) (Aldrich) were injected dropwise into 5.2 mL aqueous 0.037 M $\text{Cr}_{\text{aq}}^{2+}$ in 0.045 M HClO_4 . The concentration of $\text{CH}_3\text{Cr}(\text{H}_2\text{O})_5^{2+}$ produced was 7×10^{-3} M as determined by its absorbance at 392 nm, with $\epsilon = 246 \text{ M}^{-1} \text{ cm}^{-1}$ (20), after correction for the absorbance due to $\text{Cr}(\text{H}_2\text{O})_6^{3+}$. The product solution was used as such, without ion-exchange chromatography, with the knowledge that $\text{Cr}(\text{H}_2\text{O})_6^{3+}$ and organic by-products are innocuous in the reaction investigated.

HClO₄, NaOH, LiClO₄

Aqueous solutions were prepared and standardized as described in Part I, Experimental.

Gases

Nitrous oxide, Matheson, 98.0% minimum purity, and nitrogen, Air Products, were used to saturate solutions. Trace amounts of O₂ present in either gas were removed by passing through Cr_{aq}²⁺ scrubbing towers.

Methods

Flash photolysis

Preparation of solutions Aqueous perchloric acid was adjusted to the desired ionic strength by the addition of standardized LiClO₄. The ionic strength was calculated from Equation 3-22.

$$\mu = \frac{1}{2} \{ [\text{H}_3\text{O}^+] + [\text{Li}^+] + 4[\text{Cr}^{2+}] + [\text{ClO}_4^-] \} \quad (3-22)$$

After transferring to a 10 cm quartz spectrophotometric cell, and sealing with a rubber septum, solutions were saturated with nitrogen gas, or in some experiments, N₂O. Prior to a flash photolysis experiment, a small aliquot of Cr(ClO₄)₂ solution was injected into the cell, such that [Cr_{aq}²⁺] = 1 x 10⁻³ M after dilution.

In experiments designed to produce DCr(D₂O)₅²⁺ and study its reaction rate with D₃O⁺, aqueous Cr(ClO₄)₂ was injected into a large volume of D₂O, acidified with 5 M standardized HClO₄. Photolysis solutions

were typically 1-3% H₂O or 0.75-1.7 M H₂O. At such high molarities of D₂O, 53.4-54.4 M, essentially all, 98%, of the H₃O⁺ ions are converted to D₃O⁺ via equilibrium (23).



$$1/K_{(23)} (25^\circ\text{C}) = 11.0 (205)$$

Ionic strength was not maintained at a constant value while [D₃O⁺] was varied.

Temperature control See Part II, Experimental.

Equipment Details of the instrument and data analysis are given in the Appendix.

Spectrum of transient See Part II, Experimental.

Conventional kinetics

The reaction of CH₃Cr(H₂O)₅²⁺ with H₃O⁺ or of CH₃Cr(D₂O)₅²⁺ with D₃O⁺ was initiated by injecting a small aliquot of a stock solution containing CH₃Cr(H₂O)₅²⁺ into thermally equilibrated 0.1 M HClO₄ or DClO₄ (in D₂O) to arrive at [organochromium(III) ion]₀ = (2-6) × 10⁻⁴ M. Reactions in D₂O contained 6.9% H₂O or 3.8 M H₂O. As discussed above, the H₃O⁺ ions are effectively present as D₃O⁺ ions; a 94% conversion is calculated from equilibrium 3-23 at 51.4 M D₂O. Some reactions were carried out under a nitrogen atmosphere, in the presence of (1-2) × 10⁻³ M Cr_{aq}²⁺, and others in air; no effect on the reaction rate was noted.

The kinetic results were obtained by monitoring the loss of absorbance with time at 258 or 300 nm, where the organochromium(III) ion absorbs; because the rates are very slow, the turret assembly of a Cary 219 spectrophotometer was programmed to record absorbances at time intervals of several minutes. Kinetic cells were thermostatted by water circulating through the turret. Pseudo-first-order rate constants were obtained by plotting $\ln(D_t - D_\infty)$ versus time. The slope of such a plot, often obtained by least-squares treatment of the data, is $-k_{\text{obs}}$.

RESULTS

Detection of Transient

Flash photolysis of 1×10^{-3} M chromium(II) perchlorate, in dilute perchloric acid, with a 250 J flash, produced a transient which was detected at 380 nm, the reported (36) maximum of the $\text{HCr}(\text{H}_2\text{O})_5^{2+}$ ion. During the decay of the scattered flashlight, about 0.6 ms, an absorbance grew in which then decreased, at a rate dependent on the acid concentration, to a final absorbance slightly larger than before photolysis. The size of the transient was found to be directly dependent on the energy of the flash, as shown in Figure 3-1. This confirmed the transient was formed as a result of a reaction directly dependent on the intensity of the photolyzing flash.

Effect of Scavengers

 N_2O

Saturating the photolysis solution with nitrous oxide, instead of nitrogen gas, decreased the amount of transient produced. A 250 J flash on 1×10^{-3} M $\text{Cr}_{\text{aq}}^{2+}$ in 1×10^{-3} M HClO_4 produced a maximum absorbance change of only 0.0044 ($l = 10$ cm) at 380 nm in the presence of N_2O , as compared to 0.020 in its absence. If one tentatively assigns the identity of the transient to $\text{HCr}(\text{H}_2\text{O})_5^{2+}$, then the concentrations can be computed using the published molar absorptivity $\epsilon_{380} = 190 \text{ M}^{-1} \text{ cm}^{-1}$ (36). N_2O reduces the yield of the transient from 1.0×10^{-5} M to 2.3×10^{-6} M, a 77% decrease.

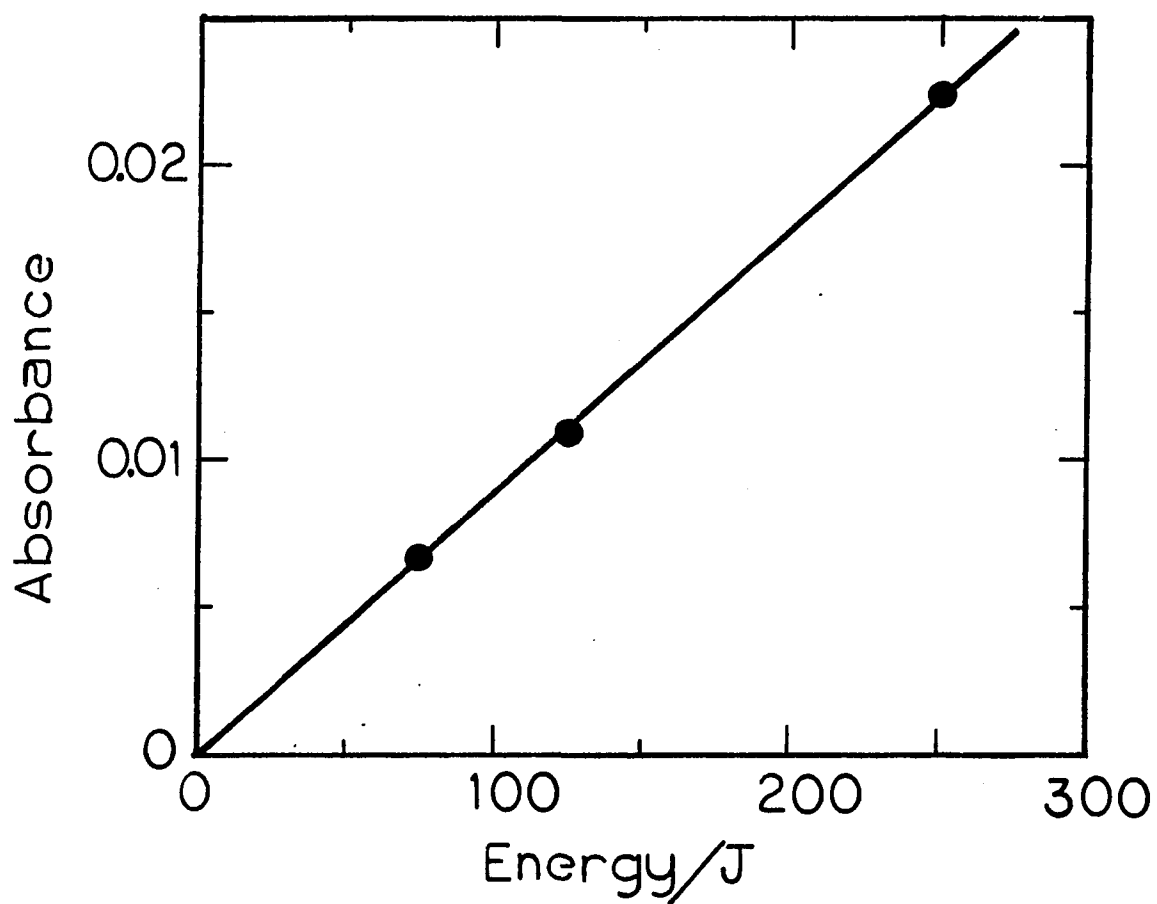


Figure 3-1. Dependence of the absorbance due to $\text{HCr}(\text{H}_2\text{O})_5^{2+}$ at 380 nm on flash energy. Cell length = 10 cm; 1×10^{-3} absorbance unit is approximately 2 mV

CH₃OH

Scavenging experiments were also designed to trap hydrogen atoms by photolysis in aqueous 5 M methanol, $[H_3O^+] = 0.1$ M. At 380 nm, no transient absorbance changes were detected, only a permanent decrease in the photomultiplier voltage. The UV-visible spectrum of the solution was recorded after flashing, and consisted of a maximum at 390 nm, and an ill-defined shoulder at about 280 nm, possibly indicating formation of the hydroxymethylpentaquo chromium(III) ion, $HOCH_2Cr(H_2O)_5^{2+}$, which has maxima at 392 and 282 nm (22,25).

To help in identifying the species, the rate of its decomposition in 0.1 M $HClO_4$ was measured. A solution containing 1×10^{-3} M Cr_{aq}^{2+} and 0.1 M $HClO_4$ in 5 M CH_3OH was photolyzed with several 250 J flashes, and the absorbance monitored at 392 nm with time. Rather than the simple loss of absorbance expected, there was an indication that a faster reacting species, also absorbing at 392 nm, was present. After its reaction was complete, however, the remaining loss of absorbance gave a pseudo-first-order rate constant of $(8.9 \pm 0.2) \times 10^{-4} s^{-1}$ at 25.0°C. In 0.1 M $HClO_4$, authentic $HOCH_2Cr(H_2O)_5^{2+}$ reacts with an observed rate constant of $k/s^{-1} = 7.1 \times 10^{-4}$, in a 50:50 CH_3OH to H_2O mixture adjusted to an ionic strength of 1.0 M (16). Considering the medium differences, the rate constants are in reasonable agreement, establishing that the $HOCH_2Cr(H_2O)_5^{2+}$ complex is formed upon photolysis of chromium(II) ion in aqueous, acidic methanol. The identity of the other, faster reacting species was not established. However, taking into consideration that

the solution was photolyzed several times, the secondary product may arise from secondary photolysis, perhaps of $\text{HOCH}_2\text{Cr}(\text{H}_2\text{O})_5^{2+}$ formed in prior flashes.

Rate of Reaction of $\text{HCr}(\text{H}_2\text{O})_5^{2+}$ with H_3O^+

Dependence on $[\text{H}_3\text{O}^+]$

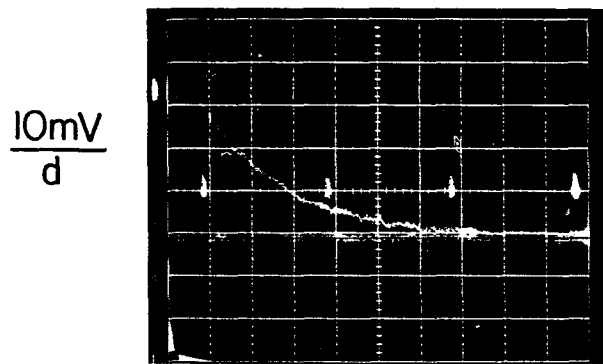
The dependence of the rate of decomposition of the transient on the concentration of acid, was investigated by monitoring the decrease of its absorbance with time as a function of $[\text{H}_3\text{O}^+]$ in the range 0.01-0.20 M. Ionic strength was maintained at 0.20 M, and the temperature was $26.0 \pm 0.5^\circ\text{C}$. Most of the kinetic data were collected at 380 nm because the largest absorbance changes were found to occur in this region. A few kinetic traces were also obtained at 330 and 420 nm, and at lower flash energies, 125 and 75 J.

Oscilloscope sensitivities of 5 or 10 mV/d ($I_0 = 1000$ mV) and time bases of from 0.2 to 5 ms/d (depending on $[\text{H}_3\text{O}^+]$) were used to follow the transients. Representative photographs of the transient decay, at four different $[\text{H}_3\text{O}^+]$, are reproduced in Figure 3-2. The kinetic data were analyzed according to a pseudo-first-order treatment in transient concentration, by plotting $\ln(D'_t - D'_\infty)^1$ versus time. Linear plots are obtained at all acidities, wavelengths of monitoring, and flash energies. In Figure 3-3, the rate plots corresponding to the photographs in

¹ D' is linearly related to D, see Appendix.

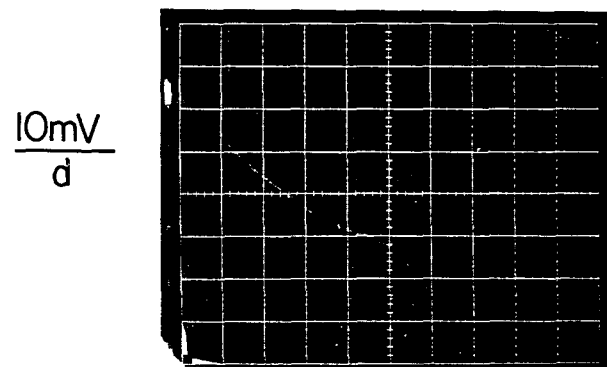
Figure 3-2. Representative photographs of oscilloscope traces showing the reaction of $\text{HCr}(\text{H}_2\text{O})_5^{2+}$ with H_3O^+ at various acidities. Monitoring $\lambda = 380 \text{ nm}$; flash energy = 250 J; $\mu = 0.20 \text{ M}$ (LiClO_4); $I_0 = 1000 \text{ mV}$; I_{t_∞} (mV) = 950 (a), 960 (b), 994 (c), 975 (d)

a) 0.010M H_3O^+



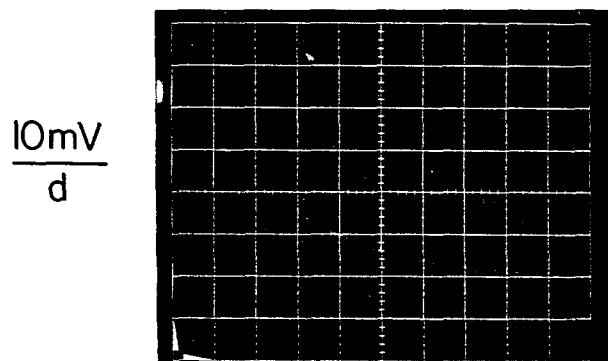
5 ms/d

b) 0.030M H_3O^+



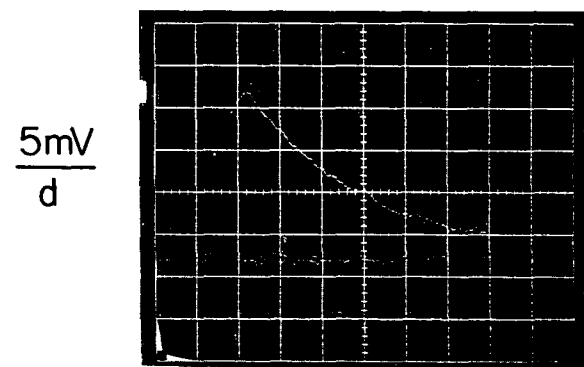
1ms/d

c) 0.080M H_3O^+



0.5 ms/d

d) 0.20M H_3O^+



0.2 ms/d

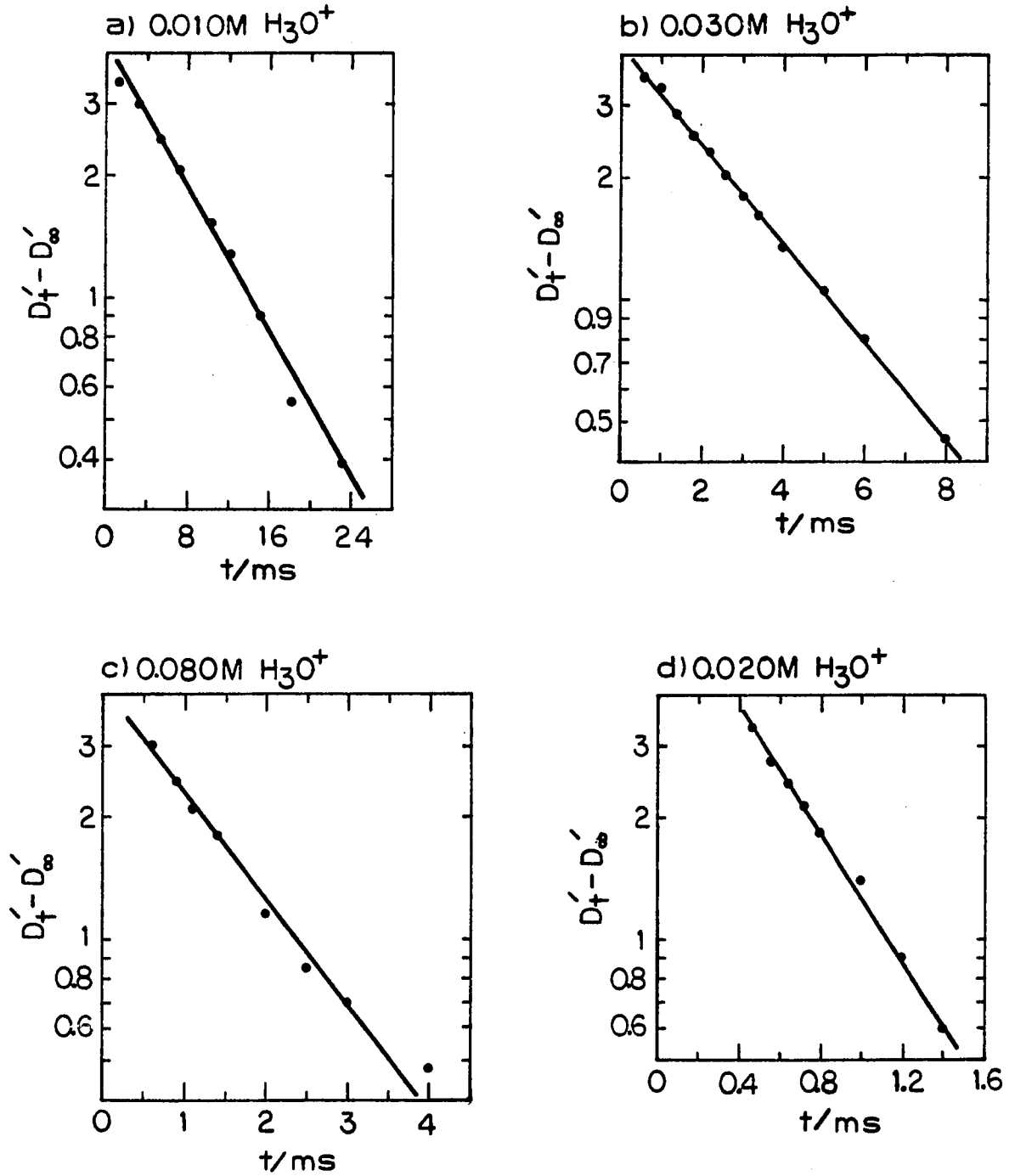


Figure 3-3. Plots of $\ln(D'_t - D'_\infty)$ versus time for photographs of Figure 3-2

Figure 3-2 are given. The pseudo-first-order rate constants, k_{obs} , are listed in Table 3-1 at the various acidities.

The experimental rate constant, k_{obs} , shows a linear dependence on the perchloric acid concentration, as evidenced by a plot of k_{obs} versus $[\text{H}_3\text{O}^+]$, Figure 3-4.

$$k_{\text{obs}} = k_0 + k[\text{H}_3\text{O}^+] \quad (3-24)$$

The slope of the line in Figure 3-4 is identified with k of Equation 3-24 and k_0 is given by the intercept. A least-squares fit of the data yields $k_0/\text{s}^{-1} = -57 \pm 46$ so it is assigned a value of zero. The value for k was obtained by dividing each entry in Table 3-1 by $[\text{H}_3\text{O}^+]$ and averaging to obtain $k/\text{M}^{-1}\text{s}^{-1} = (9.7 \pm 1.0) \times 10^3$. This suggests the transient decomposes by exclusively an acid-dependent path. Contribution from an acid-independent route appears to be negligible from the results at these acidities. Measurement of the rate of reaction at very low $[\text{H}_3\text{O}^+]$ would be necessary to prove the existence of an acid-independent term in the rate expression. However, it is definitely an unimportant reaction pathway at acidities greater than about 10^{-3} M.

Effect of temperature

The temperature dependence of the reaction of H_3O^+ with the transient was investigated by determining its rate over a 34° range in temperature. The acidity was maintained at 0.01 M HClO_4 , and the absorbance was monitored at 380 nm following a 250 J flash.

Table 3-1. Rate constants for the reaction of $\text{HCr}(\text{H}_2\text{O})_5^{2+}$ with H_3O^{+a}

$[\text{H}_3\text{O}^+]/\text{M}$	$k_{\text{obs}}/\text{s}^{-1}$
0.010	94.7 ± 4.6 (4)
0.010^b	95.4 ± 4.4 (3)
0.010^c	101.0 ± 7.3 (3)
0.010^d	104.0 ± 2.1 (3)
0.010^e	94.0 ± 6.3 (3)
0.030	283.0 ± 6.6 (3)
0.050	423 ± 63 (5)
0.060	576 ± 49 (2)
0.080	630 ± 46 (3)
0.10	931 ± 58 (6)
0.13	1330 ± 45 (3)
0.15	1365 ± 190 (3)
0.17	2010 ± 90 (3)
0.20	2200 ± 560 (6)

^aUncertainties represent 1σ ; number in parentheses is number of kinetic runs; monitoring $\lambda = 380$ nm; flash energy = 250 J, except as noted; $\mu = 0.20$ M (LiClO_4); $[\text{Cr}_{\text{aq}}^{2+}] = 1 \times 10^{-3}$ M; $T = 26.0 \pm 0.5^\circ\text{C}$.

^b330 nm.

^c420 nm.

^d125 J.

^e75 J.

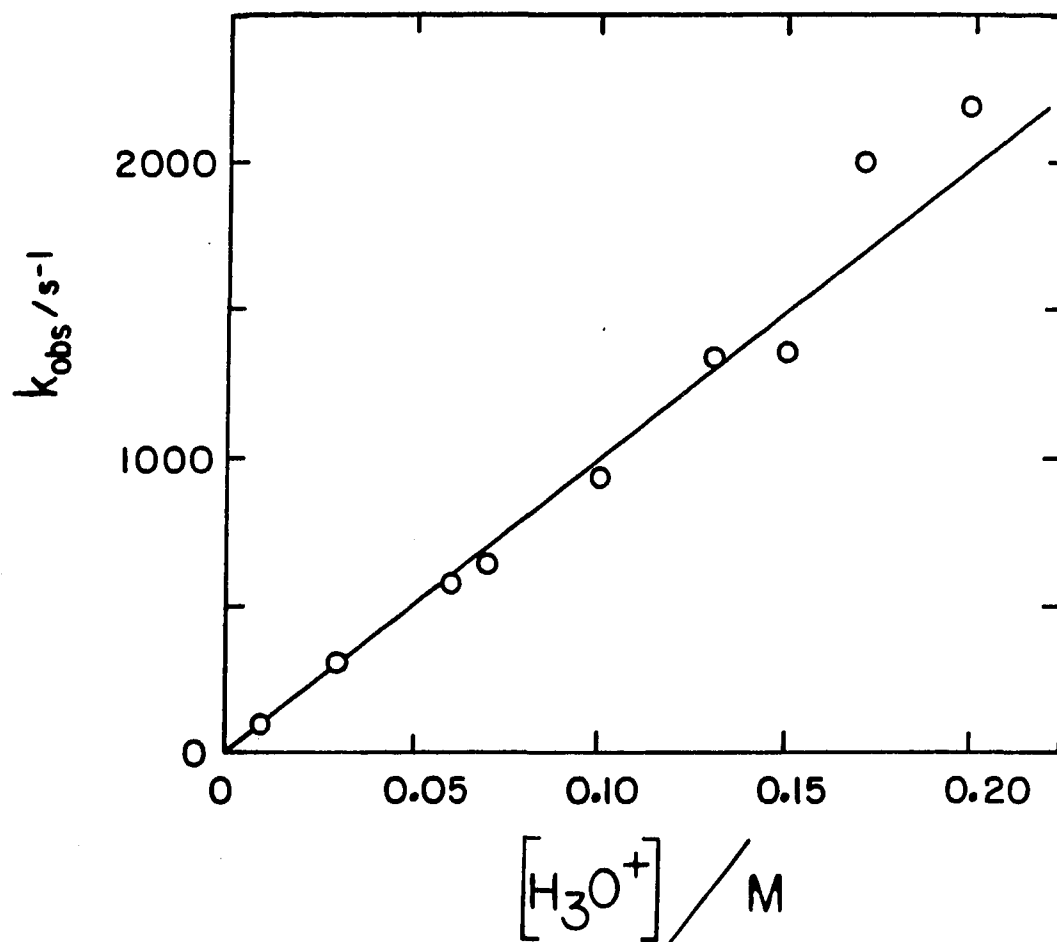


Figure 3-4. The dependence of k_{obs} on $[\text{H}_3\text{O}^+]$ for the reaction of $\text{HCr}(\text{H}_2\text{O})_5^{2+}$ with H_3O^+

Values of the second-order-rate constant k , determined at each temperature, are tabulated in Table 3-2. The rate constant k was analyzed as a function of temperature using the Eyring equation, derived from the activated complex theory of absolute reaction rates,

$$k = \frac{RT}{Nh} \exp\left(\frac{\Delta S^\ddagger}{R}\right) \exp\left(\frac{-\Delta H^\ddagger}{RT}\right), \quad (3-25)$$

where

N = Avogadro's number

h = Planck's constant

T = Absolute temperature

R = Gas constant

ΔS^\ddagger = entropy of activation

ΔH^\ddagger = enthalpy of activation.

As Equation 3-25 predicts, a plot of $\ln k/T$ versus $1/T$ should be linear with a slope given by $-\Delta H^\ddagger/R$ and $[\ln(R/Nh) + (\Delta S^\ddagger/R)]$ as the intercept. Treatment of the data from Table 3-2 accordingly resulted in a straight line, as shown in Figure 3-5. A least-squares fit of the data to Equation 3-25 gives $\Delta H^\ddagger = 6.3 \pm 0.2$ kcal/mol and $\Delta S^\ddagger = -19.1 \pm 0.7$ e.u.

Effect of ionic strength

The variation of the rate constant for the reaction of H_3O^+ with the transient was also investigated as a function of ionic strength, for the purpose of substantiating that it is correctly formulated as a dipositive cation. At a perchloric acid concentration of 0.01 M, the ionic strength was varied from 0.013 to 0.20 M by the addition of

Table 3-2. Rate constants for the reaction of $\text{HCr}(\text{H}_2\text{O})_5^{2+}$ with H_3O^+ at various temperatures^a

$T/^{\circ}\text{C}$	$10^{-4}k/\text{M}^{-1}\text{s}^{-1}$
14.4	0.637 ± 0.043
14.7	0.616 ± 0.086
20.5	0.800 ± 0.048
27.0	1.02 ± 0.035
35.5	1.50 ± 0.020
48.1	2.17 ± 0.056^b

^aUncertainties represent 1 σ of three replicate runs, except as noted; $[\text{H}_3\text{O}^+] = 0.01 \text{ M}$; $[\text{Cr}_{\text{aq}}^{2+}] = 1 \times 10^{-3} \text{ M}$; $\mu = 0.20 \text{ M}$ (LiClO_4); monitoring $\lambda = 380 \text{ nm}$; flash energy = 250 J.

^bAverage of two duplicate runs.

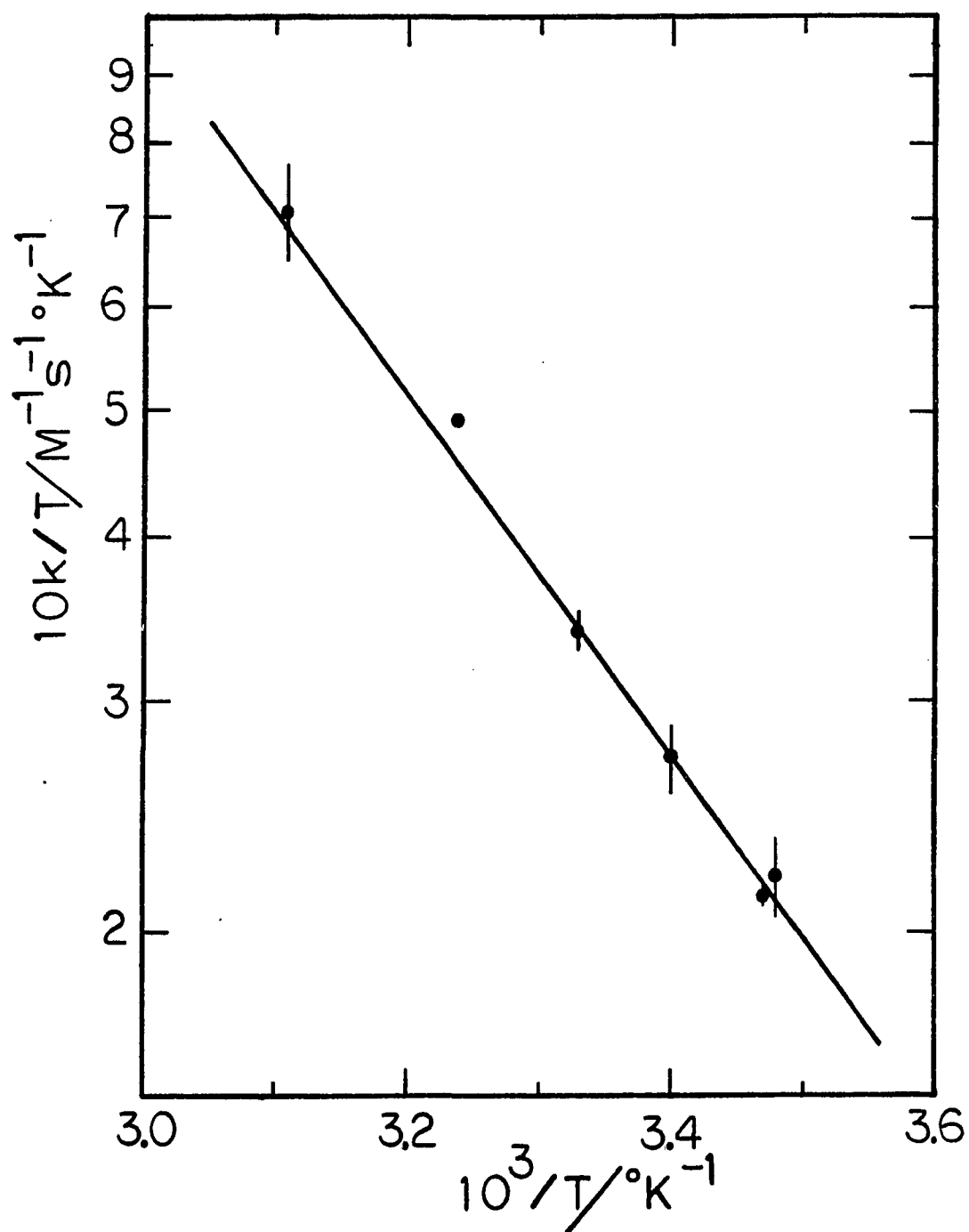


Figure 3-5. Plot of $\ln(k/T)$ versus $1/T$ for the reaction of $HCr(H_2O)_5^{2+}$ with H_3O^+

LiClO_4 . Ionic strength was calculated from Equation 3-22. A value at $\mu = 0.008 \text{ M}$ was also obtained by lowering $[\text{H}_3\text{O}^+]$ to 0.005 M . The data were treated according to Equation 3-26,

$$\log k = \log k^{\circ} + \frac{2Z_A Z_B \alpha \mu^{1/2}}{1 + \beta a \mu^{1/2}} \quad (3-26)$$

The Brønsted-Debye-Hückel equation (Equation 3-26) was presented earlier, in Part I, Results; that discussion will not be repeated here. The rate constants obtained as a function of μ are collected in Table 3-3 and the plot suggested by Equation 3-26 is given in Figure 3-6, where βa has been taken as unity.

The line on the graph has been drawn to the theoretical slope of +4 as expected for reactants of charge +2 and +1. While data points at the lower ionic strengths approximate a line with slope +4 quite well, negative deviation occurs at ionic strengths greater than about 0.07 M .

This is not surprising as the Debye-Hückel expression is generally useful only in dilute solutions, at ionic strengths less than 0.01 M . To extend its useful region, a term linear in ionic strength (77-81) is often added, so Equation 3-26 becomes,

$$\log k = \log k^{\circ} + \frac{2Z_A Z_B \alpha \mu^{1/2}}{1 + \beta a \mu^{1/2}} - C\mu \quad (3-27)$$

The kinetic data were fit to Equation 3-27 using a least-squares computer program¹ which allowed k° , $2Z_A Z_B$, and C to be treated as adjustable

¹The least-squares program was one implemented by Dr. R. B. Pfaff, Ames Laboratory.

Table 3-3. Rate constants for the reaction of $\text{HCr}(\text{H}_2\text{O})_5^{2+}$ with H_3O^+ at various ionic strengths^a

μ/M	$10^{-3}k/\text{M}^{-1}\text{s}^{-1}$
0.008 ^b	5.44 \pm 0.34 (3)
0.013	5.18 \pm 0.15 (6)
0.018	6.05 \pm 0.25 (3)
0.023	5.80 \pm 0.14 (6)
0.028	6.08 \pm 0.16 (3)
0.033	6.60 \pm 0.34 (6)
0.043	7.40 \pm 0.33 (3)
0.053	7.34 \pm 0.20 (5)
0.073	7.76 \pm 0.54 (3)
0.103	8.60 \pm 0.59 (6)
0.153	8.92 \pm 0.52 (3)
0.203	9.79 \pm 0.55 (6)

^aUncertainties represent 1 σ ; number in parentheses is number of kinetic runs; $[\text{H}_3\text{O}^+] = 0.01 \text{ M}$, except as noted; $[\text{Cr}_{\text{aq}}^{2+}] = 1 \times 10^{-3} \text{ M}$; μ adjusted with LiClO_4 ; monitoring $\lambda = 380 \text{ nm}$; flash energy = 250 J; $T = 26.7 \pm 0.3^\circ\text{C}$.

^b $[\text{H}_3\text{O}^+] = 0.005 \text{ M}$.

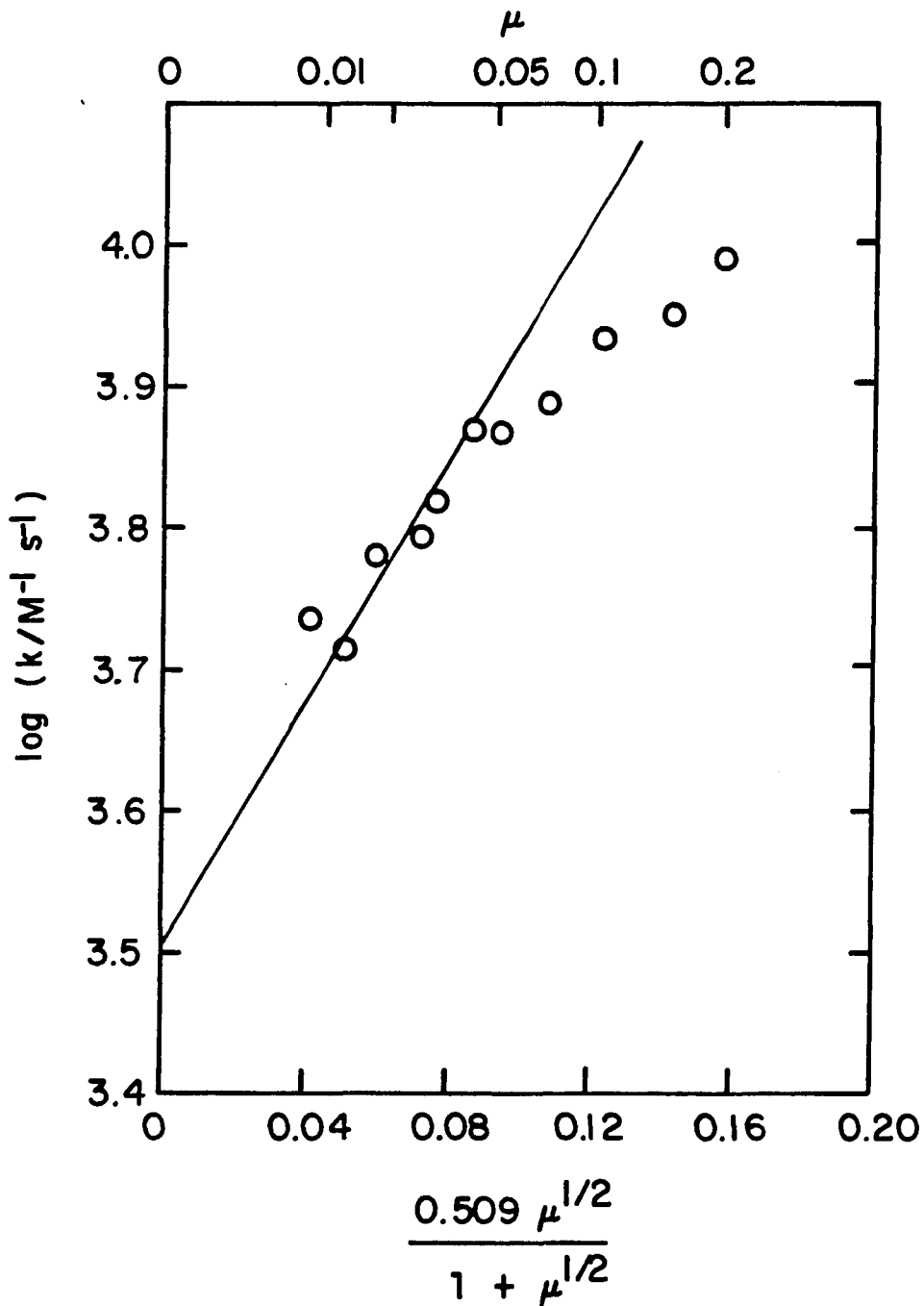


Figure 3-6. Plot of $\log k$ versus $\frac{0.509 \mu^{1/2}}{1 + \mu^{1/2}}$ for the reaction of $HCr(H_2O)_5^{2+}$ with H_3O^+ . The line is drawn to have a slope of +4

parameters. Setting $\beta_a = 1$, the following values were obtained,

$$k^{\circ}/M^{-1}s^{-1} = (3.8 \pm 0.3) \times 10^3$$

$$2Z_A Z_B = 3.3 \pm 0.6$$

$$C = 0.5 \pm 0.3.$$

Within its stated uncertainty, $2Z_A Z_B$ is approximately 4. The value for the constant C is of a reasonable magnitude (81).

Effect of deuterium substitution

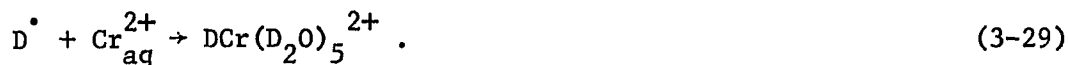
$\text{DCr}(\text{D}_2\text{O})_5^{2+}$ To obtain additional mechanistic information about the cleavage of the hydrido-chromium bond by H_3O^+ , the deuterated complex was made, and its effect on the reaction rate studied. Formation of hydrated electrons in acidified deuterium oxide, leads to deuterium atoms,



$$k_{28}/M^{-1}s^{-1} = (1.71 \pm 0.09) \times 10^{10} \quad (206)$$

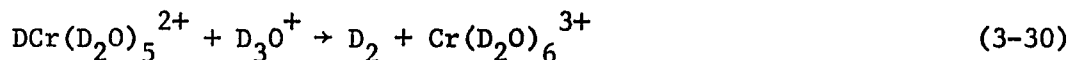
with a rate 26% slower than the analogous production of H^\bullet atoms,

Reaction 3-4. In a secondary reaction, deuterium atoms will react with chromium(II) ions to generate $\text{DCr}(\text{D}_2\text{O})_5^{2+}$,



The rate of Reaction 3-29 has not been measured, but is too rapid to follow by conventional flash photolysis.

The rate of Reaction 3-30 was investigated



over a range of $[\text{D}_3\text{O}^+] = 0.01\text{--}0.1$ M, in D_2O containing 1-3% H_2O , by monitoring the absorbance at 380 nm as a function of time. The ionic strength was not maintained at a constant value, independent of $[\text{D}_3\text{O}^+]$; it was calculated for any given solution using Equation 3-22. The rate of reaction has a pseudo-first-order dependence on $[\text{DCr}(\text{D}_2\text{O})_5^{2+}]$ as evidenced by linear pseudo-first-order rate plots obtained with a large excess of D_3O^+ . The reaction also appears to have the expected first-order dependence on $[\text{D}_3\text{O}^+]$ as suggested by an approximately linear plot of k_{obs} versus $[\text{D}_3\text{O}^+]$, curved somewhat by the variation in ionic strength. The rate constants obtained as a function of $[\text{D}_3\text{O}^+]$ and ionic strength are given in Table 3-4.

The rate of reaction of the $\text{DCr}(\text{D}_2\text{O})_5^{2+}$ complex with D_3O^+ is conveniently compared to that of the $\text{HCr}(\text{H}_2\text{O})_5^{2+}$ ion with H_3O^+ by examination of Figure 3-7, where the second-order rate constants have been plotted as a function of ionic strength on Figure 3-6. The data obtained for the deuterated complex is seen to approximate a line of the same slope as for the reaction of $\text{HCr}(\text{H}_2\text{O})_5^{2+}$ with H_3O^+ , indicating similar charges on the reactants. Again, curvature is seen at the higher ionic strengths, $\mu > 0.08$ M, as for the hydrido complex. The datum point at $\mu = 0.014$ M appears to be anomalous. The rate of reaction of the deuterated complex with D_3O^+ is much slower than the reaction in H_2O . Extrapolation to zero ionic strength affords values for k^0 of

Table 3-4. Rate constants for the reaction of $\text{DCr}(\text{D}_2\text{O})_5^{2+}$ with D_3O^+ ^a

$[\text{D}_3\text{O}^+]/\text{M}$	μ/M	$k_{\text{obs}}/\text{s}^{-1}$	$10^{-3}k/\text{M}^{-1}\text{s}^{-1}$ ^b
0.00995	0.014	13.8 ± 0.1 (2)	1.39 ± 0.01
0.0295	0.032	42 ± 3 (3)	1.4 ± 0.1
0.0487	0.054	81 ± 8 (3)	1.7 ± 0.2
0.0686	0.074	130 ± 10 (3)	1.9 ± 0.1
0.0988	0.104	200 ± 20 (3)	2.0 ± 0.2

^aUncertainties represent 1σ ; number in parentheses is number of kinetic runs; 1-3% H_2O in D_2O ; $[\text{Cr}_{\text{aq}}^{2+}] = (1-2) \times 10^{-3} \text{ M}$; μ calculated from Equation 3-22; monitoring $\lambda = 380 \text{ nm}$; flash energy = 250 J; $T = 21.6^\circ\text{C}$.

$$^b k = k_{\text{obs}}/[\text{D}_3\text{O}^+].$$

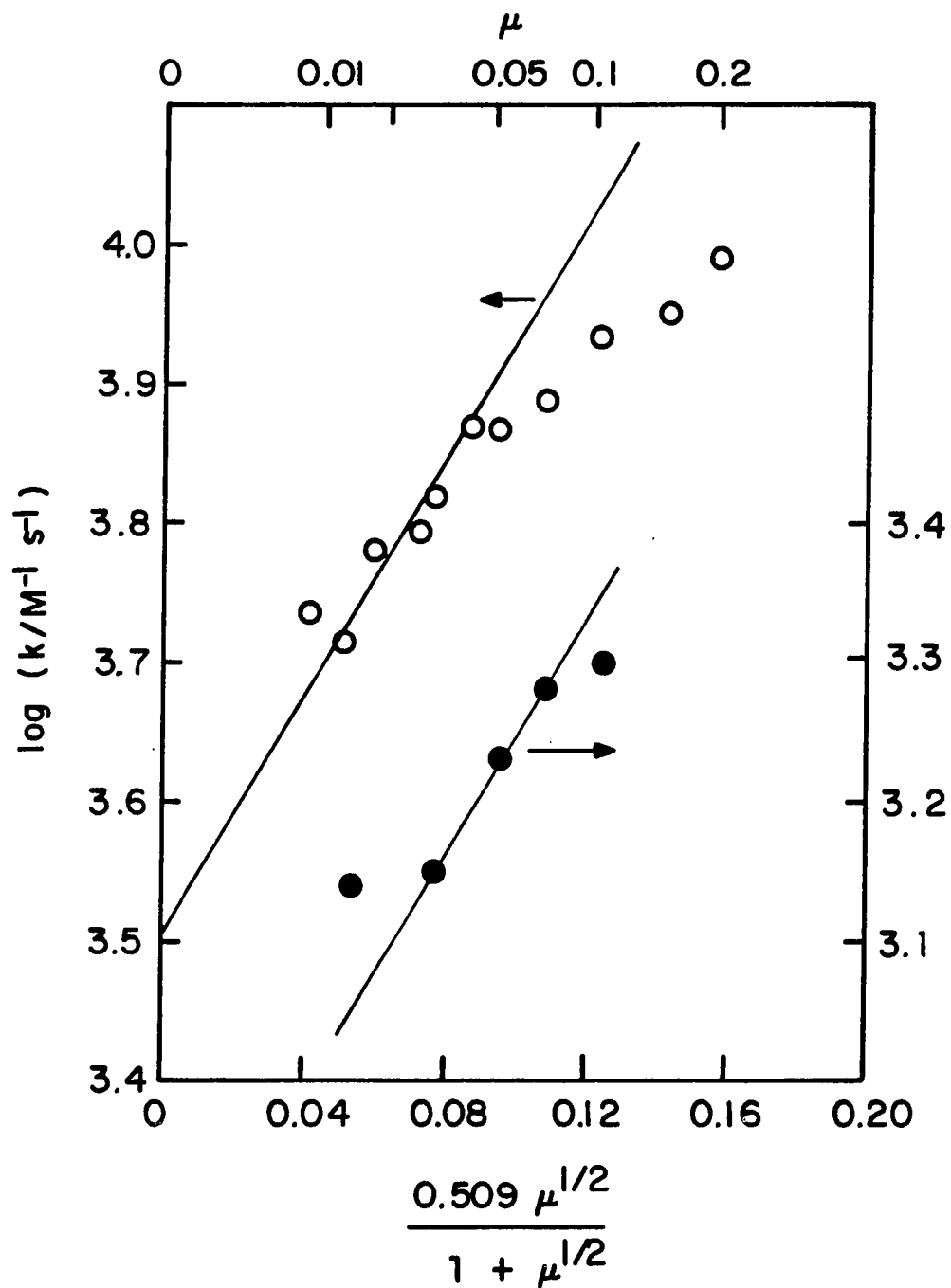
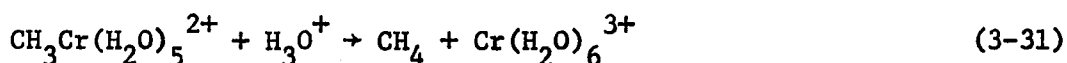


Figure 3-7. Plot of $\log k$ versus $\frac{0.509\mu^{1/2}}{1 + \mu^{1/2}}$ for the reaction of $\text{HCr}(\text{H}_2\text{O})_5^{2+}$ with H_3O^+ (open circles), and $\text{DCr}(\text{D}_2\text{O})_5^{2+}$ with D_3O^+ (solid circles). The lines are drawn to have a slope of +4

$3.2 \times 10^3 \text{ M}^{-1} \text{ s}^{-1}$ for $\text{HCr}(\text{H}_2\text{O})_5^{2+} + \text{H}_3\text{O}^+$ and $6.7 \times 10^2 \text{ M}^{-1} \text{ s}^{-1}$ for $\text{DCr}(\text{D}_2\text{O})_5^{2+} + \text{D}_3\text{O}^+$ or a ratio of $k_{\text{H}}^{\circ}/k_{\text{D}}^{\circ} = 4.8 \pm 1.2$.

$\text{CH}_3\text{Cr}(\text{H}_2\text{O})_5^{2+}$ To assess the contribution of the solvent change from H_2O to D_2O to the magnitude of the isotope effect measured, the rate of reaction of $\text{CH}_3\text{Cr}(\text{H}_2\text{O})_5^{2+}$ with H_3O^+ was compared to that of $\text{CH}_3\text{Cr}(\text{D}_2\text{O})_5^{2+}$ with D_3O^+ in D_2O (6.9% H_2O). This system was chosen for study because of the presumed similarity between H- and CH_3 -ligands, and also its reaction with H_3O^+ obeys a rate law similar (16) to the reaction of H_3O^+ with the hydridochromium(III) ion.



$$\frac{-d[\text{CH}_3\text{Cr}^{2+}]}{dt} = k_{31} [\text{H}_3\text{O}^+] [\text{CH}_3\text{Cr}^{2+}]$$

$$k_{31} (25^\circ\text{C}, \mu = 1.0 \text{ M}) / \text{M}^{-1} \text{ s}^{-1} = 4.94 \times 10^{-3} \quad (16)$$

Product studies (15,18) have shown CH_3D is formed when the reaction of $\text{CH}_3\text{Cr}(\text{H}_2\text{O})_5^{2+}$ with H_3O^+ is carried out in D_2O as a solvent.

At $[\text{H}_3\text{O}^+ \text{ or } \text{D}_3\text{O}^+] = 0.1 \text{ M} = \mu$, and $T = 24.8^\circ\text{C}$, the absorbance of the methylchromium(III) ion at concentrations of $(2-6) \times 10^{-4} \text{ M}$ was monitored with time. Second-order rate constants were obtained from pseudo-first-order rate constants by division by $[\text{H}_3\text{O}^+ \text{ or } \text{D}_3\text{O}^+]$, and are tabulated in Table 3-5. D_2O can be seen to retard the rate by a factor of $k_{\text{H}}/k_{\text{D}} = 6.3 \pm 0.3$.

Table 3-5. Deuterium isotope effect on reaction rate constants

Reaction	$k/M^{-1} s^{-1}$
$HCr(H_2O)_5^{2+} + H_3O^+$	$3.2 \times 10^3{}^a$
$DCr(D_2O)_5^{2+} + D_3O^+$	$6.7 \times 10^2{}^a$
$CH_3Cr(H_2O)_5^{2+} + H_3O^+$	$(6.2 \pm 0.2) \times 10^{-3} (5)^b$
$CH_3Cr(D_2O)_5^{2+} + D_3O^+$	$(9.9 \pm 0.1) \times 10^{-4} (3)^b$

^aValue at $\mu = 0$, obtained by extrapolation (Figure 3-7); monitoring $\lambda = 380$ nm; flash energy = 250 J; T = 21.6°C.

^b $\mu = 0.1$ M; $[D_3O^+] = 0.1$ M; monitoring $\lambda = 285, 392$ nm; T = 24.8°C; uncertainties represent 1σ ; number in parentheses is number of kinetic runs.

Spectrum of Transient

The spectrum of the transient in $0.01 \text{ M H}_3\text{O}^+$ was obtained in the region 320-450 nm, and is reproduced in Figure 3-8. A maximum occurs at $385 \pm 5 \text{ nm}$ and a minimum at $350 \pm 5 \text{ nm}$, followed by a rising absorbance into the UV region. Since optical restrictions limited measurement of UV absorbances to wavelengths $\geq 310 \text{ nm}$, the spectrum could not be obtained further into the UV.

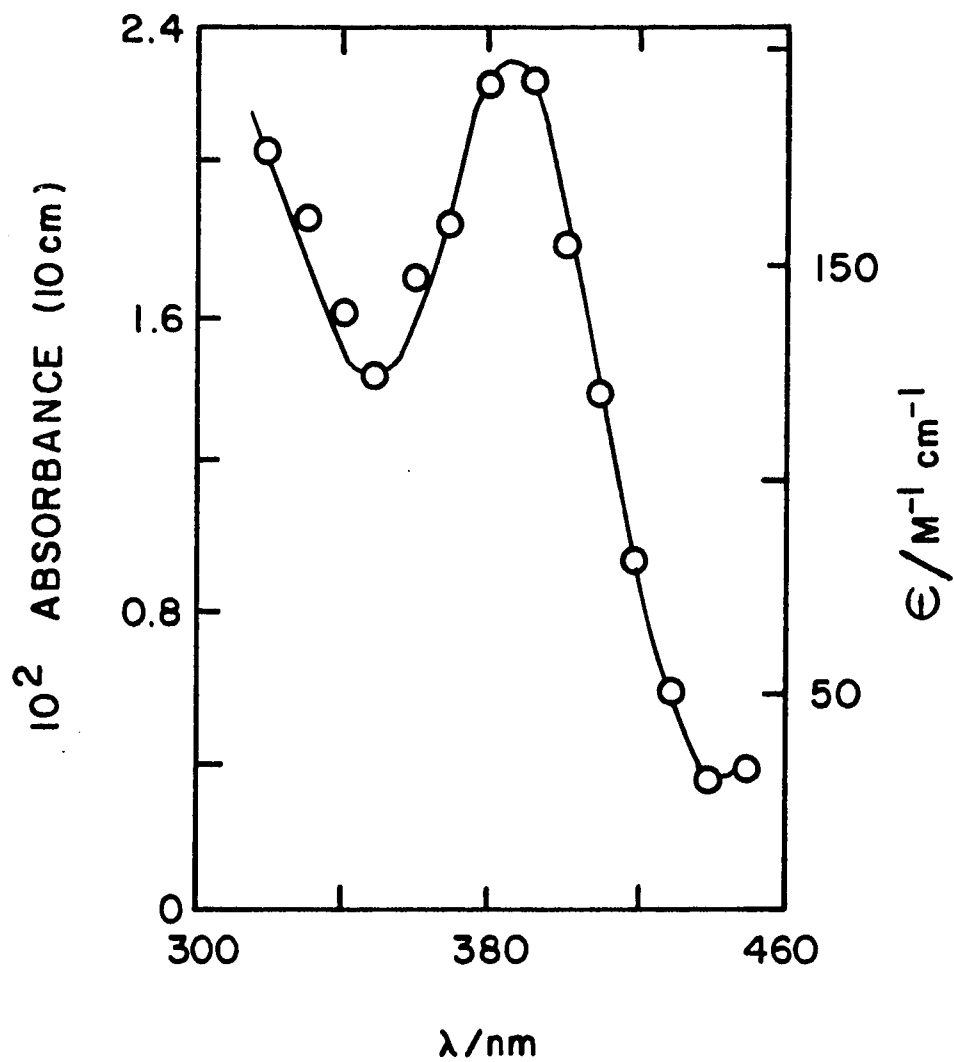


Figure 3-8. The electronic spectrum of the $\text{HCr}(\text{H}_2\text{O})_5^{2+}$ ion. Cell length = 10 cm; flash energy = 250 J. Values of ϵ are relative to $\epsilon_{380} = 190 \text{ M}^{-1} \text{ cm}^{-1}$

DISCUSSION

Assignment of Identity of Transient

The transient generated by flash photolysis of aqueous, acidic solutions of chromium(II) perchlorate can be identified as the $\text{HCr}(\text{H}_2\text{O})_5^{2+}$ ion on the basis of the following results: 1) its UV-visible spectrum is in agreement with that published (36) for $\text{HCr}(\text{H}_2\text{O})_5^{2+}$ prepared by pulse radiolysis; 2) the yield of $\text{HCr}(\text{H}_2\text{O})_5^{2+}$ was decreased or eliminated altogether upon addition of N_2O or methanol, known scavengers for e_{aq}^- and H^\cdot , respectively; 3) the rate law and rate constant for Reaction 3-16 is in reasonable agreement with prior work (36); and 4) the dependence of the rate of Reaction 3-16 on ionic strength is as expected for the reaction of H_3O^+ with a dipositive cation.

These points deserve further comment and will be individually discussed subsequently.

Spectrum

The UV-visible spectrum of $\text{HCr}(\text{H}_2\text{O})_5^{2+}$ produced by flash photolysis consists of a maximum at 385 ± 5 nm and a minimum at 350 ± 5 nm, in good agreement with the values 380 ± 5 nm and ~ 345 nm, respectively, reported by Cohen and Meyerstein (36). Absorbance maxima in the region 390 to 410 nm are characteristic of many of the organochromium(III) complexes, $\text{RCr}(\text{H}_2\text{O})_5^{2+}$ (2,20,25). Since the spectra are similar, Cohen and Meyerstein (36) assumed the same electronic transition was

responsible for the 380 nm maximum of $\text{HCr}(\text{H}_2\text{O})_5^{2+}$. Presumably another maximum at much higher energies exists as a charge-transfer-to-metal transition, but optical restrictions limited absorbance measurements in this work to $\lambda \geq 310$ nm. In the pulse radiolysis experiments, only a very intense absorption rising into the UV was observed in the region 260-310 nm, so the second maxima must lie at $\lambda < 260$ nm.

The molar absorptivity of the maximum at 385 nm, $125 \pm 15 \text{ M}^{-1} \text{ cm}^{-1}$ (see below), is about 35% lower than the value of $190 \pm 20 \text{ M}^{-1} \text{ cm}^{-1}$, obtained from the pulse radiolysis work (36). While the agreement is not excellent, the values are of a similar order of magnitude.

Scavengers

Addition of N_2O to the flash photolysis solution reduced the yield of $\text{HCr}(\text{H}_2\text{O})_5^{2+}$ by 77%. Nitrous oxide is known to be an efficient scavenger for the hydrated electron,



$$k_6/\text{M}^{-1} \text{s}^{-1} = 8.7 \times 10^9 \quad (121)$$



$$\text{p}K_7 = 11.9 \pm 0.2 \quad (122)$$

converting e_{aq}^- into OH^\bullet radicals. In acidic solution, protons compete with N_2O for the hydrated electron,



$$k_4/\text{M}^{-1} \text{s}^{-1} = 2.3 \times 10^{10} \quad (123)$$

In the presence of $\text{Cr}_{\text{aq}}^{2+}$, an additional route by which hydrated electrons can be consumed exists,



$$k_{32}/\text{M}^{-1}\text{s}^{-1} = 1.4 \times 10^{10} \quad (36)$$

The yield of H^\bullet atoms in an aqueous, acidic solution of $\text{Cr}_{\text{aq}}^{2+}$, saturated with N_2O , can be calculated from the above reaction rates. For $[\text{H}_3\text{O}^+] = 1 \times 10^{-3}\text{M}$ and $[\text{Cr}_{\text{aq}}^{2+}] = 1 \times 10^{-3}\text{M}$, in a solution saturated with N_2O at 1 atm, $[\text{N}_2\text{O}] = 0.025\text{M}$, the fraction of e_{aq}^- which react by Reaction 3-4 is,

$$\begin{aligned} & \frac{\text{Reaction Rate (4)}}{\text{Sum of Reaction Rates (4), (6), (32)}} \\ &= \frac{(1 \times 10^{-3})(2.3 \times 10^{10})}{(1 \times 10^{-3})(2.3 \times 10^{10}) + (0.025)(8.7 \times 10^9) + (1 \times 10^{-3})(1.4 \times 10^{10})} \\ &= 0.090. \end{aligned}$$

In the absence of N_2O , the fraction increases to 0.62, or an 85% decrease in the yield of H^\bullet atoms is predicted. If all H^\bullet atoms are consumed by reaction with chromium(II) ions,



$$k_1/\text{M}^{-1}\text{s}^{-1} = 1.5 \times 10^9 \quad (36)$$

rather than dimerization to molecular hydrogen, the yield of the transient $\text{HCr}(\text{H}_2\text{O})_5^{2+}$ ion would be expected to decrease by the same amount (85%), when made in the presence of N_2O , in good agreement with the reduction in yield actually measured.

The production of $\text{HOCH}_2\text{Cr}(\text{H}_2\text{O})_5^{2+}$ rather than $\text{HCr}(\text{H}_2\text{O})_5^{2+}$, when methanol is added to the flash photolysis solution, can be accounted for by the scavenging of H^\bullet atoms by CH_3OH , rather than $\text{Cr}_{\text{aq}}^{2+}$, to form hydroxymethyl radicals.



$$k_{33}/\text{M}^{-1}\text{s}^{-1} = (2.0 \pm 0.8) \times 10^6 \quad (156)$$

These radicals will subsequently be scavenged by $\text{Cr}_{\text{aq}}^{2+}$, and form $\text{HOCH}_2\text{Cr}(\text{H}_2\text{O})_5^{2+}$.



$$k_{34}/\text{M}^{-1}\text{s}^{-1} = 1.6 \times 10^8 \quad (25)$$

For solutions flashed only once, the yield of $\text{HOCH}_2\text{Cr}(\text{H}_2\text{O})_5^{2+}$, as measured by its absorbance at 392 nm where $\epsilon = 570 \text{ M}^{-1}\text{cm}^{-1}$ (22,25), can be used to calculate the concentration of H^\bullet atoms produced by a 250 J flash. If the very small amount of H^\bullet atoms lost to dimerization is neglected, the fraction which react by Reaction 3-33 is,

$$\frac{\text{Reaction Rate (33)}}{\text{Sum of Reaction Rates (33), (1)}} = \frac{(1.0 + 0.4) \times 10^7}{(1.0 \pm 0.4) \times 10^7 + 1.5 \times 10^6}$$

$$= 0.8 - 0.9.$$

Since the yield of Reaction 3-33 is given by the concentration of $\text{HOCH}_2\text{Cr}(\text{H}_2\text{O})_5^{2+}$ produced, $1.5 \times 10^{-5} \text{ M}$, $[\text{H}^\bullet]$ is calculated to be $(1.8 \pm 0.1) \times 10^{-5} \text{ M}$. Assuming this value is equal to the concentration of $\text{HCr}(\text{H}_2\text{O})_5^{2+}$ (produced in the absence of methanol), its molar

absorptivity at 380 nm is calculated from the absorbance change measured at this wavelength, 0.0223 ± 0.0011 ($l = 10$ cm), to be $125 \pm 15 \text{ M}^{-1} \text{ cm}^{-1}$.

The two scavenging experiments provide good evidence for the formation of e_{aq}^- or H^\bullet atoms from the UV photolysis of acidic solutions of chromium(II) perchlorate, in agreement with prior results obtained using continuous photolysis (124,167,168).

Reaction kinetics

The form of the rate law for Reaction 3-16 is the same as that reported by Cohen and Meyerstein (36).

$$\frac{-d[\text{HCr}^{2+}]}{dt} = (k_0 + k[\text{H}_3\text{O}^+])[\text{HCr}^{2+}] \quad (3-35)$$

These authors report $k_0 \leq 1 \text{ s}^{-1}$ and $k = (1.8 \pm 0.2) \times 10^4 \text{ M}^{-1} \text{ s}^{-1}$ at $T = 22 \pm 2^\circ\text{C}$. The ionic strength, however, was not specified. From the flash photolysis studies, at $\mu = 0.20 \text{ M}$, $T = 26.0^\circ\text{C}$, k_0 was found to be zero within experimental uncertainty, and $k = (9.7 \pm 1.0) \times 10^3 \text{ M}^{-1} \text{ s}^{-1}$, or about 46% lower than the published value. The temperature difference between the studies, even if it were significant, would predict a larger value for the warmer temperature instead of the smaller number actually measured. It is conceivable the discrepancy is due to use of a higher ionic strength in the pulse radiolysis studies, because acid concentrations as high as $1 \text{ M H}_3\text{O}^+$ were investigated by the previous workers.

Ionic strength

In order to obtain the charge on a highly reactive intermediate in a bimolecular reaction, the variation of the rate with ionic strength has often been studied. Dorfman and Matheson (207) investigated the rate of the reaction,



as a function of ionic strength to establish the charge on e_{aq}^{-} . Similarly, the ionic strength dependence of the rate of the reaction of e_{aq}^{-} with NO_3^{-} was studied in a quantitative fashion by Anbar and Hart (208). The reaction rate of the transitory CO_3^{-} anion with indole-3-propionic acid was also shown to depend on the ionic strength as predicted for a mono-negative anion (209).

When the rate constant for the reaction of $\text{HCr}(\text{H}_2\text{O})_5^{2+}$ with H_3O^{+} was treated according to the Brønsted-Debye-Hückel equation (Figure 3-6), it was seen that at $\mu < 0.07$ M, the data fit well to a line of slope +4, indicating the ionic charge of the transient was +2. At higher ionic strengths, the data were fit more successfully to an extended form of this relation, from which a value of $+(1.65 \pm 0.3)$ was predicted for the ionic charge of the transient. While either treatment supports the assignment of the identity of the transient as a dipositive cation, use of the Brønsted-Debye-Hückel equation for highly charged reactants of like sign has been criticized (80), at higher ionic strengths.

Mechanism of Protonolysis Reaction

The kinetic isotope studies were helpful in postulating a picture of the transition state. Although the effect of replacing the hydrido ligand of $\text{HCr}(\text{H}_2\text{O})_5^{2+}$ with deuterium could not be studied independently of the solvent change from H_2O to D_2O , the rate of cleavage of $\text{CH}_3\text{Cr}(\text{H}_2\text{O})_5^{2+}$ by H_3O^+ was compared to that by D_3O^+ , as an estimation of this latter component. The acidolysis of $\text{CH}_3\text{Cr}(\text{H}_2\text{O})_5^{2+}$ was previously found (16) to follow the same rate law as the protonolysis of $\text{HCr}(\text{H}_2\text{O})_5^{2+}$, suggesting both reactions occur by the same mechanism, a necessary constraint.

The magnitude of the kinetic isotope effect measured for the reaction of $\text{CH}_3\text{Cr}(\text{H}_2\text{O})_5^{2+}$ with H_3O^+ , $k_{\text{H}}/k_{\text{D}} = 6.3 \pm 0.3$, is somewhat smaller than the value estimated by using a simple harmonic oscillator model. For a transition state involving complete transfer of D^+ from D_3O^+ to the methyl group of the organochromium(III) ion, the ratio $k_{\text{H}}/k_{\text{D}}$ can be estimated (142) from a consideration of the stretching frequencies of the O-H and O-D bonds. An approximate frequency of the O-D bond is obtained from $\nu_{\text{O-H}}$ if the O-H and O-D bonds are treated as simple harmonic oscillators, which allows the stretching frequencies to be related to their reduced masses, μ ,

$$\frac{\nu_{\text{O-H}}}{\nu_{\text{O-D}}} \approx \left(\frac{\mu_{\text{D}}}{\mu_{\text{H}}} \right)^{1/2} \approx \sqrt{2}. \quad (3-37)$$

Using $\nu_{\text{O-H}} = 3600 \text{ cm}^{-1}$ or $1.08 \times 10^{14} \text{ s}^{-1}$, Equation 3-37 predicts ν_{D} as $\approx 7.64 \times 10^{13} \text{ s}^{-1}$. This results in zero-point energies ($E_0 = h\nu/2$) of

$E_{O,H} = 2.15 \times 10^4$ J/mol and $E_{O,D} = 1.52 \times 10^4$ J/mol. Dissociation of either O-H or O-D leads to atoms having only translational energy, E^* , which is identical for O + H or O + D. But since the vibrational levels lie at lower energy for O-D ($E_{O,D} < E_{O,H}$) a larger activation energy is required to cleave the O-D bond than O-H. The Arrhenius equation predicts the rate of reaction will be slower for a higher activation energy, E_a , where A is the frequency factor.

$$k = Ae^{-E_a/RT} \quad (3-38)$$

The ratio k_H/k_D can be obtained by application of Equation 3-38, with E_a for O-H given by $(E^* - E_{O,H})$ and E_a for O-D by $(E^* - E_{O,D})$,

$$\frac{k_H}{k_D} = \frac{Ae^{-\frac{(E^* - E_{O,H})}{RT}}}{Ae^{-\frac{(E^* - E_{O,D})}{RT}}},$$

which simplifies to,

$$\frac{k_H}{k_D} = e^{\frac{(E_{O,H} - E_{O,D})}{RT}}. \quad (3-39)$$

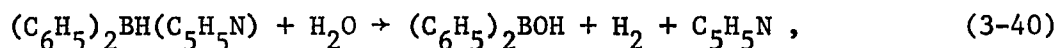
At 24.8°C $k_H/k_D = 12.7$, or about 2-fold greater than the ratio measured.

This implies cleavage of the O-H bond is probably only partially complete in the transition state.

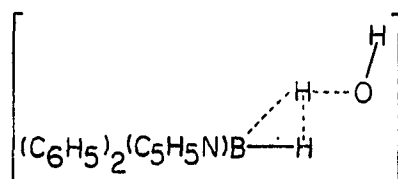
The value for k_H^0/k_D^0 experimentally obtained for the reaction of $\text{HCr}(\text{H}_2\text{O})_5^{2+}$ with H_3O^+ , 4.8 ± 1.2 , is approximately the same magnitude

as k_H/k_D for the acidolysis of $\text{CH}_3\text{Cr}(\text{H}_2\text{O})_5^{2+}$, 6.3 ± 0.3 . This suggests that substitution of the hydrido ligand by deuterium has essentially no effect on the rate of protonolysis, and, therefore, that hydrogen-chromium bond breaking is not rate-determining.

Actually, this result is not surprising for hydride-metal bonds since it appears that small kinetic isotope effects are common to the protonolysis reactions of hydrido ligands (210). Both experimentation (211-213) and calculation (214) are supportive of small isotope effects for hydride transfers. Hawthorne and Lewis (211) found that the hydrolysis of the B-H bond in pyridine diarylboranes,

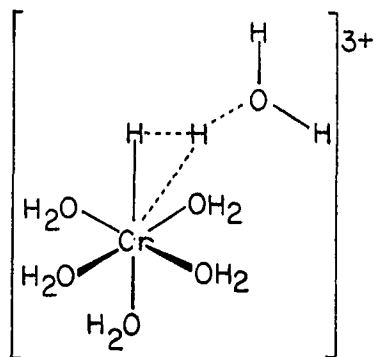


has an isotope effect of only 1.5 when the hydrido ligand was replaced by deuterium. The small effect was explained in terms of a nonlinear transition state



arising from electrophilic attack at the B-H bond where electron density is greatest. Bending rather than stretching vibrations would be expected to be involved more, in agreement with calculations based on this type of model (214).

Likewise, a three-center transition state can be pictured for the reaction of H_3O^+ with $\text{HCr}(\text{H}_2\text{O})_5^{2+}$, arising from attack of the electrophile at the H-Cr bonding electrons. In this mechanism, H-Cr bond



breaking would be of minimal importance; substitution by deuterium should not give rise to an isotope effect. However, the cleavage of the O-H bond will be expected to demonstrate an isotope effect when substitution is made by deuterium, using D_3O^+ . As in the reaction of $\text{CH}_3\text{Cr}(\text{H}_2\text{O})_5^{2+}$ with H_3O^+ , $k_{\text{H}}^{\circ}/k_{\text{D}}^{\circ}$ is smaller than that estimated (12.7) (see above) for O-H, O-D bonds. Presumably, this indicates once again that O-H bond breaking is not complete in the transition state. The formation of the H_2 molecule is clearly demonstrated by the three-center picture. After H_2 dissociation from the axial position, a transient pentaquo chromium(III) species will be formed, which will be very rapidly converted to $\text{Cr}(\text{H}_2\text{O})_6^{3+}$, in a secondary step.

While the small isotope effect in itself would be inconclusive proof for the existence of a hydride, this result, combined with the evidence presented earlier, is further justification for the assignment

of the transient generated from the flash photolysis of $\text{Cr}_{\text{aq}}^{2+}$ as the $\text{HCr}(\text{H}_2\text{O})_5^{2+}$ ion.

The large negative entropy of activation, measured for the reaction of $\text{HCr}(\text{H}_2\text{O})_5^{2+}$ with H_3O^+ , is clearly of a reasonable magnitude for formation of the highly charged (+3), and well-ordered transition state. The electrostatic contribution to ΔS^\ddagger can be estimated (215) by $-10(+2)(+1) = -20$ e.u., where +2 and +1 are the charges on the reactants. The enthalpy of activation, ΔH^\ddagger , is a small value, only 6.3 kcal/mol, reflecting the relative ease at which the H-Cr bond is cleaved by acid. This might be an indication of a relatively ionic bond to chromium, but the fact that $\text{HCr}(\text{H}_2\text{O})_5^{2+}$ exists at all demonstrates there is some degree of covalency.

CONCLUSIONS

The reaction of the isopropylpentaquochromium(III) ion with molecular oxygen follows a free-radical chain mechanism similar to the autoxidation of organic compounds. One of the propagating reactions involves a novel S_H2 attack at the chromium center, by the isopropylperoxy radical, liberating the isopropyl radical. The rate of its displacement from the organochromium(III) ion is too rapid to be occurring by a dissociative mechanism, so it is postulated the transition state involves a seven coordinate intermediate. The primary products - acetone and hexaaquochromium(III) - are readily accounted for by the decomposition of the isopropylperoxochromium(III) intermediate formed in the propagating reaction.

It is certainly reasonable to expect other organochromium(III) ions of this family to react with oxygen by a similar mechanism. From the present study, the requirements for such a scheme appear to be reactivity towards homolysis, in order to initiate the chain reaction, and the ability of the organoperoxy radical to displace the organo radical from the substrate, via an S_H2 reaction, occurring at a rate competitive with bimolecular reactions of the peroxy radical. While factors affecting homolysis of the carbon-chromium bond, within the $RCr(H_2O)_5^{2+}$ family, are reasonably well understood, S_H2 reactions at transition metal centers are extremely rare. Additional kinetic studies, exploring the latter type reaction more completely, should more clearly delineate the important factors.

The β -hydroxyethylchromium(III) ion was made by the photochemical generation of β -hydroxyethyl radicals in the presence of $\text{Cr}_{\text{aq}}^{2+}$ in dilute aqueous perchloric acid. While all three sources of $\text{HOCH}_2\text{CH}_2^\cdot$ radicals explored --(1) $\text{Cr}_{\text{aq}}^{2+}$ solutions saturated with nitrous oxide and ethylene, (2) $\text{HOCH}_2\text{CH}_2\text{Co}(\text{dmg BF}_2)_2\text{py}$, and (3) $\text{Co}(\text{NH}_3)_5\text{O}_2\text{CCH}_2\text{CH}_2\text{OH}^{2+}$ -- were successful, the first system was preferred as it was the simplest chemically. The UV-visible spectrum of $\text{HOCH}_2\text{CH}_2\text{Cr}(\text{H}_2\text{O})_5^{2+}$ supports its assignment as a sigma bonded organochromium(III) ion. The complex is highly reactive towards reactions with H_3O^+ , as expected; the rate-limiting step is assigned to a proton-assisted beta-elimination of a water molecule, followed by rapid dissociation of ethylene from a highly unstable π -bonded $\text{C}_2\text{H}_4\text{Cr}(\text{H}_2\text{O})_5^{3+}$ intermediate. This study demonstrates that functional group substitution on the organo ligand can affect the reactivity of the carbon-chromium bond substantially.

The hydrido analog to the family of $\text{RCr}(\text{H}_2\text{O})_5^{2+}$ ions was made, and the kinetics of its reaction with H_3O^+ were studied using flash photolysis. The identity of the complex is consistent with its absorption spectrum (36), published (36) rate of reaction with H_3O^+ , and the expected dependence of the rate constant on ionic strength for a +2 charged ion. The reaction rate of the deuterated complex, $\text{DCr}(\text{D}_2\text{O})_5^{2+}$, with D_3O^+ , shows a large kinetic isotope effect, similar to the reaction of the $\text{CH}_3\text{Cr}(\text{D}_2\text{O})_5^{2+}$ ion with D_3O^+ , indicating it is O-H bond breaking which is rate-limiting in both cases. Protonolysis of $\text{HCr}(\text{H}_2\text{O})_5^{2+}$ is pictured as occurring via a nonlinear three-center transition state, wherein the H-Cr bond is still intact, characteristic of cleavage reactions of hydrides.

BIBLIOGRAPHY

1. Taube, H. Chem. Rev. 1952, 50, 69.
2. Petrou, A.; Vrachnou-Astra, E.; Katakis, D. Inorg. Chim. Acta 1980, 39, 161.
3. Anet, F. A. L.; Leblanc, E. J. Am. Chem. Soc. 1957, 79, 2649.
4. Kochi, J. K.; Davis, D. D. J. Am. Chem. Soc. 1964, 86, 5264.
5. Pohl, M. C.; Espenson, J. H. Inorg. Chem. 1980, 19, 235.
6. Marty, W.; Espenson, J. H. Inorg. Chem. 1979, 18, 1246.
7. Anet, F. A. L. Can. J. Chem. 1959, 37, 58.
8. Dodd, D.; Johnson, M. D. J. Chem. Soc. A 1968, 34.
9. ^v Sevcík, P. Inorg. Chim. Acta 1979, 32, L16.
10. Malik, S. K.; Schmidt, W.,; Spreer, L. O. Inorg. Chem. 1974, 13, 2986.
11. Coombes, R. G.; Johnson, M. D.; Tobe, M. L.; Winterton, N; Wong, L.-Y. Chem. Commun. 1965, 251.
12. Coombes, R. G.; Johnson, M. D.; Winterton, N. J. Chem. Soc. 1965, 7029.
13. ^v Sevcík, P.; ^v Jakubcová, D. Collect. Czech. Chem. Commun. 1977, 42, 1767.
14. Kochi, J. K.; Rust, F. F. J. Am. Chem. Soc. 1961, 83, 2017.
15. Kochi, J. K.; Mocadlo, P. E. J. Org. Chem. 1965, 30, 1134.
16. Hyde, M. R.; Espenson, J. H. J. Am. Chem. Soc. 1976, 98, 4463.
17. Ardon, M.; Woolmington, K.; Pernick, A. Inorg. Chem. 1971, 10, 2812.
18. Schmidt, W.; Swinehart, J. H.; Taube, H. J. Am. Chem. Soc. 1971, 93, 1117.
19. Espenson, J. H.; Williams, D. A. J. Am. Chem. Soc. 1974, 96, 1008.
20. Leslie, J. P., II; Espenson, J. H. J. Am. Chem. Soc. 1976, 98, 4839.

21. Espenson, J. H.; Bakač[✓], A. J. Am. Chem. Soc. 1980, 102, 2488.
22. Bakač[✓], A.; Espenson, J. H. J. Am. Chem. Soc., in press.
23. Espenson, J. H.; Bakač[✓], A. J. Am. Chem. Soc., in press.
24. Kirker, G. W. Ph.D. Dissertation, Iowa State University, Ames, Iowa, 1981.
25. Cohen, H.; Meyerstein, D. Inorg. Chem. 1974, 13, 2434.
26. Chang, J. C.; Espenson, J. H. J. Chem. Soc., Chem. Commun. 1974, 233.
27. Ševčík[✓], P.; Jakubcová[✓], D. Collect. Czech. Chem. Commun. 1977, 42, 1776.
28. Espenson, J. H.; Samuels, G. J. J. Organomet. Chem. 1976, 113, 143.
29. Nohr, R. S.; Espenson, J. H. J. Am. Chem. Soc. 1975, 97, 3392.
30. Coombes, R. G.; Johnson, M. D. J. Chem. Soc. A 1966, 177.
31. Schmidt, A. R.; Swaddle, T. W. J. Chem. Soc. A 1970, 1927.
32. Espenson, J. H.; Leslie, J. P., II J. Am. Chem. Soc. 1974, 96, 1954.
33. Kochi, J. K.; Buchanan, D. J. Am. Chem. Soc. 1965, 87, 853.
34. Petrou, A.; Vrachnou-Astra, E.; Konstantatos, J.; Katsaros, N.; Katakis, D. Inorg. Chem., in press.
35. Johnson, M. D. Acc. Chem. Res. 1978, 11, 57.
36. Cohen, H.; Meyerstein, D. J. Chem. Soc., Dalton Trans., 1974, 2559.
37. Razuvaev, G. A.; Brilkina, T. G. Russ. Chem. Rev. (Engl. Transl.) 1976, 45, 1135.
38. Brilkina, T. G.; Shushunov, V. A. "Reactions of Organometallic Compounds with Oxygen and Peroxides" (Engl. Transl.); Iliffe Books, Ltd.: London, 1969.
39. Davies, A. G. In "Organic Peroxides", Swern, D., Ed.; Wiley-Interscience: New York, 1971; Vol. II, Chapter IV.

40. Ingold, K. U.; Roberts, B. P. "Free-Radical Substitution Reactions"; Wiley-Interscience: New York, 1971.
41. Parshall, G. W. "Homogeneous Catalysis"; John Wiley & Sons: New York, 1980; Chapter 10.
42. Khan, M. M. T.; Martell, A. E. "Homogeneous Catalysis by Metal Complexes"; Academic Press: New York, 1974; Vol. I, Chapter 2.
43. Howard, J. A. In "Free Radicals", Kochi, J. K., Ed., John Wiley & Sons: New York, 1973; Vol. II, Chapter 12.
44. Sheldon, R. A.; Kochi, J. K. Adv. Catal. 1976, 25, 274.
45. Kochi, J. K. "Organometallic Mechanisms and Catalysis"; Academic Press: New York, 1978; Chapter 5.
46. Stern, E. W. In "Transition Metals in Homogeneous Catalysis", Schrauzer, G. N., Ed.; Marcel Dekker, Inc.: New York, 1971; Chapter 4.
47. Ingold, K. U. Acc. Chem. Res. 1969, 2, 1.
48. Black, J. F. J. Am. Chem. Soc. 1978, 100, 527.
49. Davies, A. G.; Roberts, B. P. Chem. Commun. 1966, 298.
50. Davies, A. G.; Roberts, B. P. J. Chem. Soc. 1967, 17.
51. Davies, A. G.; Roberts, B. P. J. Chem. Soc. 1969, 311.
52. Davies, A. G.; Roberts, B. P. Chem. Commun. 1969, 699.
53. Allies, P. G.; Brindley, P. B. Chem. Ind. (London) 1967, 319.
54. Allies, P. G.; Brindley, P. B. Chem. Ind. (London) 1968, 1439.
55. Allies, P. G.; Brindley, P. B. J. Chem. Soc. 1969, 1126.
56. Ingold, K. U. Chem. Commun. 1969, 911.
57. Davies, A. G.; Ingold, K. U.; Roberts, B. P.; Tudor, R. J. Chem. Soc. B 1971, 698.
58. Brindley, P. B.; Hodgson, J. C. J. Chem. Soc., Chem. Commun. 1972, 202.

59. Korcek, S.; Watts, G. B.; Ingold, K. U. J. Chem. Soc., Perkin Trans. 2 1972, 242.
60. Brindley, P. B.; Hodgson, J. C. J. Organomet. Chem. 1974, 65, 57.
61. Giannotti, C.; Gaudemer, A.; Fontaine, C. Tetrahedron Lett. 1970, 3209.
62. Duong, K. N. V.; Fontaine, C.; Giannotti, C.; Gaudemer, A. Tetrahedron Lett. 1971, 1187.
63. Fontaine, C.; Duong, K. N. V.; Merienne, C.; Gaudemer, A.; Giannotti, C. J. Organomet. Chem. 1972, 38, 167.
64. Giannotti, C.; Fontaine, C.; Gaudemer, A. J. Organomet. Chem. 1972, 39, 381.
65. Giannotti, C.; Septe, B. J. Organomet. Chem. 1973, 52, C45.
66. Merienne, C.; Giannotti, C.; Gaudemer, A. J. Organomet. Chem. 1973, 54, 281.
67. Giannotti, C.; Fontaine, C.; Septe, B. J. Organomet. Chem. 1974, 71, 107.
68. Bied-Charreton, C.; Gaudemer, A. J. Organomet. Chem. 1977, 299.
69. Hedaya, E.; Winstein, S. J. Am. Chem. Soc. 1967, 89, 1661.
70. Carlyle, D. W.; Espenson, J. H. Inorg. Chem. 1967, 6, 1370.
71. Ilan, Y. A.; Czapski, G.; Ardon, M. Isr. J. Chem. 1975, 13, 15.
72. Skoog, D. A.; West, D. M. "Analytical Chemistry"; Holt, Rinehart and Winston: New York, 1965.
73. Banerjee, D. H.; Budke, C. C. Anal. Chem. 1964, 36, 792.
74. Tong, J. Y.; King, E. L. J. Am. Chem. Soc. 1953, 75, 6180.
75. Kolaczowski, R. W.; Plane, R. A. Inorg. Chem. 1964, 3, 322.
76. Montgomery, H. A. C.; Thom, N. S.; Cockburn, A. J. Appl. Chem. 1964, 14, 280.
77. Frost, A. A.; Pearson, R. G. "Kinetics and Mechanisms", 2nd ed.; John Wiley & Sons: New York, 1961; p. 150-155.

78. Davies, C. W. "Ion Association"; Butterworth and Co., Ltd.: London, 1962.
79. Rochester, C. H. Prog. React. Kinet. 1972, 6, 143.
80. Perlmutter-Hayman, B. Prog. React. Kinet. 1972, 6, 239.
81. Pethybridge, A. D.; Prue, J. E. Prog. Inorg. Chem. 1972, 17, 327.
82. Bartlett, P. D.; Funahashi, T. J. Am. Chem. Soc. 1962, 84, 2596.
83. Ingold, K. U. In "Free Radicals", Kochi, J. K., Ed.; Wiley-Interscience: New York, 1973; Vol. I, Chapter 2, pp. 65-66.
84. Kharash, M. S.; Fono, A.; Nudenberg, W. J. Org. Chem. 1950, 15, 763.
85. Sellers, R. M.; Simic, M. G. J. Chem. Soc., Chem. Commun. 1975, 401.
86. Sellers, R. M.; Simic, M. G. J. Am. Chem. Soc. 1976, 98, 6145.
87. Kochi, J. K.; Subramanian, R. V. J. Am. Chem. Soc. 1965, 87, 4855.
88. Kochi, J. K.; Bemis, A.; Jenkins, C. L. J. Am. Chem. Soc. 1968, 90, 4616.
89. Shaw, K.; Espenson, J. H. Inorg. Chem. 1968, 7, 1619.
90. Bakac^V, A., personal communication, Ames Laboratory, Iowa State University, Ames, Iowa, 1980-1981.
91. Russell, G. A. J. Am. Chem. Soc. 1957, 79, 3871.
92. Howard, J. A. In "Organic Free Radicals", Pryor, W. A., Ed.; American Chemical Society: Washington, D.C., 1978; p. 428.
93. Walling, C.; Cioffair, A. J. Am. Chem. Soc. 1970, 92, 6609.
94. Davies, A. G.; Roberts, B. P. J. Chem. Soc. B 1968, 1074.
95. Carey, L. R.; Jones, W. E.; Swaddle, T. W. Inorg. Chem. 1971, 10, 1566.
96. Swaddle, T. W. Coord. Chem. Rev. 1974, 14, 217.

97. Bushey, W. R.; Espenson, J. H. Inorg. Chem. 1977, 16, 2772.
98. Bakac^V, A.; Espenson, J. H.; Miller, L., manuscript in preparation.
99. Campano, D. D.; Kantrowitz, E. R.; Hoffman, M. Z.; Weinberg, M. S. J. Phys. Chem. 1974, 78, 686.
100. Olson, K. R.; Hoffman, M. Z. J. Chem. Soc., Chem. Commun. 1974, 938.
101. Cohen, H.; Meyerstein, D. J. Chem. Soc., Dalton Trans. 1977, 1056.
102. Papaconstantinou, E. J. Inorg. Nucl. Chem. 1981, 43, 115.
103. Middleton, B. S.; Ingold, K. U. Can. J. Chem. 1967, 45, 191.
104. Espenson, J. H.; Chen, J.-T. J. Am. Chem. Soc. 1981, 103, 0000.
105. Adams, A. C.; Crook, J. R.; Bockhoff, F.; King, E. L. J. Am. Chem. Soc. 1968, 90, 5761.
106. Evans, M. G.; George, P.; Uri, N. Trans. Faraday Soc. 1949, 45, 230.
107. Wiberg, K. B.; Mukherjee, S. K. J. Am. Chem. Soc. 1974, 96, 1884.
108. Piccard, J. Ber. Dtsch. Chem. Ges. 1913, 46, 2477.
109. Westheimer, F. H.; Novich, A. J. Chem. Phys. 1943, 11, 506.
110. Singleton, D. M.; Kochi, J. K. J. Am. Chem. Soc. 1967, 89, 6547.
111. Buxton, G. V.; Green, J. C.; Higgins, R.; Kanji, S. J. Chem. Soc., Chem. Commun. 1976, 158.
112. Buxton, G. V.; Green, J. C. J. Chem. Soc., Faraday Trans. 1 1978, 74, 697.
113. Freiberg, M.; Meyerstein, D. J. Chem. Soc., Faraday Trans. 1 1980, 76, 1838.
114. Kelm, M.; Lilie, J.; Henglein, A.; Janata, E. J. Phys. Chem. 1974, 78, 882.
115. Kelm, M.; Lilie, J.; Henglein, A. J. Chem. Soc., Faraday Trans. 1 1975, 71, 1132.
116. Schrauzer, G. N.; Windgassen, R. J. J. Am. Chem. Soc. 1967, 89, 143.

117. Brown, K. L.; Ingraham, L. L. J. Am. Chem. Soc. 1974, 96, 7681.
118. Espenson, J. H.; Wang, D. M. Inorg. Chem. 1979, 18, 2853.
119. Brown, K. L.; Ramamurthy, S., private communication, 1981.
120. "Selected Specific Rates of Reactions of Transients from Water in Aqueous Solution. III. Hydroxyl Radical and Perhydroxyl Radical and Their Radical Ions". Natl. Bur. Stand. (U.S.) Circ. 1977, No. 59.
121. Gordon, S.; Hart, E. J.; Matheson, M. S.; Rabani, J.; Thomas, J. K. Discuss. Faraday Soc. 1963, 36, 193.
122. Rabani, J.; Matheson, M. S. J. Phys. Chem. 1966, 70, 761.
123. Dorfman, L. M.; Taub, I. A. J. Am. Chem. Soc. 1963, 85, 2370.
124. Collinson, E.; Dainton, F. S.; Malati, M. A. Trans. Faraday Soc. 1959, 55, 2096.
125. Maillard, Ph.; Giannotti, C. J. Organomet. Chem. 1979, 182, 225.
126. Golding, B. T.; Kemp, T. J.; Sheena, H. H. J. Chem. Res. (M) 1981, 334.
127. Golding, B. T.; Kemp, T. J.; Sellers, P. J.; Noschi, E. J. Chem. Soc., Dalton Trans. 1977, 1266.
128. Espenson, J. H.; Shveima, J. S. J. Am. Chem. Soc. 1973, 95, 4468.
129. Kantrowitz, E. R.; Hoffman, M. Z.; Endicott, J. F. J. Phys. Chem. 1971, 75, 1914.
130. Poznyak, A. L.; Pansevich, V. V. Vesti Akad. Navuk B SSR, Ser. Khim. Navuk 1975, 6, 50; Chem. Abstr. 1976, 84: 67425v.
131. Neokladnova, L. N.; Repina, V. A.; Zotov, N. I. Zh. Neorg. Khim. 1976, 21, 149; Chem. Abstr. 1976, 85: 134090t.
132. Poznyak, A. L.; Pansevich, V. V. Vesti Akad. Navuk B SSR, Ser. Khim. Navuk 1980, 1, 18; Chem. Abstr. 1980, 92: 198517q.
133. Taube, H. Adv. Chem. Ser. 1965, 49, 107, 117.
134. Taube, H.; Gould, E. S. Acc. Chem. Res. 1969, 2, 321.

135. Butler, R. D.; Taube, H. J. Am. Chem. Soc. 1965, 87, 5597.
136. Basolo, F.; Murmann, R. K. Inorg. Synth. 1953, 4, 171.
137. Gould, E. S.; Taube, H. J. Am. Chem. Soc. 1964, 86, 1318.
138. Fan, F.-R.; Gould, E. S. Inorg. Chem. 1974, 13, 2639.
139. Dockal, E. R.; Everhart, E. T.; Gould, E. S. J. Am. Chem. Soc. 1971, 93, 5661.
140. Jackman, L. M.; Scott, R. M.; Portman, R. H.; Dormish, J. F. Inorg. Chem. 1979, 18, 1497.
141. Gould, E. S. J. Am. Chem. Soc. 1965, 87, 4730.
142. Espenson, J. H. "Chemical Kinetics and Reaction Mechanisms"; McGraw-Hill: New York, 1981.
143. Read, R. R. Org. Synth. 1927, 7, 54.
144. Breitmaier, E.; Voelter, W. "¹³C NMR Spectroscopy"; Verlag Chemie: New York, 1978, p. 208.
145. Wang, D. M. M.S. Thesis, Iowa State University, Ames, Iowa, 1978.
146. Heckman, R. A. Ph.D. Dissertation, Iowa State University, Ames, Iowa, 1978.
147. Schrauzer, G. N. Inorg. Synth. 1968, 11, 62.
148. Costa, G.; Tazher, G.; Puxeddu, A. Inorg. Chim. Acta 1969, 3, 45.
149. Ramasami, T.; Espenson, J. H. Inorg. Chem. 1980, 19, 1523.
150. Hughes, R. G.; Endicott, J. F.; Hoffman, M. Z.; House, D. A. J. Chem. Educ. 1969, 46, 440.
151. Stephen, H.; Stephen, T., Eds. "Solubilities of Inorganic and Organic Compounds"; MacMillan: New York, 1963; Vol. 1, Part 1.
152. Samuni, A.; Meisel, D.; Czapski, G. J. Chem. Soc., Dalton Trans. 1972, 1273.
153. Söylemez, T.; von Sonntag, C. J. Chem. Soc., Perkin Trans. 2 1980, 391.

154. Balzani, V.; Carassiti, V. "Photochemistry of Coordination Compounds"; Academic Press: London, 1970.
155. Orgel, L. E. Q. Rev., Chem. Soc. 1954, 8, 429.
156. "Selected Specific Rates of Reactions of Transients from Water in Aqueous Solution. II. Hydrogen Atom". Natl. Bur. Stand. (U.S.) Circ. 1975, No. 51.
157. Cullis, C. F.; Francis, J. M.; Raef, Y.; Swallow, A. J. Proc. R. Soc. London, Ser. A. 1967, 300, 443.
158. Giannotti, C.; Merle, G.; Fontaine, C.; Bolton, J. R. J. Organomet. Chem. 1975, 91, 357.
159. Khan, M. M. T.; Martell, A. E. "Homogeneous Catalysis by Metal Complexes"; Academic Press: New York, 1974; Vol. II, Chapter 1.
160. Shaw, B. L.; Tucker, N. I. "Organo-Transition Metal Compounds and Related Aspects of Homogeneous Catalysis"; Pergamon Press: Oxford, 1975.
161. Ferraudi, G. Inorg. Chem. 1978, 17, 2506.
162. Adamson, A. W.; Waltz, W. L.; Zinato, E.; Watts, D. W.; Fleischauer, P. D.; Lindholm, R. D. Chem. Rev. 1968, 541.
163. Davis, D. D.; Stevenson, K. L.; King, G. L. Inorg. Chem. 1977, 16, 670.
164. Dainton, F. S.; James, D. G. L. J. Chim. Phys.-Chim. Biol. 1951, 48, C17.
165. Cannon, R. D. Adv. Inorg. Chem. Radiochem. 1978, 21, 179.
166. Airey, P. L.; Dainton, F. S. Proc. R. Soc. London, Ser. A 1966, 291, 340.
167. Hartmann, H.; Müller, J.; Kelm, H. Naturwissenschaften 1973, 60, 256.
168. Raphael, M. W.; Malati, M. A. J. Inorg. Nucl. Chem. 1975, 37, 1326.
169. Fox, M. In. "Concepts of Inorganic Photochemistry", Adamson, A. W.; Fleischauer, P. D., Eds.; John Wiley & Sons: New York, 1975; Chapter 8.

170. Stasicka, Z.; Marchaj, A. Coord. Chem. Rev. 1977, 23, 131.
171. Davis, D. D.; Stevenson, K. L.; Davis, C. R. J. Am. Chem. Soc. 1978, 100, 5344.
172. Ferraudi, G. Inorg. Chem. 1978, 17, 1370.
173. Basco, N.; Vidyarthi, S. K.; Walker, D. C. Can. J. Chem. 1974, 52, 343.
174. Halpern, J. Annu. Rev. Phys. Chem. 1965, 16, 103.
175. Basolo, F.; Pearson, R. G. "Mechanisms of Inorganic Reactions", 2nd ed.; John Wiley & Sons: New York, 1967; Chapter 7.
176. Coffey, R. S. In "Aspects of Homogeneous Catalysis", Ugo, R., Ed.; Carlo Manfredi: Milano, 1970; Vol. 1.
177. Harmon, R. E.; Gupta, S. K.; Brown, D. J. Chem. Rev. 1973, 21.
178. Dolcetti, G.; Hoffman, N. W. Inorg. Chim. Acta 1974, 9, 269.
179. James, B. R. "Homogeneous Hydrogenation"; Wiley-Interscience: New York, 1973.
180. McQuillin, F. J. "Homogeneous Hydrogenation in Organic Chemistry"; D. Reidel: Boston, 1976.
181. Calvin, M. Trans. Faraday Soc. 1938, 34, 1181.
182. Peters, E.; Halpern, J. Can. J. Chem. 1955, 33, 356.
183. Peters, E.; Halpern, J. J. Phys. Chem. 1955, 59, 593.
184. Halpern, J.; Macgregor, E. R.; Peters, E. J. Phys. Chem. 1956, 60, 1455.
185. Webster, A. H.; Halpern, J. J. Phys. Chem. 1957, 61, 1239.
186. Korinek, G. J.; Halpern, J. J. Phys. Chem. 1956, 60, 285.
187. Halpern, J. Adv. Catal. 1957, 9, 302.
188. Meyerstein, D. Acc. Chem. Res. 1978, 11, 43.
189. Buxton, G. V.; Sellers, R. M. Coord. Chem. Rev. 1977, 22, 195.

190. Halpern, J.; Czapski, G.; Jortner, J.; Stein, G. Nature (London) 1960, 186, 629.
191. Czapski, G.; Jortner, J.; Stein, G. J. Phys. Chem. 1961, 65, 960.
192. Jayson, G. G.; Keene, J. P.; Stirling, D. A.; Swallow, A. J. Trans. Faraday Soc. 1969, 65, 2453.
193. Nenadović, M. T.; Mičić, O. I.; Muk, A. J. Chem. Soc., Dalton Trans. 1980, 586.
194. Behar, D.; Samuni, A. Chem. Phys. Lett. 1973, 22, 105.
195. Behar, D.; Samuni, A.; Fessender, R. W. J. Phys. Chem. 1973, 77, 2055.
196. Mičić, O.; Nenadović, M. T. J. Chem. Soc., Dalton Trans. 1979, 2011.
197. Lykourezos, P. A. P.; Kanellopoulos, A.; Katakis, D. J. Phys. Chem. 1968, 72, 2330.
198. Mazumdar, A. S. G.; Srinivasan, B.; Natarajan, P. R. Int. J. Radiat. Phys. Chem. 1973, 5, 51.
199. Freiberg, M.; Meyerstein, D. J. Chem. Soc., Faraday Trans. 1 1977, 73, 622.
200. Mulazzani, Q. G.; Ward, M. D.; Semerano, G.; Emmi, S. S.; Giordani, P. Int. J. Radiat. Phys. Chem. 1974, 6, 187.
201. Fiti, M.; Morar, R. Radiochem. Radioanal. Lett. 1980, 43, 137.
202. Latimer, W. "The Oxidation States of the Elements and Their Potentials in Aqueous Solutions", 2nd ed.; Prentice-Hall, Inc.: Englewood Cliffs, New Jersey, 1952; p. 33.
203. Baxendale, J. H.; Rodgers, M. A. J. Chem. Soc. Rev. 1978, 7, 235.
204. Holah, D. G.; Fackler, Jr., J. P. Inorg. Synth. 1967, 10, 26.
205. Purlee, E. L. J. Am. Chem. Soc. 1959, 81, 263.
206. Fielden, E. M.; Hart, E. J. Radiat. Res. 1968, 33, 426.
207. Dorfman, L. M.; Matheson, M. S. Prog. React. Kinet. 1965, 3, 258.

208. Anbar, M.; Hart, E. J. Adv. Chem. Ser. 1968, 81, 82.
209. Pilling, M. J. "Reaction Kinetics"; Clarendon Press: Oxford, 1975; p. 80.
210. Saunders, Jr., W. H. In "Techniques of Chemistry", 3rd ed.; Weissberger, A., Ed.; Wiley-Interscience: New York, 1974; Vol. VI, Part 1, Chapter V.
211. Hawthorne, M. F.; Lewis, E. S. J. Am. Chem. Soc. 1958, 80, 4296.
212. Kaplan, L.; Wilzbach, K. E. J. Am. Chem. Soc. 1955, 77, 1297.
213. Bartlett, P. D.; McCollum, J. D. J. Am. Chem. Soc. 1956, 78, 1441.
214. More O'Ferrall, R. A. J. Chem. Soc. B 1970, 785.
215. Benson, D. "Mechanisms of Inorganic Reactions in Solution"; McGraw-Hill: London, 1968; p. 3.
216. Porter, G.; West, M. A. In "Techniques of Chemistry", 3rd ed.; Weissberger, A., Ed.; Wiley-Interscience: New York, 1974; Vol. VI, Part 2, Chapter X.
217. Stasicka, A.; Marchaj, A. Coord. Chem. Rev. 1977, 23, 131.
218. Norrish, R. G. W.; Porter, G. Nature (London) 1949, 164, 658.
219. Porter, G. Proc. R. Soc. London, Ser. A 1950, 200, 284.
220. "Flash Photolysis". Xenon Corporation (Medford, Massachusetts) circa 1977.
221. Durante, V. A. Ph.D. Dissertation, University of California, Santa Barbara, California, 1977.
222. Gordon, A. J.; Ford, R. A. "The Chemist's Companion"; Wiley-Interscience: New York, 1972; pp. 167-168.
223. Olsen, E. D. "Modern Optical Methods of Analysis"; McGraw-Hill, Inc.: New York, 1975; pp. 73-74.
224. Matheson, M. S.; Mulac, W. A.; Rabani, J. J. Phys. Chem. 1963, 67, 2613.
225. "Rate Constants for Reactions of Inorganic Radicals in Aqueous Solution". Natl. Bur. Stand. (U.S.) Circ. 1979, No. 65.
226. Cooper, G. D.; DeGraff, B. A. J. Phys. Chem. 1972, 76, 2618.

ACKNOWLEDGEMENTS

I would like to thank Professor James H. Espenson for his guidance, encouragement, and patience throughout the course of this research. Under his direction I have had the pleasure of learning in an intellectually stimulating environment, with the freedom necessary to pursue independent thought. I am particularly grateful to Dr. Andreja Bakač^V for many useful suggestions, and also Drs. T. Ramasami and Ursula Tinner for helpful discussions. Drs. S. D. Woodruff and R. N. Kniseley provided much needed technical assistance during the set-up of the flash photolysis instrument; the expertise of the Ames Laboratory Instrumentation Group and Garry Wells of the Machine Shop were invaluable.

Special thanks are due my parents for their love, and interest in my career over the years. I am indebted to my husband Tim for his love and patient understanding; his confidence in me was especially encouraging. My son Teddy, born during the course of this work, has been a source of much pleasure, providing an exciting supplement to graduate studies.

APPENDIX

Description of Flash Photolysis Instrument

The flash photolysis technique (216,217), developed by Norrish and Porter in 1949-1950 (218,219), is useful for the study of highly reactive chemical species. A very intense, but short duration, flash of light initiates a photochemical reaction, generating a transient at a concentration such that it can be detected by some physical method. Detection is commonly accomplished by absorption spectroscopy, which can be utilized in two modes. In the first, flash spectroscopy, an absorption spectrum of the transient is obtained at a particular time after initiation. Operated in the kinetic spectrophotometry mode, an absorption at one wavelength can be followed as a function of time.

The flash photolysis instrument assembled for the present work is of the latter type, suitable for obtaining kinetic data of photochemically generated transients. It is considered a conventional microsecond unit, in which the discharge of the flashlamps requires a time on the order of microseconds. The instrument consists of two main components - the equipment necessary for production of the photolysis flash, purchased from Xenon Corporation (Model 710), and a spectrophotometer which was assembled by components. It is shown schematically in Figure A-1.

The Xenon Model 710 system is comprised of several units. The energy for the flashlamps is produced by the Model-A High Energy Photolyzing Micropulser, which is capable of delivering 5 to 2000 J. The power source consists of a bank of capacitors which are charged to a predetermined voltage. Both the capacitance and charging voltage can be varied to achieve the desired flash energy, which is calculated from

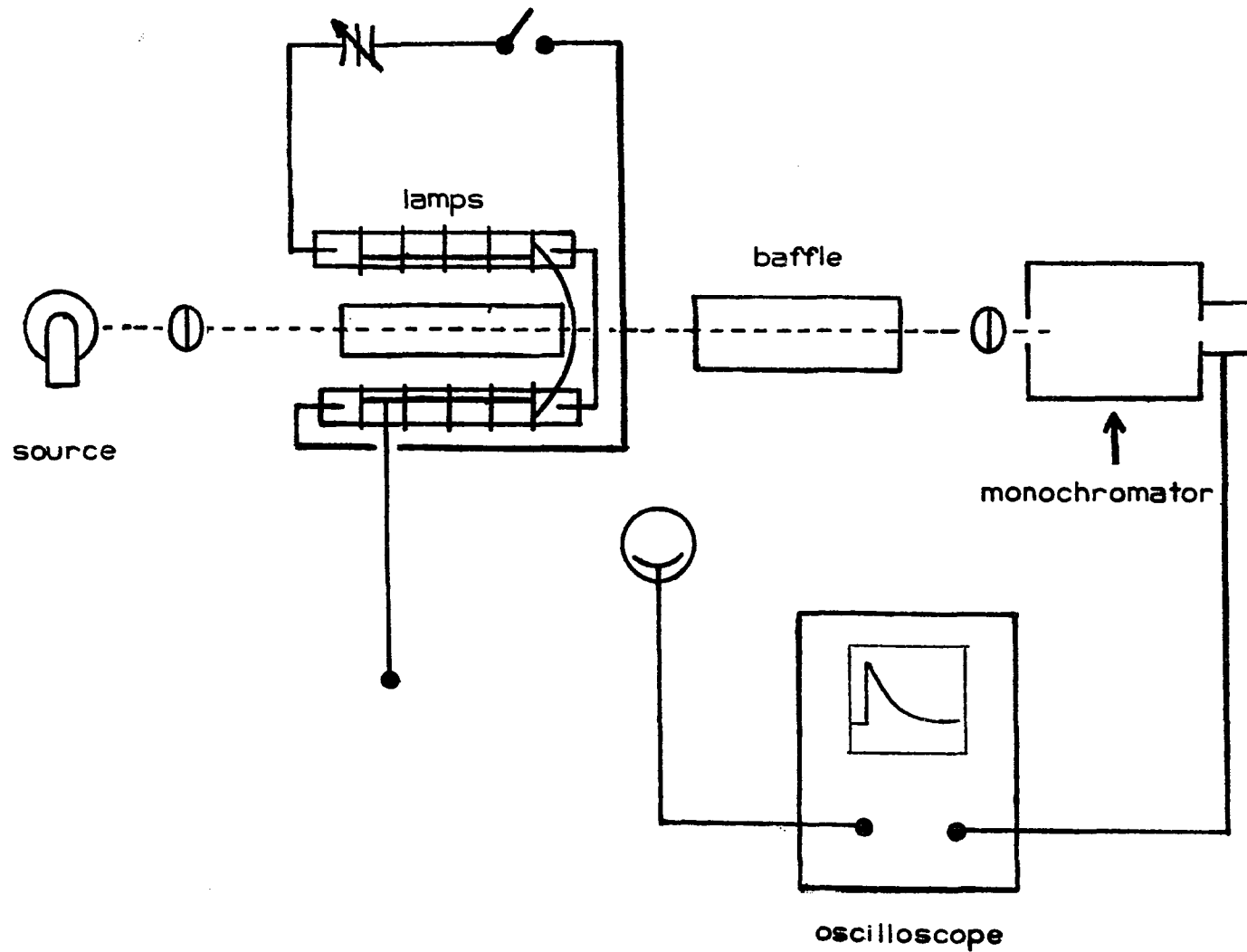


Figure A-1. Schematic of flash photolysis instrument

Equation A-1,

$$E/\text{Joules} = \frac{1}{2} C V^2 \quad , \quad (\text{A-1})$$

where C is in farads, and V is in volts. The capacitors are rated at 10 μf each; however, direct measurement lead to a smaller average value of $7.6 \pm 0.1 \mu\text{f}$. Depending upon the manner in which they are connected, the equivalent capacitance of the circuit is 3.8, 7.6, 15.2, 22.8, or 30.4 μf . The charging voltage is continuously variable from 1.5 to 10.0 kV. Maximum possible flash energies with various capacitor arrangements are summarized in Table A-1.

It is apparent from Table A-1 that a particular energy can be obtained with a variety of capacitances and voltages. Generally, higher capacitances are used so that smaller charging voltages are sufficient. The reason for this is that as the flashlamps age they become less able to "hold-off" higher voltages, and will fire before the capacitors have reached the full charge. Flash energies greater than about 200 J would be difficult if not impossible to achieve with a low circuit capacitance when using aged lamps.

The energy from the Model-A is delivered to two high intensity, fast-extinguishing Xenon FP-5-100C flashlamps, which are connected in series. These lamps are linear quartz tubes, filled primarily with xenon gas and a small amount of a nonspecified molecular gas, such as oxygen, hydrogen, or nitrogen, which serves to shorten the flash duration to about 30-80 μs , depending on the energy dissipated. The FP-5-100C flashlamps operate to a maximum of 1000 J.

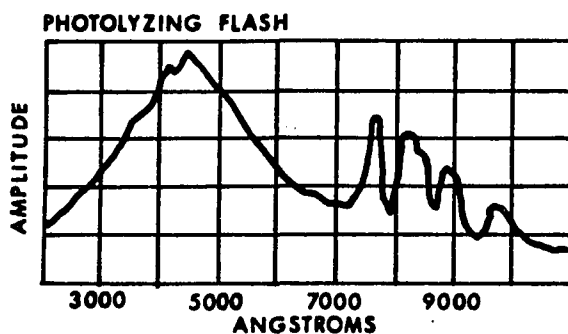
Table A-1. Maximum possible flash energies attainable with various capacitor arrangements

Maximum Energy ^a /J	Capacitor Arrangement	C_E^b / μ f.
190 (250)	2 in series 2 grounded	$C_E = [C_1^{-1} + C_2^{-1}]^{-1} = 3.8$
380 (500)	3 grounded	$C_E = C_1 = 7.6$
760 (1000)	2 in parallel 2 grounded	$C_E = C_1 + C_2 = 15.2$
1140 (1500)	3 in parallel 1 grounded	$C_E = C_1 + C_2 + C_3 = 22.8$
1520 (2000)	4 in parallel	$C_E = C_1 + C_2 + C_3 + C_4 = 30.4$

^aIf capacitors are charged to 10.0 kV. Value in parentheses is energy calculated for 10 μ f capacitors (as rated by Xenon Corporation).

^b C_E = equivalent capacitance of circuit.

The photolyzing flash has an approximately continuous spectral energy distribution, ranging from 180 nm to well past 1000 nm, as shown below.



The energy distribution can be varied somewhat by the operator's choice of circuit characteristics. For flashlight more intense in the ultraviolet region, lower capacitances and higher voltages can be employed, while the reverse increases the output of infrared radiation.

The UV spectral region can be effectively masked by slipping Pyrex glass tubes over the flashlamps, eliminating wavelengths less than about 280 nm. Alternatively, the solution to be photolyzed can be contained in an all-quartz jacketed cell in which filtration of unwanted radiation can be accomplished by solvents or solutions in the outer jacket. The UV cut-off of various solvents and solutions has been tabulated (221,222).

The flashlamps require an additional "triggering" voltage of 30-40 kV in order to accept the energy from the power source and actually fire. This is supplied from the Model-C Trigger Module through a high

voltage ceramic feed. The trigger wire is wrapped within the inter-electrode regions of the lamps, as shown schematically in Figure A-2.

The lamps are mounted parallel to one another in the FH-1275 Photo-lyzing Housing, in which electrical connections from the Model-A are made on one end of the housing using high voltage insulated cables and connectors. Electrical contact between the lamps is made through a brass holder on the other end of the housing, which also serves to secure the lamps in place. The substrate is contained in a quartz, cylindrical spectroscopic cell of 2 to 10 cm path length, and is supported on a locally machined aluminum holder, parallel to and centered between the lamps. The flashlight enters through the body of the cell, at right angles to the monitoring beam.

The Model-A and -C are operated remotely using the Model-710F remote-control panel, for safety reasons.

The spectrophotometer consists of a monitoring light source, lenses, a monochromator, photomultiplier tube, and an oscilloscope.

The monitoring source is either a 50 watt Osram quartz-halogen 64610 lamp, for visible and near UV (to 320 nm) work, or a 75 watt miniature xenon arc-lamp, an Oriel 6251 for the UV. Either lamp can be mounted in the small housing, Oriel 6302, from which the factory installed blower was removed. Cooling is accomplished instead with a filtered stream of air from the laboratory's air jet. The quartz-halogen lamp is powered by a Nobatron DC source operating at 11 volts, 4 amps. An Illumination Industries Model CA-75-18267 power supply is used for the xenon arc-lamp.

An f/1.5 UV grade silica condensing lens, in a focussing sleeve, is mounted directly onto the lamp housing. Either a collimated or focussed image of the source is possible. An additional lens, used after the condenser, provides a more intense, collimated beam than with the latter alone. The image of the source is brought to focus with the condenser, and the second lens is placed at its focal length (10 cm) from the image, producing a collimated beam of light. After passage of the monitoring light through the sample, it is directed through the baffle, which serves to eliminate some of the scattered flashlight from entering the monochromator. After emerging from the baffle the beam is focussed onto the entrance slit of the monochromator, a 0.25 meter Jarrell-Ash 82410 with f/3.6 optics. To fully illuminate the grating an f/3.6 lens is required. Because the beam of light emerging from the baffle has a diameter of 1 cm, a lens with a focal length of 3.6 cm is necessary,

$$f\# = \frac{\text{focal length}}{\text{diameter of beam}} \quad .$$

A quartz lens with a focal length of about 4 cm is in current use. Entrance and exit slits, each of 1 mm width, were chosen to maximize the light through the monochromator. With its dispersion of 3.3 nm/mm, a 3.3 nm band resolution is possible. After monochromation, the light beam is directed through the exit slit onto the photocathode of an RCA 1P28 photomultiplier tube. The light intensity is converted to a current, and amplified by the dynode chain of the PMT, shown schematically in Figure A-3. The cathode is maintained at a constant voltage, which

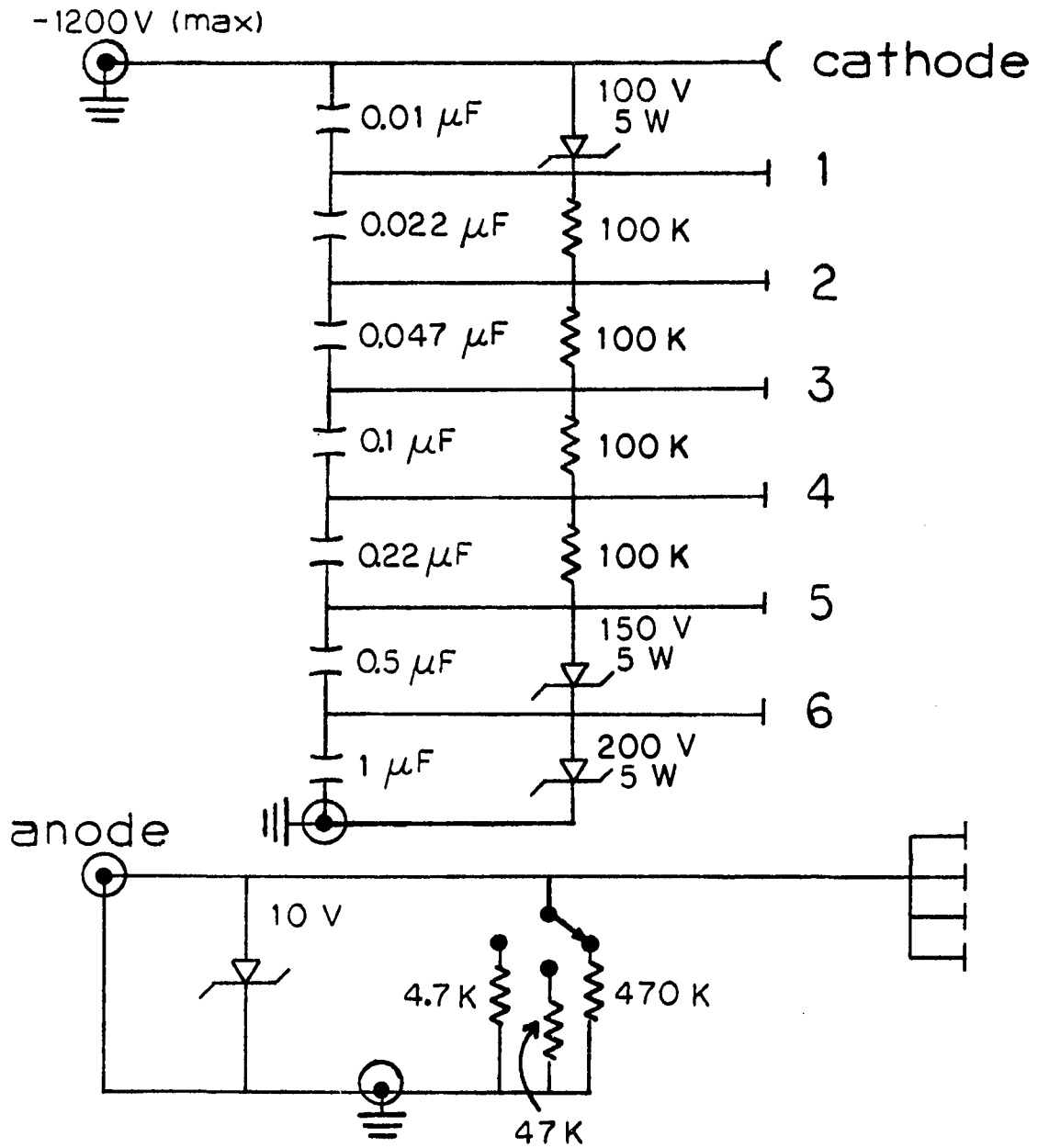


Figure A-3. Circuit diagram of PMT dynode chain

is wavelength-dependent, and ranges from 600-1200 volts. The amplified current at the anode is applied to the oscilloscope across a variable load resistance, which determines the amplification of the signal.

The oscilloscope is a Tektronix 5115 single-beam storage oscilloscope with a 5A19 N differential amplifier, featuring variable dc offset, and a 5B10 N time base/amplifier as plug-in units. The rise time of the oscilloscope and amplifier plug-in is 0.2 μ s, and the writing speed is approximately 0.2 to 0.8 divisions/ μ s. Triggering of the oscilloscope is accomplished by a Xenon Model-E optical trigger which senses photoelectrically the firing of the flashlamps. A trace of the photomultiplier voltage as a function of time after flashing the lamps is stored on the oscilloscope screen, and a Polaroid photograph is made using a Tektronix C-5B camera.

Operation of Spectrophotometer

The intensity of the light detected by the PMT at any given wavelength must be proportional to the voltage measured with the oscilloscope to obtain meaningful data. As long as the amount of anode current drawn from the RCA 1P28 tube does not exceed the manufacture's rating of 0.1 mamp, there will be a linear relation, although at strong absorptions (>80%), stray light from the monitoring beam may cause deviations.

The magnitude of the anode current (i_a) is determined by the voltage (V_a) at the photoanode of the PMT and the load resistance (R), by Equation A-2, Ohm's law.

$$i_a = \frac{V_a}{R} \quad (\text{A-2})$$

The magnitude of V_a is also dependent upon the voltage at which the photocathode of the PMT is operated, variable from 600-1200 V. Higher PMT voltages are associated with larger amounts of photomultiplier shot noise, and hence, are less satisfactory. Optimization of the load resistance is a more practical solution to maximize V_a . However, the load resistance is limited by two constraints: (1) i_a must be less than 0.1 mamp (see above), and (2) the time response of the circuit. The latter is concerned with the rise time¹ of the circuit defined by the PMT, oscilloscope, and coaxial cable connecting the two and is determined (Ref. 216, p. 408) from Equation A-3,

$$t_r = 2.2 RC \quad . \quad (A-3)$$

R can be taken as the load resistance. The capacitance of the PMT and oscilloscope are fixed; the contribution from the connecting cable can be minimized by locating the PMT and oscilloscope as close as physically possible. Typical rise times can be calculated from Equation A-3 using a nominal value of $C = 100$ pf, and the available load resistances of 4.7, 47, and 470 k Ω (see Figure A-3), to be 1, 10, and 100 μ s. Generally, a load resistance of $R = 47$ k Ω is chosen as this is a good compromise between time response and the magnitude of V_a which can be obtained. For i_a less than 0.1 mamp, the photoanode voltage may be as high as 4700 mV - more typically a maximum value of 1000 mV is chosen for V_a because it can be achieved with photocathode voltages no higher than about 700 V,

¹Rise time, t_r , is defined as the time required by the external circuit for the anode voltage V_a to rise from 0.1 to 0.9 V_a .

at almost all wavelengths, thereby minimizing the PMT noise. At wavelengths lower than about 350 nm, it is preferable to accept a smaller photoanode voltage, 500 mV, in order to avoid the large amount of noise associated with high photocathode voltages.

For very fast reactions, using $R = 4.7 \text{ k}\Omega$ may be necessary, although the transient must then have a relatively large absorbance change at the monitoring wavelength. To avoid artifacts, the rise time must always be less than the reaction time measured.

The linearity of light intensity with oscilloscope deflection should always be ascertained after any adjustment of the optical components. A spectrophotometric cell is filled with solvent, and placed in the monitoring beam inside the flashlamp housing. The monitoring wavelength and load resistance are chosen, and the voltage to the photocathode of the PMT is increased until a deflection of 1000 mV (or other value) below ground is obtained, as monitored on the oscilloscope. The cell is filled with a stable compound, absorbing at this wavelength, and the oscilloscope deflection is noted. The absorbance, D , is determined by the Beer-Lambert absorption law,

$$D = - \log \frac{I}{I_0} \quad , \quad (\text{A-4})$$

where I is the intensity (measured in mV) of the light reaching the monochromator after passage through the sample, and I_0 is the intensity measured with solvent in place. This absorbance can be compared with that from a calibrated double-beam spectrophotometer. Repeating

measurements several more times with successively more dilute samples will establish whether Equation A-4 is valid.

It is also useful to compare the spectrum of some absorbing sample with that obtained from another spectrophotometer. In Figure A-4 the spectrum of an aqueous solution of $\text{Co}(\text{NH}_3)_5\text{H}_2\text{O}(\text{ClO}_4)_3$, obtained point-by-point using the spectrophotometer of the flash photolysis instrument, is compared with that obtained from a Cary 219. Collected in Table A-2 are the voltages applied to the PMT, at each wavelength, to serve as a reference of typical PMT voltages for future users. From Figure A-4, it can be seen that deviations occur at absorbances greater than 0.7 in the visible, and greater than 0.5 in the UV. The amount of stray light (223) calculated at 340 nm is 8.8%. Because stray light is most detrimental for measurement of large absorbances, it need not be of concern in flash photolysis work, where transients are present at such small concentrations.

The quartz-halogen lamp was used for the spectrum of Figure A-4 because it is the preferred source for visible and near-UV work. The xenon arc-lamp provides more intense UV irradiation, and therefore, might be preferred at wavelengths less than about 350 nm; however, the excellent stability of the quartz-halogen lamp cannot be matched by the arc-lamp, nor its convenience of use. The xenon arc-lamp must be vented for ozone, and its very intense high energy radiation requires protection of the operator's eyes, preferably with sunglasses. Presently, absorption measurements are restricted to $\lambda \geq 310$ nm because the Jarrell-Ash monochromator suffers from scattered light and second-order diffractions at wavelengths further into the UV.

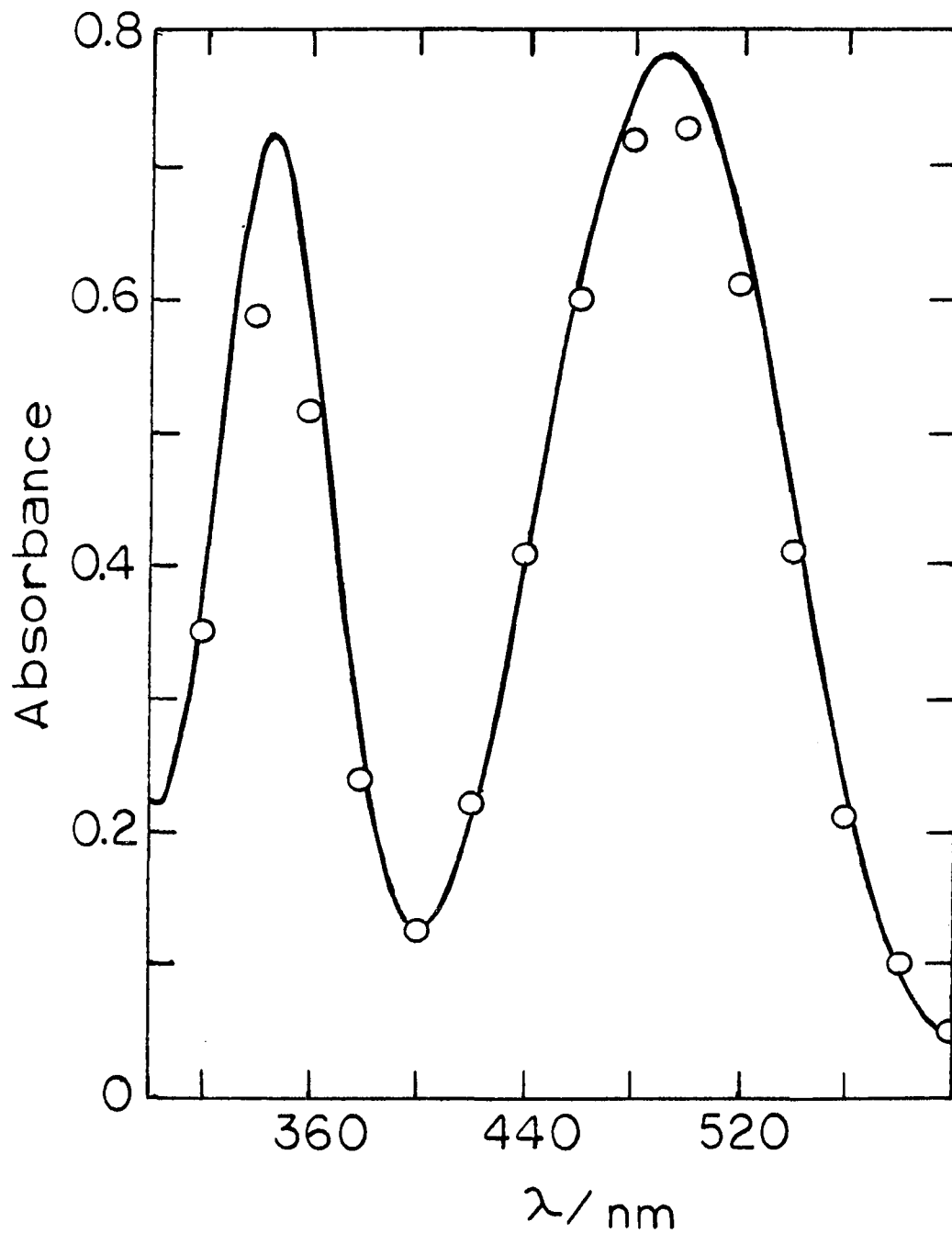


Figure A-4. The electronic spectrum of $\text{Co}(\text{HN}_3)_5\text{H}_2\text{O}^{3+}$ obtained with spectrophotometer of flash photolysis instrument (circles) and from Cary 219 spectrophotometer (line)

Table A-2. Typical PMT voltages for various wavelengths^a

λ/nm	Photocathode Voltage of PMT/V
600	690
580	670
560	665
540	660
520	660
500	660
480	665
460	675
440	675
420	680
400	695
380	720
360	750
340	830
320 ^b	935

^a $I_o = 1000$ mV, except as noted, with H₂O; cell length = 10 cm; load resistance = 47 k Ω ; quartz-halogen lamp.

^b $I_o = 500$ mV.

Operation of Flash Photolysis Instrument

This section will be presented in a format useful for actually conducting an experiment, following a step-by-step approach.

Initial equipment adjustment

1. One hour before the experiment the monitoring light and voltage to PMT (~ 500 V) are turned on; a stream of air from the laboratory jet provides cooling. The quartz-halogen lamp is run at 11 volts, 4 amps; the xenon arc-lamp must be operated at 12.5 volts, 6 amps, and the generated ozone must be vented through a hood.
2. Solvent in the desired path length cell is placed in the monitoring beam, and the monitoring wavelength is set.
3. The load resistance is selected, generally 47 k Ω .
4. The signal from the PMT is connected via a coaxial cable to the positive input of the oscilloscope. The negative input is grounded. The time base "source" is set to "line", and a sweep time of about 1 ms/div selected. The positive input is then grounded and the trace (0% T) positioned one major graticule division below the top of the screen. Ground is removed and thirty minutes before the experiment I_0 (100% T) is set to 1000 mV (or some other value) by increasing the PMT voltage. This needs readjustment every few minutes, till constant.

Actual experiment

1. The capacitance and voltage of the Model-A are adjusted to give the desired flash energy.

2. The sample to be photolyzed is placed in the monitoring beam and the housing cover closed. If it is photosensitive to the light of the monitoring source, the shutter must be used. The hood vent is centered over the housing.
3. The initial voltage of the sample is recorded, I_{t_0} , and the desired time base set.
4. Power to the Model-A, -C, -E, and remote control panel (Model-A half) are turned on.
5. The oscilloscope screen is set to the storage mode, and the time base "source" is set to "external".
6. The capacitors of the Model-A are charged from the remote control panel, and when fully charged, the lamps are triggered. If the flashlamps fail to fire - turn "high voltage" to "off", and increase the voltage output of the Model-C. Then repeat step 6.
7. The trace of light intensity, I_t , versus time will be recorded on the oscilloscope screen. The oscilloscope is triggered (manually) to record the final light intensity, I_{t_∞} . If desired a photograph is made.
8. Power to the remote control panel and Model-A and -C are turned "off" BEFORE¹ removing the sample from the monitoring source.

¹It must be understood that whenever the power to the Model-A is on, a potentially lethal situation exists should the operator make bodily contact with any portion of the circuitry driving the flashlamps, if the capacitors are charged. Hence, to be absolutely certain that the Model-A is not charged, one must ascertain the power to the Model-A (and preferably the Model-C also) are off before reaching into the housing compartment. Turning the power off causes capacitor discharge through a shorting bar inside the Model-A.

9. Often (if not always) the size of the transient will need amplification, which is achieved by using the dc off-set capability of the oscilloscope amplifier. The desired oscilloscope sensitivity is set, and with the dc off-set engaged, the trace corresponding to the light intensity before the flash is brought on screen; its optimal position on the screen can be learned only by experimentation. Steps 3-8 are repeated, plus the final light intensity should also be read with the dc off-set "off", to determine its absolute value.

Data analysis

Kinetic data consist of a trace of the light intensity, I_t , of the solution as a function of time after triggering the flashlamps. For a system where the products absorb more than the reactants, such a trace is shown schematically in Figure A-5. The line marked "a" is the ground or 0% T level (shutter closed); "b" is I_0 (100% T) (shutter open); "c" is the kinetic trace due to loss of absorbance with time upon conversion to product(s), which has a smaller molar absorptivity than the transient (for this particular example) at the monitoring wavelength; and "d" is I_{t_∞} .

Values of I_t can be converted to absorbance, D_t , by use of Equation A-4, with $I = I_t$. However, for very small transients, it can be shown mathematically that D_t will be linearly related to I_t , rather than the logarithmic relation of Equation A-4. This simplifies data analysis somewhat as the actual transmittances of the kinetic trace, measured in mV, can be used directly in kinetic plots of $\ln(D_t - D_\infty)$ versus time, for example. Or, for even further convenience, any quantity linear to

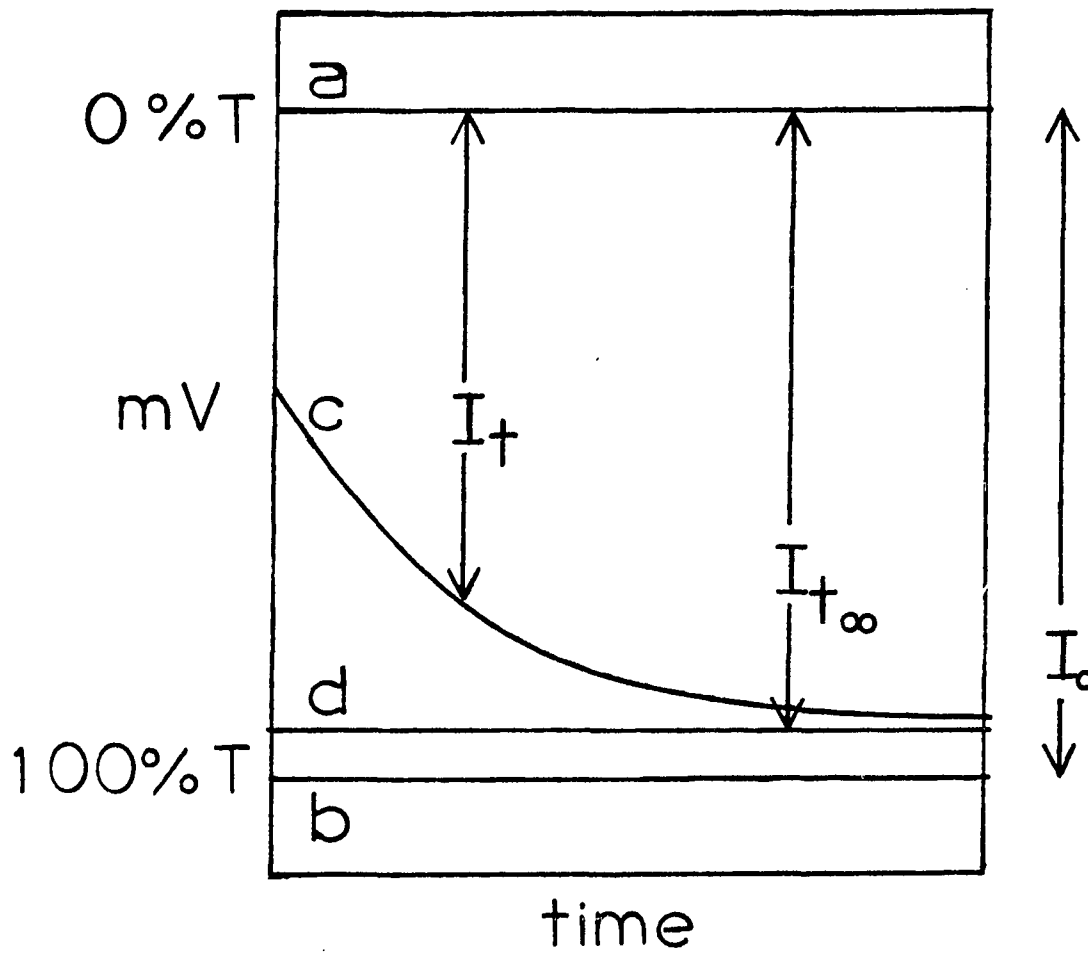


Figure A-5. Schematic of a kinetic trace for a system where $\epsilon_{\text{transient}} > \epsilon_{\text{product(s)}}$ at the monitoring wavelength. See text for identification of a - d

I_t , such as the height of the transient, measured in centimeters from I_{t_∞} , may be used directly. Generally, then, the distance from trace "c" to I_{t_∞} is measured at various times and this quantity, cm_t , or called D'_t in this thesis, used directly in kinetic analysis of the data. To convert cm_t (D'_t) to the absorbance at time t , D_t , Equation A-5 is useful,

$$D_t = \log \frac{I_{t_\infty}}{I_{t_\infty} - cm_t \left(\frac{\# \text{ mV}}{\text{cm}} \right)}, \quad (\text{A-5})$$

where I_{t_∞} is in millivolts.

In Figure A-6, the decay profile or scattered flashlight which is seen by the PMT is reproduced. This trace is obtained with the shutter closed. The decay profile limits the time at which data collection may begin to times on the order of a few tenths of a millisecond for this instrument. Its magnitude, and its duration are dependent upon the monitoring wavelength, energy of the flash, type of spectroscopic cell employed, the PMT voltage, and most importantly the time response of the circuit, i.e., the load resistance, as discussed above. The decay profile shown in Figure A-6 was obtained at 420 nm, with 250 J, no cell, 680 V on PMT, and a load resistance of 47 k Ω . Both the magnitude of the scattered flash and its duration (>0.2 ms) should be noted.

Simple chemical systems for use as calibration reactions

Br_{aq}⁻ One of the easiest transients to generate by flash photolysis is the dibromide radical anion Br₂^{•-}. Excitation of the CTTS transition of 0.1 M Br_{aq}⁻ in aqueous solution causes photoelectron production and the formation of the Br[•] atom (224), which is very

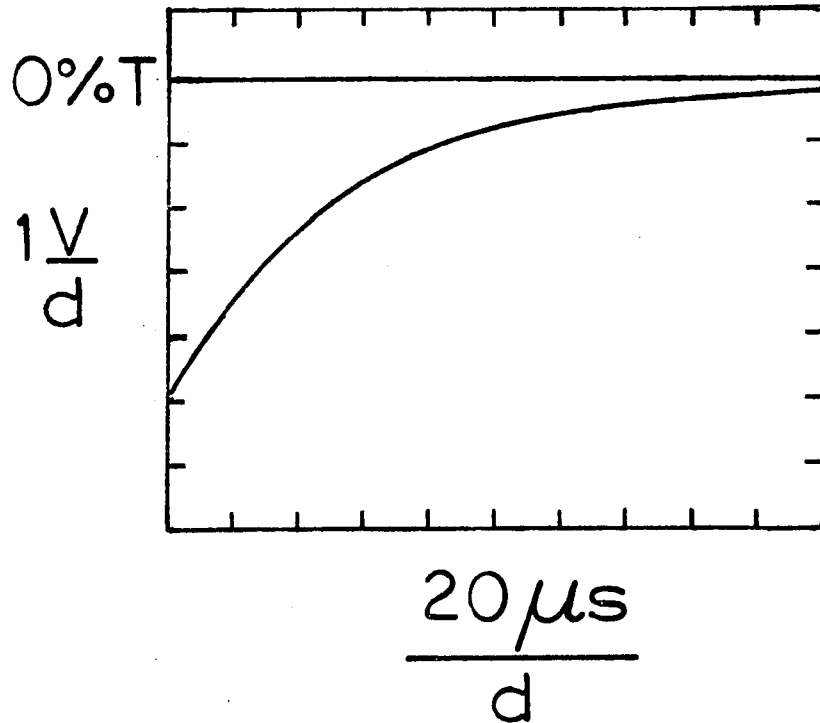
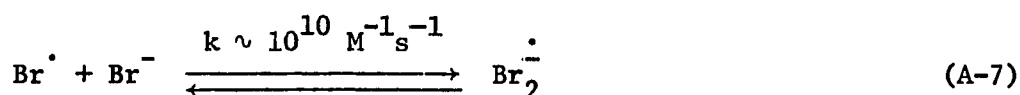


Figure A-6. Decay profile of flashlamps. Monitoring $\lambda = 420$ nm; flash energy = 250 J; no cell; 680 V on PMT; load resistance = 47 k Ω

rapidly scavenged by another bromide ion to form the intensely absorbing Br_2^- . Bimolecular reaction of the radical anions leads to formation of Br_3^- and Br^- . The reactions are summarized:

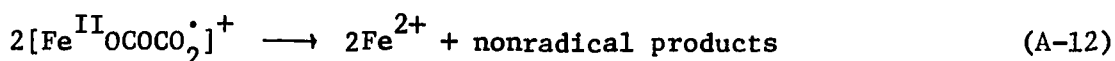
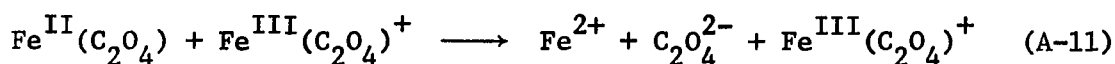
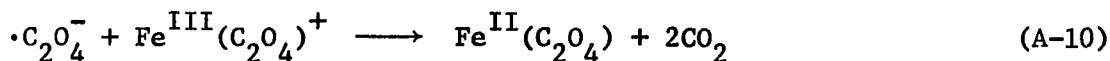
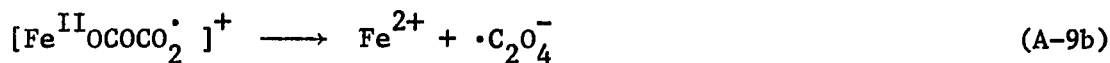


$$k_8 / \text{M}^{-1} \text{ s}^{-1} = (1.9 \pm 0.6) \times 10^9 \quad (225)^1$$

While Reactions A-6 and A-7 are so rapid that they occur within the decay profile of the flashlamps, Reaction A-8 is of a convenient rate to follow. The kinetics are monitored at 366 nm ($\epsilon = 7800 \text{ M}^{-1} \text{ cm}^{-1}$) by following the decrease in absorbance due to Reaction A-8, using a 250 J non-filtered flash, an oscilloscope sensitivity of 20 or 50 mV/div, and a time base set to 0.1 ms/div. The data are treated according to conventional second-order kinetics to evaluate k_8 .

$\text{Fe}(\text{C}_2\text{O}_4)^+$ The flash photolysis of monooxalatoiron(III) is an excellent system to study for determining the accuracy of reaction rates measured using the flash photolysis instrument because reaction rates are well known (226). In the absence of any excess iron(III), the following reactions are believed to be responsible:

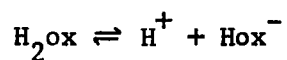
¹ k_8 is an average of the values listed in Reference 225.



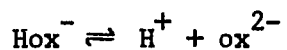
The overall reaction occurs in two stages, both leading to absorbance decreases. Reactions A-9a, A-9b, A-10, and A-12 comprise the first loss of absorbance over the time period $0 \leq t \leq 50 \mu\text{sec}$. The second absorbance loss is due to Reaction A-11 which occurs over the range $50 \mu\text{sec} \leq t \leq 5 \text{msec}$. Reaction A-11 is conveniently followed at 430 nm using a 250 J nonfiltered flash, an oscilloscope sensitivity of 20 mV/div, and a time base set at 0.5 ms/div. Recommended concentrations of the reactants are $4.99 \times 10^{-4} \text{ M Fe}(\text{ClO}_4)_3$ and $5.00 \times 10^{-4} \text{ M H}_2\text{C}_2\text{O}_4$ in 0.145 M H_3O^+ with $\mu = 0.99 \text{ M (LiClO}_4)$. The data is treated according to pseudo-first-order kinetics to obtain k_{obs} which is equal to $k_{11}[\text{Fe}(\text{C}_2\text{O}_4)^+]$. The concentration of $\text{Fe}(\text{C}_2\text{O}_4)^+$ can be calculated from a consideration of the equilibria:



$$K_f/M^{-1} = 3.9 \times 10^7 \quad (22^\circ\text{C}, \mu = 1.0 \text{ M})$$



$$K_{a_1} / M = 8.40 \times 10^{-2} \quad (\mu = 1.0 \text{ M})$$



$$K_{a_2} / M = 2.79 \times 10^{-4} \quad (\mu = 1.0 \text{ M})$$

Let $x = [\text{ox}^{2-}]$ and $y = [\text{Fe}^{3+}]$, at equilibrium, so that the stoichiometric concentration of oxalate is,

$$[\text{ox}]_{\text{Tot}} = [\text{H}_2\text{ox}] + [\text{Hox}^-] + x + [\text{Fe}^{\text{III}}]_{\text{Tot}} - y \quad (\text{A-13})$$

The above relationship can be solved for x and y , using the above three equilibria, so that $[\text{Fe}(\text{ox})^+]$ can be obtained from K_f , and hence, a value for k_{11} . Cooper and Degraff (226) report k_{11} (22°C , $\mu = 1.0 \text{ M}$) = $(2.95 \pm 0.40) \times 10^6 \text{ M}^{-1} \text{ s}^{-1}$; the activation parameters were also measured (226) so k_{11} can be calculated for any other temperature.